FRACTURE SURFACE ZONES AND CRACK-BRANCHING IN SOME BRITTLE PLASTICS

by

Brian Richard McQuillin B.A.

Presented to the University of Keele
for the Degree of Doctor of Philosophy.

Department of Physics,
University of Keele,
Keele, Staffordshire.

November, 1974.

ABSTRACT

The phenomenon of crack-branching is examined. Other, pre-branching, fracture surface zones which arise on the tensile fracture surfaces of polymethylmethacrylate, polystyrene, and an epoxy resin are then described, and an attempt is made to account for their formation.

SYNOPSIS

A detailed study of the fresh surfaces produced during the fracture of a brittle material can provide valuable information on the course and progress of the crack. When a brittle solid is broken in simple tension for example, the fracture surfaces display a characteristic sequence of markings, each of which can be related, at least in principle, with events which occured during the rupture of the solid. One such event, which appears to be common to the tensile fracture process of all brittle materials, is macroscopic crack-branching. For many materials incipient bifurcations also occur prior to the macroscopic event, and these leave many of the characteristic markings on the resulting fracture surfaces. This thesis is concerned with the phenomenon of crack-branching and, in the case of three materials, with the structure of the pre-branching fracture surfaces.

Chapter 1 is an introduction to brittle fracture and outlines the main landmarks in the development of the subject. Moving cracks are dealt with and this leads naturally to Chapter 2 which is a brief review of the energetics of moving cracks. Chapter 3 deals specifically with crack-branching, and with a simple empirical relationship which can be used to characterise the onset of branching in a given material: viz if σ is the sample strength and c_b the distance travelled by the crack before branching occurs, then the product $\sigma c_b^{\frac{1}{2}}$ has a characteristic value for a given material. An energy criterion of branching, (after Johnson and Holloway 1966), is considered to be the most satisfactory account of

the phenomenon of branching that is currently available, and this also predicts that $\sigma_b c^{\frac{1}{2}}$ = constant.

Chapter 4 describes the main experimental techniques used to examine the pre-branching fracture surfaces of three polymers: polymethylmethacrylate (pmma), polystyrene, and the Araldite epoxy resin CT200 cured with phthalic anhydride. The next three chapters, (Chapters 5, 6, and 7), decribe and discuss the fracture surfaces of pmma, polystyrene, and the epoxy resin respectively. Only in the case of the resin is it reasonably clear what processes lead to the observed structures, although even in this material it is by no means clear <u>why</u> specific events occur.

ACKNOWLEDGMENTS

I should like to express my gratitude and thanks to:-

Professor D.J.E. Ingram*:	for the use of laboratory and research facilities.
Dr. D.G. Holloway:	for his careful supervision, generously given, and for his advice and stimulating discussion.
The Technical Staff of the Physics Dept.:	for their most competent help on technical matters.
Mr. W. Brearley:	for his expert help with the experiments on oriented pmma.
Dr. J.W. Johnson:	for arranging our use of the scanning electron-microscope at Rolls Royce, Derby.
The University of Keele:	for a research studentship.

I should also like to thank my research-group colleagues, J. Lilley, G.W. Weidmann, and S.P. Gunesekera, and other colleagues in the Physics Dept., for making my stay at Keele a happy one.

Finally, I should like to thank Mrs. Margaret Greenwood, for her patience and care in typing this thesis, and my wife, Lesley, who gently whipped me into finishing this work.

---

* Now at Chelsea College, London.

CONTENTS

Abstract 1

Synopsis ii

Acknowledgements iv

CHAPTER 1 GENERAL INTRODUCTION

1.1 Introduction 1

1.2 The Strength of Solids 1

1.3 The Theoretical Strength of Solids 5

1.4 The Strength of Real Solids 9

1.5 Fracture Toughness 15

1.6 Moving Cracks 27

1.7 Fracture Surface Appearance and Crack Branching 39

1.8 Summary 45

CHAPTER 2 THE ENERGETICS OF FRACTURE

2.1 Introduction 47

2.2 Mott's Energy Expression 47

2.3 Possible Modifications to the Basic Energy Equation 53

2.4 The Dependence of Fracture Energy on Crack Speed 64

2.5 The Absorption of Energy by Multiple Cracking 67

2.6 Summary 68

CHAPTER 3 CRACK BRANCHING

3.1 Introduction 70

3.2 Provisional Experiments 73

(a) Choice of Materials 73

(b) Specimen Preparation 73

CONTENTS (continued)

(c) Experimental Measurements of $\sigma c_b^{\frac{1}{2}}$ 78

(d) Results 78

3.3 Some Previous Attempts to Explain Fracture Branching, and Why $\sigma c_b^{\frac{1}{2}}$ = Constant 80

3.4 A Closer Examination of the Measurements of $\sigma c_b^{\frac{1}{2}}$ in Relation to the Energy Criterion of Branching 97

3.5 Summary 105

CHAPTER 4 BASIC EXPERIMENTAL TECHNIQUES USED TO EXAMINE THE DETAILS OF FRACTURE SURFACES

4.1 Introduction 106

4.2 Optical Microscopy 106

(a) Light Cut Method 107

(b) The Linnik Interferometer 108

4.3 Etching Programme for CT200 Epoxy Resin 112

4.4 Electron Microscopy 113

CHAPTER 5 THE FRACTURE SURFACES OF POLYMETHYLMETHACRYLATE ("PERSPEX")

5.1 Introduction 115

5.2 Some Previous Work on the Fracture Surface Morphology of pmma 115

5.3 Crazes 120

5.4 The Role of Crazes in the Energetics of Fracture 122

5.5 The Tensile Fracture Surface Appearance of pmma 128

CONTENTS (continued)

5.6 Quantitative Measurements Relating to the Onset of each Zone 130

5.7 The Structure of Some of the Fracture Surface Zones Related to the Fracture Process 131

(a) Fracture Surface Zone A 132

(b) The Conic Zone 137

(c) Fracture Surface Zone D 155

5.8 Fracture of Oriented pmma 161

5.9 Summary and Conclusions 165

CHAPTER 6 FRACTURE SURFACES OF POLYSTYRENE

6.1 Introduction 168

6.2 Classification of the Two Zone Sequences 169

(a) Zone Sequence 1 169

(b) Zone Sequence 2 174

6.3 Identification of the Conditions Leading to the Two Zone Sequences 177

6.4 A more Detailed Examination of Some of the Fracture Surface Zones 179

(a) Zone A of the First Tensile Sequence 179

(b) Zone B of the First Sequence 185

(c) The Banded Zone (Zone C) of Sequence 1 191

(i) The Transition to the Banded Zone 192

(ii) The Development of the

CONTENTS (continued)

Banded Structure
Within the Banded Zone 200

6.5 The Relationship between Banding and Fracture-Branching 204

6.6 Discussion of Previous Results 205

(a) The Mackerel Pattern 206

(b) The Banded Structure 208

6.7 Summary and Conclusions 210

CHAPTER 7 THE FRACTURE SURFACES OF AN EPOXY RESIN

7.1 Introduction 214

7.2 Classification of the Features Which Occur in the Mist Zone 214

7.3 The Fracture Surface Topography Around the Features 214

(a) Conics 217

(b) Type 1 Features 220

(c) Type 2 Features 221

(d) Type 3 Features 222

7.4 Other Fracture Surface Markings 223

(a) The Origin of Fracture when Fracture Initiated Internally 223

(b) Craze-like Features 225

7.5 Discussion of the Formation of the Mist-Zone Features 227

(a) The Formation of Conic Features 230

(b) Type 1 Features 231

CONTENTS (continued)

(c) The Formation of Type 2 Features 233

(d) Type 3 Features 237

7.6 Further Discussion 239

7.7 Summary and Conclusions 243

REFERENCES 246

Chapter 1
GENERAL INTRODUCTION

1.1 Introduction

For most people brittle fracture is an irritatingly familiar experience: we have all seen objects broken into useless pieces because they were dropped or carelessly handled. On the other hand, brittle fracture finds a useful application in rock-blasting and sculpture, and is the basis of many industrial processes such as the production of fine particles by comminution. Unexpected failures of large structures, such as bridges, boilers and ships have also occurred as a result of brittle fracture of a component, and it is these more catastrophic manifestations which have been the greatest stimulus to research into the phenomenon.

In this chapter we introduce some of the landmarks of this research, since these form a foundation for much of the later discussion. The thesis itself is concerned with one aspect of brittle fracture; namely with the structure of the fresh surfaces which are formed as a result of brittle fracture of some polymers. We attempt to explain the morphologies of these fracture surfaces in terms of events which occurred whilst the solids were in the process of breaking.

1.2 The strength of solids

A solid can be said to have failed if either it fractures into two or more pieces, or it undergoes macroscopic permanent deformation as a result of the

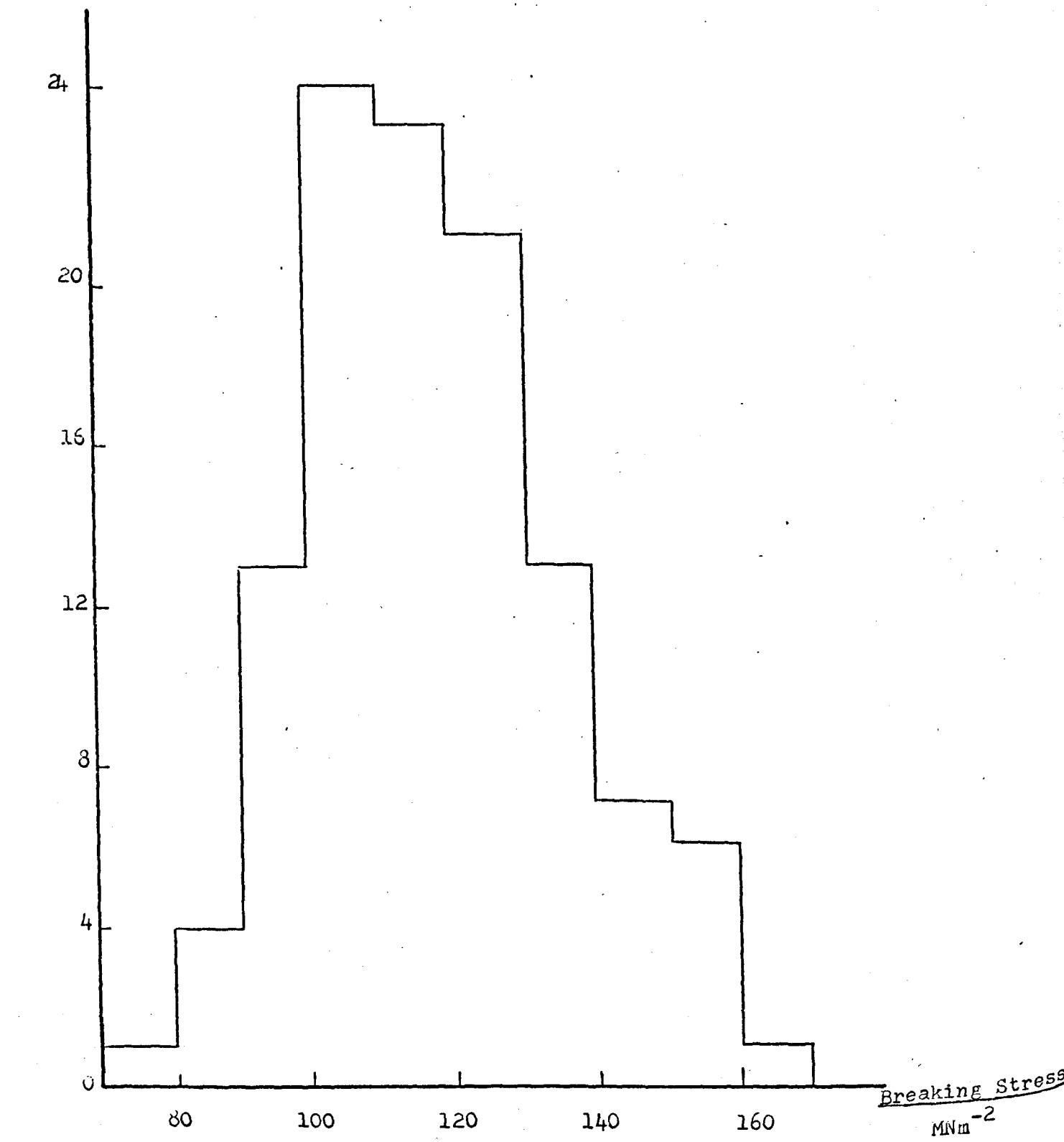

Breaking strength of Sheet Glass (After Holloway 1973).

Fig. 1.1

stresses which act upon it. A given material can exhibit both types of failure depending upon various factors such as the stress system applied, the external environment, and, in some cases, on the dimensions of the stressed sample. Where failure occurs by the propagation of a crack so that complete separation occurs without large-scale permanent deformation, the solid is said to have failed by brittle fracture, and it is this mode of failure with which we shall be particularly concerned.

Experience has shown that if a solid fails by brittle fracture the stress at which fracture occurs, that is, the strength of the solid, cannot be evaluated to the same degree of accuracy as, for example, its density or resistivity. There is, generally speaking, a large scatter in the results, even for apparently identical specimens broken under the same conditions. Figure 1.1 shows some typical results for the breaking strength of samples of sheet glass.

This inconstancy in the value of strength is a problem which has to be faced by the design engineer, and it has been common practice to include a large safety factor in designs, so that the maximum tensile stress that a component will encounter is much less than the mean value of the strength measured in the laboratory for samples of the same material. This approach, which has arisen because of the uncertainty in specifying the minimum value of strength of a component in service, has its disadvantages. For example, in some designs, such as aircraft, the increase in weight which is associated with the safety-factor may

become intolerable, particularly if the traditional engineering materials are used. As a consequence, considerable effort has been devoted to finding ways of predicting the actual stresses that a component will support without fracturing and a great deal of work has been undertaken to develop new materials with a high specific strength, so that strong, yet light components can be used for construction. Table 1.1 shows the tensile strengths of a selection of materials compared with their specific tensile strengths ($\frac{\text{tensile strength}}{\text{relative density}}$).

Table 1.1

Material	Tensile Strength / MNm^{-2}	Specific Tensile Strength / MNm^{-2}
Steel	2000	256
Alumin alloy	300	107
Mild steel	460	59
Carbon fibre	3200	1700
Plastics	100	80

It is clear from this table that whereas carbon fibres and steel have comparable strengths, the former are far superior in terms of specific strength. The high specific strength of these fibres combined with their high stiffness, (large value of Young's modulus), has led to the development of carbon fibre reinforced composites in recent years.

1.3 The theoretical strength of solids

In principle the strength of a solid is related to the attractive forces between its constituent atoms. Once the atomic arrangement and the nature of the forces between the atoms are known, then the strength of the solid should be calculable. At present, however, there is insufficient knowledge of the mutual interaction between the atoms, their response to applied stresses, and their dynamics, to enable anything approaching a complete description to be made, and even if this information were available the complexity of the resulting calculations would be enormous. As a result, calculations of theoretical strength have involved varying degrees of approximation, although in no case is the dynamic nature of the atomic system taken into account, and so even in their most elaborate form the calculations are for solids at 0 K.

The simpler calculations relate the ideal strength to other macroscopic physical properties. For example, Polanyi, (1921), Orowan, (1955), and others, obtained rough estimates of the ideal cleavage strength σ_{th} in terms of the equilibrium surface energy T, the interplanar separation, b, of planes perpendicular to the tensile axis, and the appropriate Young's modulus, E. Polanyi assumed Hookean behaviour up to fracture, and equated the increase in surface energy to the release of strain energy stored in a layer of thickness equal to the interatomic separation, b. This produced a value for σ_{th} of:

$$\sigma_{th} = (4ET/b)^{\frac{1}{2}} \qquad (1.1).$$

Orowan assumed that the atomic force separation law was Hookean, and the strain energy term now included a contribution from the atomic interaction at separations higher than that corresponding to σ_{th}.
This gave:

$$\sigma_{th} = (2ET/b)^{\frac{1}{2}} \qquad (1.2)$$

Orowan (1934, 1945,6) also proposed a different argument in which it was assumed, more realistically, that the atomic stress-displacement curve could be represented to a first approximation by half a sine-curve, chosen to give the correct modulus at zero displacement. σ_{th} was then taken to be the maximum value of this curve. Orowan assumed that the work done in raising the stress to this maximum value, which is equal to the work done in separating a pair of adjacent atomic planes, was just equal to the energy of the freshly formed surfaces. This gave:

$$\sigma_{th} = (ET/b)^{\frac{1}{2}} \qquad (1.3)$$

These simple arguments produce values of σ_{th} which are of the same order of magnitude as those obtained from more refined calculations, and they have the added attraction of being applicable to all solids. In the case of crystalline materials the values of E, T and b, will depend upon the particular crystalline plane across which fracture occurs, and although this is not true of the amorphous materials such as glass and many polymers,

there is still sufficient uncertainty in the measured values of T and b to introduce a factor of four variation in σ_{th}, over and above any variations introduced as a result of the particular assumptions made in the derivations. To take the case of glass, estimates of T vary between 0.54 J m^{-2}, obtained by extrapolation from the liquid state to room temperature (Griffith 1920), and 1.75 J m^{-2}, estimated from the heat of vapourisation of silica (Charles 1961). Some authors have used 3.5×10^{-10}m as the value of b, obtained by dividing the molar volume by Avogadro's number and taking the cube root, (Condon 1954), and others have taken the Si-O bond length of 1.6×10^{-10}m, (e.g. Charles 1961).

More refined calculations of σ_{th} have been advanced using specific models of atomic bonding. Of these, most success has been achieved with ionic and van der Waals' solids, in which the interatomic forces are best understood. Even here, however, the available models of interatomic forces are only approximate, and the potential functions which have been used tend to become increasingly unreliable as strain increases and symmetry decreases and the atoms become polarised.

Much of this latest theoretical work has been undertaken on NaCl, and this therefore provides a suitable case for comparison with experiment. The measured value of breaking strength for NaCl whiskers,

MATERIAL	THEORETICAL STRENGTH MNm^{-2}	EXPERIMENTAL STRENGTH MNm^{-2}
Sodium Chloride	4300	~ 10 (polycrystalline) ~ 1000 (whisker)
Iron	40 000	2000
Silica Glass	16 000	50
Diamond	200 000	1800
Graphite	1400	15

TABLE 1.2

COMPARISON OF THEORETICAL AND EXPERIMENTAL STRENGTHS

(very fine single crystals), is 1.08×10^3 MNm^{-2}, and this can be compared with the theoretical value as calculated from Orowan's, (1946), equation of 4.3×10^3 MNm^{-2} and the theoretical value obtained from a more refined analysis, (MacMillan 1972), of 2.5×10^3 MNm^{-2}. Thus the simple theory provides an overestimate of the strength of NaCl of about a factor of four, and even the most accurate calculation to date gives a value of σ_{th} which is higher by a factor of two than the measured value.

The discrepancy between σ_{th} calculated by any of these methods, and the strength of materials measured in the laboratory is normally much greater than this, and any variations in the predicted values become relatively insignificant in comparison. Table 1.2 compares calculated values of σ_{th} as obtained from Equation 1.3, with measured values of strength for a selection of materials.

It is obvious that the immense differences between the theoretical strength and observed values cannot be accounted for in terms of any approximations made in the calculations; we have already seen that the alternative approximations lead to variations in σ_{th} of a factor of four at most. Clearly, at least one assumption on which all the calculations are based is in error.

1.4 The strength of real solids

The discrepancy between the fracture strength of

real solids and the theoretical cleavage strength is mirrored in the difference between the measured and calculated values of shear strength of crystalline solids. The reason for these discrepancies is that in both cases the theoretical estimates are for perfect solids. Fracture is assumed to occur by simultaneous parting of two adjacent planes of atoms over the whole cross section, and shear failure is assumed to occur when two planes of atoms slide across each other such that every atom in those parts of the planes which remain in contact is involved in the shearing process. The low values of fracture and shear strengths have been explained in terms of structural imperfections which localise the processes of fracture and shear so that at any one time only a few atoms are involved, and fracture and shear failure occurs progressively across the specimen. The imperfections which are the chief cause of failure in ductile materials are dislocations, whereas cracks and sharp notches lead to the low values of fracture strength, and it is with these latter types of flaw that we shall be primarily concerned.

The effect of a sharp notch or crack in a material is to increase the stress in the material in the neighbourhood of the tip of the notch, so that bonds may be broken in this localised region even though the average stress over the whole cross-section is much less than the theoretical strength. Fracture can then occur by localised rupture of the bonds near to the tip of the

crack and spread progressively across the specimen. This stress magnifying effect of cracks and notches has been the subject of many theoretical and experimental investigations.

Inglis (1913) and Kolosoff (1914) independently derived an expression for the stress at each end of an elliptical slit in a two-dimensional plate in terms of the average stress acting normal to and remote from the slit, (σ), the length of the slit, (2c), and the radius of its tips, (ρ). They obtained the following result for σ', the stress at each end of the slit:

$$\sigma' = \sigma\left[1 + 2\left(\frac{c}{\rho}\right)^{\frac{1}{2}}\right] \simeq 2\sigma\left(\frac{c}{\rho}\right)^{\frac{1}{2}} \text{ if } \rho \ll c \qquad (1.4)$$

For a brittle solid, in which little or no plastic distortion occurs in the highly stressed region near to the tip of the notch, it will be relatively easy to introduce notches which severely weaken the solid. In materials in which plastic deformation does occur, however, the high stresses close to the ends of the slit will induce plastic flow in this region, and the tips of the notch will as a consequence become blunted by this process. Higher applied stresses will then be needed to rupture the solid.

Equation 1.4 was derived for an elastic continuum, and it is therefore only strictly applicable to real solids if ρ is much larger than the distance between their atoms. For a <u>crack</u> in an ideally brittle solid ρ will be of the same order as the distance between the atomic centres, and for this case a different approach is

needed. Griffith (1920) used an energy argument to calculate the critical stress required to maintain the stability of a pre-existing crack in a perfectly brittle solid. If the applied stress exceeded this value then the crack would extend, whereas if the applied stress were reduced then the crack would shorten. Although the actual expression that Griffith derived is unlikely to be applicable to any real material, the principle on which his derivation was based is of fundamental importance, and underlies the present theoretical treatment of brittle fracture. Using Inglis's, (1913), solution for the stresses around a slit in a two dimensional sheet, Griffith obtained the result that the total increase in energy due to the introduction of a crack in a previously uncracked specimen of unit thickness was

$$4Tc - \frac{\pi\sigma^2c^2}{E}$$

Here, T is the surface energy per unit area of fracture surface, c is the crack half-length, and σ is the applied stress.

This result is valid for both constant strain, (fixed grip), conditions and constant stress, (dead loading) conditions. The decrease in strain energy of the specimen appears entirely as surface energy in the former case, and in the latter case the work done by the displacement of the ends of the specimen just exceeds the increase in strain energy by $\frac{\pi\sigma^2c^2}{E}$.

Griffith postulated that the determining factor in the fracture process was that the surface energy of the fresh surfaces formed when the crack lengthened must be less than the elastic energy lost by the cracked body plus that lost by the loading system. This provided an energy criterion for fracture. For an ideally brittle solid this can be expressed as follows:

$$\frac{d}{dc}\left(4Tc - \frac{\pi\sigma^2c^2}{E}\right) \leqslant 0 \qquad (1.5)$$

Equation 1.5 implies that the stress required to cause crack extension must be greater than σ_c where,

$$\sigma_c = (2TE/\pi c)^{\frac{1}{2}} \qquad (1.6)$$

This expression gives the necessary and sufficient conditions for the stability of a pre-existing crack in a thin elastic sheet. Similar expressions have been subsequently derived using Griffith's criterion for thick sheets and for various other crack geometries, and these differ from equation (1.6) only in terms of their numerical coefficients.

If equation 1.6 is compared with Equation 1.3 we find that

$$\sigma_{th}/\sigma_c = (\pi c/2b)^{\frac{1}{2}} \simeq (c/b)^{\frac{1}{2}} \qquad (1.7)$$

Clearly, since $b \sim 10^{-10}$m, only a very short crack is required to seriously impair the strength of a truly brittle solid.

MATERIAL	SURFACE ENERGY Jm^{-2}	FRACTURE ENERGY Jm^{-2}
Sodium Chloride	0.15	0.31
Alumina	1.13	20
Steel	1.0	~1000
Soda Glass	0.3	4
Perspex	~0.5	230

TABLE 1.3

COMPARISON OF SURFACE ENERGY AND FRACTURE ENERGY

1.5 Fracture toughness

Griffith's criterion underlies the present theoretical approach to the fracture of flawed solids. By pointing out the deleterious effect of small cracks on the strength of brittle solids he also pioneered the current view which acknowledges that it is virtually impossible to build a structure from components which do not contain flaws. In this section we shall look at some of the developments of Griffith's original ideas.

Griffith's criterion is now normally expressed as follows: a crack will extend only if the rate of release of strain energy is greater than the energy required to form the new surfaces.

$$\frac{\delta U}{\delta c} \geqslant 2S \quad \text{for a solid of unit thickness} \qquad (1.8)$$

In this expression, U is the elastic strain energy, and S is the snergy required to form unit area of fracture surface. Griffith assumed that the energy required to create unit area of fracture surface by extension of a crack was the surface energy of the solid, (which is equivalent to its surface tension). Experiments have shown, however, that the energy needed to create unit area of fracture surface in a solid is generally much greater than its surface energy. Even glass, commonly regarded as the archetype brittle solid, requires $\sim 4\ Jm^{-2}$ to form unit area of fracture surface, compared with its surface energy of $0.3\ Jm^{-2}$. Table 1.3 shows some values of surface energy compared with the measured

energy required to form unit area of fracture surface.

Possible reasons for these discrepancies include electrostatic, viscoelastic and plastic effects. In metals and many nominally brittle polymers, limited plasticity in the vicinity of the crack-tip is recognised as the dominant energy absorbing process in fracture however. For these materials, Griffith's criterion can still be applied and an expression for σ_c can be derived, provided the plastic as well as the elastic energy required to create new fracture surface is taken into account.

Orowan, (1948), and, independently, Irwin (1948), were the first to use Griffith's criterion to calculate the critical stress for a material which undergoes a finite amount of plastic deformation before new fracture surfaces are formed. They derived an expression similar to the one obtained by Griffith for σ_c except that T, the surface energy, was replaced by the sum of the elastic and plastic work done in forming unit area of new fracture surface. They denoted this new energy term by γ, the fracture energy of the material. Since, in general, the plastic work done is much greater than the elastic, then γ is nearly equal to the plastic work done in forming unit area of fracture surface by crack propagation. Thus, for a solid which undergoes a finite amount of plastic deformation,

$$\sigma_c \simeq (2\gamma E/\pi c)^{\frac{1}{2}} \qquad (1.9)$$

where γ is the fracture energy of the solid.

Equation 1.9 is valid only if the zone of plastic distortion is small compared to the crack length and specimen dimensions, for only under these conditions can the stored strain energy in the body be calculated on the assumption of purely elastic behaviour.

For a crack in a perfectly brittle material, σ_c, (in Equation 1.6) gave the value of the applied stress required to maintain the stability of the crack. If the applied stress was less than σ_c then the crack would close up, and in the absence of any applied stress the crack length would become zero. When plastic deformation occurs at the tip of the crack however, the crack could still be of finite length even in the absence of any applied stress, since the plastic displacement could prevent crack healing. This is one main reason why cracks can exist in nominally brittle materials even when there are no stresses acting. The interpretation of σ_c in Equation 1.9 is therefore slightly different from that of Equation 1.6, which was for an ideally brittle solid. In Equation 1.9, σ_c, represents that value of the applied stress which must be exceeded if the crack is to extend. (A possible exception to this is glass. It is now generally agreed that plastic distortion occurs during the fracture of glass, but it has been recently demonstrated (Wiederhorn and Townsend (1970); and Rowley, Wiedmann, and Holloway, (to be published)) that crack healing may occur in this material.)

The modified Griffith theory, which includes inelastic contributions to the energy expended as the crack advances, was taken a stage further by Irwin and Kies, (1952). They suggested that the value of the strain energy release rate which equalled the energy dissipated during crack growth might provide an improved fracture criterion. They argued that if the process by which the crack lengthened was independent of the loading or specimen geometries, then extension of the crack would begin at a critical value of the strain energy release rate. This critical value could then be regarded as a material property, and could be measured by experiment.

In a later paper, Irwin, (1956), suggested that the strain energy release rate could be regarded as a force acting on unit length of crack front, tending to cause extension of the crack. This force, denoted by G, would have the critical value G_c when crack extension began. G_c is equal to twice γ , the fracture energy of the material.

Although it was assumed by Irwin that the critical value of crack driving force, G_c, was a material property, this had to be borne out by experiment for specific materials. These experiments have shown that <u>in general</u> G_c can be considered a material property. This does not mean that its value necessarily remains constant during fracture however, or that it takes on the same value for all strain rates, temperatures etc.

Irwin also showed that G could be related to the elastic stress field in the immediate vicinity of the crack tip in terms of the stress intensity factor, K. The stress intensity factor relates the stress field in the neighbourhood of the crack tip to the geometry of the specimen and the conditions under which it is loaded.

Three modes of crack surface displacement were distinguished and any arbitrary displacement could be resolved into a combination of these three modes. The modes were:

Mode 1: the opening mode, in which crack-surface displacements occur normal to the crack plane.

Mode 2: the forward shear mode, in which crack surface displacements occur by shearing in the crack plane normal to the leading edge of the crack.

Mode 3: the parallel shear mode, in which displacements occur in the crack plane and parallel to the leading edge of the crack.

Of these three, Mode 1 is of most practical importance.

Using the stress function solutions of Westergaard (1939) Irwin obtained an expression of the form

$$\sigma_{ij} = K_M (2\pi r)^{-\frac{1}{2}} f_{ij}(\theta) \qquad (1.10)$$

for the stresses σ_{ij}, near the tip of a planar crack in an infinite sheet. Here, r and θ are polar co-ordinates in a co-ordinate system with the origin at the crack tip,

SPECIMEN GEOMETRY	VALUE OF K_I	ADDITIONAL NOTES
Single edge-notch plate of width W, and notch-length c.	$\sigma\sqrt{W\tan(\pi a/W)}$	σ=applied stress
Single edge-notch plate of width W, and notch-length c where W/c> 10.	$\sigma\sqrt{\pi c}$	σ=applied stress
Parallel cleavage, with each cantilever arm of width H, and a crack of length c and width b.	$\frac{Pc}{bH^{3/2}}\left[3.46+2.38(H/c)\right]$	P =applied load

TABLE 1.4

VALUES OF STRESS INTENSITY FACTOR

the subscript M refers to the mode of crack surface displacement under consideration, and the function $f_{ij}(\theta)$ depends upon the particular stress component σ_{ij} and the mode, M, but its value is independent of the method of loading and the specimen geometry.

The important parameter in expression 1.10 is K, the stress intensity factor, since this is the only parameter which relates the stress field close to the crack tip to the specimen geometry and the loading conditions. K is defined by the condition that σ_{ij}, for which $f_{ij}(\theta) = 1$ when $\theta = 0$ is given by

$$(\sigma_{ij})_{\theta = 0} = K(2\pi r)^{-\frac{1}{2}} \qquad (1.11)$$

Thus if K can be calculated for various specimen geometries and loading conditions, then the stress field close to the crack tip can be evaluated. More importantly, if two cracks have identical stress intensity factors associated with them, even though the specimen and loading geometries might be quite different, the material close to both crack tips will be under the same stresses. This shifts the mathematical problem to one of calculating K for various loading and specimen geometries. A few such calculations are given in Table 1.4, all of which are for opening mode surface displacements.

Irwin applied virtual work arguments to relate K to G. He considered the stresses which would be needed to close a segment of crack border, and showed that the opening mode crack extension force was related to K_I by the following expression:

$$G_I = K_I^2/E \qquad (1.12)$$

Thus if $G=G_c$ provides a valid criterion for crack extension then for an elastic material this is equivalent to the attainment of a critical stress at the tip of the crack (from expression 1.11).

The expression given in Equation 1.12 is only strictly valid for thin plates where the stress in the thickness direction is zero, a condition called plane stress. For thick plates, where thickness direction stresses develop as a consequence of non-uniform Poisson's ratio contraction near to the tip of the crack, the thickness direction strain is considered to be equal to zero. This state is called plane strain, and for this state, Equation 1.12 takes the form:

$$G_I = K_I^2 (1-\nu^2)/E \qquad (1.13)$$

where ν is Poisson's ratio.

For practical materials in which limited plastic distortion occurs close to the crack tip, plane strain conditions will hold if the length of the plastically deformed region is small compared with the thickness of the specimen. Under these conditions and if the length of the plastic zone is small compared to length of crack, it is still possible to apply elasticity theory to calculate the stress field immediately outside the zone of plastically deformed material, since this field will be relatively unaffected by a small zone of plasticity. The stresses which exist within the plastically deformed zone remain unknown however, unless certain assumptions are made

about the properties of the material. For the case of an elastic-perfectly plastic material, the stresses within the plastic zone can be regarded as constant, and equal to the flow stress of the material. On the basis of this assumed material behaviour, a characteristic parameter, with the dimensions of length can be derived, which defines the boundary between elastic and plastic response.

Various expressions have been derived for such a characteristic parameter. For example, Irwin, (1960), argued that the elastic stress distribution around a crack with a plastic-zone at its tip would be identical to that around a crack in a perfectly elastic material, provided the length of the elastic crack was $c^* = c + R$, where c was the actual length of the crack, and R was obtained from Equation 1.11 by substituting σ_Y, (the flow stress), for σ_{ij}, and R for r. This gave:-

$$R = (1/2\pi).(K_I^2/\sigma_Y^2) \qquad (1.14)$$

When $K_I = K_{IC}$, $R = R_C$, and this defined an effective plastic zone size, and could be used as a simple fracture criterion.

When a crack exists in a material with a plastic zone at its tip, the crack faces will be separated from each other due to the plasticity. This displacement has been termed the crack-opening displacement, or COD. Wells, (1963), suggested that a critical COD might be used as an alternative fracture criterion.

Wells showed that:

$$G_{IC} = \sigma_Y \alpha_c \quad \text{where } \alpha_c = \text{critical value the COD} \tag{1.15}$$

a result which can be obtained from simple energy considerations.

It is not necessary for the shape or size of the plastic zone as predicted from such models of plasticity to correspond to the real situation. The parameters which are derived from such models are useful because they enable plasticity to be related to directly measurable quantities, such as the applied stresses acting at the boundaries of the specimen.

The three macroscopic parameters, G_{IC} K_{IC} and γ, the fracture energy, can all be used as measurements of how difficult it is to propagate a crack through a material. This is, they all serve as measures of the toughness of a solid. They are useful only because it has been shown experimentally that they are material properties. K_{IC} is now known as the Fracture Toughness of a solid, and enjoys a wider use in engineering than the other two toughness parameters. This is largely because it provides a single material dependent parameter from which the load carrying capacity of a component containing cracks of a known or assumed maximum size can be calculated. On the other hand, it is the fracture energy which is most directly related to the dissipative processes occurring at the tip of a crack, and therefore from the physical point of view this is probably the more interesting parameter. As yet, particularly for the amorphous

x35 000

Possible microstructure of an Epoxy Resin (acid etched).

Fig. 1.4

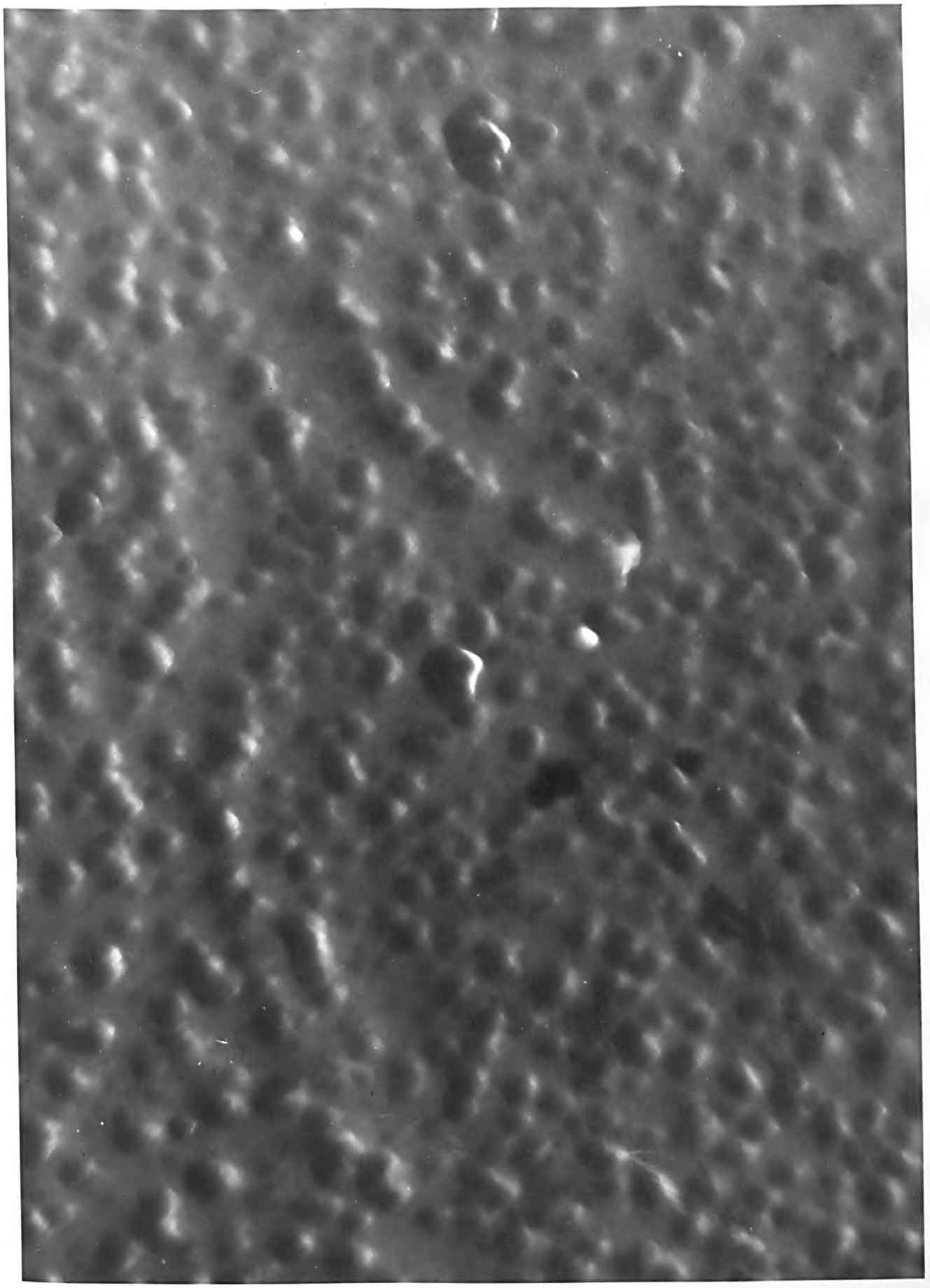

x 35 000

Possible microstructure of an Epoxy Resin (Sputter Etched)

Fig. 1.5

materials examined in this work, very little is known about the mechanisms of plastic flow at crack tips, or the factors which limit the extent of plastic deformation. One factor which might be of direct relevance in limiting plastic deformation in a material is its microstructure. Unfortunately, for the amorphous materials, as their name suggests, there is very little information currently available on their microstructures, and as a consequence we are a long way from understanding the physics of the fracture process in these materials. (Some provisional experiments with one of the materials examined in this work, (the Araldite epoxy resin system CT200 + HT901), successfully revealed a consistent structure, which may have been a genuine microstructure of this nominally amorphous solid. Specimens were sputter etched by argon-ion bombardment, and others were chemically etched at 343K with N/66 chromic acid. With both methods a surface structure of similar scale was produced, as shown in the electron micrographs, (Figs 1.4 and 1.5.)

1.6 Moving Cracks

In most practical situations it is the fracture toughness of the material which commands greatest interest, and the behaviour of the system after the critical condition is attained is of secondary importance. For this reason rather less attention has been paid to the kinetic aspects of fracture and the dynamics of crack propagation.

The behaviour of the moving crack nonetheless poses many interesting problems, both at a theoretical and an experimental level. A great deal of information about the course and progress of the fracture can be obtained from an examination of the fresh surfaces which are formed by the fracture, and in the next section we discuss some general findings of such examinations. In this section we deal with some of the problems associated with moving cracks.

For an edge crack of length c in a thin sheet which is loaded in uniaxial tension,

$$G_I = \frac{\pi\sigma^2 c}{E} \qquad (1.16)$$

where σ is the applied tensile stress.

When σ reaches σ_c so that $G_I = G_{IC}$ crack extension will occur. As the crack grows, G_I increases and surplus energy is available during each further increment of crack growth at constant applied stress in excess of that required for the formation of new fracture surfaces. The longer the crack gets the greater this surplus energy becomes, and it is converted into kinetic energy as the crack accelerates. There is an obvious upper limit to the speed of the crack, however, set by the rate at which information of the crack tip position can be transmitted through the specimen, since this sets the rate at which additional energy can be made available for further increase in kinetic energy. Clearly, the crack cannot travel faster than the speed at which this information is conveyed to the unbroken part of the sheet; i.e. the

speed of sound in the material.

This general upper limit to the crack speed is too high however, since as the crack gets longer, a larger amount of material must be displaced in the lateral movement of the crack walls. A steadily increasing mass of material has therefore to be displaced for each additional increment of crack extension, and the kinetic energy of the crack will increase with crack length as well as with crack speed. Mott, (1948), argued that a stage would eventually be reached when the energy release rate would only just be sufficient to provide the additional kinetic energy associated with increase in crack length, and would not be sufficient to raise the speed of the crack any further. As a consequence the crack speed would, he argued, be limited to a certain maximum value. Using a dimensional argument to derive an expression for the kinetic energy associated with the crack, Mott obtained the result that:

$$v_{max} = (2\pi/k)^{\frac{1}{2}} v_1 \qquad (1.17)$$

where v_{max} is the limiting speed of the crack; v_1 is the longitudinal wave velocity in the material; and k is a numerical constant, the value of which depends to what extent the material surrounding the crack contributes to its kinetic energy.

Mott did not evaluate k. Hiorns and Venables (1961) assigned a value of unity to k, although they did not justify so doing. Perhaps the most widely accepted estimate

of k, however, is that due to Roberts and Wells, (1954). These authors obtained a value of k equal to 44, which gives a theoretical terminal speed of $0.38v_l$, for a material with a Poisson's ratio of 0.25. Roberts and Wells argued that the value of k would depend upon the volume of material to which displacements due to the motion of the crack were transmitted. This, they argued, would depend upon the distance travelled by the elastic waves in the time taken for the crack to extend throughout the specimen. They assumed that after a time t, the crack half-length was $v_{max}t$, and the volume of material of interest was defined by the region of radius $v_l t$ centred at the origin of the crack. (Figure 1.6)

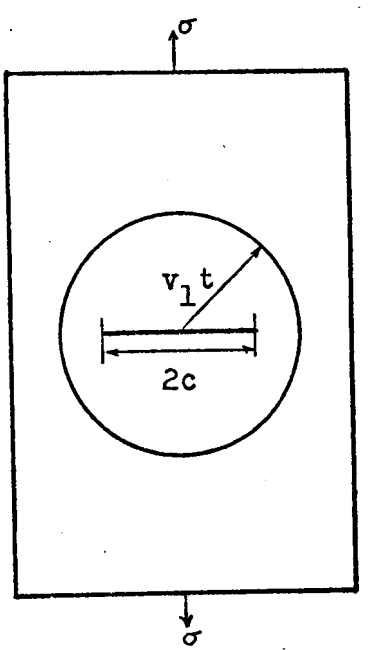

Figure 1.6

Showing the region over which the Westergaard displacement field was integrated.

Combining this stress wave restriction with Mott's expression for v_{max}, Equation 1.17, then,

$$r/c = (k/2\pi)^{\frac{1}{2}} \qquad (1.18)$$

where $r = v_l t$.

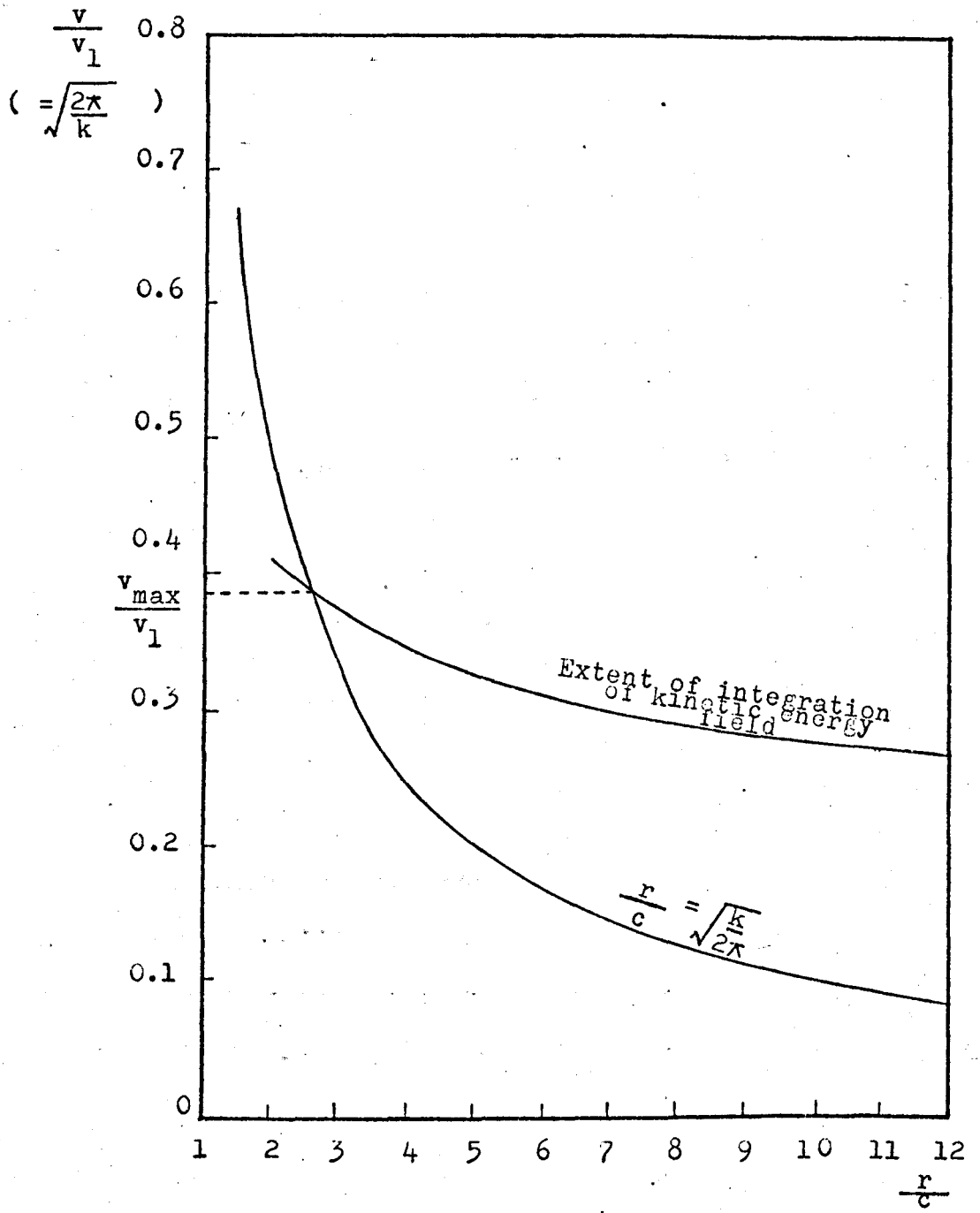

Showing Roberts and Wells' calculation of v_{max} (After Roberts and Wells 1954).

Fig. 1.7

By integrating Westergaard's, (1939), solution for the displacement field around a crack using numerical methods, they were able to evaluate $(2\pi/k)^{\frac{1}{2}}$ as a function of r/c, and by plotting this on the same graph as Equation 1.18, they found that unique value of k which satisfied both the general displacement field integral, and the stress wave restriction. Their results are reproduced here as Figure 1.7.

Roberts and Wells concluded that the "influence of stress waves appears to be to limit the volume of material to which kinetic energy must be supplied, rather than to modify the stress distribution from the static values about the crack", (Roberts and Wells 1954, page 821.) This conclusion has recently been the subject of criticism by various theoretical workers, (see for example, Erdogan, 1967), who take cognisance of the dynamic changes in the crack tip stress field and produce the result that the terminal speed of the crack is higher than that predicted by Roberts and Wells. The value obtained for v_{max} by these workers equal to $\sim 0.9 v_2$, where v_2 is the transverse wave velocity in a material of Poisson's ratio of 0.25 ($0.9v_2 \simeq 0.6v_1$ for such a material). This value of the terminal speed is equal to v_R, the velocity of surface waves in the material, (Love 1944), and it is therefore argued that the crack can be regarded as the motion of a surface disturbance in a non-dissipative medium.

The underlying criticism of the Mott-Roberts and Wells's theory is that there is no justification for assuming

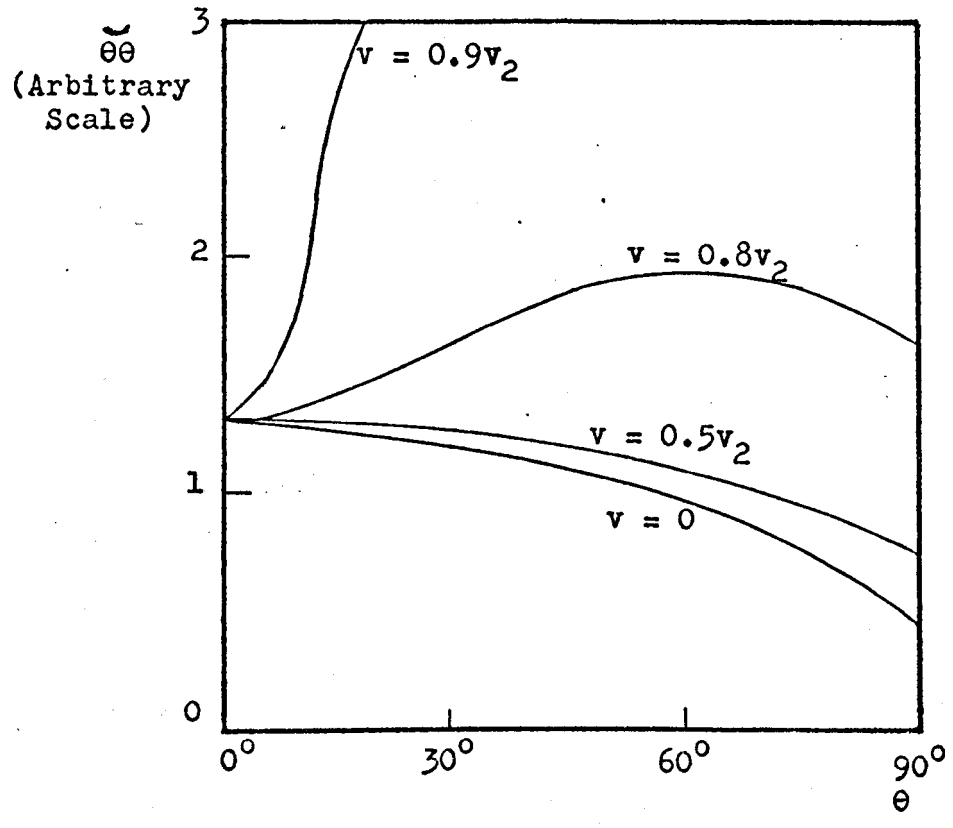

(a)

Showing dependence of the hoop stress $\tilde{\sigma}_{\theta\theta}$ on crack speed.

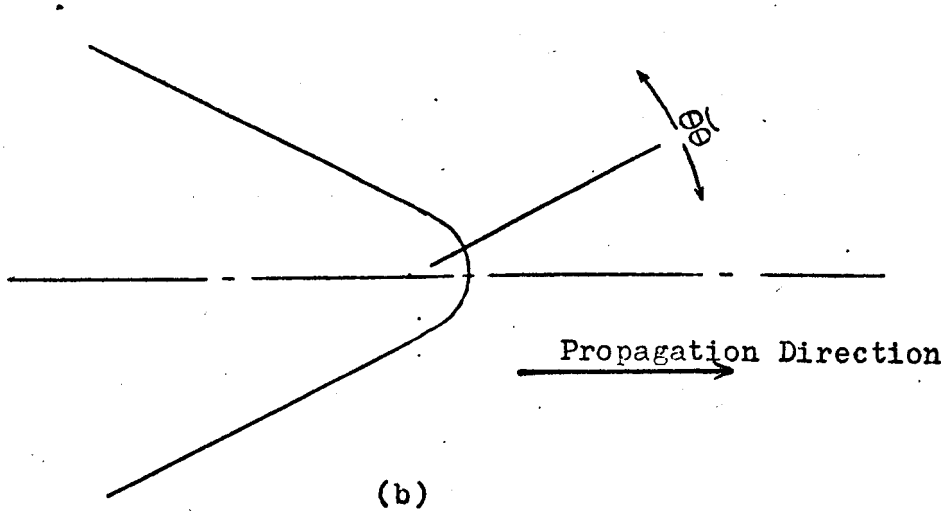

(b)

Illustrating the meaning of the term "hoop stress" at the crack-tip.

Fig. 1.8

that the stress and displacement fields close to the moving crack are the same as those around a static crack of the same length. It is argued that any misrepresentation of the stresses in the vicinity of the crack tip is likely to alter the value of the energy exchange which occurs in this region, and therefore the predicted value of the terminal speed of the crack will not be the correct one.

Although these theoretical modifications to the value of the terminal speed of the crack are inherently interesting, they seem to the author to be of little consequence when real materials are considered, since refinements to Roberts and Wells's analysis which take account of changes in the crack tip stress field around a moving crack serve only to shift the predicted terminal speeds further away from the experimentally measured values! It would seem to be more likely, as was the case with theoretical predictions of the ideal strength of a material, that at least one, possibly tacit, assumption on which these theories are based is in error.

The analysis which predicts a limiting crack speed of v_R assumes that the crack runs in a straight path for the whole of its journey across the specimen. Yoffé, (1951), and Craggs, (1963), have shown that in an elastic isotropic solid this is unlikely to be the case. They predict that at speeds of $\sim 0.8v_2$ the stress distribution around the crack tip is such as to provide higher stresses normal to two symmetrically inclined planes than on the crack plane itself. Yoffé produced the graph shown here as Figure 1.8

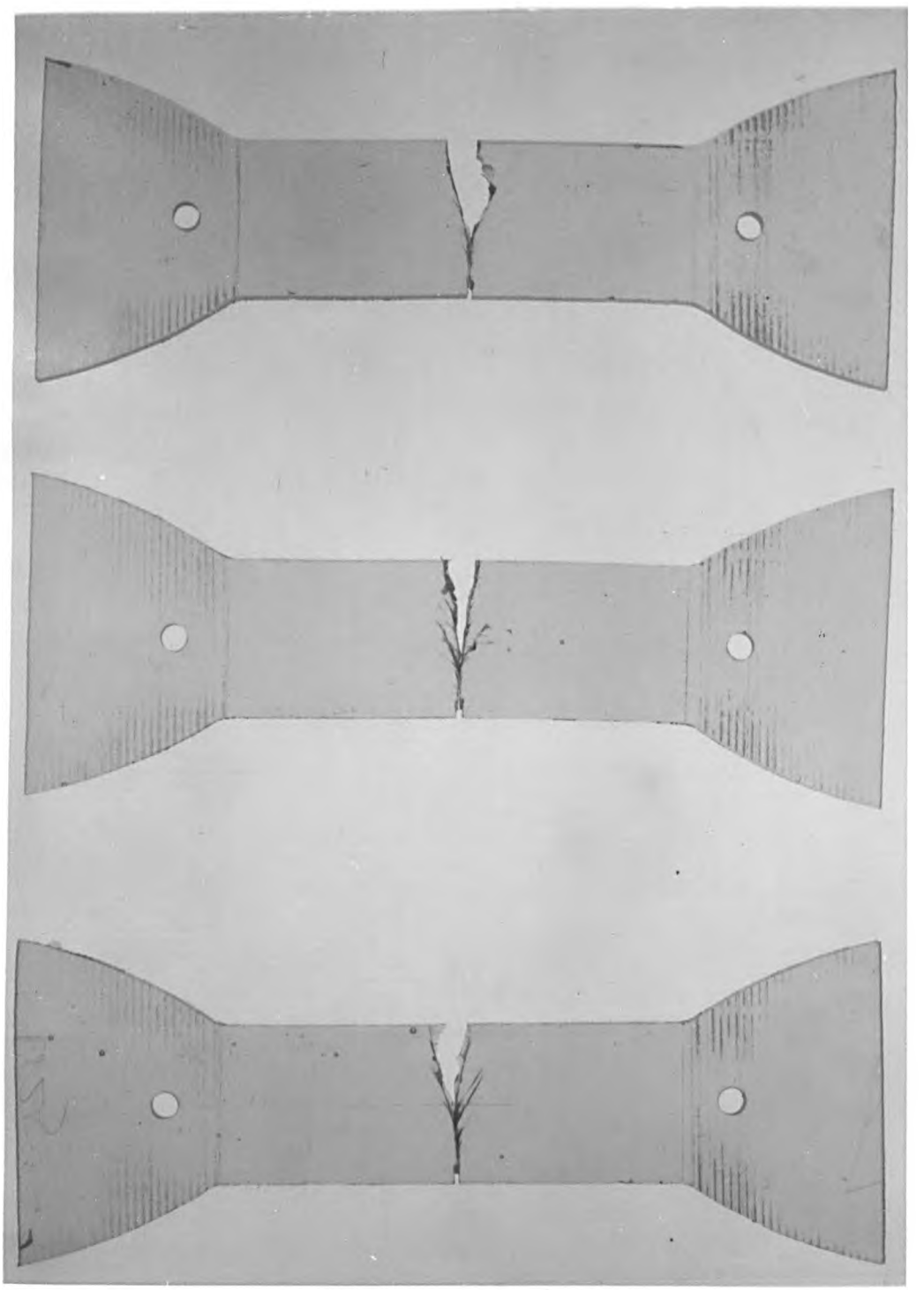

Crack-Branching in an Epoxy Resin.

Fig. 1.9

which shows the relation between the hoop stress $\widetilde{\theta\theta}$ very close to the crack tip and the polar coordinate θ at various fracture speeds. This graph shows that at low fracture speeds the maximum hoop stress occurs for θ equal to zero, (i.e. in the plane of the crack). At speeds of $0.8v_2$ the hoop stress has a local minimum at $\theta = 0$, and maxima now occur on either side of $\theta = 0$. At speeds of $0.6v_2$ the $\widetilde{\theta\theta}$ curve tends to become flat, and equal stresses will then exist over a wide arc about the leading edge of the crack.

This redistribution of stress has been interpreted in the following manner. It has been argued that once the crack speed is such as to produce equal stresses over a wide arc ahead of the crack tip, then the crack may curve away from its earlier plane of propagation, and this would lead to the formation of branches. In this situation it was argued that the crack could never attain a speed much greater than about $0.6v_2$, since any tendency for increase in speed above this value would be opposed by the redistribution of stresses around the crack tip and branching would ensue. The crack speed would therefore effectively be limited to the value at which branching occurs, i.e. $\sim 0.6v_2$.

Observations made on the fracture surfaces of many brittle solids broken under uniaxial tension show that branches may indeed be formed, (see Figure 1.9), and Yoffé's argument has often been proposed as the explanation of this event (see, for example, Field 1971). We shall see later however, that this explanation of crack branching

MATERIAL	$\frac{v_{max}}{v_1}$	REFERENCE
Glass	0.28	Schardin ('59)
pmma	~0.30	Schardin ('59)
Cellulose Acetate	0.27	Smith and Ferguson ('50)
Pitho Steel	0.24	Anthony and Congleton ('70)
Diamond	0.40	Field ('71)

TABLE 1.5

VALUES OF EXPERIMENTAL TERMINAL SPEED (v_{max})

AS A RATIO OF LONGITUDINAL SPEED (v_1)

is unlikely to be the correct one for most brittle materials.

Experimental measurements of crack speeds have been made, (e.g. by Schardin, 1959), on a selection of materials, and these have shown that cracks do in fact attain a terminal speed, but for nominally homogeneous isotropic solids such as glass, perspex, and epoxy resins, the measured values of the terminal speed are less than the value predicted theoretically by any of the theories to date. Some measured values are given in Table 1.5.

For anisotropic materials such as diamond, where the crack is constrained to a particular cleavage plane, the measured terminal speeds are closer to some of the theoretical values, (the lower ones), although it should be borne in mind that all the theoretical predictions of v_{max} were for isotropic solids.

The discrepancy between theoretical and experimental values of the terminal crack speeds in isotropic solids has not yet been satisfactorily explained; the general argument - that real materials are not ideally elastic, homogenous, isotropic solids, and it is therefore not surprising that their terminal speeds differ from that predicted for the ideal case - is singularly unenlightening.

Plastic distortion at the crack tip might be one cause of the discrepancy in a given solid however. Although Roberts and Wells allowed for limited plasticity in their energy balance equation, the imposed stress wave restriction on the volume of material to which kinetic energy was supplied assumed that the solid was purely elastic.

Saibel, (1948), has argued that the stress wave speed in the plastic zone is likely to be lower than that in the normal material, and if correct this would presumably alter the limits of integration in the Westergaard displacement field integral and thereby alter the numerical value of k. Bearing in mind the size of the plastic zone compared with the overall crack-length, however, such an effect is likely to be of second order only.

A more likely explanation lies in the observation that as the fracture spreads across a specimen of an amorphous solid, it can no longer be regarded as a single propagating crack. The fracture soon involves many cracks, as is discussed in the next section, and these would provide alternative opportunities for energy dissipation and thereby limit the kinetic energy, and hence the speed of the main crack. This point is discussed in more detail in the next chapter.

1.7 Fracture Surface Appearance and Crack Branching

The fracture surfaces which are formed by brittle fracture of a solid are often extremely complex; the surfaces display a variety of markings. The range and distribution of these fracture surface markings depends to a large extent upon the nature of the material, the stress system which induced fracture, and the external environmental conditions in which the fracture took place.

Fracture Surface of Perspex

Fig. 1.10

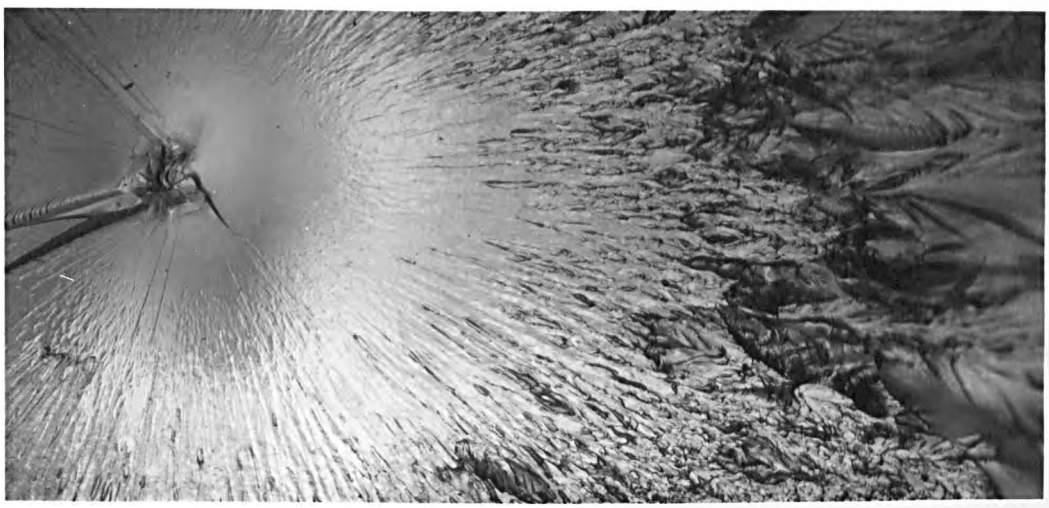

Fracture Surface of an Epoxy Resin

Fig. 1.11

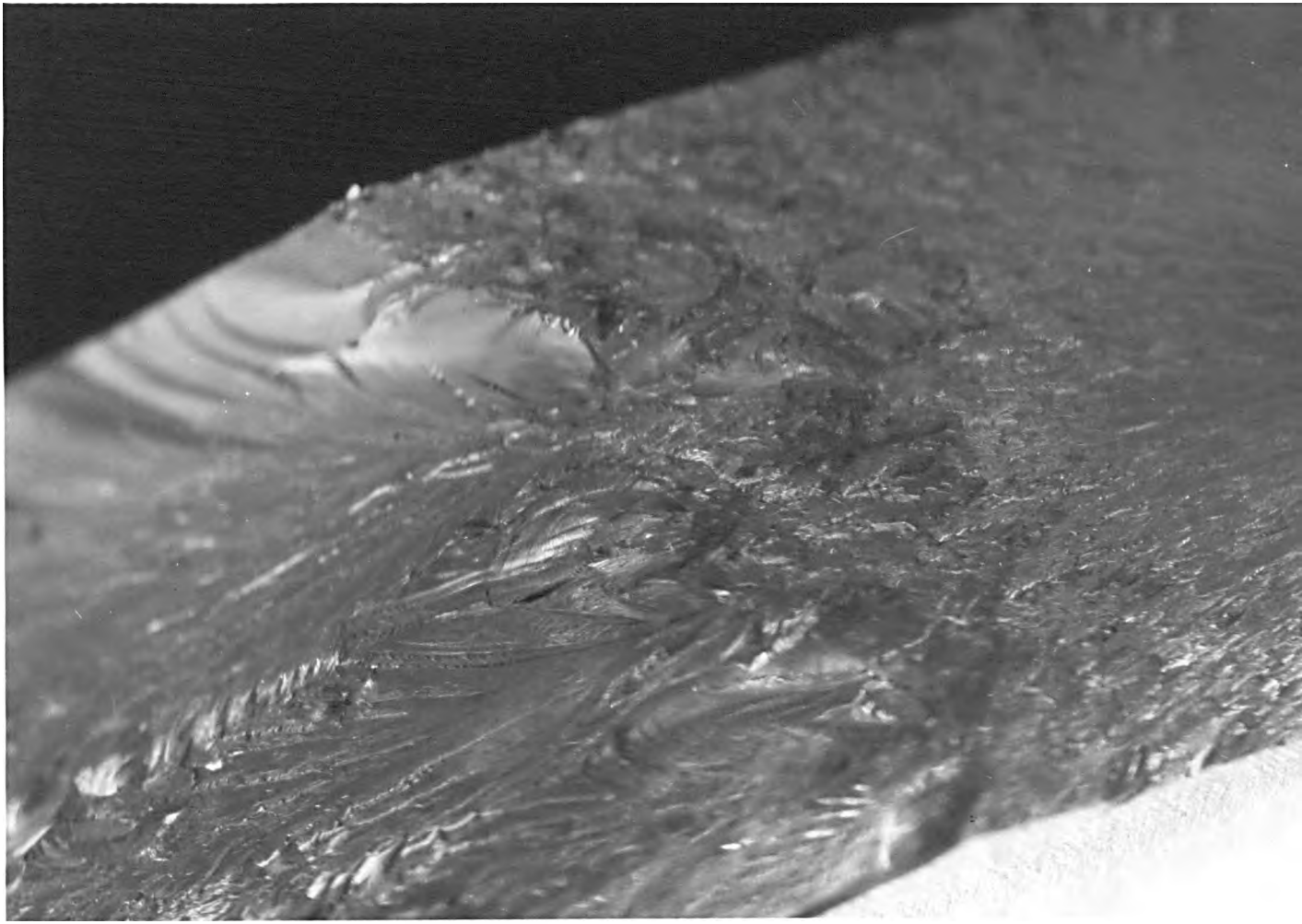

Fig. 12

Branching zone in an Epoxy Resin

When solids are broken under uniaxial tension, the fracture surfaces which are formed can generally be divided into at least three distinct zones, each zone being distinguished from the others in terms of the features which it displays. Figures 1.10 and 1.11 show, respectively, a general view of the fracture surface of Perspex, and a similar view of the fracture surface of an epoxy resin, (Araldite CT200 + HT901), and illustrate the division of the fracture surfaces into different zones.

The detailed structure of each zone can vary considerably from one material to another, as Figures 1.10 and 1.11 illustrate, but in all cases the first zone is relatively smooth compared with those which follow it, and the final zone is produced as a result of branching of the fracture front, (Figure 1.12). Furthermore, the sequence of zones which are produced on a fracture surface of a given material is reproducible from one specimen to another, and this observation enables certain generalisations to be made, if only at a qualitative level, about the fracture process in a given material. Much of the work to be described in this thesis is concerned with a detailed survey of the features which occur on the fracture surfaces of a selection of polymers, and as a consequence more detailed descriptions of particular features and a discussion of the processes by which they are produced will be postponed until later chapters. What is of interest here is that for a given sequence of zones on a fracture surface of any of the materials examined in this work, and for materials examined elsewhere, (e.g.

Johnson and Holloway, 1967, Congleton and Petch, 1970), it is generally true that each zone has a rougher appearance than its predecessor. This suggests that there may be a common factor in the fracture process in a wide range of materials. A closer examination reveals that the progressive roughening of the fracture surfaces would seem to arise from the formation and restricted propagation of many localised cracks close to the general fracture plane, and it is the occurrence of these subsidiary cracks which is the common feature in the fracture process in all the materials examined. Where the materials can differ is in the density and distribution of these subsidiary cracks, and in the mechanisms by which these cracks are formed.

We have already mentioned that the final fracture surface zone of each material is produced as a result of branching of the fracture front, and for certain materials it has been established empirically, (e.g. Johnson, 1963), that the onset of this final fracture surface zone, and hence fracture branching, can be characterised by the following simple relationship:

$$\sigma c_b^{\frac{1}{2}} = \text{constant} \qquad (1.19)$$

where σ is the applied tensile stress at fracture, and c_b is the distance from the origin of fracture to the onset of the final fracture surface zone, i.e. c_b is the distance travelled by the fracture before branching occurred. The value of the constant in this expression varies from one

material to another, and part of the work described in this thesis was to ascertain whether this simple empirical expression held for a selection of polymers. This was found to be the case, and it was also found that a similar expression held for the onset of many of the other fracture surface zones in these materials, although clearly, the value of the constant differed for each zone.

Although this simple expression, (Equation 1.19), has been known to hold for some time, at least for the case of glass, (e.g. Shand, 1954), there is as yet no complete and entirely convincing explanation as to why it holds, either for the branching zone or the other fracture surface zones. The form of equation 1.19 is similar to that of the stress intensity factor of an edge crack in a sheet loaded in simple tension (Paris et al 1964), viz

$$K_I = A . \sigma . c^{\frac{1}{2}} \qquad (1.20)$$

where A is a factor which depends on the specimen geometry with respect to the size of the crack and on the speed of the crack. This suggests that the empirical relationship 1.19 can be couched in terms of fracture mechanics parameters and branching would then occur at a critical stress intensity factor, K_{IB}, which is represented by the empirical relationship 1.19. Because of the complex situation which exists when a crack branches, the absolute magnitude of A, in Equation 1.20, is not easy to calculate however, but in Chapter Three we suggest that at least the

effects of the proximity of a free edge in a sheet, and reflected stress waves from these edges might be of secondary importance only in their bearing on the magnitude of K_{IB}.

Recouching the relationship, 1.19, in this form brings us no closer to understanding why branching occurs of course, and it is not yet clear even how it occurs. The experimental fact that branching occurs in a wide range, if not all, brittle materials suggests that there may be a general explanation for this event which is to a large extent material independent. We have already met one possible candidate for this general explanation in Yoffé's analysis of the stress distribution around a rapidly moving crack, but as we shall see in Chapter Three , it is unlikely that this provides a feasible explanation for the materials examined in this work, or for other materials which have been investigated elsewhere (e.g. Johnson, 1963). Furthermore, Yoffé's analysis predicts that the fracture surface would be smooth up to the onset of branching and this is manifestly not the case (see Figures 1.10 and 1.11).

1.8 Summary

In this chapter, several basic ideas have been introduced which will be used in the rest of the thesis, and it is worth summarising these here in list form.

(1) The discrepancy between the low fracture stress of brittle materials and the high cohesive forces between

their atoms can be explained by the presence of notches or cracks which locally magnify the applied stress. A tough solid is less sensitive to flaws, since the plastic flow at the tip of a crack in a tough solid blunts the tip, and it is more difficult for a blunt crack to propagate and hence cause failure.

(2) Once a crack begins to move under constant load it soon attains a limiting speed, and eventually branches. The measured values of the limiting speed are less than the theoretical predictions for many isotropic, homogeneous solids.

(3) The fracture surfaces of tensile specimens of many brittle materials can be divided into at least three distinct zones, which for a given material always occur in a regular sequence. The first zone is near the origin of fracture, and is smooth; the second zone(s) have a rougher appearance and contain many local subsidiary cracks; the third zone corresponds to where branching has occurred.

CHAPTER 2

THE ENERGETICS OF FRACTURE

2.1 Introduction

The intention in this chapter is to examine the energetics of moving cracks. No attempt is made to give an exhaustive or critical survey of all the previous work in this field, although some of the results which have been previously obtained are extended using simple physical arguments. We begin with Mott's, (1948), energy expression from which he derived a value of v_{max}, the terminal speed of a crack. This is then extended to give the speed of the crack as a function of its length, and a comparison is made with a previous result obtained by Berry, (1960). Possible modifications to the energy release rate arising from the finite speed of the crack are then explored, and a simple expression is derived for the ratio between G_I for a moving crack, and G_I for a static crack of the same length. Finally, it is noted that the fracture energy may be speed dependent, and that the production of numerous subsurface cracks during the fracture process is probably the main reason why the experimental terminal speed is less than the theoretical prediction.

2.2 Mott's Energy Expression

We have seen in Chapter 1 (Section 1.6) that Mott extended Griffith's energy balance equation so that it

applied to moving cracks. He argued that once the crack had attained a significant speed then the kinetic energy associated with the lateral displacement of the crack walls became an important factor in absorbing part of the energy given to the crack by the system.

Mott wrote down an expression for the total energy of the crack, (as opposed to the total energy of the cracked sheet), in the following form:

$$-\frac{\pi\sigma^2c^2}{E} + \frac{k\rho v^2c^2\sigma^2}{\Sigma E^2} + 4Tc = \text{constant} \qquad (2.1)$$

The first term in this expression is the energy available when a crack has grown from zero to a length of 2c. In the case of constant strain, (fixed grip), conditions this energy is supplied by release of part of the strain energy stored in the specimen, and in the case of constant stress, (dead loading), conditions the energy is supplied by part of the work done during the movement of the load that results from the introduction of the crack.

The second term represents the kinetic energy of a crack of length 2c travelling with a speed v, and was derived by Mott on dimensional grounds. In this expression k is a numerical constant, (see Chap. 1, section 1.6).

The third term represents the surface energy associated with the crack surfaces: the 4 arises because the analysis was for a crack extending at each end.

It was assumed that the applied stress, σ , and the modulus, E, remained constant for all crack lengths,

which is only formally valid if the length of the crack approaches zero. In practice however, if the width of the specimen is always very much greater than the length of the crack then the applied stress and the modulus will be unchanged as the crack extends.

Mott assumed, at least implicitly, that the constant on the right hand of equation 2.1 was finite, for in order to eliminate it he differentiated 2.1 with respect to c. By setting dv/dc = 0 he obtained an expression for the speed of the crack given by:

$$v = \left(\frac{2\pi E}{k\rho}\right)^{\frac{1}{2}}\left(1-\frac{4T}{\pi\sigma^2 c}\right)^{\frac{1}{2}} \qquad (2.2)$$

The derivation of this expression has been criticised on the grounds that it assumes the speed of the crack is constant, (e.g. Erdogan, 1967). This criticism is probably unjustified however, since it was Mott's primary aim to estimate the terminal speed of the crack, and Eq. 2.2 as derived serves for this purpose.

Since Mott argued that the terms on the left hand side of Equation 2.1, when summed, gave the total energy of the crack when it had reached a length of 2c, then the constant on the right hand side must, in fact, be equal to zero. This constant is only finite if the summed terms exceed the total energy of the crack, as would be the case if 2c were the new length of an initially smaller pre-existing crack. In this case the energy given to the crack by the system, and the energy associated with the surfaces produced by extension of the crack, would both be smaller than the corresponding values of

these quantities in Eq. 2.1

Setting the constant on the right hand side of Eq. 2.1 equal to zero, an expression for the speed of the crack as a function of its length can then be obtained directly. This expression is exactly the same as Eq. 2.2.

If the crack is now allowed to extend to a length 2c from an initial pre-existing length of $2c_o$, then by considering the total energy of the crack it is possible to obtain an expression for the crack speed as a function of its length, which predicts a speed at a given crack length slightly less than the value given by Eq. 2.2. This of course would be expected, since the crack to which Mott's total energy equation referred had a finite kinetic energy associated with it for any length >0, whereas in this second case, the crack is at rest at some finite length.

The energy given to the crack as it extends from $2c_o$ to 2c is

$$\frac{\pi\sigma^2}{E}(c^2 - c_o^2) \qquad (2.3)$$

and the surface energy associated with the growth of the crack will be,

$$4T(c - c_o) \qquad (2.4)$$

The kinetic energy, which depends on the overall length of the crack would be unchanged however.

The revised energy balance for the crack is thus:

$$\frac{-\pi\sigma^2}{E}(c^2 - c_o^2) + \frac{k\rho v^2 c^2 \sigma^2}{2E^2} + 4T(c - c_o) = 0 \qquad (2.5)$$

or, $$\frac{-\pi\sigma^2 c^2}{E} + \frac{k\rho v^2 c^2 \sigma^2}{2E^2} + 4Tc = \left(4Tc_o - \frac{\pi\sigma^2 co^2}{E}\right) = \text{constant} \qquad (2.6)$$

but in this case of course, the left-hand side is not the total energy of the crack.

Rearrangement of Eq. (2.6) produces the following expression for the speed of the crack as a function of its length:

$$v = \left(\frac{2\pi E}{k\rho}\right)^{\frac{1}{2}}\left(1 - \left(\frac{co}{c}\right)^2 - \frac{4TE}{\pi\sigma^2 c}\left(1 - \frac{co}{c}\right)\right)^{\frac{1}{2}} \qquad (2.7)$$

which reduces to Eq. 2.2 if $c_o = 0$.

No fracture condition has yet been introduced. If Griffith's criterion for crack stability is now incorporated, it is possible to express Eq. 2.7 in a more useful form. According to this criterion, the pre-existing crack of length $2c_o$ will remain stable only if the applied stress has a value σ_c defined by the Griffith Equation, (Eq. 1.6),

viz: $$2TE = \pi \sigma_c^2 c_o. \qquad (2.8)$$

If the right-hand side of this equation is substituted into Eq. 2.7 for 2TE, we obtain:

$$v = \left(\frac{2\pi E}{k\rho}\right)^{\frac{1}{2}}\left(1 - \frac{co}{c}\right)^{\frac{1}{2}}\left(1 + \frac{co}{c} - \frac{2\sigma_c^2 co}{\sigma^2 c}\right)^{\frac{1}{2}} \qquad (2.9)$$

The applied stress acting on the sheet, σ, must exceed σ_c if there is to be any crack growth beyond $2c_o$; which means that

$$v > \left(\frac{2\pi E}{k\rho}\right)^{\frac{1}{2}} \left(1 - \frac{c_o}{c}\right) \qquad (2.10)$$

It is unlikely that σ will exceed σ_c by a large amount, especially since the (unstable) equilibrium defined by the Griffith Equation will be destroyed if one end of the crack moves slightly before the other, and the number of fracture surfaces produced is momentarily only two. Therefore, to a good approximation we can say that,

$$v \simeq \left(\frac{2\pi E}{k\rho}\right)^{\frac{1}{2}} \left(1 - \frac{c_o}{c}\right) \qquad (2.11)$$

This expression for v can be derived by at least two other methods. The first is to diffentiate Eq. 2.6 with respect to time, (without assuming $dv/dt = 0$), and solve the resulting diffential equation. The second, which is much less direct, is to consider the total energy of the cracked sheet and any work done on the sheet, and thereby obtain an expression for the kinetic energy of the crack. By equating this expression for the kinetic energy with Mott's dimensional expression, and then incorporating a fracture criterion into the result, Eq. 2.11 can be obtained. The main danger with this approach is that it is relatively easy to omit an energy term from the argument. Berry (1960), has used this indirect approach to derive an expression for

speed against crack length, but he considered the two extreme cases when $\sigma = \sigma_c$ and $\sigma = \infty$ when presenting his final result. This refinement would appear to be unnecessary, however, unless we were concerned with fracture from a pre-existing notch rather than from a pre-existing crack.

In general, energy arguments can be easily confused. For this reason we feel that where possible the most direct approach is probably the best. In the particular case of the energetics of moving cracks it would seem an unnecessary complication to include the boundary conditions of the sheet and surface energy terms, which are not a direct consequence of crack extension, into the analysis, especially since all these additional terms eventually cancel in the final equation. By considering the energy balance for the crack the same result can be arrived at much more directly, and consequently, with less chance of error.

2.3 Possible Modifications to the Basic Energy Equation

Equation 2.6 was derived for a perfectly brittle solid. An obvious development is to include a plastic work term in the energy required to create new fracture surfaces. This can easily be achieved by replacing T, the surface energy, by γ, the fracture energy. This produces an energy equation for the crack of:

$$-\frac{\pi\sigma^2c^2}{E} + \frac{k\rho v^2c^2\sigma^2}{2E^2} + 4\gamma c = \left[4\gamma co - \frac{\pi\sigma^2co^2}{E}\right] = \text{const.} \quad (2.12)$$

This refinement does not alter the general form of the speed equation, (Eq. 2.11), although it could lead to a change in the magnitude of k, Mott's constant of proportionaltiy, as was suggested in Chapter 1.

The expression which has so far been used to represent the energy given to the crack was derived, initially by Griffith, by integrating the strain field over the whole of the cracked sheet. When the crack is moving at high speeds however, these limits to the integration would be too generous, since at this stage only that portion of the volume of sheet close to the crack will be aware of its real position. The material outside this volume will, depending on its distance from the crack, "see" a range of effective crack lengths which are shorter than the real crack length at any instant, and as a consequence only supply energy to "cracks" of these sizes. This would lead to an overall reduction in the energy supplied to the crack.

There have been several theoretical attempts to estimate the energy release rate under dynamic conditions. These have involved finding the elastic stress field when the crack tip is moving, and then calculating the amount of energy which leaves the material by way of the crack tip by using virtual work arguments. We propose a much simpler argument below, which gives an order of magnitude estimate for the energy release rate when the crack is moving at a constant speed v, and which illustrates the main physical principles involved.

In his book, The Mechanical Properties of Matter, Cottrell, (1963), gives a simple physical argument for estimating the strain energy released by the formation of a crack in a specimen held at constant strain. He argues that close to the crack surfaces the stress would be relaxed to zero, whereas at large distances from the crack the stress would be unchanged, and therefore, approximately, a region of radius c around the crack would be relieved of its strain energy. This is illustrated in Fig. 2.1 for an edge crack, of length c.

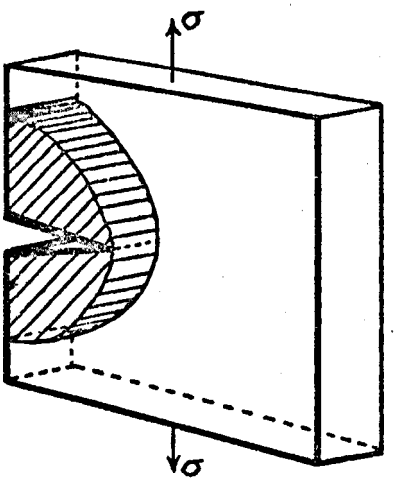

Fig. 2.1

Perhaps surprisingly, this simple argument gives a value for the strain energy released which is just half the value obtained by integrating the whole strain field.

It seemed feasible that by extending this simple physical argument an approximate value could be obtained for the strain energy released during incremental growth of a moving crack, and hence for the strain-energy release rate under dynamic conditions.

Consider first a quasi static extension of a crack from length c to a new length (c + dc). The energy released by this extension of the crack is equal to the product of the strain energy per unit volume, (calculated by Cottrell to be $\sigma^2/2E$), and the new volume which is relieved of its strain energy by the crack extension. Following Cottrell's reasoning, this new volume will be a semi-annulus centred at the edge crack's origin, Fig. 2.2.

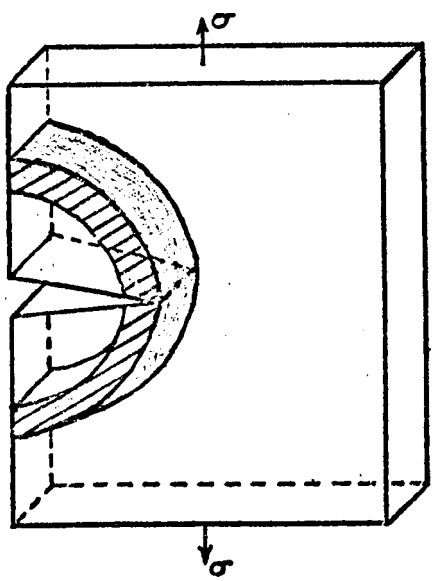

Fig. 2.2

The magnitude of this semi-annular volume is approximately π c dc w, where w is the specimen thickness. Thus, the strain energy released during this quasi-static increment of crack extension is

$$dE = \frac{\pi \sigma^2 c \, w \, dc}{2E} \qquad (2.13)$$

or, per unit thickness, the strain energy released is,

$$dE = \frac{\pi \sigma^2 c \, dc}{2E} \qquad (2.14)$$

$$\text{Thus, } \frac{dE}{dc} = G_s = \frac{\pi \sigma^2 c}{2E} \qquad (2.15)$$

where G_s denotes the strain energy release rate under quasi-static conditions of crack extension.

Now let the crack extend from c to (c + dc) at a finite speed v. In this case, the volume of material relieved of strain energy is determined by the distance travelled by the stress wave conveying the information of the instantaneous crack tip position to the unbroken sheet. The actual volume will depend upon the speed of the crack, v, and the longitudinal speed of sound in the material, v_1. In reality this stress wave travels in all directions away from the crack-tip, but by direct analogy with the preceding argument for quasi-static growth of the crack we shall assume that the stress wave travels away from the crack plane along a portion of an annulus centred at the crack origin. The volume of this portion is then a first approximation to the actual volume relieved of strain energy during the incremental growth dc of the crack. Figure 2.3 illustrates this volume for the first incremental extension of the crack, dc.

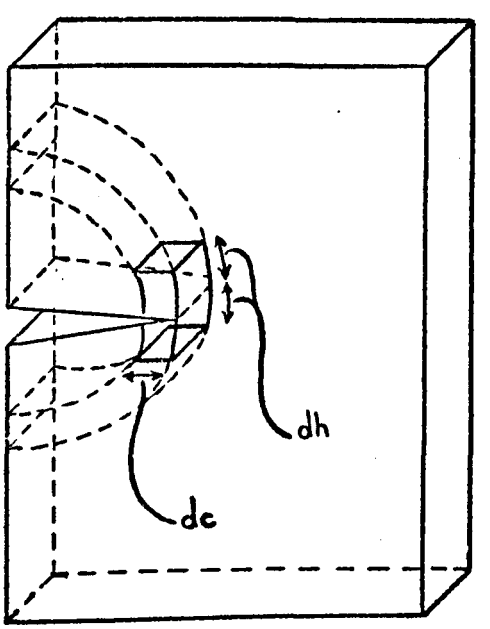

Fig. 2.3

If dh is the average arc-length of this volume on either side of the crack plane, then,

$$dh = (v_1/v)\, dc \qquad (2.16)$$

and the volume of material relieved of its strain energy is,

$$2\, dh.\, dc.\, w \qquad (2.17)$$

where w is the thickness of the sheet.
Thus, the strain energy relieved per unit thickness is,

$$dE = \frac{\sigma^2 v_1}{E v}.\, dc^2 \qquad (2.18)$$

i.e.

$$\frac{dE}{dc} = \frac{\sigma^2 v_1}{E v}\, dc \qquad (2.19)$$

If the crack continues to grow at the same speed for a further distance dc, then the volume of material relieved of its strain energy <u>during</u> this second increment of crack growth is just twice the value given by Equation 2.17. This is because during the second increment, not only does the original stress wave relieve new material of strain energy, but also a second stress wave leaves the crack-tip and this relieves an equal volume of its strain energy. Fig. 2.4 illustrates diagramatically the total volume relieved of its strain energy during this second increment of crack extension, where as before, a direct analogy has been made with Cottrell's simple argument.

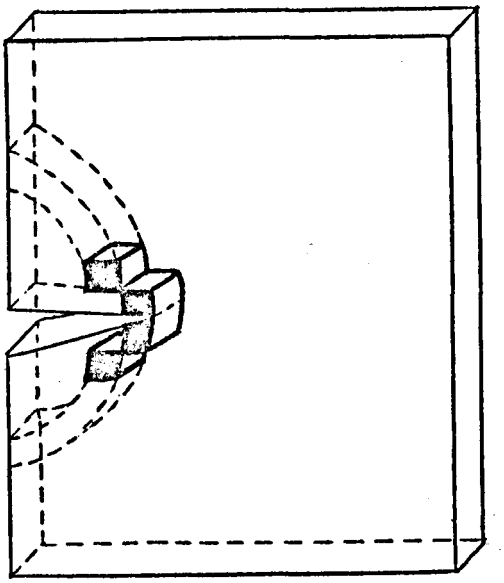

Fig. 2.4

In general, the change in stored strain energy during an increment dc of crack growth, when the crack is travelling at a speed v, is,

$$dE = \frac{\sigma^2}{E} m\,(^{v}1/v)dc^2 \qquad (2.20)$$

where mdc is the distance from the crack tip along the crack plane to the material which is totally relieved of its strain energy, Fig. 2.5.

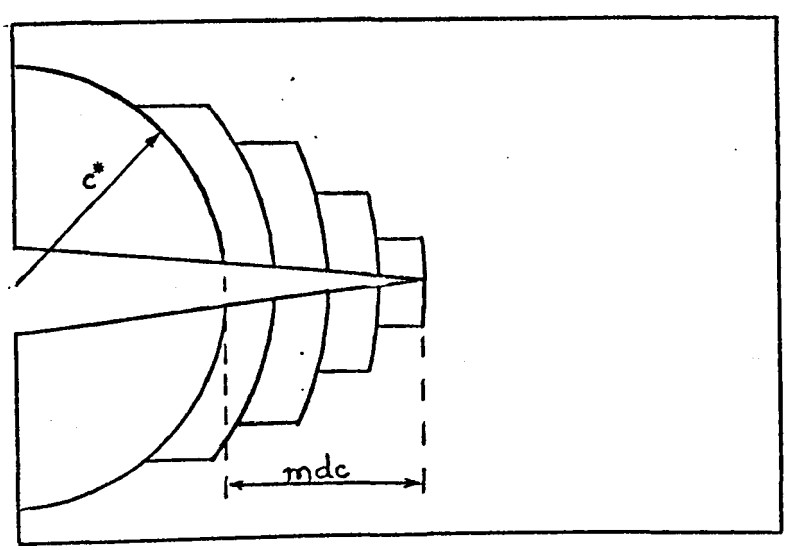

Fig. 2.5

If the radius of the first full semi-circular annulus encountered from the crack tip direction is c^*, and the

total length of the crack is c, then,

$$c - c^* = mdc$$

and
$$\pi c^* = 2\, m(v_1/v)\, dc \qquad (2.21)$$

from which
$$m = \frac{c}{dc(1 + 2v_1/\pi v)} \qquad (2.22)$$

Thus, from Equations 2.20 and 2.22 , the change in strain energy during a dc increment of crack extension is:

$$dE = \frac{\pi\sigma^2 cdc}{E}\,(v_1/(\pi v + 2v_1)) \qquad (2.23)$$

or
$$\frac{dE}{dc} = G_D = \frac{\pi\sigma^2 c}{E}\,(v_1/(\pi v + 2v_1)) \qquad (2.24)$$

where G_D denotes the energy release rate under these dynamic conditions.

Comparing Equations 2.15 and 2.24, the ratio of G_D to G_S is given by:

$$\frac{G_D}{G_S} = \frac{1}{(1 + \pi v/2v_1)} \simeq \frac{1}{(1 + \frac{v}{v_1})} \qquad (2.25)$$

which suggests that apart from speeds approaching the terminal value, there is very little difference between the dynamic and static value of energy release rate. At measured terminal speeds, which are typically $0.3v_1$, the difference is of the order of 30%.

At least for speeds up to the experimentally measured terminal values, this result, based on the

preceding rather naive analysis, compares favourably with other more refined calculations. For example, Eshelby (1969), has considered the case of a crack moving arbitrarily in Mode III, and has shown that G_D, (in our terminology), is of the form:

$$G_D = \frac{\pi\mu}{4} ((1 - v/v_2)/(1 + v/v_2))^{\frac{1}{2}} B^2(x) \qquad (2.26)$$

where $c_o + x$ is the current length of a pre-existing crack of length c_o; v_2 is the shear wave speed; and $B(x)$ is a function which can be expressed in terms of complete elliptical integrals of the first and second kinds. The ratio of G_D/G_S for a crack of length $c_o + x$ is,

$$\frac{G_D}{G_S} = \frac{(1 - v/v_2)^{\frac{1}{2}}}{(1 + v/v_2)^{\frac{1}{2}}} \frac{B^2(x)}{B_S^2(x)} \qquad (2.27)$$

where $B^2(x)/B_S^2(x)$ increases from unity to $4/\pi$ as x increases from 0 to infinity, (Eshelby, 1969). Therefore, to a first approximation,

$$G_D/G_S = \frac{(1 - \frac{v}{v_2})^{\frac{1}{2}}}{(1 + \frac{v}{v_2})^{\frac{1}{2}}} \qquad (2.28)$$

Although this analysis was developed for Mode III, Eshelby argued that it should be applicable to Mode I if v_2 is replaced by v_R, the Rayleigh wave speed. Substituting for v_R in the preceding equation, the ratio of G_D/G_s is given by,

$$G_D/G_S = (1 - v/v_R)^{\frac{1}{2}} / (1 + v/v_R)^{\frac{1}{2}} \qquad (2.29)$$

Fig. 2.6

Ratio of G_D/G_S against normalised crack speed.

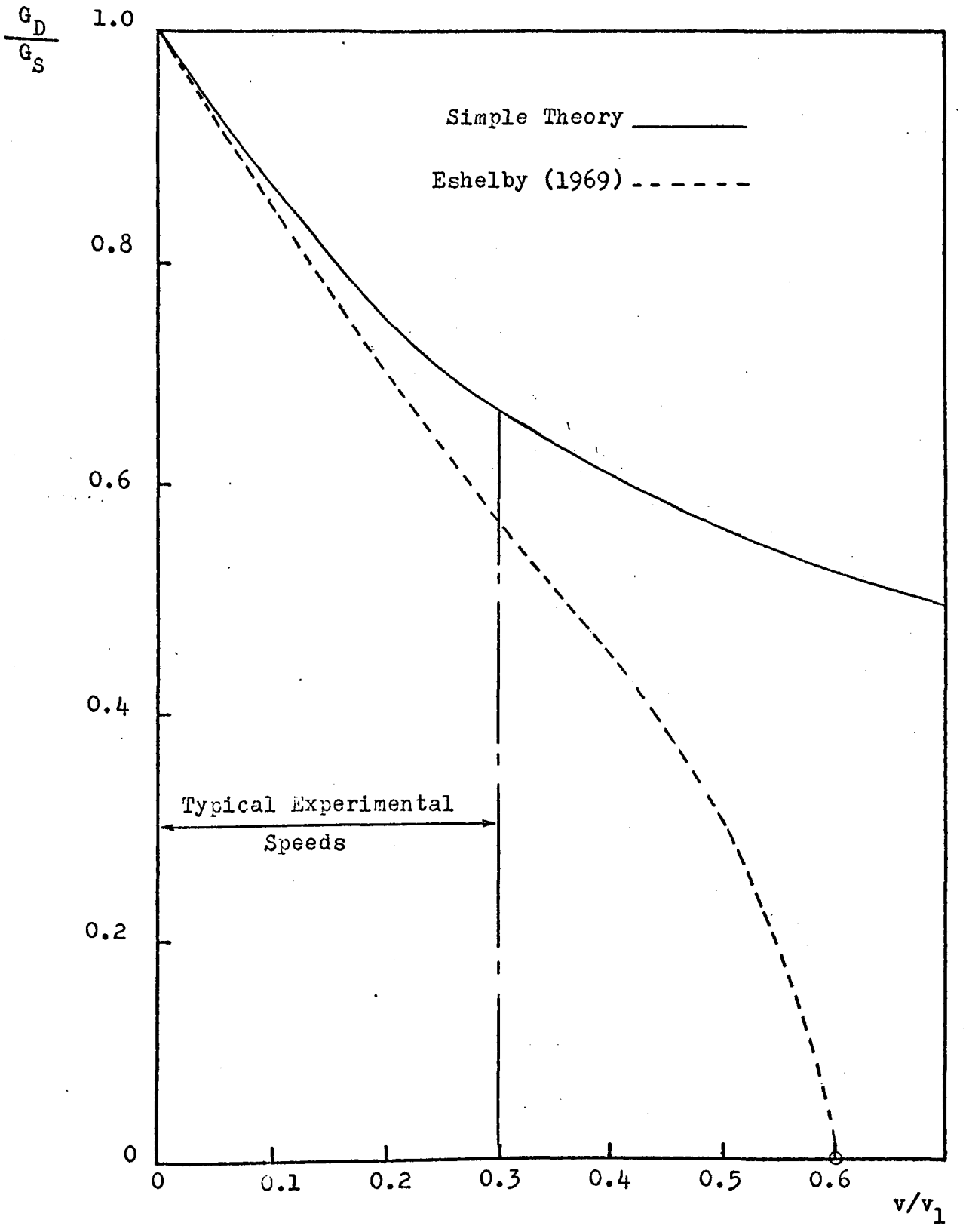

Figure 2.6 compares the ratio of G_D/G_S as predicted from this analysis, and as predicted from our more naive analysis. (It has been assumed that the Poisson's ratio is 0.25, which means that $v_R \simeq 0.6v_l$.)

For speeds in excess of experimentally measured terminal values the ratio of G_D/G_S as predicted by our analysis deviates from that of Eshelby's. The reasons for this are at least two-fold; firstly, in making the comparison between the static and dynamic situations we have considered strain energy released only from material behind the crack tip, and secondly, it was assumed that the energy density obtained from this strain relieved material could be calculated from the statically determined value. If the comparison between G_D and G_S is evaluated solely from a consideration of the changes in stored strain energy from material behind the crack tip, then we ignore the important physical point that the material ahead of the crack is unable to accommodate the crack's arrival if the speed of the latter is in excess of v_l. If the comparison between G_D and G_S had been calculated on the basis of a consideration of changes in stored strain energy in the material ahead of as well as behind the crack tip, then the contributions of the former in the dynamic case would have tended to zero as v approached v_l, and the ratio between G_D and G_S would have been correspondingly smaller.

The assumption that the energy density was always a fixed value, derived from Cottrell's simple static argument, is probably the more significant shortcoming of our model,

however. The more refined analyses which consider a crack with a steadily increasing length, (as opposed to a moving crack of constant length similar to that considered by Yoffé, 1951), predict that the stress intensity factor tends to zero as the crack speed approaches the appropriate wave speed, which implies that the energy density obtained from the strain relieved material gradually decreases as v increases.

Whatever the shortcomings of the simple physical argument previously described, it has the principal advantage of indicating, perhaps more clearly than more refined analyses, the main physical reason for a reduction in the energy release rate for a dynamic crack as compared with a static crack of the same length. Moreover, in line with more sophisticated analyses, it indicates that the magnitude of this reduction is relatively small at speeds less than the measured terminal speed.

2.4 The dependence of fracture energy on crack speed.

There is considerable experimental evidence to suggest that the fracture energy of many materials changes with crack speed. For example, Williams, (1971), has measured the fracture energy of pmma as a function of speed and his results show that at least for speeds up to $\sim 0.1 ms^{-1}$ the fracture energy increases. Griffiths, (1969), has argued, again from experiment, that the fracture energy of Araldite CT200 epoxy resin decreases with crack speed.

None of these results provide direct quantitative information on the magnitude of any changes in fracture energy at speeds approaching the terminal value, however. At present, it is only possible to extrapolate trends which have been established for lower crack speeds into these high speed regions.

Exactly why fracture energy changes with speed is, for most materials in which the phenomenon is known to occur, not yet understood. It is quite possible that it is not the speed per se which directly affects the fracture energy, but some speed dependent variable such as the temperature of the material at the tip of the propagating crack. It is very difficult to isolate the effect of crack speed from these other variables so as to ascertain which one is directly responsible for any fracture energy changes. From the point of view of the energetics of fracture an attempt to make such a distinction would in one sense be an academic one; for provided the fracture energy does change with speed, even if the cause of the change is not speed but some speed dependent variable, then such changes should be taken into account, at least in principle, when evaluating the energetics of fracture in a material.

In energy balance equations similar to those discussed earlier, it is normally assumed that the fracture energy of the material is independent of crack speed. Indeed, in a more general sense any dependence of fracture

energy on speed is rarely incorporated into fracture mechanics analyses, and where it is, a simplifying assumption is invariably made to keep the mathematics tractable. For example, Kostrov (1964), has assumed that under dynamic conditions the plastic-zone length, (the magnitude of which is related to the fracture energy), is linearly dependent on crack length; and Glennie (1971), has argued that the flow stress of steel is linearly dependent on the crack-tip strain rate. Glennie also suggested that the increase in resistance to plastic deformation might account for the low terminal speeds of cracks in steel as measured by experiment. On its own however, an increase in flow stress does not provide a guarantee that the fracture energy will increase, since volume of plastic distortion is also a relevant factor. If, following Wells (1963), we assume that the zone of plastic distortion can be characterised by the crack-opening displacement, (see Chapter 1), then any variations in this quantity would also affect the fracture energy. It is at least a priori possible that changes in the crack-opening displacement could more than compensate for changes in material flow-stress under dynamic conditions. This contingency aside, Glennie's proposal that an increased resistance to plastic flow might account for the discrepancy between the predicted and measured values of the terminal speed, is on physical grounds quite feasible, and, if nothing more, this would alter the speed profile from that predicted by Equation 2.7. There is a much more likely explanation of the discrepancy however; viz that the available

energy is shared amongst several cracks.

2.5 The absorption of energy by multiple cracking.

So far in this chapter the discussion has centred on the energy absorbed by a single moving crack. As was indicated in Chapter 1 however, the fracture process in real materials involves more than one crack; soon after fracture has commenced many subsidiary cracks are produced, and ultimately macroscopic branching of the whole fracture front occurs. The production of these subsidiary cracks is likely to be the main reason for the discrepancy between experimentally measured terminal speeds and the predicted values.

The kinetic energy of a crack depends on its length as well as its speed, and the terminal speed is set by the stage at which the available energy is only just sufficient to satisfy the kinetic and fracture energy demands of crack extension, with no surplus available for increasing the crack speed. In a situation where in addition to the main crack many subsidiary cracks propagate over a finite distance, the available energy is shared between these and the main crack. Consequently, less energy is supplied to the main crack, and the stage at which the speed of the main crack is limited may be reached quite early on in the fracture process. Provided the energy demands of the subsidiary cracks keep pace with the increase in available energy as the fracture extends, and experiment suggests that this is the case,

then the maximum speed of the main crack should be restricted to this early and relatively low value for the rest of the fracture process. The actual terminal speed would depend on how early in the fracture process subsidiary cracks are formed.

If this reasoning is correct, then the discrepancy between the theoretical and experimental values of terminal crack speed arises because one of the underlying assumptions of the theory is in error; viz that the fracture occurs by the propagation of a single crack. In this respect the reason for the discrepancy is analogous to the reason for the discrepancy between the theoretical and experimental values of strength. In the former case, it is assumed that one crack only is involved in the fracture process, and the analysis deals with the maximum speed of this crack under these conditions. In the latter case, it is assumed that solids are flawless, and the analysis deals with the strength of such perfect solids.

2.6 Summary

This chapter has dealt briefly with the energetics of moving cracks. Mott's energy balance equation was considered, and from this a value for the terminal speed of a crack was derived. This was compared with Mott's own value and that derived by Berry. The effect of crack speed on energy release rate was then considered, and a

simple physical argument was used to derive an approximate expression for the ratio of G under dynamic conditions to G under static conditions, for a given crack length. The result, in common with more refined analyses indicated that there was very little difference between the two values until the speed of the crack reached its (measured) terminal value, and then the difference was $\sim 30\%$. Possible variations of fracture energy with crack speed were then noted, and we concluded with the suggestion that the finite propagation of subsidiary cracks during fracture of real materials was likely to be the main reason for the discrepancy between the measured and predicted values of terminal speed.

In the next Chapter the phenomenon of crack branching is examined. This phenomenon, it is concluded, can most satisfactorily be explained in terms of an energy argument proposed initially by Johnson and Holloway, (1966).

CHAPTER 3

CRACK BRANCHING

3.1 Introduction

When a brittle solid is broken in tension, a stage may be reached when the fracture continues simultaneously along two separate paths at a small angle to each other. This phenomenon is called crack-branching, and forms the subject of this chapter.

Of all the events which occur as the fracture spreads across a specimen, the formation of a branch is perhaps the most striking, and probably for this reason it has attracted more attention than the other, pre-branching fracture-surface structures. However, since crack-branching is merely one stage in the development of the fracture process, it should be examined within the context of this fracture process as a whole; the physical importance of the phenomenon can then be placed in perspective with the other events which occur during fracture.

By placing the formation of a branch within the context of the other events which occur during the fracture of glass, Johnson and Holloway (1966) were led to an energy criterion for branching, which, as we shall see later, is probably the most satisfactory account of the phenomenon which is currently available. By lightly etching pre-branching fracture surfaces of glass with dilute HF they

revealed numerous small cracks which penetrated the exposed surfaces. It was suggested that the presence of these cracks could mean that the mechanism of crack bifurcation was available well before gross fracture branching actually occurred, and the boundary to gross fracture branching might therefore demarcate a physical transition in the fracture process determined by the availability of sufficient energy to propagate continuously two of these cracks over a large distance.

This distinction, between the mechanism of crack bifurcation and the continued propagation of more than one crack is not widely acknowledged. For example, in many of the publications on crack branching, (e.g. Field 1970), crack bifurcation and crack branching are treated as one and the same phenomenon; crack bifurcation is regarded as an isolated event confined to the branching boundary. For the materials examined in this work there is ample evidence of numerous small cracks below the exposed surfaces prior to macroscopic branching, and there is no reason to suppose that the mechanism which led to these cracks is any different from that which led ultimately to branching. Consequently, in line with the approach taken by Johnson and Holloway, our study of crack branching has been separated into the two aspects of how, (by what mechanism), a crack bifurcates, and why, only after a certain stage in the fracture process the multiple cracks so produced continue to propagate simultaneously over large distances. In this chapter we shall be concerned with the second of these problems.

For many materials it is now well established that if c_b is the distance from the fracture origin to the onset of branching, and σ is the tensile breaking stress, then,

$$\sigma\, c_b^{\frac{1}{2}} = \text{constant} \qquad 3.1$$

The value of the constant is different for different materials, but for a given material it is always the same, (Clark and Irwin 1965, Congleton and Petch 1966, Johnson and Holloway 1966, Anthony and Congleton 1968).

Any satisfactory account of crack branching should, in principle, predict that $\sigma\, c_b^{\frac{1}{2}} = \text{constant}$, although the theoretical account of branching which until quite recently was almost universally accepted, does not do so. In fact, there have been very few attempts to explain the significance of Eq 3.1, but of those that are available, again, the energy criterion of Johnson and Holloway would appear to be the most satisfactory.

In the next section we describe some experiments conducted to establish whether Eq 3.1 was applicable to a selection of polymers. Some attempts to account for crack branching are then outlined, and this is followed by a closer examination of the implications of one of these; viz the energy criterion of Johnson and Holloway. It should be noted that the experiments described in the next section were in the nature of a preliminary survey, and they could usefully have been extended to loading conditions other than simple tension and to environments other than air at room temperature.

3.2 Provisional Experiments

(a) Choice of materials

The materials chosen for this early work fell into two categories; a thermosetting resin, with and without fillers, and some thermoplastics. The resin was the Araldite epoxy system CT200 + HT901, (CIBA-GEIGY Ltd., Duxford, Cambridge), which is manufactured primarily for casting and laminating purposes. The thermoplastics were: polymethylmethacrylate, (pmma), polystyrene, polycarbonate, toughened-polystyrene, acetyl copolymer, and styrene acrylonitrile. The pmma was obtained from I.C.I. Ltd., the polystyrene from B.P. Ltd., and from Borst Bros. Ltd., and the other thermoplastics from Borst Bros. Ltd., (Borst Bros., Hitchin, Herts.)

Using this range of solids it was possible to measure the product $\sigma c_b^{\frac{1}{2}}$ for materials which had been stiffened and toughened in different ways.

(b) Specimen Preparation

Each thermoplastic was purchased in sheet form. Rectangular specimens were cut from the sheets with a band saw, and although initially the sawn edges were milled parallel and smooth, on later specimens filing was used for this purpose which proved adequate and saved considerable time.

The pmma, polystyrene, and polycarbonate sheets were available in $\frac{1}{4}$" ($\sim$6mm) and $\frac{1}{8}$" ($\sim$3mm) thicknesses, and the other thermoplastics were available in $\frac{1}{4}$" ($\sim$ 6mm) thickness sheets. Specimens of various widths ranging

from ~ 6mm to ~ 50mm, and length of ~ 250mm were cut from these sheets.

To produce a range of strengths and to ensure rupture away from the grips in which the specimens were held in the testing machine, notches were introduced into many specimens of each material. Using a number of different cutting tools, notches which varied in length and sharpness could be produced quite easily. Sharp notches were produced with a scalpel by carefully pressing the blade into the side of a specimen; blunter notches were produced by sawing the side of the specimen with a hacksaw, (a very blunt notch), with a jeweller's saw, and in some cases with a tungsten wire affixed to the frame of a coping saw. Sometimes, to produce a long sharp notch the edge of a specimen was in the first instance sawn, and the scalpel was pressed firmly into the end of the saw-cut. Although it was unnecessary to keep detailed records of the dimensions of the notches, care was taken to align the notches roughly perpendicular to the applied tension direction. This was achieved by scibing a thin line perpendicular to the edge of a specimen and using this as a guide when introducing the notch.

In general the manufacturers' recommendations were followed to anneal the materials, although some difficulty was encountered in finding satisfactory annealing conditions for polystyrene. The compression moulded polystyrene often underwent significant deformation and/or internal

bubbling on heating, and a selection procedure was adopted so that only those specimens which, after annealing, showed no significant deformation and internal bubbling, were used for the tensile tests. The specimens were annealed at 383 K for two hours and then slowly cooled to room temperature over a period of seven hours. (It is perhaps worth noting that much of the previous work on the fracture of polystyrene has been undertaken on un-annealed compression moulded material, (see e.g. Murray and Hull 1970)).

The unfilled epoxy resin was cast into dumb-bell shaped specimens using specially designed steel moulds. These moulds produced specimens $1\frac{1}{2}$" ($\sim$ 37mm) or $\frac{3}{4}$" ($\sim$ 19mm) wide, and were designed so that the specimens were thinner along the shank than in the dumb-bell ends. There was a gradual change in thickness along the length of each specimen so as to reduce the possibility of stress magnification at a sharp step.

The epoxy specimens were cured by the following schedule recommended by the manufacturer:

viz. CT200 resin: 100 parts by weight

HT901 curing agent (phthalic anhydride): 30 parts by weight.

These stoichiometric quantities of resin and curing agent were heated together at 408 K ($\pm$ 5 K) for sixteen hours.

Prior to curing, the CT200 resin was pre-heated to 413K until it became fluid and the curing agent, HT901, which was in powder form, was then added. The mixture was stirred until the curing agent had completely

"dissolved", and the reaction was allowed to continue in the mixing vessel at 413K for ~ 15 minutes, by which time the viscosity had increased significantly. This partially cured resin was then added to the moulds which had been pre-heated to 408K. The resin was allowed to partially cure and thereby increase its viscosity, so that leakage from the moulds could be kept to a minimum.

The inner surfaces of the moulds had been previously treated with Releasil (No. 7) silicon grease so as to facilitate removal of the specimens. This treatment involved baking the Releasil on at ~ 573K, and was effective for the production of about thirty specimens from each mould.

After curing the moulds were dismantled, the specimens were removed, then annealed at 403K for ~ 5 hours and slowly cooled to room temperature over about 12 hours.

The composite specimens based on this resin were already available in the laboratory as the arms of broken Double Cantilever Beam specimens (Berry 1963). These arms had a cross section of 10mm x 7mm and were ~ 250mm long. The composites tested had aluminium powder, and silica flour as fillers in proportions specified in table 2.1.

Material	Parts by weight HT901 per 100 parts by weight resin.	Parts by weight filler/100 parts by weight resin.
CT200+Al	15	10
CT200+SiO_2	30	30

Table 2.1

MATERIAL	$\sigma c_b^{\frac{1}{2}}$ ($MNm^{-3/2}$)	NUMBER OF SPECIMENS	RANGE OF c_b ($mx10^{-2}$)
pmma	4.17 ± 0.09	60	0.8 -3.0
polystyrene	1.74 ± 0.04	60	0.5 - 2.8
polycarbonate	3.64 ± 0.15	20	0.7 - 2.5
toughened polystyrene	3.64 ± 0.18	18	0.7 - 2.8
acetyl copolymer	1.87 ± 0.12	14	0.5 - 3.0
styrene acrylo-nitrile	6.60 ± 0.42	16	1.0 - 2.8
CT200	2.70 ± 0.08	50	0.7 - 3.5
CT200 + Al	3.00 ± 0.18	17	0.2 - 0.6
CT200 + SiO_2	3.26 ± 0.14	18	0.2 - 0.6

TABLE 3.2

VALUES OF $\sigma c_b^{\frac{1}{2}}$

These specimens were cured and annealed by the same schedules used for the unfilled resin.

(c) Experimental Measurements of $\sigma c_b^{\frac{1}{2}}$

The basic experimental procedure was to fracture the specimens in tension, evaluate the fracture stress, and measure the distance from the origin of fracture to the onset of branching. A Dennison T42U Universal Testing Machine was used for the tensile tests. The specimens were aligned perpendicular to serrated steel wedge fixed grips using a plumb-line and tri-square, and the load was recorded on a dial indicator. By fracturing weakened specimens of pmma which had been aligned by this technique, the crack was found to propagate perpendicular to the edges of the specimen, thereby indicating severe bending stresses were absent.

The branching distances were measured with a travelling microscope, and the value recorded for each specimen was the average of the measurements obtained from both fracture surfaces.

(d) Results

The results are tabulated in Table 3.2 which gives the mean values of $\sigma c_b^{\frac{1}{2}}$ for each of the materials tested, together with the standard error of the mean in each case.

These results show that the product $\sigma c_b^{\frac{1}{2}}$ is constant for each material. It is interesting to note that the value of $\sigma c_b^{\frac{1}{2}}$ varies by a factor of three only for the whole range of materials tested; and within the accuracy of the experiment $\sigma c_b^{\frac{1}{2}}$ is the same for the polycarbonate and toughened polystyrene.

For a stationary edge-crack penetrating a specimen loaded in uniaxial tension, K_I is proportional to $\sigma c^{\frac{1}{2}}$, where c is the length of the edge-crack and σ is the applied stress, and it might therefore seem a feasible interpretation of the above results that for each material, branching occurs at a critical value of K_I or G_I. Indeed, Congleton and Petch, for example, have argued from the constancy of $\sigma c_b^{\frac{1}{2}}$ in glass and some other materials that branching occurs at a critical value of $K_I = K_B$, where K_B is equal to $\pi^{\frac{1}{2}}\sigma c_b^{\frac{1}{2}}$. However, this expression for K_B is the approximate solution for K_I for a stationary crack of length c_b in a specimen of width W, when $c_b < W/10$, and it is not <u>a priori</u> obvious that the value of K_I at branching should be of this magnitude; at best this is a first approximation to the actual value. A complete solution for K_I under the conditions which obtain at branching should, in principle, take into account the speed of the crack, the affect of the proximity of the free edges of the sheet on the crack-tip stress field*, and, possibly, that at or immediately after branching, two cracks are involved in the fracture process. To the author's

---

* Although in principle the proximity of the free edges of the sheet should influence the crack-tip stress field, and hence K, the observation that in resin specimens in which fracture originated internally and close to one edge, the branching distance was the same on either side of the origin, provides circumstantial evidence that the effect of the free edges might be of second order only. The results of Table 3.2 support this since they imply that for specimens of a given strength the branching distance is independent of specimen width.

knowledge no complete solution for K or G which includes all these factors is yet available. At the present time therefore, we cannot specify with certainty the exact magnitude of K or G at branching, even though the preceding results suggest that in a given material K or G is constant when branching occurs.

3.3 Some previous attempts to explain fracture branching, and why σc_b^2 = constant

At least until quite recently, the most widely accepted explanation of crack-branching, although one which did not account for the empirical fact that $\sigma c_b^{\frac{1}{2}}$ = constant, was Yoffé's calculation of the redistribution of elastic stresses around the tip of a crack travelling at high speeds, (Chapter 1, Section 1.6). The formation of two local stress maxima symmetrically displaced about the crack-plane would, it was suggested, lead to branching of the crack. Since these stress maxima occur at a crack-speed of $\sim 0.6v_2$, the condition for crack branching has been stated in terms of the attainment of this critical speed. It is extremely unlikely that this theory can account for crack branching in real materials however, for it conflicts with much of the experimental evidence that is now available, perhaps the most important of which is the speed measurements which have been made. If we consider the measurements which have been made on glass, (e.g. Schardin 1959), two points emerge: firstly, the terminal speed in this material is less than $0.6v_2$, and secondly, the terminal

speed is reached and maintained well before branching occurs. The former observation is a less serious objection to Yoffé's theory than the latter since the main principle of the theory that the stresses are redistributed might still be retained, even though the predicted speed at which this occurs is in error. The second observation, that the terminal speed is reached and maintained well before branching occurs, is the more serious objection since it is explicit in the theory that branching occurs when the crack attains a critical speed. If, perhaps more logically, the predicted bifurcation were associated with the first of the sub-surface cracks formed earlier in the fracture process before branching occurs, the theory might be retained to account for the appearance of these cracks. (Indeed, in the region where these cracks first form, at least for glass, the speed of the crack approaches its terminal value.) However, this interpretation would leave the later macroscopic branching event to be explained in some other way.

These latter comments reveal one major limitation of this account of crack branching; being essentially a mechanism of crack-bifurcation it can make no distinction between bifurcation prior to and at branching. There are other, less important, criticisms of Yoffé's theory, such as the predicted angle between branched cracks not being observed in practice, but it is felt that the comments which have already been made justify a search for an alternative explanation of branching.

As it stands the preceding theory of crack-branching provides no explanation for the empirical fact that $\sigma c_b^{\frac{1}{2}}$ = constant. Bateson, (1960) used a critical speed criterion as the basis for an explanation of this fact. Bateson, who was concerned with glass in particular, assumed that branching occurred when the crack attained its terminal speed, and argued that the value of $\sigma c_b^{\frac{1}{2}}$ would depend primarily on the terminal crack-speed and the surface energy of the material. We have already noted that surface energies of many brittle solids are lower than their measured fracture energies, and in this respect Bateson's model need modifying. This would only affect the magnitude of $\sigma c_b^{\frac{1}{2}}$ however, and not the underlying reasoning of Bateson's argument.

Bateson derived an expression for the crack speed by considering the lateral displacement of a small volume of material at the crack-tip. He argued that at rupture, the released strain energy in this small volume would be converted into "distortion energy", and, as the crack extended the small volume would attain kinetic energy as it moved laterally out from the crack plane. He assumed that the kinetic energy of the crack was associated with material on the crack boundary only, and that energy was conserved at the crack tip. An expression for the crack speed was derived in terms of the speed of transverse waves, v_2, and by differentiating this with respect to time, Bateson obtained an expression for the acceleration of the crack as a function of the applied stress, crack-tip

radius, and some physical constants of the material.

He then assumed that the acceleration of the crack was constant, and elementary mechanics were applied to calculate the distance travelled by the crack before it reached its terminal speed, which ex hypothesi was the distance travelled before branching occurred. From this distance c_b, and knowing the applied stress, σ, Bateson obtained the expression:-

$$\sigma\, c_b^{\frac{1}{2}} = \left(v_{max}/v_2\right)\left[T.E\,(1 + \nu)\right]^{\frac{1}{2}} = \text{const.} \quad 3.2$$

If the assumptions on which this result is based are for the moment accepted, the value of $\sigma c_b^{\frac{1}{2}}$ obtained experimentally can be compared with the value predicted from Equation 3.2. For glass, for which the theory was developed, experimentally $\sigma c_b^{\frac{1}{2}} = 1.9\ MNm^{-3/2}$ (Johnson and Holloway 1966), whereas using typical values for the quantities in Equation 3.2 the predicted value is $0.15\ MNm^{-3/2}$. (The experimental value of v_{max} and the fracture energy, rather than the surface energy, for glass have been substituted into Equation 3.2). For pmma, $\sigma c_b^{\frac{1}{2}} = 4.2\ MNm^{-3/2}$ experimentally, and from Bateson's equation $\sigma c_b^{\frac{1}{2}} = 0.54\ MNm^{-3/2}$. In both cases the predicted value of $\sigma c_b^{\frac{1}{2}}$ is an order of magnitude too low. It should be pointed out that Bateson realised his theory gave poor agreement with experiment for glass.

There are two assumptions on which Bateson's analysis is based: (i) the crack branches when it attains its terminal speed, and (ii) the acceleration of the crack is uniform up to the terminal speed.

It is not a priori obvious why a crack should branch when it attains its terminal speed, (Bateson made no reference to stress redistribution), and this assumption is known to be contrary to experiment for many materials, (Schardin 1959), where the terminal speed is reached well before branching occurs.

The second assumption of uniform acceleration is directly opposed by the expression for crack speed obtained in Chapter 2, (Equation 2.11), which on differentiation with respect to time predicts that the acceleration of the crack is greater during the early stages of its growth, and in this respect is at least in qualitative agreement with experiment. Furthermore, Bateson's own expression for crack speed can be expressed in the form,

$$v = Av_2(1 - B/c)^{\frac{1}{2}} \qquad 3.3$$

where A and B are constants, and when differentiated this does not in fact predict uniform acceleration as Bateson assumed.

The assumption of uniform acceleration would therefore appear to be unjustified, and this undermines the derivation which was based on this assumption.

In view of these objections to Bateson's analysis, it is not considered to provide a satisfactory explanation of the empirical fact that $\sigma c_b^{\frac{1}{2}}$ = constant, and in any case it predicts a value for this constant which is an order of magnitude too low.

In a series of papers, (Congleton and Petch 1967, Anthony and Congleton, Petch and Sheils 1968, Anthony and Congleton 1970), an explanation of crack branching was proposed which predicted that $\sigma c_b^{\frac{1}{2}}$ = constant. As presented, the model is couched in terms of growth of "Griffith cracks" ahead of the main crack. Griffith cracks are small cracks which have often been assumed to exist in brittle materials, and in particular in glass, as an inherent part of the structure, even though there is no direct experimental evidence for their presence. Although phrased in terms of Griffith cracks the existence of these are not in fact central to the proposed model, since all that is required is that new cracks can form in the unbroken material ahead of the main crack; i.e. that a secondary nucleation mechanism is operative, in which new cracks form at local stress-raising inhomogeneities within the material.

It was argued that branching occurred as a result of the growth of Griffith cracks ahead of the main crack. The growth of Griffith cracks, they argued, was controlled by the stress-field of the main crack, and the criterion for branching was that the stresses due to the main crack had to be high enough to cause "persistent extension of a ... Griffith crack" (Congleton and Petch 1967, p.758). In the earlier publications they argued that the "persistent growth" condition could only be satisfied if the centre of a Griffith crack of length 2c was located at a distance c ahead of the main crack. In the later work this was

modified to nc ahead of the main crack, where $n \geqslant 2$. In Congleton et al (1968), the importance of this "persistent growth" condition was stated explicitly. It was argued that unless a Griffith crack grew "persistently" then its growth would be arrested as soon as the main crack swept past. This is tantamount to saying that when the main crack reaches the end of the Griffith crack both must be travelling at the same speed, and more importantly, they must maintain that speed. This very important point will be returned to later.

Westergaard's (1939) stress solution was used to obtain an expression for the stress normal to the crack plane at a distance nc ahead of the crack tip: viz

$$\sigma \left(c_b/_{2nc}\right)^{\frac{1}{2}}$$

provided $nc \ll c_b$

Using the Griffith-Orowan equation for the critical stress required to extend a pre-existing crack, the Griffith crack will extend when,

$$\sigma \left(c_b/_{2nc}\right)^{\frac{1}{2}} \simeq \left(\frac{2\gamma E}{\pi c}\right)^{\frac{1}{2}} \qquad 3.4$$

Rearranging,

$$\sigma\, c_b^{\frac{1}{2}} = 2\left(\frac{n\gamma E}{\pi}\right)^{\frac{1}{2}} \qquad 3.5$$

They were unable to predict the value of n theoretically, (even though its magnitude is fundamental to their criterion of persistent extension), although it was suggested that $n \geqslant 2$, and they proceeded to evaluate

its actual value experimentally. To do this, they argued that $\pi^{\frac{1}{2}}\sigma\, c_b^{\frac{1}{2}} = K_B$ when K_B = critical value of K_I at branching, and hence

$$K_B = 2(n\gamma E)^{\frac{1}{2}} \qquad 3.6$$

They further argued that since $K_{Ic}^2 = G_{Ic} \cdot E = 2\gamma E$ then,

$$\frac{K_B^2}{K_{Ic}^2} = \frac{4n\gamma E}{2\gamma E} = 2n \qquad 3.7$$

But since,

$$\frac{K_B^2}{K_{Ic}^2} = \frac{c_b}{c_o} \qquad 3.8$$

then

$$\frac{c_b}{c_o} = 2n \qquad 3.9$$

For a given material the ratio $\frac{c_b}{c_o}$ has a characteristic value, and therefore so does n, and since both c_b and c_o are amenable to measurement, the actual value of n can be found.

A tacit assumption underlying this approach is that the mechanism of crack branching is always the same; viz the growth of small secondary cracks ahead of the main crack. Whether these secondary cracks are an inherent part of the structure or are nucleated at local stress-raising sites is in the present context of academic interest only. What is of more importance is that by developing a criterion for branching which is mechanism dependent the authors restrict its applicability to those materials in which it is known that this mechanism operates. We shall see later that it is not sufficient to assume

that a given mechanism operates in every material; a mechanism can be shown to operate only after a careful examination of the fracture surfaces has been undertaken, and even then it is not always entirely clear which mechanism is operative, (see Chapters 5, 6, 7,).

At best, then, this criterion in terms of the stress required for persistent extension of an advanced crack, is restricted to those materials in which the mechanism of crack bifurcation is known to be the growth of small cracks ahead of the main crack, and for these materials it predicts that $\sigma c_b^{\frac{1}{2}}$ = constant. The magnitude of the constant cannot be predicted theoretically however, because of the unknown factor n which appears in the final result. The fact that n can be determined experimentally in no way justifies the criterion, since the observation that c_b / c_o is constant, (= 2n), is a matter of empirical fact with which any theory of crack-branching must be consistent. There would appear to be no critical test to which the criterion for crack-branching can be subjected, and we must conclude that the validity of the criterion remains unproven.

The requirement that two cracks must be travelling at the same speed, and that they must maintain this speed is central to an energy criterion of branching proposed by Johnson and Holloway (1966). Johnson and Holloway argued that the branching boundary demarcates that stage in the fracture process at which the rate of release of energy by the system is sufficient to create continuously two cracks, and to maintain the kinetic energy associated

with each. This criterion of branching, unlike the previous one, is mechanism independent: it says nothing about how crack division occurs. Because of this, and in common with all energy arguments, it will only provide a necessary condition for branching. For most materials at least, this is of no consequence since it seems that in practice a mechanism is always available before it is needed in the creation of the branch.

By differentiating Mott's energy equation (Eq. 2.1) with respect to crack length, and assuming that when branching occurred the crack speed was constant at its terminal value, and that at this stage 8 fracture surfaces were produced, (4 at each end of the crack), they obtained the following expression, which was based on the energy changes occurring during an increment of crack growth at branching :

$$\underline{\text{viz}} \quad \left(-\frac{2\pi\sigma^2 c_b}{E} + \frac{K\rho v_{max}^2 \sigma^2 c_b}{E^2} + 8\gamma \right) = 0 \qquad 3.10$$

Rearranging,

$$\sigma c_b^{\frac{1}{2}} = \left[\frac{8\gamma E}{\left(2\pi - \frac{k\rho v_{max}^2}{E}\right)} \right]^{\frac{1}{2}} = \text{constant} \qquad 3.11$$

Although this analysis was derived for the particular case of glass, it should be applicable to other materials since it is based on general energy principles.

There are two major assumptions on which the analysis is based: firstly, the rate of release of strain-energy at branching is the same as that for quasi-static growth

of a single crack of the same length; and secondly, the speed of the crack is constant when branching occurs and equal to the terminal value. It was suggested in Chapter 2 that the static value of energy release-rate is likely to be an overestimate for a crack travelling at high speed. A modification of the first term in Equation 3.10 to take account of crack-speed would alter the predicted value of $\sigma c_b^{\frac{1}{2}}$ given by Equation 3.11, but not undermine the basic criterion which Johnson and Holloway proposed. The second assumption, that the crack speed is constant at its terminal value when branching occurs, is consistent with many experimental speed measurements which have been made in certain materials, (e.g. Schardin 1959), but has recently been questioned (e.g. Anthony et al 1970). However the general notion that the speed of both cracks must be equal to some constant value would seem to be a prerequisite if branching is to occur, otherwise, as pointed out by Congleton and Petch, one crack would unload the other. Thus, the assumption that $dv/dc = 0$ would appear to be justified, even if, as some authors have suggested, the constant speed is not the terminal value.

The theoretical value of $\sigma c_b^{\frac{1}{2}}$ that Johnson and Holloway obtained for glass is $0.95 MNm^{-3/2}$. They used Roberts and Well's estimate of $k = 44$, Schardin's value of $v_{max} = 1.5 \times 10^3 \ ms^{-1}$, and took typical values for the other quantities. For pmma, again using $k = 44$, their expression predicts that $\sigma c_b^{\frac{1}{2}} = 1.94 \ MNm^{-3/2}$,

which compares with 4.17 $MNm^{-3/2}$ obtained experimentally in this work. (At the time of writing there is no data on v_{max} for the other polymers and we are therefore unable to use Equation 3.11 to predict values for $\sigma c_b^{\frac{1}{2}}$ for these materials.) If a dynamic correction is made to the rate of release of strain-energy, then the predicted values of $\sigma c_b^{\frac{1}{2}}$ for glass and pmma become closer to the experimental values. A dynamic correction of the order implied by the naive analysis presented in Chapter 2, and by Eshelby's more refined analysis at speeds equal to the experimental terminal speed, give theoretical values of $\sigma c_b^{\frac{1}{2}}$ for glass and pmma respectively of ~ 1.5 $MNm^{-3/2}$ and ~ 3.8 $MNm^{-3/2}$. Thus a dynamic correction to the rate of release of strain energy will reduce, at least to some extent, the discrepancy between theory and experiment obtained by this analysis.

Any correction to the predicted value of $\sigma c_b^{\frac{1}{2}}$ implied by the recent questioning of the assumption that $v = v_{max}$ at branching, is less easily accounted for. Indeed, there are good physical grounds for assuming that $v = v_{max}$ at branching, even for materials for which no speed measurements have been made. If two cracks are to travel simultaneously over large distances, and therefore at the same speed, some constraint must be imposed on the speed of both cracks. One obvious physical constraint is the terminal crack-speed, which imposes an upper limit. It would be possible, of course, for one crack to overtake the other if the speed of either crack

fell below this upper limit, and to allow for this contingency Johnson and Holloway argued that each crack must be continuously supplied with kinetic energy. This last point has been questioned by Congleton and Petch, who argued that it was an unnecessary requirement to include kinetic energy into the energy balance equation at branching, since the kinetic energy of the secondary crack, (N.B. they presupposed the mechanism), could be obtained from the kinetic energy of the existing length of the main crack; i.e. the speed of the main crack dropped. When offering this alternative to Johnson and Holloway's energy balance equation they assumed that n (in Equation 3.5) was equal to unity, and gave the following expression for $\sigma c_b^{\frac{1}{2}}$:

$$\sigma c_b^{\frac{1}{2}} = 2(\gamma E/\pi)^{\frac{1}{2}} \qquad 3.12$$

It was argued that exactly this expression could be obtained if branching occurred when it was energetically possible for the Griffith-Orowan Equation to be satisfied for double the normal amount of fracture energy. However, the subsequent modification to their expression with $n \geqslant 2$ implies that branching occurs only when there is sufficient energy to satisfy the Griffith-Orowan Equation for 2n times the normal amount of fracture energy. But at branching only twice the normal amount of fracture energy is needed in the creation of the two cracks and an energy surplus would result; the most obvious sink for this surplus energy is the kinetic energy of the cracks. Ironically, their modified expression for $\sigma c_b^{\frac{1}{2}}$ indirectly supports the energy balance equation proposed by Johnson and Holloway, which in an earlier paper Congleton and Petch had suggested was incorrect.

It was the same authors who questioned the assumption that the crack-speed at branching was equal to the terminal speed. On the basis of two sets of crack-speed measurements they concluded that, in glass at least, the crack speed at branching depended on specimen strength, being higher for low strength specimens.

The first set of measurements (Congleton and Petch 1967), was obtained by the well known Wallner-line technique, (Wallner 1939). A Wallner-line marks the intersection of the crack-front with a stress wave, and by using the stress wave as a timing device, the average speed of the crack can be ascertained. A Wallner line can only be observed on an otherwise smooth fracture surface. Thus, for specimens broken in tension, Wallner lines will only be observed on the smooth area of fracture surface which surrounds the origin of fracture.

Wallner-lines enable the <u>average</u> speed of the crack between two points to be estimated, as described below.

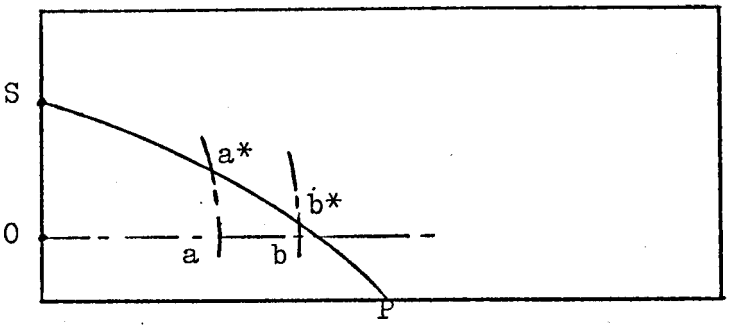

Fig. 3.1
Wallner-Line

SP represents the Wallner-line, and O marks the origin of fracture. The time taken for the crack to

move from a to b is the same as the time taken for the stress wave to travel from a* to b*. The average speed of the crack is thus:

$$\overline{v} = \frac{ob - oa}{(sb^* - sa^*)/v_2} \qquad 3.13$$

where v_2 is the transverse wave speed.

Thus:

$$\overline{v} = \frac{(ob - oa)}{(sb^* - sa^*)} v_2 \qquad 3.14$$

The second set of speed measurements, which were considered to complement the Wallner-line results, were obtained by evaporating a metallic resistance-grid onto the side of each specimen and timing the crack as it travelled between successive grid-bars. This was accomplished by recording on an oscilloscope with a calibrated time-base the change in potential difference as the spreading crack ruptured each grid-bar in turn, (Anthony et al 1970).

In common with the Wallner-line technique this method measures average speed between two points. However, in the discussion of the results they proceed as if the measurements were of absolute crack-speeds at given distances from the origin of fracture. It is effectively argued that because the measured values of crack-speed are roughly equal in each specimen at a given distance from the tip of a constant-length pre-introduced notch,

regardless of the radius of the notch, (and hence specimen strength), then the rate of increase of crack-speed with crack-length is the same in all specimens. Thus, it is concluded, in specimens where the branching distance c_b is short, the speed at branching is relatively low.

However, in order to reliably estimate dv/dc from average crack-speed measurements alone, it is necessary for several such readings to be taken over successive distances. If, to take an extreme example, only one reading of average crack-speed were made over equivalent regions on each specimen, it would not necessarily follow that dv/dc was the same in each case just because the measured values of $\bar{v}$ were comparable: provided the (instantaneous) speed is roughly the same when timing begins, then a whole range of crack accelerations over the measured distance will give values of $\bar{v}$ which are approximately equal.

In the actual resistance grid experiments, the number of average speed readings taken on a given specimen before branching occurred depended on the value of c_b. In all specimens where c_b was much larger than the minimum grid spacing (1mm), and where several readings of $\bar{v}$ were made over successive distances, the values of $\bar{v}$ became roughly constant and equal to the terminal speed by the time branching occurred. The conclusion that the speed at branching could be less than the terminal speed was based on the speed measurements made on three high strength glass specimens. For these specimens, the branching distance

enabled at most only two successive readings of the average speed to be made before branching occurred. This, however, is an insufficient number of readings to allow any definite conclusion to be drawn about the rate of change of (absolute) crack-speed with crack-length over the branching distance, c_b. A similar criticism can be made about the Wallner-line experiments; and the conclusion that branching can occur at speeds less than v_{max} must at the present time be considered unproven. We therefore feel justified in assuming in accordance with the majority of Congleton et al's evidence and other published results (e.g. Schardin 1959), and because even in materials where no data is yet available there are good physical grounds for so doing, that the speed of the crack at branching is equal to the terminal value.

Summary

In this section some attempts to account for crack branching and attempts to explain the empirical fact that $\sigma c_b^{\frac{1}{2}}$ = constant at branching have been discussed. Of these, the energy criterion of Johnson and Holloway would appear to be the most satisfactory; this states that branching occurs when there is sufficient available energy to create continuously two cracks and to maintain the kinetic energy of both. In its original form the analysis predicts values of $\sigma c_b^{\frac{1}{2}}$ for glass and pmma which are in reasonable agreement with experimental values, although a dynamic correction to the energy release-rate improves

the agreement. Johnson and Holloway assumed that at branching the crack-speed had attained its terminal value. This assumption is in agreement with much of the currently available experimental data, although it apparently conflicts with a conclusion of Congleton and co-workers, who claimed to show that branching could occur, (at least in high strength glass specimens), at speeds which were significantly less than the terminal value. This conclusion, we have suggested, is open to doubt.

3.4 A closer examination of the measurements of $\sigma c_b^{\frac{1}{2}}$ in relation to the energy criterion of branching.

The theoretical expression for $\sigma c_b^{\frac{1}{2}}$ based on the energy criterion of branching predicts that branching will occur when $\sigma c_b^{\frac{1}{2}} = A (E \gamma)^{\frac{1}{2}}$, where A is a numerical constant, E is the Young's modulus, and γ is the fracture energy of the material concerned. It must be possible, of course, to express any dimensionally consistent theoretical expression for $\sigma c_b^{\frac{1}{2}}$ in this form, and alternative expressions will differ in respect of the physical parameters which affect, or are assumed to affect, the magnitude of A. Thus, the expression for $\sigma c_b^{\frac{1}{2}}$ based on the energy criterion of branching, states that the magnitude of A will depend on the speed of the crack, the longitudinal wave speed, and the extent to which the material surrounding the crack contributes to its kinetic energy. Congleton and Petch's expression is based on the assumption that A^2 is a multiple of crack-length,

MATERIAL	$\sigma c_b^{\frac{1}{2}}$ ($MNm^{-3/2}$)	SOURCE OF $\sigma c_b^{\frac{1}{2}}$	YOUNGS MODULUS (GNm^{-2})	FRACTURE ENERGY	SOURCE OF FRACTURE ENERGY	$\sigma c_b^{\frac{1}{2}}$ AS "$n(\gamma E)^{\frac{1}{2}}$"
CT200	2.7	This work	3.2	~100*	Griffiths (69)	$4.7(\gamma E)^{\frac{1}{2}}$
CT200 + Al	3.0	This work	3.8	~100*	Griffiths (69)	$4.8(\gamma E)^{\frac{1}{2}}$
CT200 + SiO_2	3.3	This work	6.0	~160*	Griffiths (69)	$3.3(\gamma E)^{\frac{1}{2}}$
pmma	4.2	This work	3.0	280	Linger (67)	$4.5(\gamma E)^{\frac{1}{2}}$
polystyrene	1.7	This work	3.1	90*	This work	$3.3(\gamma E)^{\frac{1}{2}}$
polycarbonate	3.6	This work	2.6	540	McGeehin (70)	$3.1(\gamma E)^{\frac{1}{2}}$
glass	1.9	Johnson (63)	70	4.3	Linger (67)	$3.5(\gamma E)^{\frac{1}{2}}$
alumina	7.1	Congleton (68)	390	17	Congleton (68)	$2.8(\gamma E)^{\frac{1}{2}}$

TABLE 3.3

and that its magnitude depends on the distance between the tip of the main-crack and the centre of a pre-existing secondary crack when the latter begins to extend, and we have already suggested reasons why this assumption may not be entirely satisfactory. By re-writing experimental values of $\sigma c_b^{\frac{1}{2}}$ in terms of a multiple of the product $(\gamma E)^{\frac{1}{2}}$, it was found that for a wide range of materials the experimental value of A was substantially constant, even though the values of γ and E varied quite considerably from one material to another. In this section we note that the measured constancy in A suggests a simple means of estimating fracture energy from the $\sigma c_b^{\frac{1}{2}}$ measurements in a given material, and propose a qualitative explanation for this constancy.

Table 3.3 shows $\sigma c_b^{\frac{1}{2}}$ values in terms of a multiple of $(\gamma E)^{\frac{1}{2}}$ for a selection of materials. Since the crack is travelling at high speed at branching, where possible a "dynamic" value of γ has been used in compiling the table. In such cases the value of γ is marked with an asterisk. Several polymers for which it was previously recorded that $\sigma c_b^{\frac{1}{2}}$ was constant are omitted from the table because of the current lack of data on their fracture energy values.

The most notable feature of Table 3.3 is that when $\sigma c_b^{\frac{1}{2}}$ values are expressed in the form of multiples of $(\gamma E)^{\frac{1}{2}}$, in each case the multiple is very roughly the same; it has a maximum value of 4.8 for CT200 resin + Al and a minimum value of 2.8 for alumina. This result is

MATERIAL	$\sigma_c^{\frac{1}{2}}$ b ($MNm^{-3/2}$)	E BY 3-POINT BEND (GNm^{-2})	PREDICTED FRACTURE ENERGY (Jm^{-2})
toughened polystyrene	3.6	3.2	290
acetyl copolymer	1.9	2.8	90
styrene acrylo-nitrile	6.6	3.8	820

TABLE 3.4

PREDICTED VALUES OF FRACTURE ENERGY

thought to be of more than academic interest since if it is generally true for isotropic materials that $\sigma c_b^{\frac{1}{2}} \sim 3.8(\gamma E)^{\frac{1}{2}}$ then it should be possible to estimate the fracture energy of a material from its $\sigma c_b^{\frac{1}{2}}$ value. Thus, for a material for which $\sigma c_b^{\frac{1}{2}}$ has been measured, γ is given by:

$$\gamma \sim \frac{\sigma^2 c_b}{14E} \qquad 3.15$$

This method of estimating γ would be particularly useful, for example, in the case of materials which are difficult to fabricate into suitable double-cantilever beam specimens, and it might also provide a useful check on single edge-notch fracture energy measurements (Berry 1963). For the polymers excluded from Table 3.3, the predicted values of γ are given in Table 3.4.

The validity of this method of measuring γ relies on the assumption that $\sigma c_b^{\frac{1}{2}} \sim 3.8(\gamma E)^{\frac{1}{2}}$ for most if not all isotropic brittle materials. Clearly, with the relatively small number of materials for which this has been found to be the case, the generalisation to all isotropic brittle materials must be treated with a certain reservation. As with all generalisations, the larger the number of individual cases which can be found the more plausible the generalisation becomes, although an underlying theoretical justification or a plausible model is normally required before it becomes fully acceptable to assume that each new instance can be treated as a further particular case of the generalisation.

None of the theoretical accounts of branching previously considered predict a constant multiple of $(\gamma E)^{\frac{1}{2}}$ explicitly. However, a consideration of the terms which affect the multiple in the expression for $\sigma c_b^{\frac{1}{2}}$ based on the energy criterion of branching suggests that the multiple should in practice remain substantially constant, and this adds a degree of support to the preceding method of measuring γ .

The expression for $\sigma c_b^{\frac{1}{2}}$ based on the energy criterion of branching can be expressed in the following form:

$$\sigma c_b^{\frac{1}{2}} = \left[\frac{8}{2\pi f(v) - \frac{kv_{max}^2}{v_1^2}} \right]^{\frac{1}{2}} . (\gamma E)^{\frac{1}{2}} \qquad 3.16$$

This differs from Johnson and Holloway's original expression by the factor f(v) which represents a dynamic correction to the energy release-rate in Equation 3.10. As discussed in Chapter 2, the value of f(v) decreases with increasing crack-speed, and in Equation 3.16 its magnitude will therefore depend on v_{max}, the terminal crack-speed, and on v_1 the longitudinal wave speed in a given material.

For those isotropic materials for which v_{max} has been measured, f(v) has the same value in each case to within 6%, (using Eshelby's (1969) expression for f(v) as given in Chapter 2), and even if the maximum spread is doubled on either side of the mean of the known values, f(v) still varies by only 13% throughout the whole range. It therefore seems reasonable to expect that, in practice, f(v) will remain substantially constant.

Of all the terms in Equation 3.16 perhaps the one of most uncertain magnitude is k, the numerical constant in the dimensional expression for kinetic energy used by Johnson and Holloway, although derived initially by Mott, (see Chapter 1). We noted in Chapter 1 that Hiorns and Venables (1961) assigned a value of unity to k although gave no justification for so doing, and that the most widely accepted value was Roberts and Wells' estimate of 44. This latter value was previously used to predict $\sigma c_b^{\frac{1}{2}}$ values for glass and pmma, and since these agreed quite well with experimental values of $\sigma c_b^{\frac{1}{2}}$, especially when a dynamic correction was incorporated into the analysis, this lent some support to this choice of value for k in these cases. However, it is not a priori obvious that k will always have the same magnitude, or that in any case its value will be exactly equal to 44 in real materials. k is effectively a measure of the extent to which the material surrounding the crack contributes to its kinetic energy, and the magnitude of k will therefore be largely dependent on the volume of material disturbed by the passage of the crack; the greater the terminal speed of the crack, the smaller this volume will be.

Mott argued that the volume of material disturbed by a crack progressing through a sheet of unit thickness would on dimensional grounds be proportional to kc^2. If, following Roberts and Wells, we consider the simple case of a crack travelling at a constant speed v_{max} for all values of crack length c, then the volume of material disturbed by the crack at any instant will depend on the

furthest distance travelled by the stress-waves generated by the crack. For a crack which has been in motion for a time t, the furthermost wavefront will have travelled a distance r from the crack origin, where $r = v_1 t$, and $t = c/v_{max}$, (Fig. 3.2)

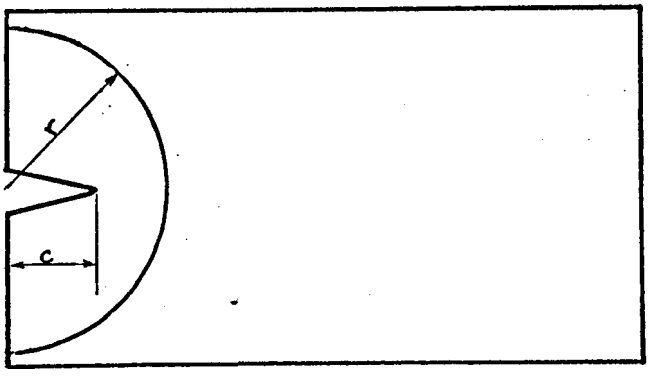

Fig. 3.2

Distance covered by furthermost wavefront.

In this case, $kc^2 \propto r^2$

and hence, $k \propto v_1^2 / v_{max}^2$

The expression $k(v_{max}^2 / v_1^2)$, which appears in the denominator of Equation 3.16, should therefore remain substantially constant, since variations in (v_{max}^2/v_1^2) are largely compensated for by variations in k.

A consideration of the likely variation in the two terms f(v) and $k (v_{max}^2 / v_1^2)$ therefore suggests that, in practice, the denominator of Equation 3.16 should remain substantially constant, and hence $\sigma c_b^{\frac{1}{2}} \simeq$ (Universal constant) $\times$ $(\gamma E)^{\frac{1}{2}}$. If the energy criterion is accepted as a generally correct explanation of the significance of the branching boundary, which is the author's view, then this constancy in the predicted multiple of $(\gamma E)^{\frac{1}{2}}$ provides additional support for the previously described method of measuring γ, which relied on the assumption that $\sigma c_b^{\frac{1}{2}} \simeq$ (Universal constant) $\times$ $(\gamma E)^{\frac{1}{2}}$.

3.5 Summary

This chapter was concerned with the phenomenon of crack-branching, and in particular with the empirical fact that, for a wide range of materials, $\sigma c_b^{\frac{1}{2}}$ = constant. Several attempts to explain branching and to account for this simple empirical relationship were examined, and of these, the energy criterion of Johnson and Holloway was found to be the most satisfactory. For several materials it was found that $\sigma c_b^{\frac{1}{2}} \simeq 3.8(\gamma E)^{\frac{1}{2}}$, where γ is the fracture energy of the material, and this suggested a simple means of estimating γ directly from the $\sigma c_b^{\frac{1}{2}}$ value. This method presupposed that $\sigma c_b^{\frac{1}{2}} \simeq 3.8(\gamma E)^{\frac{1}{2}}$ was generally true. A plausible justification for this assumption was obtained from an examination of the predicted expression for $\sigma c_b^{\frac{1}{2}}$ based on the energy criterion. This examination suggested that <u>in practice</u> $\sigma c_b^{\frac{1}{2}}$ would be expected to be approximately equal to (Universal constant).$(\gamma E)^{\frac{1}{2}}$.

The energy criterion of branching is, by its very nature, mechanism independent: it says nothing about how a branched-crack forms. This second aspect of branching, together with a general survey of the pre-branching events, occupies most of the remainder of this thesis, and constitutes the main bulk of experimental work.

CHAPTER 4

BASIC EXPERIMENTAL TECHNIQUES USED TO EXAMINE THE DETAILS OF FRACTURE SURFACES

4.1 Introduction

Up to now we have been primarily concerned with the problem of why, at branching, two cracks continue to propagate simultaneously over large distances. We now move to a different area of experimental work, undertaken to provide some information about the mechanism of crack division in three polymers: viz. polymethylmethacrylate, polystyrene, and an epoxy resin, (Araldite CT200).

The general method of fractography was employed as the main experimental procedure. This involves an examination of the fresh surfaces produced by breaking a specimen under known conditions, in this case under tension. The basic principle of this method is that events involving local or general perturbations of the crack-tip are effectively 'sculptured' on to the fracture surfaces, and by examining these surfaces one can learn much about these events, all of which occurred whilst the solid was in the process of breaking.

In this Chapter the techniques used to make the fracture surface observations are outlined, the main bulk of which involved optical microscopy.

4.2 Optical Microscopy

For the detailed optical examinations a Vickers Projection Microscope was used, and for examining the

coarser fracture surface markings and relatively large areas of fracture surface, a low power, (x 5 to x50), zoom stereo-microscope was employed.

For quantitative work on the topography of the fracture surfaces three methods were needed to cover the whole range of fracture surface features encountered. The height of some of these features relative to the surrounding fracture surface was less than a micron, whereas the larger features protruded by several hundred microns above the surrounding fracture surface. If the height, (or depression), of a fracture surface feature came into this latter category (i.e. $\gg 1\mu$), the fine focus control on the Vickers microscope could be utilised. For features displaced from the surrounding local fracture surface level by $\sim 1\mu$, a "light cut" method was employed, and for features displaced by less than 1μ a specially designed Linnik interferometer was used. A brief description of these two latter methods is given below.

(a) Light Cut Method

The light cut method is a particularly convenient means of measuring elevations or depressions of the order of a few microns and is most suitably employed if the change in level is relatively abrupt so that a sharp step is formed on the fracture surface.

The method involves placing a parallel line graticule between the light source and the objective lens, so that shadows are cast upon the surface under investigation, which is illuminated by oblique illumination. If the

surface is optically smooth, the shadows will be a facsimile of the graticule. If there is a region of fracture surface which is raised or depressed, then as the shadows pass over this region they will be displaced laterally by an amount which depends on the change in elevation. By measuring the displacement of the shadows the relative height of one area of surface with respect to an adjacent area can be ascertained. Except for very sharp steps, the method is limited to the measurements of level differences of $\sim 1\mu$.

(b) The Linnik Interferometer.

This instrument is essentially a Michelson Interferometer adapted for the study of the microtopography of surfaces, (Tolansky, 1955). Its advantage over other interference techniques is that no reference plate is required close to the surface under investigation. This enables high power objectives to be used with relative ease in situations where surface asperities would normally keep a reference plate sufficiently far from the surface to make it impossible to form low order fringes.

The optical arrangement is shown in figure 4.1, and Figs. 4.2 and 4.3 show the actual instrument.

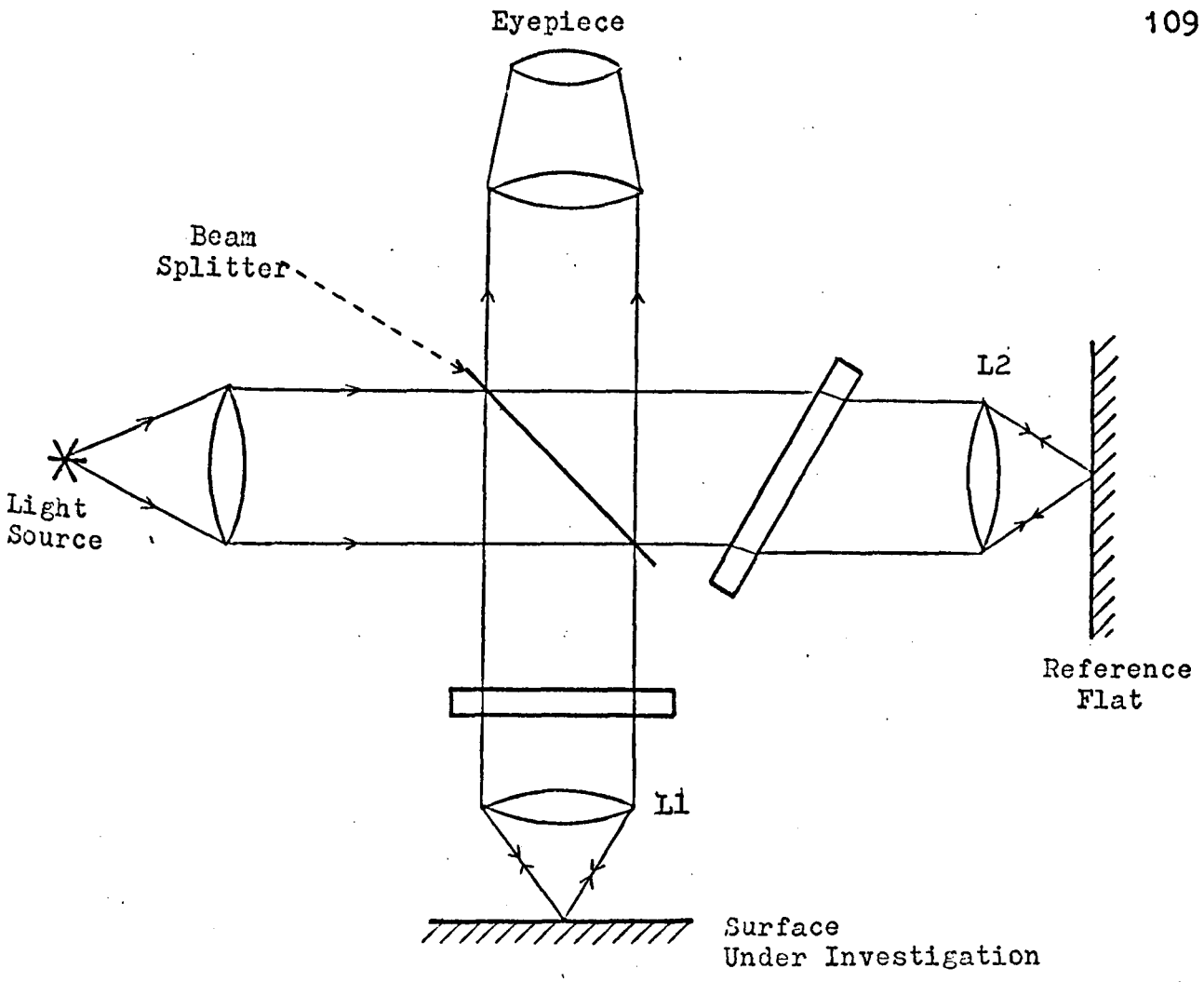

Optical Arrangement of Linnik Interferometer.
Fig. 4.1

A parallel light beam was projected on to a beam splitter. One of the beams which emerged was passed through a glass block and then through an objective L1 on to the surface under investigation, and the other was passed through a second glass block then through a similar objective L2 on to a flat, (although in this instrument not optically flat), reference plate, (Fig. 4.1). The glass blocks were incorporated into the light path of each beam to compensate for any difference in the lengths of the two light paths. Both glass blocks could be rotated in planes perpendicular to the light beams.

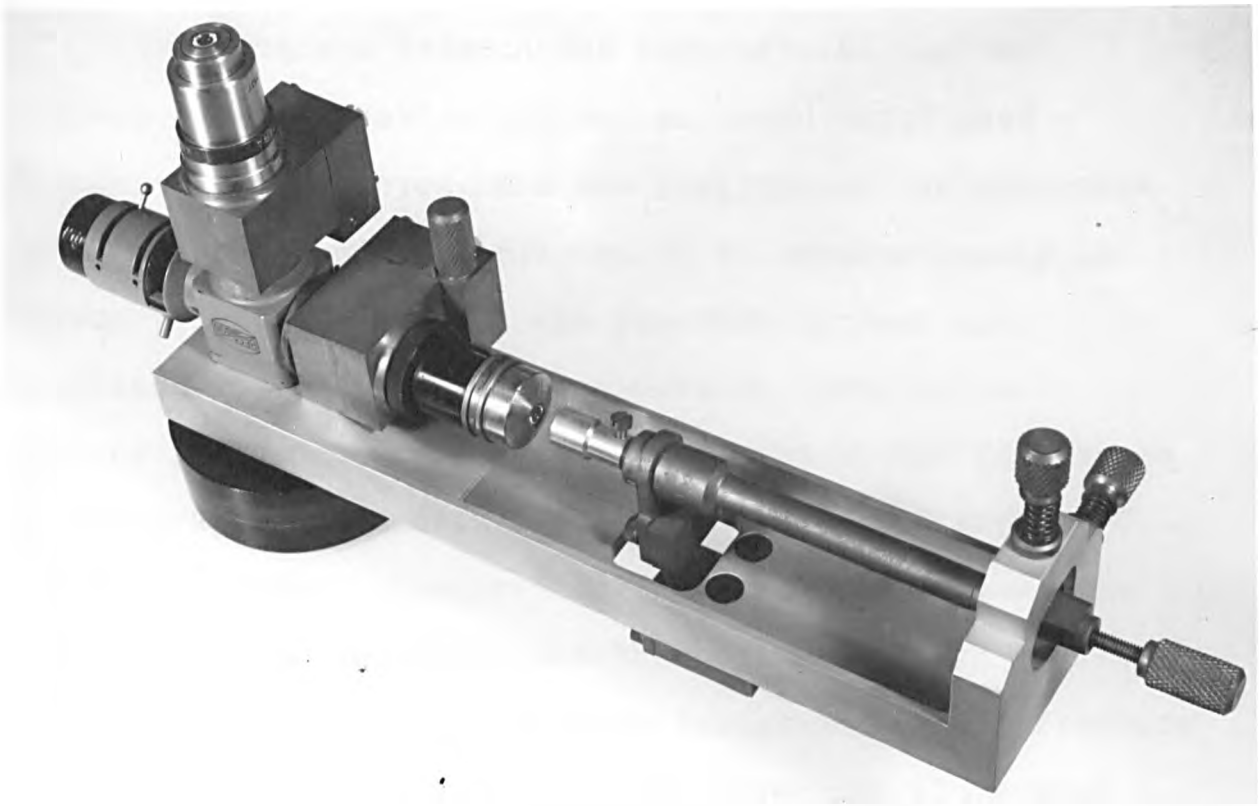

Linnik Interferometer.

Fig. 4.2

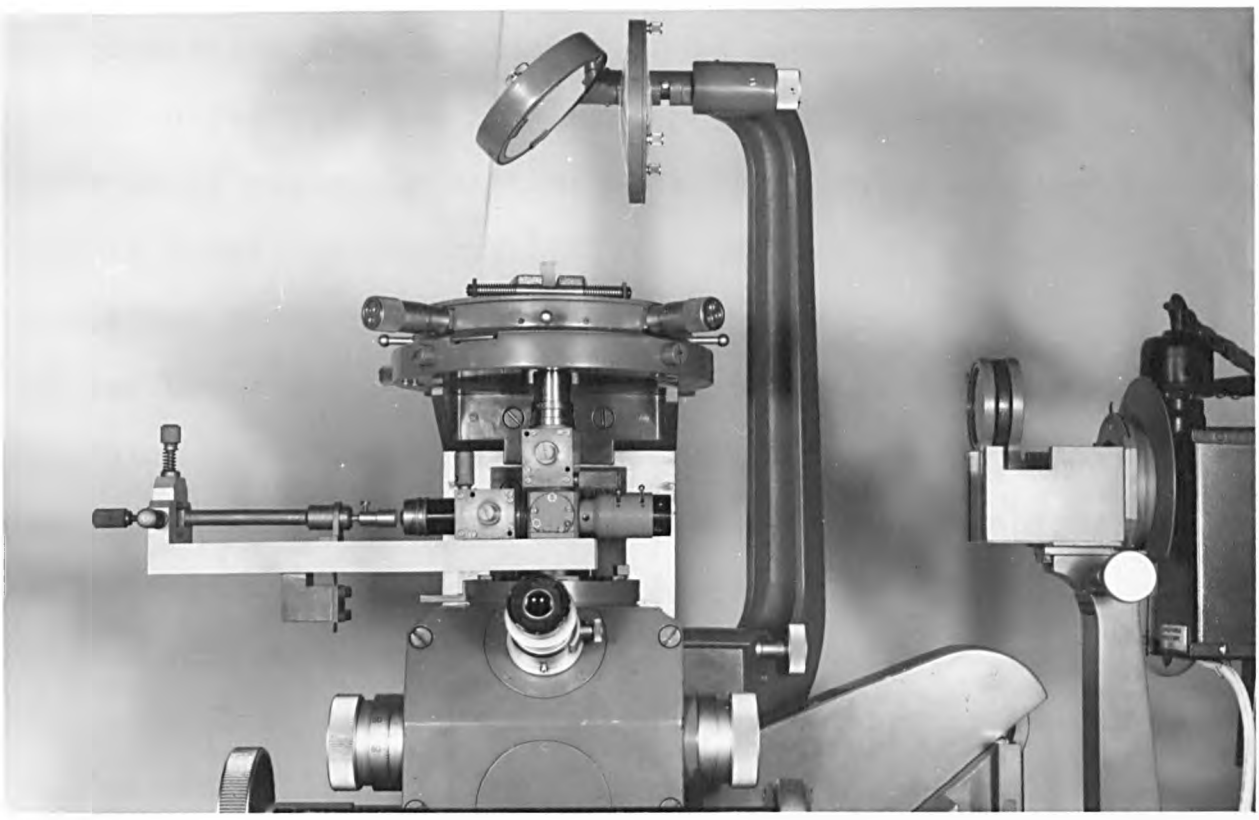

Linnik Interferometer mounted on the Projection Microscope.

Fig. 4.3

The distance between the objective L1 and the surface under investigation was adjusted until good focussing was achieved, and the position of the reference plate was subsequently adjusted to be simultaneously in focus. In this way both the fracture surface and localised interference fringes were in view, and a contour pattern was produced as a result of the difference in topography between the fracture surface and the reference plate. Compared to the fracture surface, the reference plate was flat, and the contour pattern therefore mapped out the surface topography of the fracture surface under investigation. The reference plate used was a microscope slide cover-slip which approximately matched the reflectivity of the plastics examined, and thereby enabled fringes of good contrast to be obtained.

The main drawback of this instrument was that the two objectives were un-matched. In commercial instruments matched objectives are obtained by sorting through literally hundreds of nominally matched objectives until a suitable pair is found, (Tolansky, 1963). The use of matched objectives guarantees that the glass path lengths of the two beams are the same, which greatly facilitates obtaining low order fringes. In this instrument, the difference in glass path lengths through the two objectives was compensated for by careful adjustment of the two glass blocks on a trial and error basis. For monochromatic light, critical adjustment was not absolutely necessary, but for white light the settings had to be critically adjusted since with white light, only low order fringes can be observed.

Once the instrument had been adjusted elevations of the order of $\lambda/10$ could be measured. For sharp steps it was necessary to use white light fringes, but in most cases, where one level sloped to another, monochromatic sodium light was used.

As well as information about the surface topography. it was also useful to determine the extent and position of subsurface cracks which had formed during the fracture process. To obtain this additional information one could often utilise the fringe patterns formed as a result of reflections from the interfaces associated with a sub-surface crack. If the crack sloped away from the fracture surface the angle of this slope could also be obtained by the normal thin wedge method.

A second approach, used in the case of the epoxy resin, was to gradually etch away the top layer of fracture surface so as to reveal the sub-surface cracks directly.

4.3 Etching Programme for CT200 epoxy resin

The etching procedure was developed as part of a more general programme to attempt to reveal the microstructure of the resin. After a series of tests with a variety of acids of various concentrations, N/6 chromic acid was found to be a suitable etchant for dissolution of the fracture surface. The resin was sequentially etched in this acid for one minute at a time at 343K. After each 1 minute etch the specimen

was washed in distilled water, carefully dried, and then examined under the Vickers microscope. By keeping a continual check on the extent to which the specimen had been etched in this way, over-etching of the specimen and complete removal of the subsurface crack, was avoided.

4.4 Electron Microscopy

Both scanning and transmission electron microscopy were used on occasions, although in general the observations made provided very little additional information beyond that obtained from the optical microscopy. For the transmission electron microscope, carbon replicas of surfaces were made by carbon evaporation, and these were removed from the surfaces by submerging the specimen in liquid nitrogen. The different coefficients of expansion of the carbon and the polymer broke the bond between the two, and the carbon could then be removed by immersing the coated specimen in water, and relying on the surface tension of the water to peel the carbon away.

Scanning electron microscopy, mainly of the fracture surfaces of polystyrene, was undertaken at Rolls Royce Ltd., Derby, through the courtesy of Dr. J.W. Johnson.

The electron microscope observations did not prove of great value, mainly because much of the useful information was obtained from an examination of the location and structure of sub-surface features. The electron microscope is, of course, restricted to the surface only.

In the next three Chapters the results of a detailed examination of the fracture surfaces of polymethylmethacrylate, polystyrene, and CT200 resin are presented, and then discussed. The photographic evidence is contained in a separate volume, and textual references to photographs in this volume are always preceded by the word "Plate". Reference to figures in the main volume are preceded by the word "Figure". Figure numbers and plate numbers have been kept separate, and where possible the plates have been arranged so that they may be compared.

CHAPTER 5

THE FRACTURE SURFACES OF POLYMETHYLMETHACRYLATE ("PERSPEX")

5.1 Introduction

It is probably true to say that the fracture surface morphology of polymethylmethacrylate, (pmma), has been examined more extensively than that of any other glassy polymer. Despite this, we feel that a sufficient number of problems remain to render further discussion worthwhile.

This chapter begins with a very brief review of some of the previous work undertaken on the fracture surface morphology of pmma, and the notion of a craze is introduced, which we shall require for some of the discussion in this, and in the following two chapters. The results of our own findings are then discussed in some detail.

5.2 Some previous work on the fracture surface morphology of pmma.

The fracture surface structure of pmma has been subject to investigation since the early 1950's; for example, Zandman, (1954), observed a change in the fracture surface appearance as the applied rate of loading was altered, and Wolock, (1958), noted a change with increasing molecular weight comparable to that reported by Zandman. Zandman's results are reproduced here as Fig. 5.1.

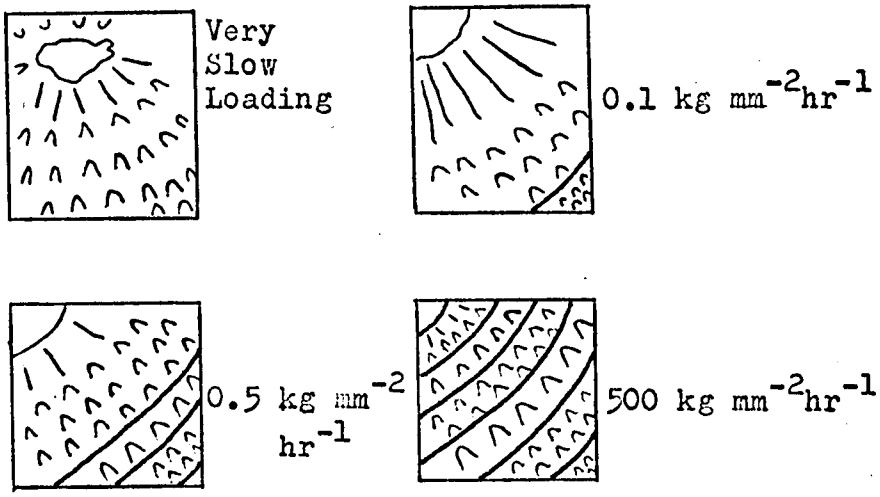

Figure 5.1.

(After Zandman 1954)

Although Zandman concluded that the observed changes were due to the applied loading rates, he also reported that specimen strength increased at higher loading rates. It is therefore possible that the increased strength associated with the higher rates of loading was in fact responsible for the changes in fracture surface appearance. Our own results suggest that this is likely to be the case.

The effect of temperature on the fracture surface appearance has also been reported, (Wolock et al 1959). A change in structure was noted for temperatures above 320 K. The same authors investigated the effect of pre-orientation of the polymer, and again a change in structure was observed, although the photographs in the original publication are not of sufficient quality to allow a direct comparison with unoriented specimens to be made.

In the late 1950's and early 1960's particular attention was devoted to the now famous coloured hues which arise on the fracture surfaces of pmma. One of the earliest reports of the presence of these colours was in 1956 by Busse, et al. Berry, (1959), and Wolock

et al (1959), both independently reported the presence of the colours, although the first attempt to explain their origin was by Higuchi, (1958). Later, Berry, (1959), and Newman et al, (1962), proposed a similar model to Higuchi's.

It was proposed that the colours arose as a result of reflections from the interfaces of a thin film, which was generated by the fracture process and remained on the resulting fracture surfaces. They argued that as a result of the high stresses near to the tip of the crack, the molecular chains in the material immediately ahead of the crack were oriented normal to the propagation direction. This oriented polymer was then broken by the oncoming crack, to leave a thin layer on each fracture surface with a refractive index sufficiently different from that of the bulk material to cause reflections at the interface between the film and bulk material, and thence interference effects.

Berry, (1961), gave the following diagram to illustrate the process.

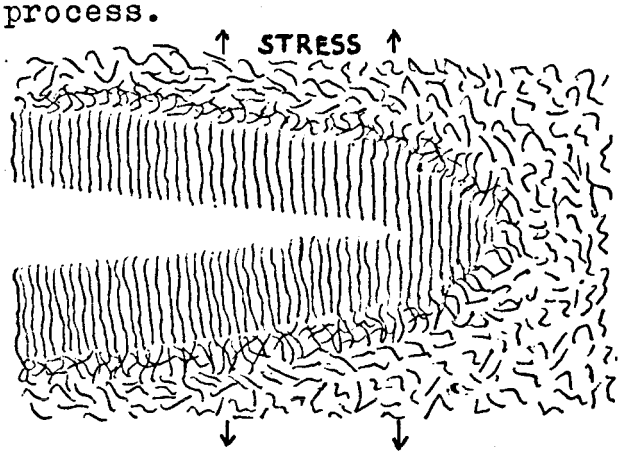

Fig. 5.2
(After Berry 1961)

The plastic work required to orient the polymer chains was also thought to be responsible for the high

value of the measured fracture energy compared to the calculated value of the surface energy: i.e. $\sim 150 Jm^{-2}$ compared with the calculated value of surface energy $\sim 0.5\ Jm^{-2}$, (Berry, 1961).

Higuchi assumed that the colours were formed by first order interference, and estimated the film thickness to be between 400 and 700nm. Newman et al, (1962), produced a gully across the film with a soft swab, and estimated the depth of this gulley to be $\sim$ 200nm. They proposed that the film thickness was of this order.

If specimens were left in laboratory air for long periods the surface colours vanished although the time taken varied markedly from specimen to specimen, (Wolock et al 1960). It was noted that the disappearance of the colours occurred by the fading of the original tint rather than by a colour change. The same authors reported that some organic solvents and organic solvent vapours accelerated the removal of the colours, although in this case, a change of colour appeared to be involved, (Wolock et al 1964).

They also noted that the colours rapidly disappeared on heating a specimen to 343 K, but here again a fading of the original tint was thought to occur.

In apparent conflict with this last observation, is the observation made by Kambour, (1965), that a shift to a lower order colour occurred when the fracture surface was heated locally with a hot needle, a result which

also implies disagreement with Higuchi's proposal that the surface colours were first order. Our own observations confirm that different sequences of colour disappearance do occur under these two conditions; viz general heating of the whole area, and local heating with a hot needle. In the latter case however, it is difficult to distinguish the effects of local heating from the inevitable mechanical compression of the surface film which occurs in locating the needle.

The proposal that the surface film was merely oriented polymer is no longer accepted. Indeed, Berry, (1964), criticises his earlier model on several accounts. For example, he argues that the high degree of orientation required to cause the pronounced difference in refractive index between the film and the bulk polymer, would demand a large contraction of the film in the transverse direction, which is not observed. (Some contraction is observed, but this is insufficient to allow for the large elongation in the longitudinal direction implied by this model). Berry also noted that in oriented pmma, it is easier to propagate a crack parallel to the alignment direction than normal to the alignment. But, he argued, if the surface layer were simply a region of oriented polymer, then one might expect lower energy requirements when a crack is propagated normal to the alignment direction. (In proposing this objection, Berry tacitly assumes of course, that the mechanism of plastic deformation is identical in oriented and unoriented material).

The currently accepted explanation of the surface colours is that a thin layer of craze remains on the fracture surfaces, and this gives rise to thin film interference effects in reflected illumination. This view is similar to the previous one, in that both account for the surface colours in terms of thin film interference, but it differs in that a craze is thought to have a structure different from oriented polymer.

5.3 Crazes

When subjected to a tensile stress many thermoplastics become flecked with small crack-like markings. The development of these marks is time dependent, is accelerated by the presence of certain organic solvents, and the marks rapidly lengthen and slowly thicken. These small marks are called crazes, Plate 5.1.

Like cracks, crazes reflect light, are planar, and the plane of the craze is normal to the direction of the principal tensile stress; indeed, Maxwell, (1949, 1950), Russell, (1950), Wolock et al, (1959), and others, thought that crazes were small cracks, but Hsiao and Sauer, (1950), demonstrated that a specimen completely traversed by crazes through its cross section was still load bearing. In 1953 the latter authors reported that the growth characteristics of crazes differed from those of cracks.

Crazes usually start at the surface of a specimen or at foreign inclusions within the polymer, (Newman et al 1957). Bessonov, (1959), demonstrated that surface crazes were

wedge-shaped, the apex of the wedge pointing away from the surface; and postulated a craze structure in the form of filaments aligned normal to the major axis of the craze and parallel to the applied tension direction. In 1962, on the basis of electron microscopy and X-ray diffraction studies, Spurr and Niegisch reported a fibrillar structure within polycarbonate crazes, and, although they were observed with more difficulty, within pmma and polystyrene crazes. More recently, Kambour, (1968), proposed that polystyrene crazes contained oriented material, on the basis of low angle X-ray scattering experiments.

Kambour, (1964), measured the refractive index of 'craze matter' in pmma. He measured the critical angle for total internal reflection at the craze-polymer interface, and calculated a value of 1.32 for the refractive index of the craze, compared with 1.5 for the normal polymer. Using the Lorenz-Lorentz equation he evaluated the average density of the craze, and concluded that pmma crazes contained $\sim$40% voids. On the basis of this result Kambour argued that the crazes were regions within the polymer which had undergone a substantial molecular alignment in the direction of applied tension, and in which a large proportion of the volume was occupied by voids. He subsequently examined the size and shape of the voids using electron microscopy, and concluded they were spherical holes $\sim$20nm in diameter, and, on the basis of some liquid exchange studies, (1969), that they were interconnected.

Kambour found that the same basic model of a craze; viz: an aggregate of interconnected spheroidal holes $\sim$ 20nm in diameter embedded in a matrix of oriented polymer, served for a variety of different thermoplastic polymers.

The refractive index of the surface film left on pmma fracture surfaces was also determined by Kambour, (1964), again from measurement of the critical angle at the film-polymer interface. The refractive index was found to be 1.32, equal to the refractive index of crazes in this material. He concluded that the fracture surface layer was a film of craze, and that the fracture process involved the formation and subsequent rupture of a craze. Supporting this view is the later work of Murray and Hull, (1969), for example, in which they claim that in compression-moulded polystyrene, cracks are nucleated by the formation of cavities within larger crazes.

It is now generally agreed that crack propagation in many thermoplastics involves the formation and rupture of crazes.

5.4 The role of Crazes in the energetics of fracture.

Plate 5.2 shows a field of crazes surrounding the crack tip in a rectangular specimen of pmma. The crack had been loaded by driving a wedge into its open end. The formation of crazes in the region surrounding the tip of a loaded crack has been noted by several authors, (e.g. Hull 1970, Sternstein *et al* 1968.). The crazes formed around

a crack or notch are thought to grow perpendicular to the major principal tensile stress direction when this stress exceeds a certain fixed value, (Sternstein et al 1968).

The craze which is formed parallel and contiguous to the crack plane, (the crack-tip craze), is of particular importance, since in general it is this craze which ruptures when the crack extends. (The other crazes do rupture when the crack extends very slowly or when the crack is advancing very rapidly during the latter stages of tensile fracture, (see later).)

Kambour, (1966), examined the crack-tip craze in pmma. He viewed this craze through the side of a specimen in a direction normal to the crack plane, and from the optical interference fringes produced by reflections from the craze-polymer interfaces, he estimated the shape and thickness of the craze as a function of its distance from the crack tip. Fig. 5.3 illustrates his results.

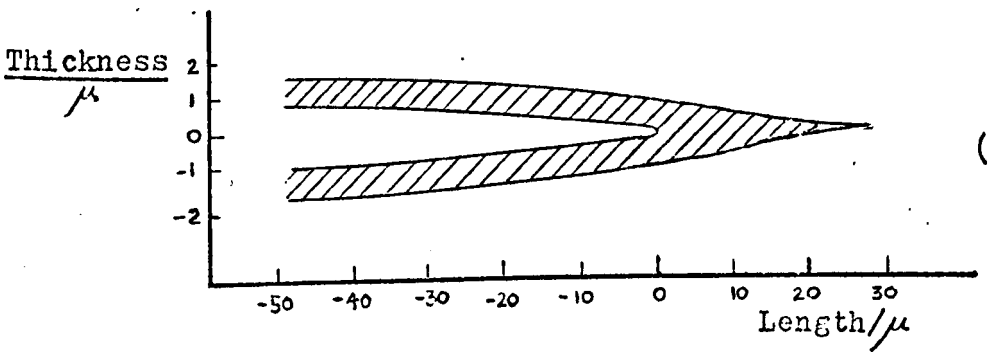

Fig. 5.3

(After Kambour (1966))

These dimensions were, of course, for a craze which had grown ahead of a static crack, and it was tacitly assumed that the refractive index of the craze was constant for the whole of its length.

Using 540nm monochromatic light he observed six fringes in the craze when the specimen was under zero applied

stress, and this number gradually increased as the applied stress increased, and reached a maximum of nine when crack extension was imminent. By relaxing the applied stress to zero, the fringe number reverted to six, and on the basis of this reversibility in the number of fringes, Kambour argued that he was extending the craze elastically. The Lorenz -Lorentz equation was used to calculate the strain which the craze underwent, and he concluded that 100% elastic strain occurred as the applied stress was increased from zero to the maximum value prior to crack extension. (In fact Kambour seems to have made an algebraic error in this calculation: re-calculation shows the extension to be $\sim$67%).

He argued that the elastic energy required to extend the crack-tip craze was entirely dissipated when the craze broke, and this was the most significant sink of energy dissipation. Taking Berry's, (1962), value of 140 Jm^{-2} as a reference for the fracture energy of pmma, void formation was estimated to contribute $\sim$2%, plastic work of craze formation to contribute $\sim$14%, and elastic extension of the craze to contribute $\sim$40% to this fracture energy. (This latter value is based on 100% strain. Using the corrected value of 67%, the contribution made by elastic extension of the craze is reduced to $\sim$18%).

More recent experiments, (Linger 1967), have shown that the fracture energy of pmma is approximately twice that reported by Berry, and consequently the percentage contributions made by the above processes are about half the stated

amounts. Thus, by considering energy dissipation processes in the crack-tip craze, about 25% of the total fracture energy can be accounted for, and this value can be obtained only if 100% elastic extension is assumed. With 67% elastic extension, the total contributions amount to $\sim$16% of the measured value.

Therefore, even if Kambour's arguments concerning the three main contributions to the overall fracture energy are correct, and even here there is some doubt, it seems unlikely that a full explanation can be given of the measured fracture energy if only the crack-tip craze is considered. Our own experiments have shown that whenever a stress sufficient to cause crack extension was applied to a specimen, a field of crazes similar to that shown in Plate 5.2 had already been established. The energy required to form these crazes should therefore be included in any inventory of energy dissipation processes. Most of the work on the fracture of pmma has concentrated on the crack-tip craze, because it is here where it is thought that most information will be derived on the conditions of crack growth. However, just because the condition for crack growth is governed by the craze at its tip, it does not follow that the fracture energy can be attributed solely to the formation and rupture of that single craze. To concentrate on the crack-tip craze alone is to underestimate the total amount of plastic work involved during the formation and extension of a crack. By tacitly ignoring all crazes other than the crack-tip craze it is

not surprising that Kambour can, at best, account for only ~ 25% of the total energy requirements for crack extension.

During the course of his discussion, Kambour refers to the 'plastic work of craze formation', and, as we have seen, distinguishes this from the energy required for craze extension and the energy required to form the voids within the craze. This being the case, then it is not clear what is meant by the former statement, if according to Kambour's own proposal a craze is a region of oriented polymer with significant void content. If the craze does contain oriented polymer then there seem to be two possible interpretations of the subsequent elastic extension of the craze. Firstly, the elastic energy of craze extension is configurational, and the chains at zero applied stress are incompletely aligned. Application of stress completes the alignment of chains between voids into a parallel array. If this is the case, it is difficult to account for the plastic/elastic transition that Kambour proposes, since there is no fundamental difference in the process of craze extension from its formation through to its rupture. Yet, Kambour argues that the craze undergoes 60% plastic strain, followed by a further 100% elastic strain. Alternatively, if the chain segments between voids are already fully, or almost fully aligned in the pre-existing crack-tip craze, then the elastic energy would be equal to that required to stretch these already aligned chains. In this case, it is difficult to account for the large amount of strain which apparently occurs on applying the load.

The experiment from which Kambour concluded that the craze underwent a large elastic extension is itself inconclusive, since it does not allow for elastic energy atored within the specimen as a whole. It is quite feasible, for example, that the crack-tip craze was extended and compressed plastically as a result of elastic relaxation in the specimen. If this were the case, then the same reversibility in fringe numbers could easily occur, and this could be misconstrued to mean elastic extension of the craze. Clearly, a more refined experiment is required to examine this possibility.

More recently, a model has been proposed which goes some way towards removing some of the problems associated with the 'traditional' view of craze formation based largely on Kambour's work. The crazing process is likened to 'foaming'; i.e. the emphasis is laid on voiding. According to this model, proposed initially by Haward, (1973), the crazing process consists of the simultaneous formation of many voids, the average separation between them being such that the plastic zone of any one void overlaps those of its neighbours. The interpenetration of plastic zones is considered to be necessary, since calculation shows that the formation of a single void would be most unlikely at stresses below the yield stress. The mechanism of plastic deformation which is thought to occur between voids is not discussed in any detail.

According to this model the craze is no longer considered to be a local highly oriented matrix containing voids; it resembles an open-cell foam. Therefore, in

Kambour's terminology, the plastic work of craze formation is the work done in forming this foam structure. Whether this foam undergoes some degree of orientation as it is strained is then a separate question. In the case of pmma there is circumstantial evidence to suggest that the craze film left on surfaces exposed by fracture is not in fact highly oriented. This is discussed in a later section.

In the next section the tensile fracture surface appearance of pmma is described, and although based largely on our own observations it is recognised that in some respects the descriptions duplicate previously published work.

5.5 The Tensile Fracture Surface Appearance of pmma

Specimens of pmma broken under uniaxial tension at a fracture stress sufficiently high to cause branching display a characteristic sequence of markings, Plate 5.3. This sequence can be divided into the series of distinct zones shown schematically in Fig. 5.4.

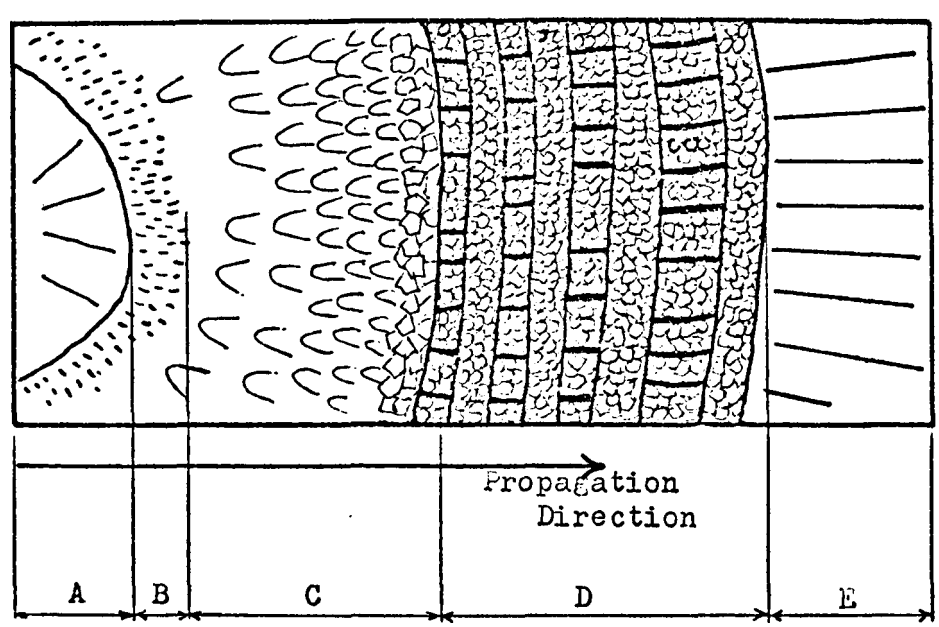

Fig. 5.4 Plan view (Not to Scale)

The first zone, (Zone A), surrounds the origin of fracture and is highly reflecting. When viewed in reflected white light, patches of colour can be seen over its surface. This zone ends quite abruptly, and there is a complete change in fracture surface appearance at the start of zone B. This second zone displays coloured hues; it consists of elongated features of one colour on a smooth background of another colour. Sometimes zone B contains an isolated hyperbolic-shaped feature, similar to those shown in Plate 5.4, although there is a definite boundary after which many such features are produced. This boundary marks the onset of the third zone, designated C in Fig. 5.4, and also referred to as the 'Conic Zone'. The conic shaped features formed in the early part of this zone have in most cases a set of roughly circular interference fringes associated with them. These fringes are concentric about the 'focus' of the feature, and have been likened to a distorted set of 'Newton's Rings' (Kambour 1965). The conic features are superimposed on a mottled background structure, Plate 5.5. This background structure exists between conics and within conic boundaries, although the general direction of the mottling is different in the two cases. Between conics it lies in a direction roughly parallel to the general direction of fracture propagation, whereas within conics it is radial about the 'foci' of the features. Small striations also invariably radiate from the conic foci, and where these meet the conic boundary they are terminated.

Zone D consists of a series of relatively rough regions of surface, separated by smoother regions, the overall effect being a series of bands lying roughly normal to the general direction of fracture propagation, Plate 5.6. The structure of the surface in the smoother areas is identical to that at the end of the conic zone. The rougher regions consists of a series of 'plateaus' at different levels, and the structure of each 'plateau' also resembles the end of the conic zone. Between each plateau, there is a sharp step up or down to its neighbour. The transition to this zone is not well defined, and before a definite banded appearance is produced there are normally isolated patches of the rougher surface, Plate 5.7.

As distance from the fracture origin is increased within zone D the width of successive rough regions increases, although the spacing between them, (i.e. the width of the smoother strips), is relatively unchanged. Furthermore, with high strength specimens a few wide rough strips are produced, whereas a larger number of narrower strips are formed with lower strength specimens.

The final fracture surface zone, (labelled E in Fig. 5.4) corresponds to where the fracture has branched.

5.6 Quantitative measurements relating to the onset of each zone.

The measurements described in Chapter 3 were extended to each zone boundary in turn. The results are presented in Table 5.1.

TABLE 5.1

Zone Boundary	Magnitude of $\sigma^2 c$ for this zone boundary (MNm^{-3})
Zone B	0.67 ± 0.05
Conic Zone (Zone C)	1.17 ± 0.07
Zone D	4.71 ± 0.13
Branching Zone (Zone E)	17.39 ± 0.18

These results show that a critical value of $\sigma^2 c$ can be associated with the onset of each zone, and this is why we suggested earlier that Zandman's reported change in the fracture surface appearance with applied loading rate, was in fact more likely to reflect the changes in strength which accompanied the different loading rates: our results indicate that the stronger the specimen the shorter the distances from the origin of fracture to the onset of each zone, and this is just what Zandman observed.

5.7 The Structure of some of the Fracture Surface Zones Related to the Fracture Process.

In the time available it was not possible to examine every zone with equal thoroughness. We concentrated mainly on those structures which it was felt would provide most information on the mechanism of branching in this material. Furthermore, as indicated in the introductory paragraph of this chapter, many of the structures have been examined prior to this work, and attempts have been

made to relate them to the fracture processes. These earlier interpretations have been incorporated into our own discussion, and in some cases they were the starting points of our own investigations. To a large extent this made our task easier, although it is felt that many of the interpretations so far offered are far from satisfactory, either because they are incomplete or because they tend to oversimplify the situation.

(a) Fracture surface zone A.

Zone A has generally been considered to have formed by slow growth of the crack, (e.g. Wolock 1963), and the end of this zone to mark the onset of catasrophic failure, (e.g Beardmore 1968). In no case, however, has evidence been put forward to support either of these claims, other than that zone A surrounds the origin of fracture.

It seemed *a priori* possible, however, that if zone A were produced during slow crack propagation, then the structures found on this zone would be similar to those formed when the crack is known to propagate slowly. To investigate this possibility, a crack was grown slowly in pmma by double cantilever cleavage, and the fracture surfaces so produced were compared with zone A. Finite crack growth could be observed several hours after the initial deflection of the cantilever arms had occurred, even though the deflection remained constant, but the rate of crack growth was very slow, ($\sim$ mm hr^{-1}), arguably slower than would occur at the early stages of

tensile fracture. Nonetheless the fracture surfaces so produced were very similar to zone A, which is consistent with the view that this zone was produced by slow crack growth.

Plate 5.8 shows a detail in zone A from a typical tensile specimen, and Plate 5.9 shows a detail of the fracture surface produced by the method just described. In both cases there are broad dark lines which lie roughly parallel to the general direction of propagation. These lines correspond to sloping surface between two different levels. The fracture surface between these dark lines in both cases has a fine stippled appearance, and is traversed by isolated thin linear features which lie roughly perpendicular to the general direction of fracture propagation.

Whilst a crack was propagating between the two cantilever arms observations were made of its tip through the side of the specimen in a direction parallel to the crack plane, using a low power stereo microscope. It was found that crack extension was discontinuous, and involved the rupture of more than one craze. Typically, the crack would pause and during the pause period, a craze either above or below the general crack plane would rupture slowly, and the tip radius of the main crack would slowly increase. Eventually, the main crack and the ruptured off-axis craze joined, the region between the two seeming to undergo significant yielding. The crack then proceeded by further growth and rupture of the off-axis

craze, with the craze ahead of the crack taking on a tapered shape similar to that proposed by Kambour.

The implication of these observations is that zone A of the tensile sequence was formed by the rupture of more than one craze. This is consistent with the existence of different levels of fracture surface separated by sloping regions. Furthermore, the high degree of permanent deformation which was always observed when two cracks at different levels joined, suggests that the production of these sloping regions of fracture surface possibly involved significant local yielding of the polymer, over and above that involved in the production of individual crazes.

The fine linear features which lie roughly normal to the direction of propagation, can, under suitable illumination conditions, give rise to complex interference patterns, Plate 5.10. Sometimes two sets of superimposed fringes of different spacing can be observed. These fringes suggest that a thin wedge of refractive index different from the bulk polymer and oblique to the general fracture plane exists beneath the exposed surface. The thin linear feature which is present on the surface, is thought to mark either the intersection of the wedge with the fracture surface, or some perturbation of the fracture surface caused by the proximity of this wedge.

Fig. 5.5 is a diagramatic sketch of one of these wedges. The two sets of interference fringes which were

sometimes observed are thought to arise from the interference of reflections from the boundaries of the two regions shown cross-hatched in the diagram.

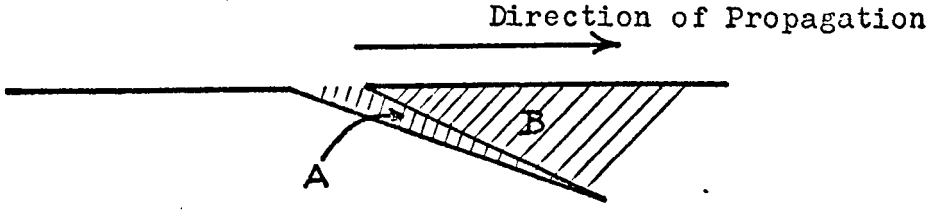

Fig. 5.5

The first of these, labelled A, corresponds to the thin oblique wedge of different refractive index, and the second to the intervening material between this wedge and the exposed surface.

These wedge structures and the linear features on the exposed surface with which they could be associated were not investigated in great detail, although it would appear that they arose only when several roughly parallel crazes were produced during the fracture process. It seems possible that the wedge structures correspond to oblique crazes formed between two such parallel crazes.

Similar linear features were observed on the fracture surfaces of the other two materials examined, (viz: polystyrene and CT200 epoxy resin), and in the case of the polystyrene again they arose whenever the fracture process involved the formation of several roughly parallel crazes. Furthermore, Hull (1970), has shown that when a crack is propagated through a field of pre-formed parallel crazes in Polystyrene, so that the crack runs parallel to the crazes within this field, then oblique secondary crazes are formed during fracture

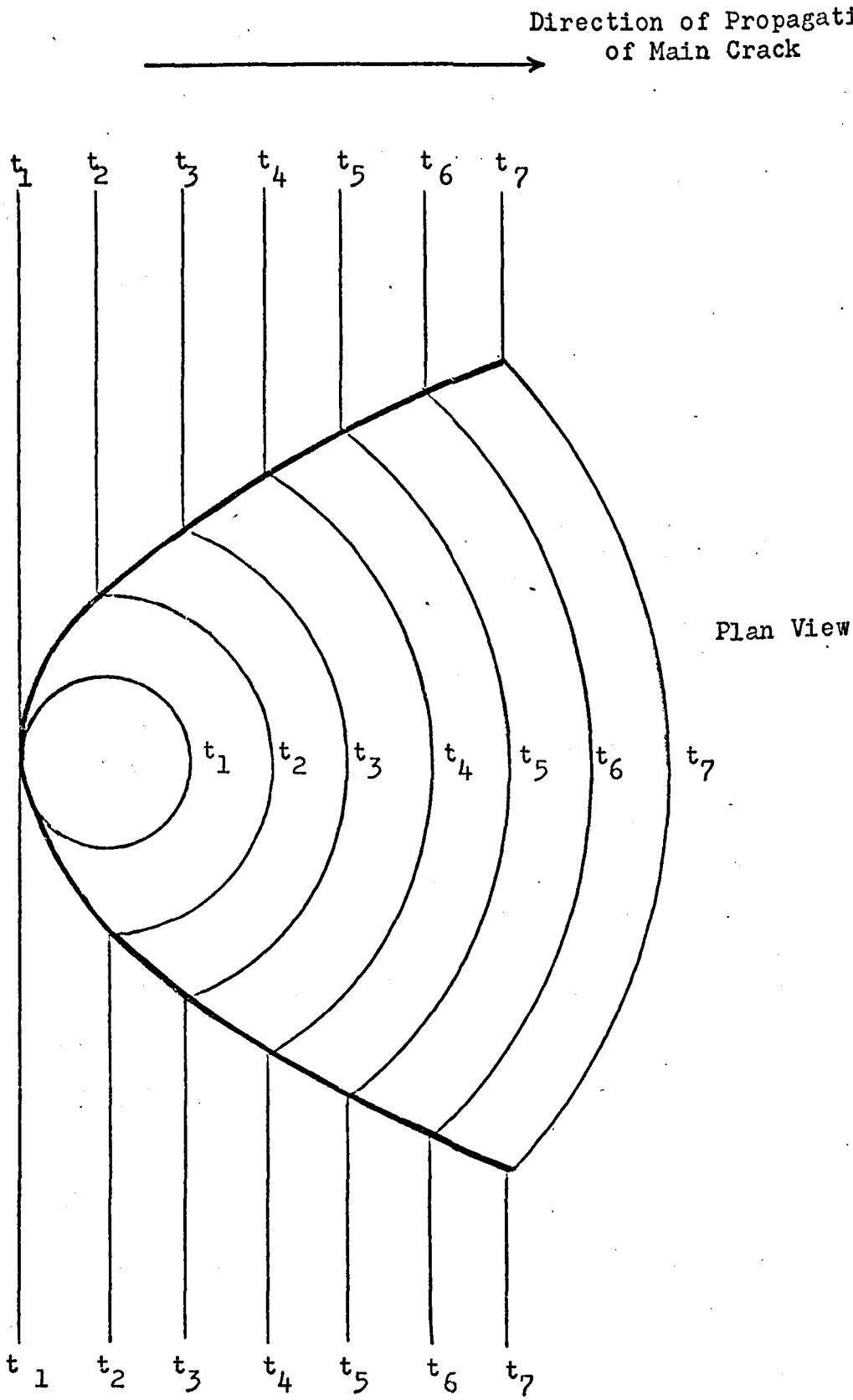

Formation of Conic Feature
(After Berry 1964)

Fig. 5.6

which link the pre-existing parallel crazes. On the resulting fracture surfaces the oblique crazes leave fine linear structures similar to those just described. Recent experiments in this laboratory, (Lilley and Holloway 1973), have revealed the presence of craze-like marks around the tips of loaded cracks in CT200 resin so that, in this case also it is possible that the fine lines correspond to the interaction of an oblique craze with the exposed surface.

(b) The Conic Zone (Zone C of Fig. 5.4)

Schwarzl et al (1956), offered an explanation for the formation of the conic features which is now generally accepted. As it stands, however, the model merely accounts for the general shape of the boundary of such features.

Schwarzl argued that a conic feature would be formed if a crack with a relatively straight leading-edge interacted with a secondary crack of circular perimeter, growing radially. A plan view of the proposed interaction is shown in Fig. 5.6. The shape of the resulting feature would depend upon the relative speeds of the two interacting cracks.

An assumption which is implicit to this model and which is not normally made explicit, is that a "conic feature" will be produced only if the perpendicular distance between the planes of the two interacting cracks is less

than their "collision cross-section"; i.e. less than twice the average radius of curvature of their tips. If the perpendicular distance is greater than this, then it does not follow that a conic feature, (in the sense of a conic shaped line boundary, and from hereon called a Conic feature), will be formed, although the locus of the points of interaction of the main and secondary cracks may still be conic-like. Other features can be produced which resemble Conics in shape but have significantly different morphologies: examples of these are discussed in Chapter 7.

To see why this "collision cross-section" condition must be imposed, consider Fig. 5.7.

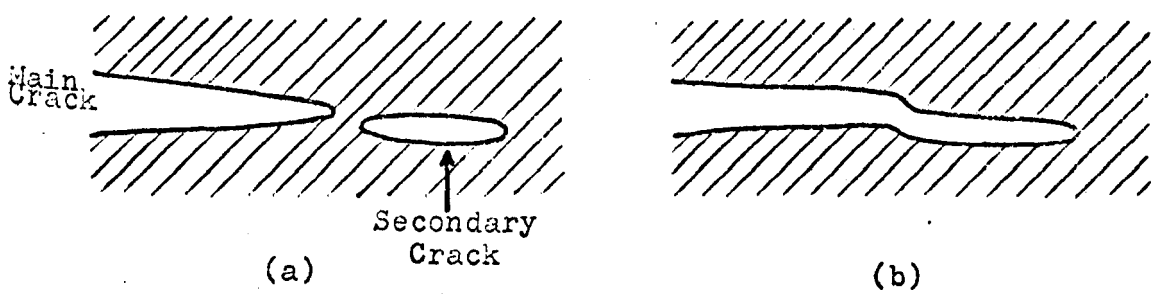

Fig. 5.7

In this figure two cracks approach, the perpendicular distance between the two crack planes being less than the average of the two crack tip radii. When the cracks meet, (Fig. 5.7b), they effectively 'collide' and leave a sharp step on the resulting fracture surfaces. When viewed from a direction normal to the surface, this step will appear as a fine line.

When the distance between the two cracks is greater than the average crack-tip radius, the two cracks

can overlap prior to joining; the resulting boundary of interaction will not then be a simple fine line and should show interference effects in reflected illumination, Fig. 5.8.

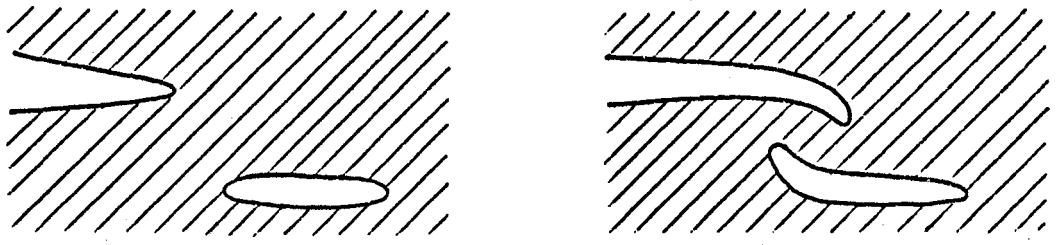

Fig. 5.8

Although detailed measurements have shown the level difference across Conic boundaries always to be less than the tip radius of a static crack in pmma, it was rarely the case that the boundary was a simple step on the fracture surface. The boundary was often a ridge of material typically 0.3μ in height on the matching features found on both fracture surfaces, and on occasions interference effects could be detected along the boundaries, Plate 5.11. These observations suggest that although the inter-planar separation of the two cracks was less than their "collision cross section", the interaction between them possibly involved local drawing of the intervening material as they came into close proximity, thus leaving a slightly raised ridge on both fracture surfaces along the locus of the points where the two cracks joined. This possible modification to the basic interaction is shown in Fig. 5.9 , (p. 140).

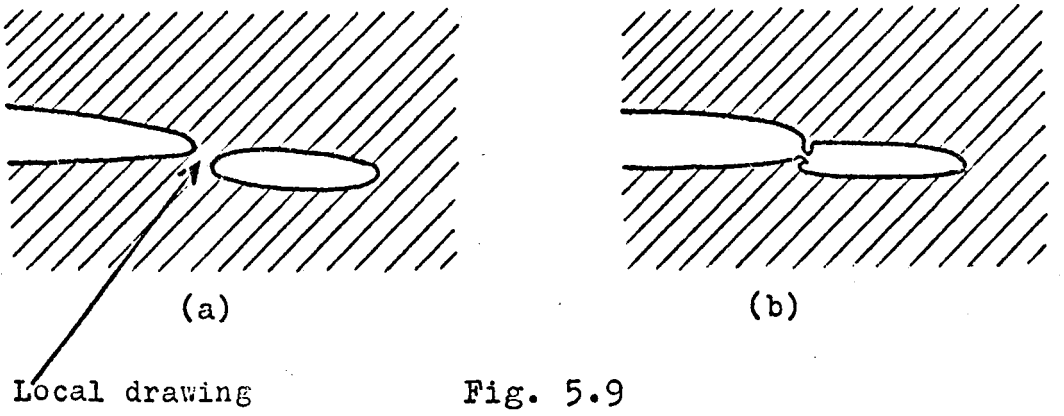

Fig. 5.9

The magnitude of the level difference across Conic boundaries indicates that the secondary cracks leading to Conics are formed within a thin band, approximately 1μ wide on either side of the crack plane, as shown in Fig. 5.10

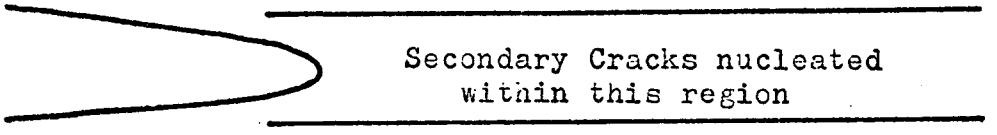

Fig. 5.10

The most obvious implication of this geometrical restriction is that the secondary cracks were all formed within the main crack-tip craze. If they were nucleated beyond the end of the crack-tip craze, it is difficult to see why they were <u>always</u> nucleated within such a restricted band on either side of the main crack plane. Only at the start of the next zone does local cracking occur outside this narrow band, and the fracture surface features so formed are then quite different and require $\sigma^2 c$ to pass the next critical value corresponding to the C-D zone transition.

Evidence in support of the view that the secondary cracks giving rise to Conics were nucleated within the main crack-tip craze comes from the 'Newton's rings' which are associated with Conics. The presence of such

ring patterns implies that the craze film undergoes a change in thickness within Conic boundaries. The order of the fringes indicates that the film is thinnest near to the focus of a Conic, and progressively thickens as the boundary is approached. Moreover, the shape of the fringes indicates that the thickening of the film is not symmetrical in all directions away from the focus: it thickens more rapidly in a direction towards the closed end of the feature, than in the direction away from the closed end. The interference patterns which resemble Newton's rings are observed only within the boundaries of the Conics formed in the early part of the conic zone. The Conics formed in the later stages of this zone, (which are reminiscent of polygons rather than conics), normally have a single rather hazy coloured area surrounding the focus, and no more. The colour of this region of interference contrast is invariably a dull yellow. In the following discussion, concerning the Newton's rings fringes, we refer only to Conic features formed in the early stages of the conic zone.

The microscope attachments described in the preceding chapter were utilised to investigate the curvature of the top surface of craze film within Conic boundaries. It was found that although there was some curvature, it was insufficient and often in the wrong sense to account for the order and the sequence of the interference fringes observed. For example, in white light, fringes up to

third order red were observed, corresponding to a thickness of ~750 nm, and a thickness change from the focus to the boundary of the Conic of about 600nm, since immediately around the focus the fringe was invariably a dull grey. The change in the level of the top surface was at most about 250nm, and sometimes no curvature at all could be detected. At the focus itself a sharp dip or rise of the exposed surface was detected in most cases, and there was a male-female match between these sharp asperities on complementary features.

The most important implication of these observations assuming that the craze layer has uniform optical density, is that the 'Newton's ring' fringes arise from a variation in the thickness of the craze film caused by a significant curvature of the bottom surface of this film: that is, the craze-polymer interface is closer to the exposed surface within a conic feature than it is elsewhere.

Fig. 5.11 is a schematic representation of two sections through a typical Conic feature, based upon these observations.

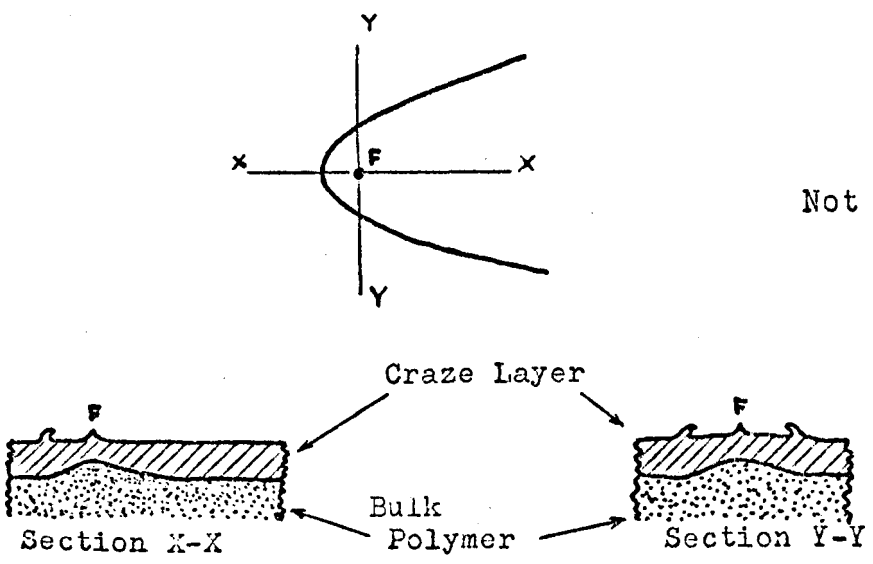

Fig. 5.11

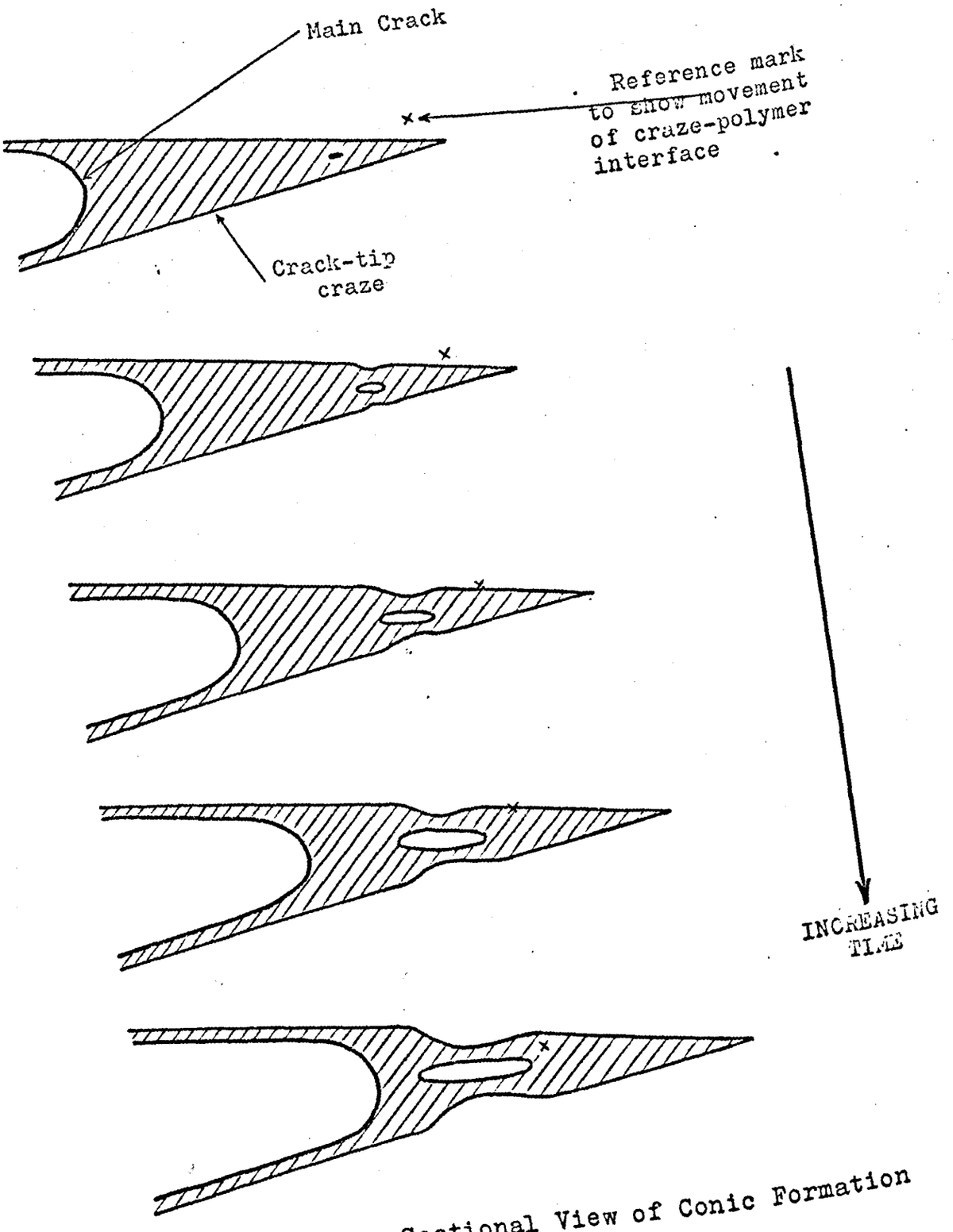

Sectional View of Conic Formation

Fig. 5.12

Given that we are correct in thinking that the entire craze-film thickness produces the observed fringes, then it is possible to account for the formation of a Conic feature in terms of an advanced rupture within the crack-tip craze if it is assumed that craze thickening occurs predominantly by movement of the craze-polymer interface through the material; i.e. by the formation of new crazed material rather than by extension within the initial interfaces. Once a local rupture has occurred within the main crack-tip craze, this will unload the craze above and below it, and thereby prevent further growth of this local section of craze. As the secondary rupture grows, more and more craze will become unloaded in this way, and consequently a progressive change in thickness of the craze layer will occur on either side of the secondary fracture, and it will be at its thinnest in the region where the secondary fracture was first nucleated. Fig. 5.12 illustrates the process of Conic formation.

If, on the other hand, the predominant mode of craze thickening were progressive extension of the previously crazed material within the initial interfaces, then one would expect the top surface of the craze film to be curved and the bottom surface to be relatively planar. In the next Chapter it is suggested that this is the case in polystyrene; i.e. that there could be an important difference in the process of craze thickening in the two materials.

According to Kambour's model of a craze as a region of highly oriented polymer containing voids even before it is ruptured, then the surface film having formed from the rupture of such a region should consist of highly oriented material, or show evidence of significant relaxation following rupture. One piece of evidence which suggested that the craze film on pmma was not highly oriented came from experiments undertaken initially to investigate the disappearance of surface colours, (in particular those within Conic boundaries), when a specimen was heated. Although the colours disappeared, the fine structure on the top surface and the level differences, for example across Conic boundaries were, as far as could be detected, unchanged. Plate 5.12 shows the effect of locally heating a surface with a hot needle, in a similar manner to that described by Kambour, (1965). No significant change in the appearance of the fine structure or in the level differences across Conics occurred during such thermal treatment. Neither were any changes in surface structures apparent when a specimen was heated in the oven at 346 K.

Kambour argues that the disappearance of the colours arises because the craze layer collapses, and this interpretation is consistent with his model of the craze film as a highly oriented layer. If this were the case however, one would expect a change in level difference across some Conic boundaries and some evidence of change in fine structure on the surface, since it would be unlikely for no differential shrinkage to occur throughout the whole craze layer. The almost pristine nature of the surface structure

of the thermally treated craze layer suggests that the disappearance of the surface colours is unlikely to result from thermal relaxation of highly oriented material.

Of the two methods of thermal treatment of the surface layer, (viz: local heating with a hot needle, and general heating over the whole surface), general heating is perhaps a better test for thermal collapse, since the any ambiguity associated with mechanical compression arising from location of the hot needle is avoided. Under conditions of general heating, as reported earlier, the interference colours become gradually less saturated, although no change in the order of the interference occurs. Evidently under these conditions the colours disappear by the destruction of the reflectivity of the lower boundary rather than by progressive reduction of the film thickness, which is further circumstantial evidence against significant orientation in the craze layer. This change in the saturation of the colours might be produced, for example, if heating accelerated the infusion of water vapour into the pores of the craze. This would cause an increase in the refractive index of the surface film and hence a reduction in the reflectivity of the film-polymer interface and lead to the observed decrease in fringe contrast.

The model of a craze as an open-cell foam, (Haward, 1973), which may or may not undergo significant drawing between voids is consistent with the apparent absence of significant relaxation in the fracture surface layer on heating,

provided the material between voids does not undergo significant orientation either during the formation of the basic craze structure, or during subsequent rupture of this crazed material. The former requirement may be consistent with the hypothesis that craze thickening occurs in this material by the creation of new craze matter, (i.e. in the context of Haward's model the transfer of more normal polymer into a foam-like structure), rather than by extension of the crazed material within the initial interfaces. (Whether this suggested mode of craze thickening is in fact consistent with the apparent absence of orientation in the craze layer would depend on the mechanism of craze i.e. foam extension: it is possible that extension of the craze may not occur by increasing the orientation of the polymer molecules between voids, but by an increase in the total void volume, in which case craze thickening could occur by extension of the material between the initial interfaces with no significant orientation taking place.)

So far in the discussion on the formation of Conics, no attempt has been made to explain why many localised ruptures occur within the crack-tip craze. We have shown that the formation of a significant number of Conics occurs only after a critical value of $\sigma^2 c$ has been attained and this suggests that a critical value of K or G might be associated with the condition for their formation, although why this should be awaits more detailed information on

the conditions of craze rupture in this material. The secondary cracks will apparently extend within the tapered section of craze, whereas the main crack will extend only after the craze has thickened to some maximum, and evidently critical value, (which for a static crack is thought to be about 2μ ,(Kambour, 1965)). This apparent contrast between the behaviour of the secondary cracks and the main crack suggests that the fundamental condition for craze rupture might not be a simple one. Evidently it cannot be the attainment of a critical craze strain, (or craze thickness), and on its own a critical stress condition carries its own difficulties since, at least with current craze models, the stress within the craze is considered to be substantially constant and equal to the crazing stress. The fact that Conics are produced only when the crack is extending rapidly indicates that advanced ruptures within the crack tip craze occur only when the rate of creation of craze ahead of the crack is high, and this might provide the clue to their formation. It is possible, for example, that under conditions of rapid craze formation there is insufficient time for uniform development of the craze throughout the whole of its volume, and inhomogeneities are created within the craze interfaces which could act as stress raising sites for the nucleation of secondary cracks. On the other hand, it is possible that such inhomogeneities are a characteristic of the craze structure per se, (such as a foam structure with a variety of void sizes), but under the quasi-static

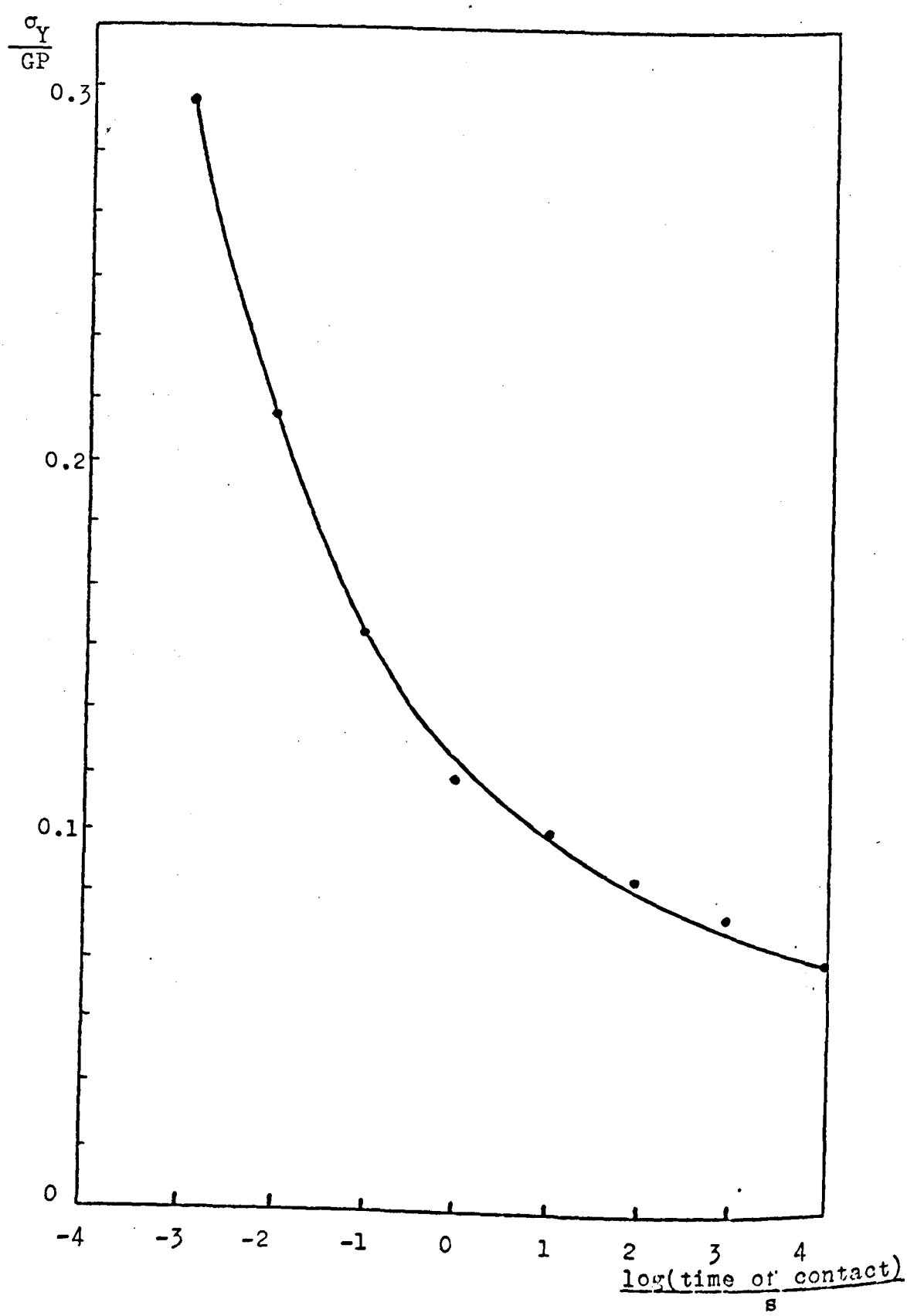

Flow-stress of pmma as a function of time.

Fig. 5.13

crazing stress their stress raising effects might be insufficient to cause local ruptures. However, if the crazing stress increased with the effective crack-tip strain rate, (i.e. with crack speed), secondary cracks might then form at such sites. Circumstantial evidence that the crazing stress does increase with crack speed comes from the observation that the flow-stress of pmma, as measured by diamond indentation, decreases with the load duration of the diamond pyramidal indentor. The results are shown in Fig. 5.13, and if coupled with the observation of Haward et al (1971) that changes in the flow stress correspond to similar changes in the crazing stress, (a result also implied by the work of Beardmore, 1968), they suggest that the crazing stress is likely to increase with crack speed. The fact that crack speed is largely determined by the value of G might then account for the requirement that G must exceed a certain minimum value before Conics form.

The tentative nature of the preceding discussion is a reflection of the current lack of understanding of the fundamental conditions for craze rupture, and the structure of the craze itself. Any attempt to relate a macroscopic parameter to the fundamental condition for the process of Conic formation is complicated by the fact that the process occurs within the plastic zone, although as just suggested the value of G might be indirectly related to Conic formation through the crack speed. What is more certain is that as the next fracture surface zone, (zone D), is approached the number of secondary nucleations per unit

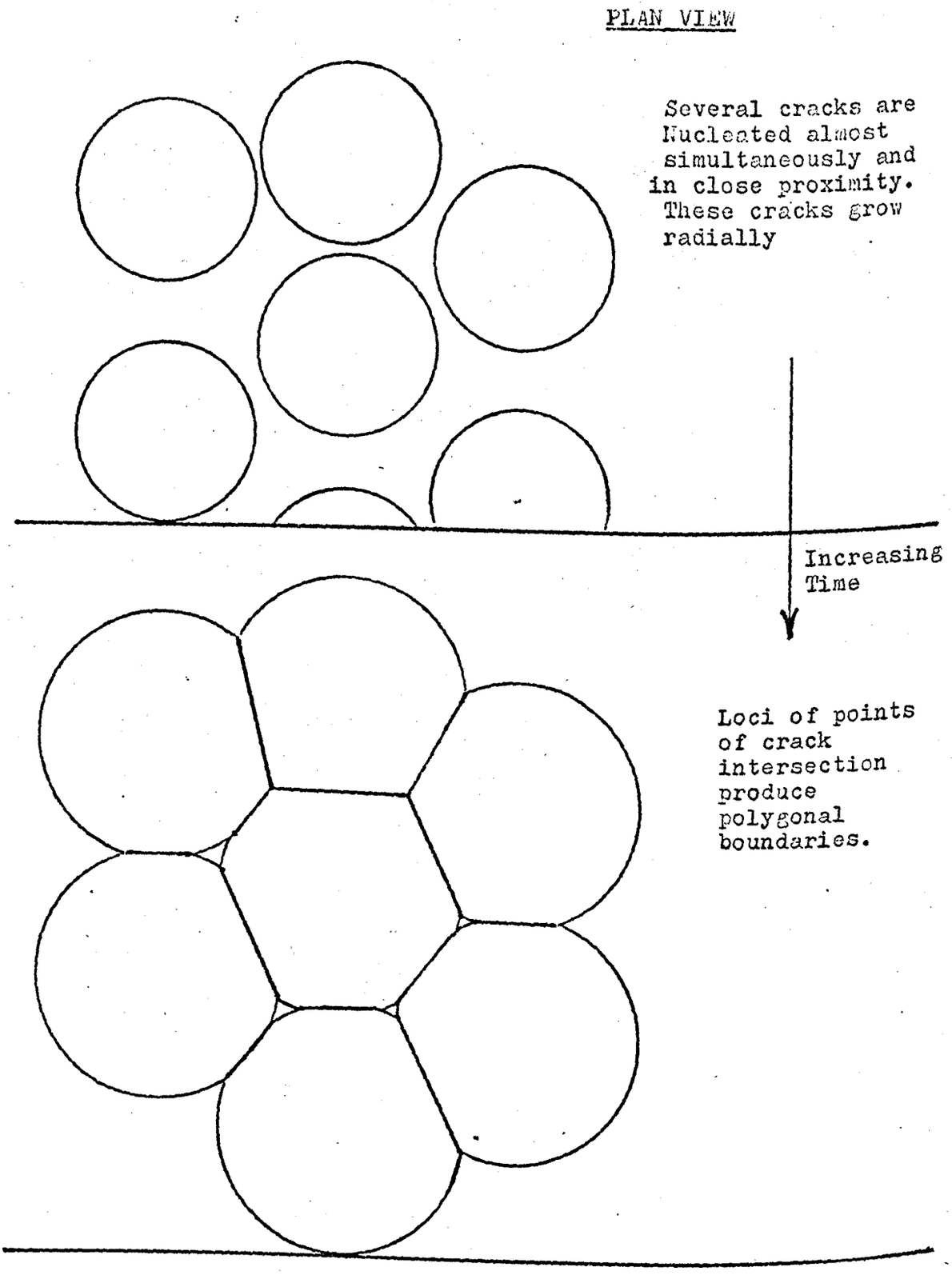

Formation of "Polygonal Conics" in latter part of Conic Zone.

Fig. 5.14

area of fracture surface gradually increases, Plate 5.7. Indeed, immediately prior to the onset of the next zone it would appear that simultaneous nucleation of many secondary cracks occurs over large areas of craze plane, as can be inferred from the "polygonal" shape of the boundaries of the secondary cracks in the later stages of Conic zone, Plate 5.13. Fig. 5.14 illustrates how such polygonal boundary shapes arise if many secondary cracks are nucleated almost simultaneously and in close proximity.

Under these conditions the fracture speed might well approach or even exceed the maximum value of crack speed predicted theoretically, and there is some evidence that this is the case, (Schardin, 1959). Furthermore, simultaneous nucleation of secondary cracks within the craze of the main crack would account for the failure to observe Newton's Rings within the boundaries of the 'Conic' features thereby produced, for coalescence of secondary cracks within a region of craze of roughly uniform thickness, will not lead to any significant variation in craze film thickness.

The general view advanced in this section has been that Conic features are formed by interactions between cracks within the craze associated with the main crack. In the early part of the Conic zone the secondary cracks are thought to join with the main crack, whereas in the latter stages the secondary cracks coalesce. This model of Conic formation implies that the crack-tip craze is longer when the crack is moving than it is under quasi-static conditions. To see why this is the case, consider

the following argument.

In Fig. 5.15 the dotted line shows the instantaneous position of the main crack front when a secondary rupture has just nucleated, and the full lines show the position of the main and secondary cracks when they first meet.

Fig. 5.15

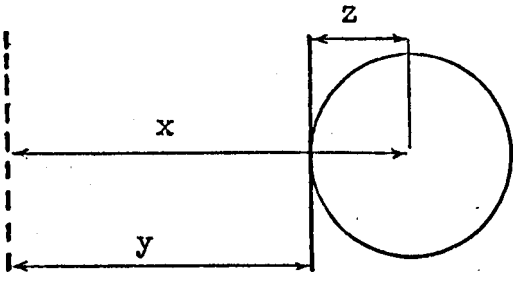

The distance x,(= y + z), is the distance between the instantaneous position of the main crack and the origin of the secondary crack when the latter has just nucleated; y is the distance travelled by the main crack from its position when the secondary crack has just formed, to where the two cracks first meet; and z is the distance travelled by the secondary crack, parallel to the plane of the main crack and towards the latter, when the two cracks first meet.

Fig. 5.16 is a sketch of a typical Conic as formed in the early part of the Conic zone. On this figure z is the distance from the 'focus' of the Conic to its closed end, and r corresponds to the increase in radial growth of the secondary crack, whilst the main crack traverses the distance z.

Fig. 5.16

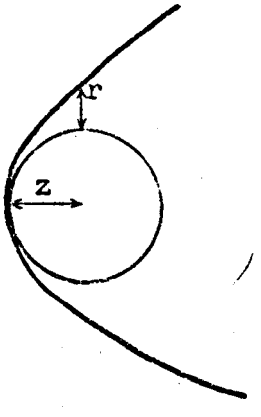

If the simplifying assumption is now made that both cracks are always travelling at constant, but not necessarily equal, speeds, then it is possible to calculate the minimum value of x, (Fig. 5.15).

Let the speed of the main crack be v_m, and the speed of the secondary crack be v_s, then referring to Fig. 5.15,

$$z = v_s t \qquad 5.1$$

$$\text{and } y = v_m t \qquad 5.2$$

where t is the time taken for the main crack to travel distance y, and the secondary crack to travel distance z.

Now referring to Fig. 5.16, when the main crack extends an additional distance z after the cracks first meet, the secondary crack extends laterally by a distance r.

Thus, $$v_s = v_m . r/z \qquad 5.3$$

From 5.3 and 5.1,

$$z^2 = (r . v_m . t) \qquad 5.4$$

Therefore, from 5.4 and 5.2,

$$z^2 = r . y \qquad 5.5$$

Hence

$$x = y + z = z + z^2/r \qquad 5.6$$

For a typical Conic formed in the early part of the Conic zone, $z \sim 25\mu$ and $r \sim 18\mu$, and hence $x \sim 63\mu$, which according to the view that Conics originate in the crack-tip craze, implies that the crack tip craze is longer when the crack is moving than it is under static conditions, (when it is $\sim 25\mu$). This indicates that once the crack is moving some of the available energy

goes to increase the volume of crazed material ahead of the advancing crack, and not all to increasing the crack speed, (compare Mott's argument in Chapter 2). Furthermore, Kambour has proposed that the thickness of the craze film increases with crack speed.

It should be noted however, that additional energy requirements associated with a change in the dimensions of the crack-tip craze do not in themselves mean that the fracture energy is greater when the crack is moving than during quasi-static crack extension: the total amount of crazing has to be considered. During the formation of the Conic zone for example, it would appear that very few off-axis crazes are produced, whereas during quasi-static crack growth many off-axis crazes are formed, and it is therefore possible that although more energy may be required to form the crack-tip craze, the overall fracture energy is less during the formation of the Conic zone than it is during slow crack growth.

(c) Fracture Surface Zone D.

The onset of zone D demarcates the first stage following the termination of zone A at which surface asperities again exceed $\sim 1\mu$.

It will be remembered that the basic structure of this zone consists of a series of rough strips of surface, separated by relatively smooth strips. The rough strips consist of a series of "plateaus" at different levels (the level difference being in excess of 1μ), the fine structure of which, in common with that of the smooth strips, is similar to the end of the Conic zone; i.e. it

consists of polygonal shaped 'Conics'. This suggests that although fracture now occurs at different levels, the mode of fracture at each is similar to that which produced the later Conic zone; viz multiple interactions between approximately coplanar, circular cracks. To the author's knowledge no specific attempt has been made to account for the structure of zone D, other than to describe it as representing 'stick-slip' behaviour, and to relate it in a general sense to crack branching, (e.g. Andrews 1967). However, any complete account of the structure of zone D must at least in principle explain why there is a change in mode of fracture at the onset of the zone; why this mode of fracture occurs discontinuously; and, closely associated with this second aspect, why there is a need for a finite and relatively smooth mode of propagation before the start of each rough strip.

Detailed matching experiments established that rough strips on one surface coincided with rough strips on the other, Plate 5.14, and that the fine structure on each rough strip matched in detail with that on the complementary rough strip, Plates 5.15 and 5.16. Observations were also made from the side, in a direction parallel to the general plane of propagation, and these revealed the presence of a "fan" of craze-like markings at, or close to the beginning of each rough strip, Plate 5.17. Many of these features extended beneath the next relatively smooth region of surface, and sometimes even under the following rough strip.

To ascertain whether the features were crazes or cracks, two simple tests were undertaken which provided circumstantial evidence in support of the majority being crazes. Firstly, specimens were heated in an oven at 346 K. It is known that crazes become at least optically invisible after heat treatment at this temperature and it seemed reasonable that if the features were crazes they too would disappear after this heat treatment. Plate 5.18 shows the result of heating the sample shown in Plate 5.17, and it is clear that most of the component features of the 'fan' have disappeared. Secondly, specimens were immersed in methanol for several hours. It is known that pmma crazes disappear after immersion in methanol, and again the majority of the component features of the 'fan' disappeared after immersion.

To the author's knowledge there is no simple conclusive test to distinguish between crazes and cracks, other than their growth characteristics under static, or quasi-static conditions. Clearly it is not possible to use this test in the present situation. Under dynamic conditions, similar to that which obtains here, it is common practice to assume that specific features are either crazes or cracks, (see, e.g. Hull 1970). The circumstantial evidence just described supports the hypothesis that the majority of the features comprising the 'fans' are crazes. The few remaining features which were substantially unaffected by the heat or solvent treatments are thought to be open cracks, formed by the

rupture of some members of the 'fan' craze field. This view is supported by the general "plateau" structure of the rough strips which indicates that secondary cracking has occurred within the fan-shaped crazefield, the secondary cracks so formed having subsequently joined by further cracking between the different levels.

The fracture mechanism which leads to the rough strips is therefore considered to be secondary nucleation. Given this, it is fairly clear what happens as the fracture progresses through zone D, although at this stage it is only possible to speculate on why it happens. The rough strips are produced when independent crack nucleations occur in separate crazes within the fan, and the smooth strips when rupture occurs within a single craze. In both cases, craze rupture occurs by the coalescence of approximately coplanar, circular cracks.

Zone D immediately precedes fracture branching in pmma, and it is instructive to compare its general morphology with that in the corresponding region, (the mist zone), formed on the fracture surfaces of glass and of the epoxy resin examined as part of this work, (Araldite CT200). In these two materials the mist zone consists of many isolated 'elements' which are of a few basic types and which are apparently randomly distributed. The 'elements' are formed by an interaction between the main crack and a smaller subsidiary crack. In contrast, the structure of zone D on pmma is much more ordered: when subsidiary cracking occurs it does so over most of the

specimen width, and when it ceases, again it does so over most of the specimen width.

The average size of the individual glass and resin mist features gradually increases as the branching zone is approached, and the average width of the rough strips on pmma gradually increases as branching is approached. This gradual increase in mist-feature size is thought to reflect the amount of energy available in the case of the glass and the resin, (e.g. see Johnson, 1963), and it seems likely that the width of the rough strips on pmma is also determined by the availability of energy. If so this would account for the formation of wider rough strips on the fracture surfaces of stronger specimens.

Although it is possible to account for the width of the rough strips in terms of availability of energy, it is not possible to explain in terms of energy alone why the formation of the rough regions, (i.e. why secondary nucleation), occurs discontinuously, or why during those stages when secondary nucleation occurs, it does so across the whole specimen width. If these two aspects could be resolved then we would be closer to understanding <u>why</u> the zone D structure is produced.

The fact that secondary nucleation occurs across the whole fracture front, (rather than at isolated and independent sites as in glass and the resin), is likely to be related to the formation of the 'fan-shaped' craze field, within which the secondary cracks are nucleated. This field is produced across the whole width of the

specimen, and thus provides crazes across the whole specimen width in which secondary nucleations can occur. The formation of this craze field could in principle be related to the overall fracture rate or to the local stress distribution. It is possible, for example, that the rapid fracture speed which is thought to occur when a craze fails by coalescence of secondary cracks within it, (which is the mode of failure which immediately precedes each fan-shaped craze field), might lead to a redistribution of stresses just ahead of the effective crack tip similar to that predicted by Yoffé, (see Chapter 3). This redistribution of stress could lead to the growth of crazes oblique to the initial fracture plane across the whole fracture front. The general orientation of the crazes within the fans is certainly consistent with this possibility, if it is assumed that under such dynamic conditions crazes still grow normal to the major principal stress.

The simultaneous nucleation of secondary cracks along the whole fracture front will effectively 'blunt' the 'crack-tip', and thereby lead to a reduction in stress level in the unbroken material. This reduction in stress level might explain the need for finite extension of a single crack beyond each array of secondary cracks; this could re-establish the stress level to a sufficiently high value to enable new secondary cracks to form within the next craze fan. (In the case of glass and the resin this requirement would not be expected since the subsidiary

cracks are formed at local sites, apparently randomly distributed, and the single main crack should still be largely responsible for the general stress level in the unbroken sheet.)

At the time of writing these ideas must be regarded as tentative, although it is hoped that enough has been said to illustrate the nature of the problems involved in any attempt to account for why the zone D structure is formed. It is an underestimation of these problems to describe the process as 'stick-slip', and this label helps very little in understanding the mechanisms involved.

From the point of view of crack branching, the mechanism leading to the branched cracks is considered to be a special case of secondary nucleation: viz: nucleation of independent circular cracks within some members of a fan-shaped craze field. When there is sufficient energy to rupture continuously at least two of these crazes across the whole fracture area, so that the kinetic energy of each fracture is maintained, then branching will occur.

5.8 Fracture of Oriented pmma

Some provisional experiments were conducted to compare the fracture surface morphology of oriented pmma, when broken in both directions with respect to orientation, with that of the normal material.

Specimens of cast pmma were pre-heated to 383 K in an electrically heated enclosure specially made for the purpose. They were then strained until the final strain

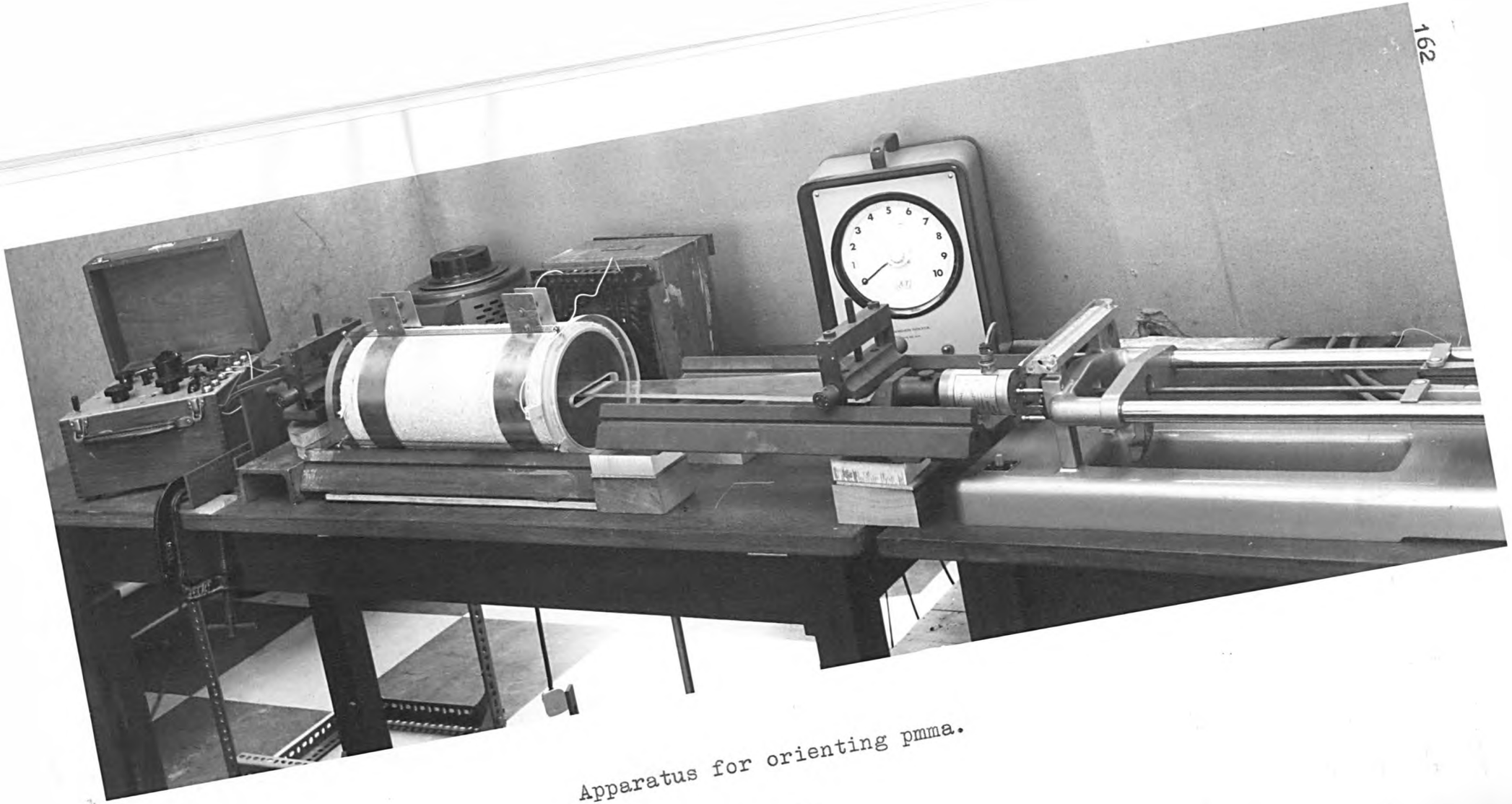

Apparatus for orienting pmma.

Fig. 5.17

was between 85% and 95%. The apparatus is shown in Fig. 5.17. The temperature was recorded with a thermocouple and the heating current was adjusted manually to maintain a uniform temperature. Preliminary tests showed that the temperature was reasonably constant for about 3/8 the length of the enclosure on either side of its centre, and all test specimens were cut from that part of the strained sheet which was located within this section of the oven. After straining to the desired amount, the load was maintained and the temperature allowed to return to ambient over a period of $\sim$6 hours.

Plate 5.19 shows a fracture surface of a specimen loaded parallel to the orientation direction, the nominal strain being $\sim$85%. Prior to rupture such specimens underwent visible permanent deformation. Microscopic examination showed that a field of 'shear bands' had formed, similar to those observed by Bowden (1970) in polystyrene. It was not established whether their formation alone was responsible for the overall deformation, or whether their formation was a consequence of specimen orientation per se, or to the high breaking stress required to rupture these oriented specimens.

As Plate 5.19 shows, the fracture surface is different from that of unoriented material. Notably, no structure similar to that of zone D is present, and relatively few Conics have formed. Following the Conic zone the surface is continually 'rough'. The onset of both these zones could be characterised by a critical value of $\sigma^2 c$, the values of which varied with the degree of orientation as shown in Table 5.2.

Nominal % strain	$\sigma c^{\frac{1}{2}}$ to onset of "rough" region $MNm^{-3/2}$
85	3.66±0.11
95	4.08±0.12

TABLE 5.2

$\sigma c^{\frac{1}{2}}$ FOR ORIENTED pmma LOADED PARALLEL TO ORIENTATION

Nominal % strain	$\sigma c^{\frac{1}{2}}$ to onset of "bands" $MNm^{-3/2}$
85	1.59±0.05
95	1.49±0.09

TABLE 5.3

$\sigma c^{\frac{1}{2}}$ FOR ORIENTED pmma LOADED NORMAL TO ORIENTATION

Plate 5.20 shows the fracture surface of a specimen loaded normal to the orientation direction. In the case of these specimens no observable shear bands or any signs of macroscopic permanent deformation occurred prior to rupture. One notable feature of the morphology in this case, is the series of 'bands' which have formed roughly normal to the crack propagation direction. The onset of this 'banded' zone could again be characterised by a critical value of $\sigma^2 c$, the magnitude of which depended on the amount of orientation, Table 5.3.

There was insufficient time to examine the structure of the oriented material in any detail. However, the preliminary observations described above clearly indicate that the fracture process varies quite considerably with pre-orientation of the polymer. A more detailed examination of the fracture surface morphology of the oriented material might provide valuable clues to the behaviour of the normal material.

5.9 Summary and Conclusions

The tensile fracture morphology of pmma has been described, and a general discussion of some of the fracture processes leading to this morphology has been given. The importance of crazing has been emphasised. In the course of the discussion an attempt was made to identify the important problems associated with the fracture process, although in the time available many

of these were left unresolved. These problems included the structure of the craze, the process of craze thickening, the conditions for craze rupture, and the formation of the 'fan-shaped' craze field.

We argued that Haward's model which likens a craze to an open-cell foam was in many respects to be preferred to the older, Kambour model of a craze as a local region of oriented polymer containing voids. It was suggested that the predominant process of craze thickening in pmma was the production of new craze rather than the extension of the previously crazed material within the initial interfaces. The condition of craze rupture was considered to be problematical because of the apparent difference between the behaviour of the main crack, and the secondary cracks formed within the main crack-tip craze.

The Conic zone was of particular interest because it appeared as though throughout the whole of this zone the fracture progressed through the single craze associated with the tip of the main crack, although the mode of craze failure involved the extension of many localised cracks formed within this craze, in addition to extension of the main crack. The quantitative measurements of $\sigma^2 c$ suggested that the formation of Conics might be related to a critical value of G. Why this should be awaits more insight into the detailed mechanisms of craze rupture than is currently available, although it was suggested that Conic formation might be indirectly related to G through crack speed.

In zone D localised cracking occurred outside the main crack-tip craze, although only intermittently, to produce a series of rough strips of surface. Why this was so was not resolved, although it was suggested that the simultaneous nucleation and finite growth of many secondary cracks might preclude further nucleations, because of the associated reduction in stress level in the unbroken sheet.

Finally, in pmma, whenever a craze ruptures, whether it be by extension of the main crack or by coalescence of smaller, circular cracks, the rupture always occurs roughly midway between the craze interfaces. This can be inferred from the thickness of the layer of craze film left on the resulting fracture surfaces. By contrast, in polystyrene, in addition to this mode of craze rupture there is a second mode in which rupture occurs at or very close to the craze-polymer interfaces. Several other differences in the fracture processes of the two materials are evident, and these are discussed in more detail in the next Chapter. The fact that there <u>are</u> differences is in itself particularly interesting, since macroscopically the two materials are quite similar, and it is common practice, even in the context of fracture, to liken them.

CHAPTER 6

FRACTURE SURFACES OF POLYSTYRENE

6.1 Introduction

Fracture of polystyrene at 293K involves the formation and rupture of crazes, (see e.g. Kambour 1966). A study of the fracture surfaces of polystyrene specimens broken in simple tension indicated however, that the fracture process was in many respects quite different from that involved in tensile fracture of pmma. For example, on some areas of fracture surface a layer of craze film was clearly visible, whereas the matching area on the other fracture surface was devoid of any detectable craze layer. Very abrupt transitions in the mode of rupture also occurred, which could be related to dense fields of craze-like marks beneath the exposed surfaces. The topography of the craze film within Conics was also quite different, and Conic features occurred only on areas of fracture surface produced during slow crack growth.

One of the more surprising results of a preliminary examination of tensile fracture surfaces of polystyrene was the discovery of the existence of two alternative sequences of fracture surface zones, Plates 6.1 and 6.2. The sequence shown in Plate 6.1, (referred to as Sequence 1), contains five major zones, one of which consists of alternate rough and smooth surface, *prima facie* similar in form to the rough and smooth strips which constitute

zone D on pmma surfaces. We shall see later, however, that there are several important and fundamental differences between the two structures. The other sequence, (referred to as Sequence 2), also consists of five major zones, but in this case no large area consisting of alternate rough and smooth strips of surface is formed.

In the next section the detailed structures of each sequence are described; the discussion then devolves around those aspects of the fracture process which suggest marked differences between the behaviour of this material and pmma, and which are felt to have some bearing on the mechanism of crack branching.

6.2 Classification of the Two Zone Sequences

(a) Zone Sequence 1

Fig. 6.1 is a sketch of the main zones comprising the first zone sequence.

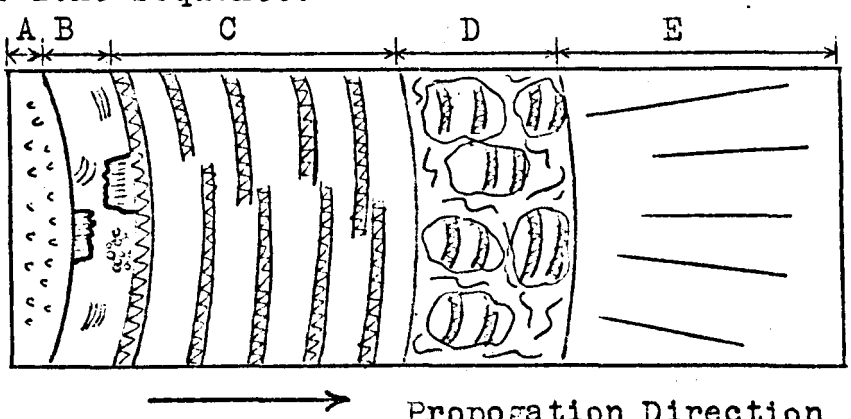

Fig. 6.1 Not to scale.

To the unaided eye, zones A and B cannot be distinguished, but even at low power on the optical microscope two quite different regions can be seen. The first of these, Zone A, is transparent and contains many small Conic-like features,

most of which are roughly hyperbolic or elliptical in outline. At high magnifications, (~ x 500), a graininess covering the whole zone can also be resolved.

The detailed structure of the surface in zone B varied considerably from one specimen to another, although careful observation showed that the different structures could be classified into three basic types. The first of these consists of small, irregularly shaped 'islands' which are higher than the surrounding fracture surface, and which display interference contrast, Plate 6.3. These 'islands' become gradually smaller as the boundary of the next zone is approached. The second structure consists of a few relatively large, but irregularly shaped areas which normally display thin-wedge interference patterns, Plate 6.4. These areas are separated by featureless regions which show no interference effects, and are usually formed either contiguous to the boundary demarcating the start of zone B, or contiguous to the boundary demarcating the end of this zone. In the latter case, the interference fringes produced indicate that the apex of the thin wedge lies along the zone boundary. Plate 6.5 illustrates a case where white light fringes reached a dull grey at the zone boundary, indicating that the wedge was very thin in this region. The third structure, illustrated in Plate 6.6, appears to be less random than the other two. It consists of a series of relatively rough strips of fracture surface separated by smooth regions. Any crenulations on one rough strip are invariably reproduced

on adjacent ones, and the rough strips display interference contrast in reflected illumination. This structure has been likened to the markings on mackerel, (Hull and Murray, 1970), and consequently has been categorised as the Mackerel pattern; we shall adopt this terminology here.

Comparison of matching fracture surfaces showed that in all three cases a region displaying interference effects on one surface correlated with an area devoid of any interference effects on the other. In no case was there a detailed match between the size and shape of complementary structures; the area devoid of interference was invariably slightly larger. For example, Plates 6.7 and 6.8 show two matching fracture surfaces containing the second basic structure just described. It is clear that although the regions showing interference effects on one surface coincide with featureless areas on the other, there is no detailed correspondence of the boundaries of these regions.

Significant drawing is involved in the production of all three structures. A particularly striking example of this can be seen in Plate 6.9 which is a scanning electron micrograph of the 'island' structure. (Immediately after this micrograph was taken the drawn fibrils began to collapse in the electron beam.)

The observations outlined above suggest that the basic structures formed in zone B are produced by a craze

which has ruptured in such a way that a thick layer of craze film remains on one fracture surface, and a very thin, or even no craze film is left on the other. It is evident that this craze has ruptured whilst retaining a tapered shape, since the craze close to the boundary of the next zone is much thinner than in earlier parts of zone B. The drawing suggests that the craze did not rupture completely by crack propagation.

The transition from zone B to zone C is always very sharp even when specimens are viewed under the scanning electron microscope, (Plate 6.10). The transition also involves an abrupt change in the level of the fracture surface. Scanning electron microscope observations further suggested that the fracture surface at the end of zone B sloped up or down to the B-C zone boundary, (Plate 6.10).

By viewing a specimen from the side in a direction parallel to the fracture surface, a dense field of craze-like markings was observed beneath the exposed surface, and these splayed-out into a 'fan-shape', the apex of the fan coinciding with the abrupt transition between zones B and C. These features resemble the 'fan-shaped' craze fields which were associated with the rough strips of zone D of pmma; they also disappeared on heating and on immersion in methanol. By focussing into the specimen the field of craze-like markings was found to extend along the whole length of the boundary between the two zones, so that

in three dimensions the field had a wedge shape, with the apex of the wedge running along the B-C zone boundary.

Zone C consists of a series of equispaced, relatively rough strips of surface, separated by smooth surface. This structure will be referred to as the banded structure, and zone C as the banded zone. The width of a band is taken to be equal to the width of one of the rough strips, and the band spacing as the width of a smooth region separating the rough strips. To a first approximation the bands were parallel to one another, and lay in a direction roughly perpendicular to the propagation direction, Plate 6.11. Observation from the side of a specimen showed that each band could be related to a fan of craze-like markings. Plate 6.12 shows a side view of a specimen containing a stopped crack which had been propagated by driving a wedge into its open end. The formation of a series of fans is quite evident, and each of these was found to correspond to a band on the resulting fracture surfaces. Plate 6.13 shows a particular fan whose position coincides with a fortuitous mark on the side of the specimen. Plate 6.14 shows the onset of a band on the fracture surface of the same specimen, and it can be seen that the mark also coincides with the beginning of the band. These two micrographs illustrate that the apex of the fan coincides with the onset of the band, a result which was found to be quite general.

Sometimes, striations originating on one of the rough strips extend into, and occasionally even cross, the next smooth region. The smooth regions have a structure similar to the island structure of zone B, and as the next rough strip is approached this island structure falls below the limit of resolution, Plate 6.15. Sometimes the island structure is formed as a series of miniature bands which are reminiscent of rib marks formed on the fracture surfaces of glass, (Murgatroyd, 1942), Plate 6.16.

There is no well defined transition between the banded zone and the next zone, (designated zone D on Fig. 6.1). Within zone D the fracture progresses at many different levels, and at each of these isolated patches of the banded structure are produced. The fracture surface is now macroscopically much rougher than at any previous stage, Plate 6.17.

Finally, branching of the whole fracture front occurs to produce zone E, the branching zone.

(b) Zone Sequence 2

Fig. 6.2 is a diagrammatic sketch of the second zone sequence; again the letters A to E refer to the five main zones.

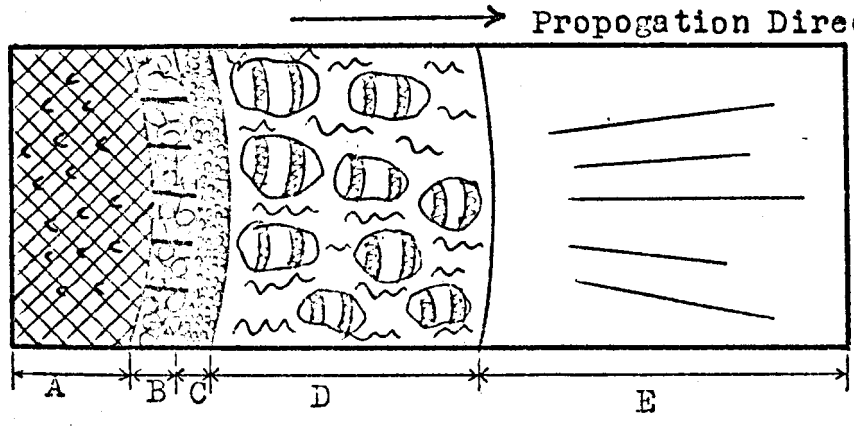

Fig. 6.2

Not to scale.

When viewed in reflected illumination the first zone, designated A on the Figure, is a milky/silvery colour. Observation through the side of a specimen in a direction parallel to the fracture surface showed that beneath the area of fracture surface occupied by zone A there was a dense field of crazes, Plate 6.18. By focussing into the specimen from this direction it became evident that the crazes were not generally parallel to the fracture surface above them. The milky colour of zone A is thought to arise from multiple reflections and scattering from these subsurface, non-parallel crazes.

The surface structure of zone A is similar to that of zone A of the first sequence: i.e. it contains many Conic-like features and a fine graininess, Plate 6.19. Apart from these features the fracture surface is planar, suggesting that it is produced by the rupture of a single craze, even though many crazes are formed.

Zone B consists of a tangled web of slivers superimposed on a fracture surface consisting of several plateaus at different levels, Plate 6.20. Plate 6.21 shows a detail of Plate 6.20, and illustrates that the plateaus have a fine structure similar to the island structure which occurs in some zones of the previous sequence.

The different fracture surface levels in this zone suggest that several crazes are now rupturing simultaneously, and the fine structure of each level indicates that the individual crazes rupture in a similar way to that occurring

in zone B of the previous sequence. The formation of many slivers and the presence of sharp steps between plateaus indicates that final severence occurs by secondary cracking between the initial non-coplanar interfaces formed by rupture of the different crazes.

Zone C of the second sequence is relatively planar, and is transparent, Plate 6.22; perhaps it could legitimately be classified as the end of zone B rather than a zone of independent status. The island structure previously described recurs here and the scale again decreases as the next zone boundary is approached, Plate 6.23. The indications are that zone C results from the rupture of the predominating members of a craze field, other members of which can be seen beneath the exposed surfaces, and that the rupture mode is similar to that occurring in zone B of the previous sequence: i.e. at or very close to the craze-polymer interface, and within a tapered craze.

It is clearly not always a single craze which ruptures to form this zone, since level differences can be detected within it, with a sharp step from one level to the other, Plate 6.24.

The transition between zones C and D is very abrupt. There is normally a detectable level difference across the zone boundary, and the boundary is normally at a level slightly different from the fracture surface on either side, Plate 6.25. Remarkably, where zone C had several discrete levels the transition between zones C and D coincided on each of these, Plate 6.26.

The surface structure of zone D is similar to the structure of zone D of the first sequence, and the final zone, designated E on Fig. 6.2 corresponds to where the fracture has branched, and both sloping regions of surface on the two halves of the broken specimen are deeply furrowed.

6.3 Identification of the Conditions Leading to the Two Zone Sequences

The formation of two alternative tensile zone sequences was, of the materials examined, unique to polystyrene. The polystyrene used in all experiments was obtained from two suppliers: Borst Bros. Ltd., and B.P. Ltd., and at first we considered the two zone sequences to be a consequence of using different grades of material. This view was supported by the consistent production of the Type 1 sequence with the B.P. material. It transpired, however, that both sequences could be obtained on the fracture surfaces of different specimens cut from the same original sheet, (purchased from Borst Bros. Ltd., grade of polystyrene unspecified). Grade of material could not therefore be solely responsible for the formation of the two sequences.

Communication with B.P. Ltd., revealed that the polystyrene which they had supplied contained a mineral oil additive, to serve as a lubricant in the moulding process. Borst Bros. unfortunately "kept no records on whether their material contained a mineral oil lubricant", although the raw pellets which they normally processed

(i.e. Hostyren N), contained no such additive. It seemed possible that the universal production of the Sequence 1 in B.P. material was related to the presence of the mineral oil, and the formation of Sequence 1 in the Borst material on certain occasions was controlled by a similar chemical, this time introduced as a contaminant.

To test this hypothesis we acquired specimens of two grades of material from B.P. Ltd., which were essentially the same except that one contained mineral oil additives. These materials were ; Carinex KLP 35, and Carinex KLP 31 U/L. The only known difference between these is that the latter contains 6.5% of solubles of which the majority are mineral oil and low molecular weight polystyrene. When broken under simple tension the KLP 31 U/L material gave rise to the Sequence 1 and the KLP 35 gave rise to Sequence 2. These results confirmed the first part of the hypothesis, that the presence of mineral oil was a controlling factor in the production of Sequence 1. To test the second part of the hypothesis, Borst material was deliberately contaminated with substances which it was thought could have been introduced accidentally in the normal laboratory and workshop situation; viz machine oil, which could easily have been introduced during the shaping of the specimens, and sebum, which could easily have been introduced during handling. Also, some specimens were prepared carefully so as to minimise the possibility of contamination. At every stage these specimens were

handled with clean gloves, and they were cut using a band saw which had been thoroughly cleaned with CCl_4. Several hours were allowed before the band saw was used, so that the CCl_4 had time to evaporate.

Sequence 1 was produced in all tests in which machine oil was deliberately introduced. In the presence of sebum a high proportion of samples gave rise to Sequence 1, and the carefully prepared, unhandled specimens always gave rise to Sequence 2.

The results of these experiments support the hypothesis that the production of Sequence 1 relies on the presence of certain chemicals. Although the mechanism by which the contaminants or mineral oil act is not entirely clear, it is perhaps worth noting that the craze field around a sharp notch in a specimen of B.P. polystyrene consists of a few, relatively large crazes, while that around a sharp notch in Borst material is a dense field of much smaller crazes. These observations indicate that the effect of mineral oil is to reduce the number of crazes, conceivably by acting as a crazing agent which is released by the crazing process, so that once a craze is formed it will tend to grow at the expense of the nucleation of new crazes.

6.4 A more detailed examination of some of the fracture surface zones.

(a) Zone A of the first tensile sequence.

The surface structure of zone A of the first tensile sequence consists of small Conic features and a fine

graininess. Most of the Conics were approximately hyperbolic in outline, which indicates that the speed of the secondary crack was comparable with that of the main crack when they joined. The level difference across Conic boundaries was never greater than a few microns, which means that the secondary cracks leading to Conics were consistently formed within a narrow band on either side of the main-crack plane. This geometrical restriction suggests that the secondary cracks were nucleated within the crack-tip craze.

The process of Conic formation in polystyrene is thought to be similar to that in pmma; viz both involve local ruptures within the crack-tip craze, and the Conic boundary is formed by an interaction between the periphery of this local rupture and the main crack front. However, there are significant differences between Conic morphologies in the two materials and the average speed of fracture during Conic formation is also quite different. In pmma it will be recalled, Conics are formed on an area of fracture surface produced during rapid fracture propagation, and the interference patterns within Conic boundaries are formed by a reduction in craze-layer thickness caused by curvature of the craze-polymer interface. By contrast, the Conic features in polystyrene are formed when the fracture is propagating relatively slowly, and the interference patterns are produced by a gradient of craze-layer thickness related to a change in level of the top surface of the craze film (i.e. the fracture surface),

rather than to a change in the level of the craze-polymer interface.

Much information on Conics, and the general mode of fracture through zone A was obtained from early experiments designed to examine slow crack growth in polystyrene. The double torsion configuration (Outwater and Gerry, 1966), was found to be the most suitable arrangement for this purpose: this consists of the application of equal torques to the two arms of a rectangular pre-cracked specimen. A simple jig was made so that a specimen could by held under load whilst being examined under a low power stereo-microscope.

These early experiments showed that the crack-tip craze in B.P. polystyrene had a tapered shape, similar to that of pmma, and that during slow crack growth this tapered craze moved forward with the crack so that the distance between the tip of the crack and the tip of the craze remained substantially constant. In B.P. polystyrene very few crazes were produced on either side of the main crack plane during slow crack growth. On the other hand, slow crack growth in Borst polystyrene frequently led to the production of a very dense field of crazes on either side of the main crack, and this made observation of the crack-tip craze very difficult. Careful observation of a stopped crack in this material showed, however, that the crack-tip craze was in fact tapered.

The fracture surface produced during slow crack growth in double torsion had an identical structure to zone A

of the first tensile sequence; i.e. Conics and a fine graininess were present. This indicates that Conic features can form during slow crack growth in this material, which suggests that the tensile zone A could have been produced during a slow extension of the crack. Careful observation of a stopped crack loaded in double torsion revealed small circular marks within the tapered crack-tip craze, and further extension of the crack led to the development of Conics at each site where these small marks were originally observed. This provided very strong evidence that the Conics were produced by local ruptures within the crack-tip craze.

The topography of the fracture surface within Conic boundaries was investigated with the microscope attachments described in Chapter 4. On one of the pair of matching features the fracture surface sloped from the boundary down towards the focus to produce a 'cone-shaped' indentation in their fracture surface: the material within the boundary of the matching feature was raised above the surrounding fracture plane, and sometimes had a shallow indentation surrounding its focus, giving it a superficial resemblance to a small 'volcano'. Plates 6.27 and 6.28 show matching areas of fracture surface containing Conic features, and Fig. 6.3 is a schematic representation of a section through matching Conics, based on the observed topography of the surface within Conic boundaries.

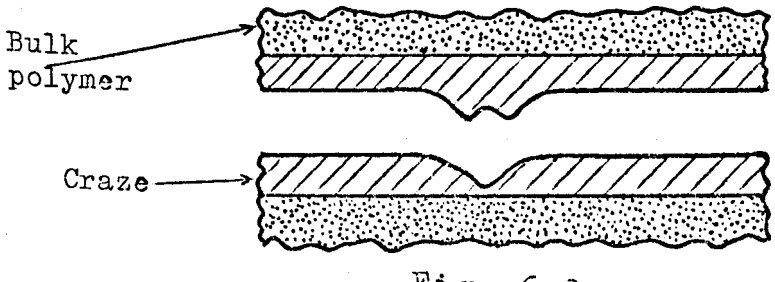

Section through matching Conics showing morphology around foci.

Fig. 6.3

The significant curvature of the top surface of craze film within Conic boundaries in polystyrene suggests that the predominant craze thickening process is internal expension of the crazed material formed within the initial tapered interfaces. This could occur either by molecular orientation and/or by increased void volume. Moreover, the topography of the matching surfaces suggests that the secondary crack was nucleated close to one interface of the tapered craze. Fig. 6.4 illustrates how a significant curvature of the top surfaces of matching craze film could occur if the main process of craze thickening were internal expansion. The reason for the shallow indentation in the raised Conic feature is not yet entirely clear, although it might be due to post-fracture relaxation.

The mechanism of craze thickening basic to this account of Conic formation contrasts with that proposed for pmma, where from an examination of the topography of the surface within Conic boundaries we suggested that the predominant craze thickening process was accretion of new craze matter. This difference might be of fundamental significance to the fracture process in the two materials.

A second basic difference, in this case between the detailed craze rupture processes in polystyrene and pmma, can be inferred from a comparison of the craze films on matching fracture surfaces. In polystyrene a layer of craze film is present on both matching surfaces of zone A. This indicates that rupture of the craze film occurs somewhere between, and not at, the craze-polymer

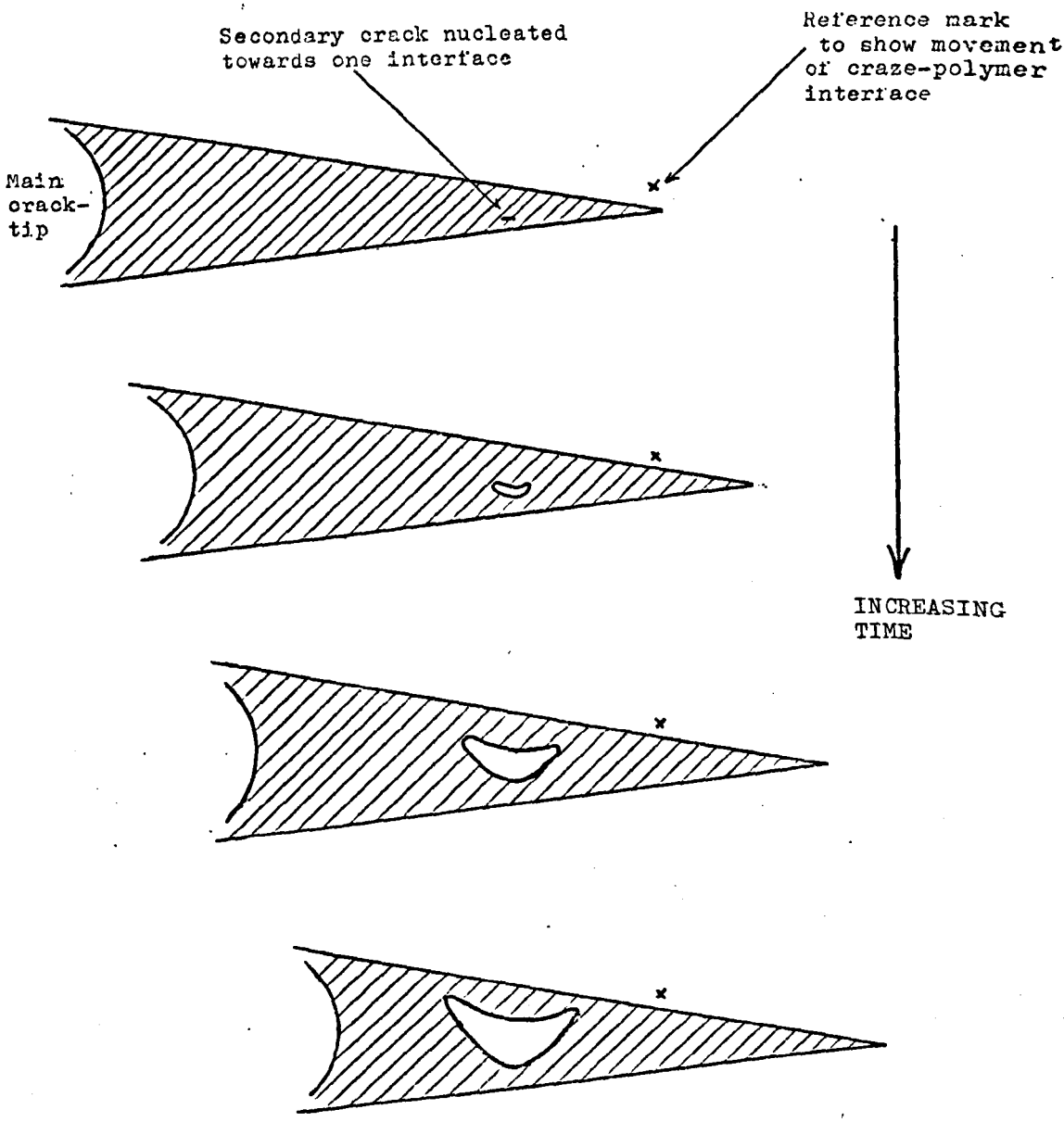

Sectional Views of Conic Formation in Polystyrene.

Fig. 6.4

interfaces. However, this general mode of craze failure in which the main crack advances roughly through the centre of the craze occurs in polystyrene in the formation of the A-zone only. Following the termination of this zone a second mode of craze rupture is evident; local ruptures occur at or close to the craze polymer interfaces before the main crack has attained the full thickness characteristic of zone A, so that these ruptures extend into the tapered craze. This second mode of craze failure does not occur in pmma, although in polystyrene it predominates.

(b) Zone B of the first Sequence

Zone B of the first sequence marks an important transition in the fracture process; local ruptures now occur at or close to the craze-polymer interfaces, the craze no longer grows to a constant thickness before rupture but rather preserves a tapered form, and final parting involves significant drawing of the crazed material between local interfacial ruptures. The pattern of interfacial ruptures evidently determines the form of the resulting fracture surface structure, and three basic structures have been observed; viz the island structure, the wedge structure, and the Mackerel pattern. The island structure forms when roughly circular ruptures occur on both interfaces; the wedge structure when a large area ruptures on one interface; and the Mackerel pattern when a series of roughly linear ruptures occur along alternate sections of both interfaces.

There are at least two, possibly related problems associated with this general mode of craze failure: firstly, why does the craze retain its tapered shape, and secondly, why does failure of this tapered craze result from interfacial rupture rather than from rupture approximately along the middle of the craze.

As far as can be ascertained from observation, the tip of the tapered craze-film at the end of zone B coincides with the apex of the first craze-fan of the banded zone, (zone C). We might therefore propose that the formation of the fan inhibits growth of the tapered crack-tip craze. This proposal, although speculative, is at least consistent with the sharpness of the B-C zone boundary which implies that the boundary was established before fracture had extended to it. In principle the subsequent interfacial ruptures within the tapered craze might arise, because the craze polymer interface is oblique to the maximum tension direction and this leads to shear stresses at the interfaces sufficiently large to cause local shear failure. Alternatively, if this zone marks the transition from slow propagation (zone A) to rapid propagation (zone C), the interfacial ruptures might be a local strain rate effect. At present it is not entirely clear why a craze fails by interfacial rupture, although the proposal that growth of the main crack-tip craze is impeded by the formation of the first fan of crazes is considered to be a feasible hypothesis to account for the tapered shape of the remnant craze-film.

As recorded earlier, there are three basic patterns of interfacial rupture within zone B. The conditions which determine in which of these three ways a given section of tapered craze will rupture on a given occasion is as yet unresolved, although the pattern of rupture does seem to be influenced by the local, and even by a transient, stress distribution. The local fracture surface structure within the smooth strips of the banded zone, which was similar in form to that of zone B, was influenced by striations, Plate 6.29. Although striations were not generally formed within zone B the local surface structure might still be influenced by transient changes in stress within the craze brought about by the passage of a stress pulse. Indeed it was noted in the earlier general description section that the structure of the smooth strips between bands sometimes included rib-marks, along which the island pattern had a slightly different appearance. This observation implies that the pattern of interfacial rupture can be influenced by stress pulses and was investigated in more detail. The results are discussed below, following a brief account of the nature of rib-marks.

Rib-marks were first observed on the fracture surfaces of glass, (Murgatroyd, 1942), and it is now well established that they are slight ripples in the fracture surface produced by temporary changes in the direction of maximum tension which affects the whole crack front simultaneously. These transient changes in the direction

of maximum tension are caused by the arrival of a suitable stress pulse at the crack-tip. One of the simplest ways to produce rib-marks is to subject a specimen to an impact blow with a sharp object so that a conchoidal fracture is produced. Plate 6.30 shows a typical fracture surface produced in this way with polystyrene. Rib-marks are clearly visible. The formation of bands along segments of some rib-marks can also be seen, and this phenomenon is discussed in more detail in the next section, since it suggests that stress pulses may also be an important factor in the formation of bands.

The rib-marks in polystyrene, as well as leading to a change in the surface structure, also correspond to a slight ripple in the fracture surface. Given that a crack in this material is preceded by a craze, a stress pulse is unlikely significantly to deflect the crack-tip, as it does in glass, and give rise to the ripple on the fracture surface, since extension of the crack is most likely to occur along the path of the already formed craze. However, a stress pulse may influence the pattern of rupture within the crack-tip craze and it may also cause a transitory deflection of the craze-tip. If the fracture subsequently follows this deflected craze a rippled fracture surface will result. In principle the associated change in surface structure which occurs along the surface ripple could arise because once the maximum tension reverts to its original direction, the

slopes of the rippled craze are then oblique to the maximum tension direction thus leading to shear stresses at the interface sufficiently large to cause local shear ruptures.

If interfacial ruptures can be produced in this manner then we might expect the same effect to occur in pmma. Conchoidal fracture surfaces of pmma certainly display rib-marks, and along the rib marks the fracture surface structure is affected, although in pmma a detectable layer of craze occurs on both surfaces. The different behaviour of these two materials could be related to the manner of craze thickening which occurs in the two cases. In polystyrene, the material within the craze is thought to extend as the craze thickens. Shear stresses produced by a tensile stress on an oblique interface will therefore act on a stable interface, since although the craze-polymer boundary moves through space as the craze thickens, it does not move through the polymer. In pmma however, the interfaces actually move through the polymer as the craze thickens, and the shear stresses are therefore constantly being established at different parts of the polymer. A priori the shear stresses may not be applied to a given region of polymer, (i.e. a given set of interatomic bonds), for long enough to cause local rupture. Alternatively, the existence of shear stresses along the interface in pmma might affect the rate of movement of the interface into the polymer rather than cause rupture.

As well as interfacial rupture, the failure process within the polystyrene zone B also involves extensive drawing of the intact sections of craze between local ruptures. Similar drawing has been observed within the smooth strips separating the bands of zone C, and here too the craze retains its tapered shape. It would therefore appear that significant drawing of the craze only occurs on areas of surface formed by failure of a tapered craze, which implies that the material between the tapered interfaces is capable of undergoing further permanent deformation after it has formed. This implication is clearly consistent with the proposed mechanism of craze thickening in this material, (viz: internal expansion), for according to this mechanism the crazed material between local interfacial ruptures is far from the maximum expansion it can tolerate, and is therefore capable of further expansion during the failure process. This could occur either by molecular orientation and/or by increased void volume, and could lead to the drawn edges and fibrils which are observed.

In this section we have described the appearance of zone B and tentatively suggested how it might be formed. It may be useful to conclude with a simple summary which will also serve to distinguish between what is regarded as established fact, and what is tentative, or even speculative hypothesis.

Zone B is formed by the failure of a tapered craze. This craze fails by local ruptures along its interfaces

and drawing of the intact sections of craze between these local interfacial ruptures. Three basic patterns of interfacial rupture can occur, giving rise respectively to the island structure, the wedge structure, and the mackerel pattern. The extent and pattern of interfacial rupture can be influenced by stress-pulses. The following "explanations" are, inevitably, tentative. The tapered shape of the craze film on the fracture surfaces may arise because thickening of the crack-tip craze is impeded by the formation of a craze-fan at its tip. Interfacial rupturing of this craze might arise by local shearing, or as a result of the effective strain rate during the formation of zone B. The effect of stress pulses may be two-fold: firstly, they may influence the pattern of interfacial ruptures as they pass through the tapered craze, and secondly they may lead to a deflection of the craze-tip to produce a subsequent surface ripple. The structure along the rippled section of craze might also be influenced by local shear stresses which occur when the maximum tension reverts to its original direction.

(c) The banded zone (zone C) of Sequence 1.

The banded zone of Sequence 1 consists of a series of rough strips of surface separated by smooth strips. Any complete account of the structure of this zone must explain why there is a transition in the mode of fracture at the beginning of the zone, (i.e. from rupture of a single tapered craze to rupture of several crazes), and

why this mode of fracture occurs discontinuously, to leave a series of rough bands on the fracture surface. In the following discussion we shall deal first with the transition to the zone, and then with the development of the fracture through the zone.

(i) The transition to the banded zone

As noted in the previous section, the transition to the banded zone is very sharp. Fracture surface observations suggest that the boundary coincides with the intersection of the tip of the tapered craze of zone B with the apex of a fan-shaped craze field, as shown diagramatically in Fig. 6.5.

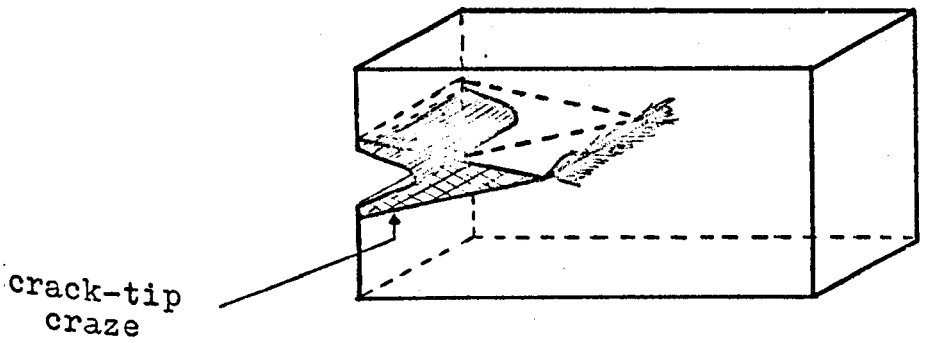

Fig. 6.5

It is not obvious from a post-fracture study of the surfaces what the sequence of events in time was during the production of this region of fracture surface; it is possible, for example, that rupture occurred within members of the fan-shaped craze field before complete separation occurred within the tapered craze. The sharpness of the boundary indicates, however, that the fan-shaped craze field forms before fracture extends to the zone boundary, as is explicit in Fig. 6.5.

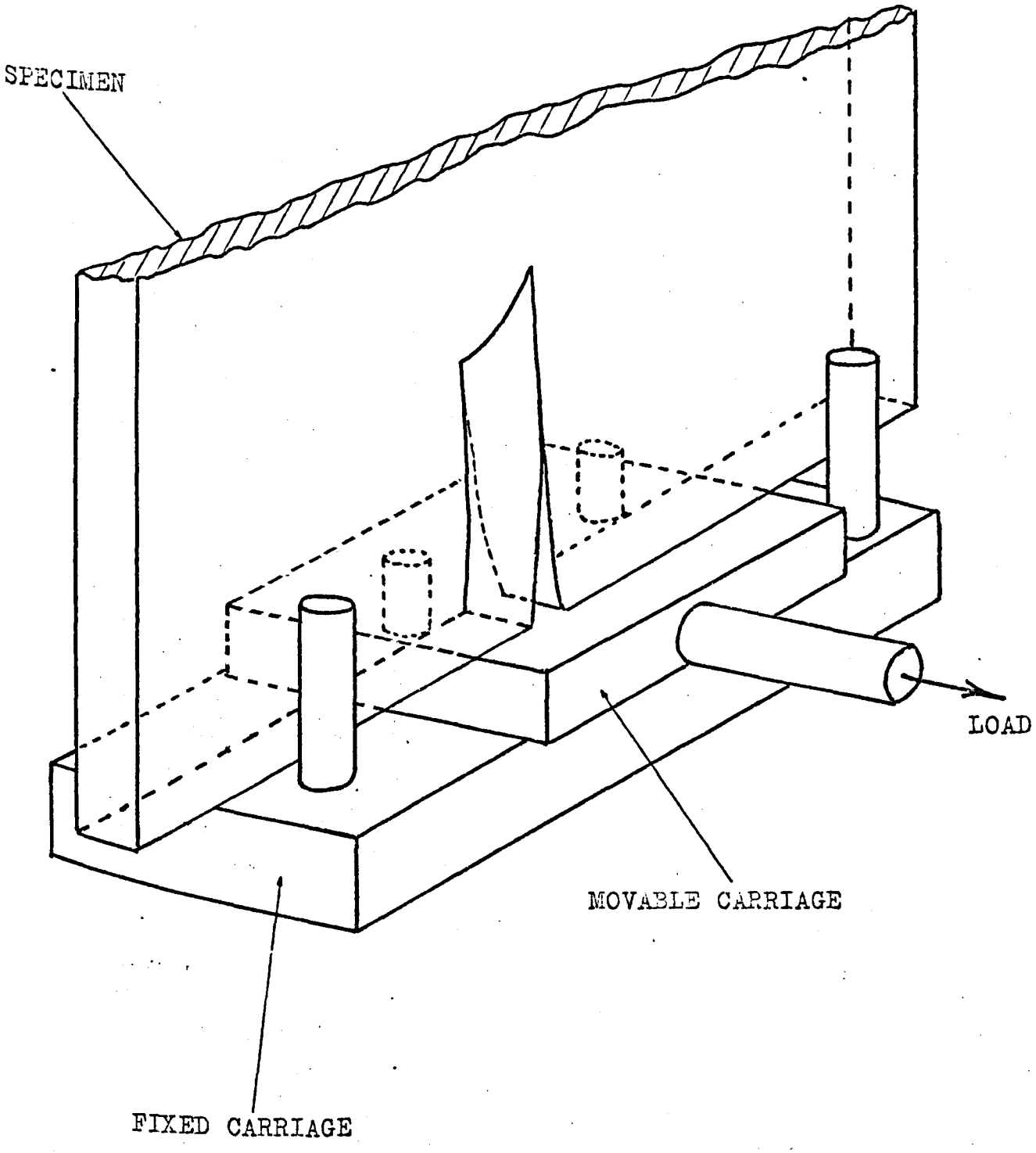

Illustrating mode of action of the Double-Torsion Apparatus.

Fig. 6.6

An unsuccessful attempt was made to determine the chronology of the fracture process near the beginning of the banded zone, using the double torsion configuration described earlier. The transition to a banded zone produced under double torsion always occurred so rapidly that visual resolution of the sequence of events was impossible. However, the experiments did provide some valuable information on the transition to the banded morphology. It was found that, even for constant displacement of the two arms of the specimen, crack propagation was discontinuous; the crack would alternatively pause, often for many hours, and then either propagate rapidly, and form the banded structure, or propagate slowly and form a structure similar to the tensile A-zone. This alternation, pause-propagate-pause, continued until the crack reached the end of the specimen.

This behaviour was investigated quantitatively, for it implied that the banding process could commence at a wide range of values of G. The quantitative measurements were made using the apparatus shown diagramatically in Fig. 6.6. The specimen was positioned between the four loading pins so that the pre-introduced crack ran along the common centre line of both pairs of pins. The two fixed pins were in contact with one side of the specimen, and the moveable pins were in contact with the other side. By displacement of the movable carriage in a direction normal to the plane of the specimen and away from the fixed pins, equal torques were applied to each arm of

the specimen. The load was applied by a Hounsfield Tensometer, and measured with an Ether load-cell.

To evaluate G we assumed that the double torsion specimen consists of a linear, isotropic elastic material, and each arm of the cracked specimen is equivalent to a rectangular beam of length equal to the crack length. From strain energy considerations expressions for G are then readily derived: thus, in terms of the applied load, (from Weidmann, 1973),

$$G = 3 F^2 r^2 / \mu b t^4$$

where F = applied load

r = separation between loading pins on one arm of the specimen

t = specimen thickness

μ = rigidity modulus

b = half-width of the specimen

Twenty-five specimens were examined and the results showed that the value of G corresponding to the onset of slow growth regions ranged between 3200 Jm^{-2} and 400 Jm^{-2}, and those corresponding to the onset of the banded regions ranged between 1500 Jm^{-2} and 180 Jm^{-2}. There was thus an order of magnitude variation in each and a large overlap between the two ranges, which indicates that the transition from the slow fracture mode, (giving rise to a surface structure identical to the tensile A-zone), to the more rapid banding-mode cannot be characterised by a critical value of G. For comparison purposes a few samples of pmma were broken under double torsion conditions. For

this material, a fracture morphology similar to the tensile zone D, (the analogue of the banded zone in polystyrene), could be produced under double torsion only if the crack initiated from a fairly blunt notch; even when it was produced it soon expired as the crack-length increased at constant deflection, and did not recur. In pmma, the "banded" regions occurred at a value of $G \sim 4.5\ kJm^{-2}$. The different behaviour of polystyrene and pmma under double torsion indicates that the process of banding is quite different in the two cases. It is relevant to emphasise this here since similarities between the formation of the two band structures have been assumed, (e.g. Hull, 1970).

The general behaviour of polystyrene under double torsion, in which areas of fracture surface consisting of many bands alternate with smooth areas, implies that the banded structure is controlled by the operation and availability of a particular mechanism. The alternative, that it is controlled by the availability of energy is not viable, since having stopped it can recur at a later stage, following a pause or slow growth region, when the available energy is even less. Fracture surface observations showed that the prominence of individual bands at the end of a double-torsion banded section was less marked than either the bands formed during the early part of that section, or those formed at the beginning of

the next banded section. This suggests that the effectiveness of the mechanism leading to individual bands gradually diminishes and eventually expires, rather than stopping abruptly. On the other hand, when the mechanism next recurs, (i.e. at the beginning of the next banded section), it does so abruptly, and with full effectiveness. Plates 6.31 and 6.32 show respectively, the latter end of one double torsion banded region, and the beginning of the next banded region; an area produced by slow crack growth separates the two regions.

An indication that stress pulses might be an important factor in the formation of individual bands came from the conchoidal fracture surface observations described earlier; as noted then, individual bands had formed along segments of some of the rib-marks. The hypothesis that all bands are stress-pulse induced would be consistent, in principle, with the double torsion result that the banded structure can occur over a wide range of values of G, with the sharpness of the transition to the banded zone on tensile specimens, and possibly with the mode of expiry of the banding process during double torsion fracture.

At the present time one can only speculate on how stress pulses might lead to bands, but it seems a priori possible that if the deflection of a craze leads to rib-marks, this might also lead to the formation of a band. A band, rather than a rib-mark might occur, for example, if the deflection of the craze tip happened to be particularly large, or sharp, so that when the pulse

has passed shear stresses lead to local interfacial failure close to the craze-tip, Fig. 6.7..

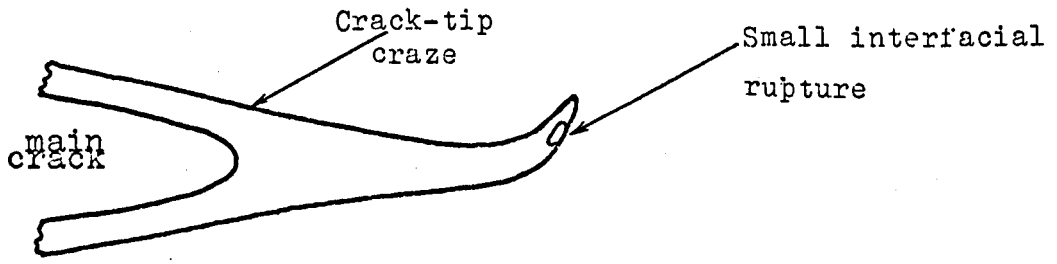

Fig. 6.7

The small 'hole' ahead of the main crack will increase the stress level in the uncrazed material, and could thereby lead to the formation of a fan of crazes ahead of the main crack-tip. The production of such a craze-fan near a small hole in a specimen loaded in tension has been observed directly, (Sternstein et al, 1968). It is worth noting that if the first band of the tensile banded zone is produced by this mechanism, this would account for the slope in the fracture surface at the end of zone B, and for the sharp transition between zone B and the banded zone.

The general hypothesis that all bands are stress-pulse induced, if linked with the double torsion result that banding can occur at any value of G above 180 Jm^{-2}, suggests that provided G exceeds this minimum value, an individual band can occur whenever, and possibly only when a suitable stress pulse arrives at the crack-tip craze. Individual bands do not form in isolation however; whenever a band is formed it is followed by others. This suggests that the first band might trigger suitable conditions for

the formation of the second, and so on; i.e. within a given banded zone the process of band formation is self-regenerative. This possibility is discussed in the next section.

It may be useful to summarise briefly the material of this section; again this will enable established facts to be separated from the more tentative hypothesis.

The transition to the tensile banded zone is extremely sharp, and along the zone boundary, the apex of the first fan of crazes coincides with the tip of the tapered craze of zone B. The formation of a series of bands can occur over a wide range of values of G as shown by the double-torsion experiments.

The chronology of the fracture process at the end of zone B and the beginning of the banded zone is not known, and it may be important to avoid the tacit assumption that events leaving characteristic features on the fracture surface necessarily occurred in time in the same order as they appear on the fracture surface. For example, the sharpness of the boundary of the banded zone suggests that the craze-fan which leads to the first band was produced before complete failure of the tapered craze of zone B had occurred, even though this fan is formed at the end of the tapered craze.

Individual bands can be induced by stress pulses. The hypothesis that <u>all</u> bands are stress-pulse induced, although tentative, would be consistent with several of

the observations; viz the sharpness of the transition to the tensile banded zone, the occurrence of banding over a wide range of values of G, and, possibly, with the mode of expiry of the banded structure within the banded regions formed on double torsion fracture surfaces, (see next section). It is not entirely obvious how a band might be stress-pulse induced, although the formation of bands along rib-marks on conchoidal fracture surfaces suggests that the basic mechanism responsible for rib-marks may also be responsible for banding. Craze-deflection has been suggested as a possible mechanism: a rib-mark forms when the deflected craze returns to its original plane of propagation, and a band when local rupture occurs within the deflected craze. This local rupture acts as a stress-raising site and enables a fan of crazes to develop in the material immediately ahead of the deflected craze.

(ii) The development of the banded structure within the banded zone.

Before discussing the development of the banded structure it is useful to review briefly the experimental facts relating to the structure within a given tensile banded zone.

The rough strips, (i.e. the bands), arise from the rupture of several members of a fan-shaped craze field, and the smooth strips, (i.e. the spaces between bands), from the rupture of a single craze. In all cases,

individual crazes fail by interfacial rupture and local drawing, and in the smooth strips at least, the craze retains its tapered shape. The width of the bands is substantially constant throughout the banded zone and is independent of specimen strength. It is instructive to compare this last observation with the development of the 'bands' within zone D on pmma fracture surfaces; (zone D is the analogue of the banded zone on polystyrene). In pmma the width of the bands gradually increases throughout zone D, and increases with specimen strength, which suggests that the termination of any given band is controlled by the availability of energy. In polystyrene, the constant band-width implies that the termination of any given band is not related directly to the availability of energy. It would appear that the termination of each individual band is controlled by a mechanism rather than by energy. Thus, in polystyrene, a mechanism leads to the development of a fan of crazes, some of these crazes subsequently rupture simultaneously, and the multiple ruptures are eventually arrested, not because there is insufficient energy to maintain them, but because some mechanism prevents their further growth.

We proposed in the previous sub-section that individual bands were stress-pulse induced. It was also noted that once a band had formed it was followed by others to produce a zone consisting of many bands. If each band within such a zone is stress-pulse induced, then it seems possible that the banding process throughout the zone is

self-regenerative; it is conceivable that stress-pulses generated during the formation of any given band are of suitable magnitude and type to lead to the formation of a new fan of crazes, at the site of which a new band is formed, and so on. As stated this 'self-regenerative' mechanism of banding offers only a very general outline of the process which might occur during the formation of the banded zone of the first tensile sequence. Until it is known whether individual bands are invariably stress-pulse induced, and if so, what the detailed mechanism of stress-pulse interaction is, and until more information is available on the exact sequence of rupture leading to secondary, tertiary, etc., pulses, any attempt to develop this 'self-regenerative' mechanism into a more complete account must remain purely speculative; it would presuppose a specific mechanism of stress-pulse interaction with the crack-tip craze, and assume a specific rupture sequence to account for the production of further stress-pulses. At the present stage, therefore, there is little value in attempting a more complete description of the detailed fracture process within a given zone of bands. The essence of the proposed mechanism - *viz*: self-regeneration - nonetheless has certain implications relating to the rupture process within a given banded zone. It is known that the apex of each craze-fan coincides with the tip of the tapered craze which ultimately ruptures to form the preceding smooth strip. To account for this in terms of the self-regeneration

mechanism, it is necessary to assume that one member of each craze fan extends beyond the main field of crazes as shown in Fig. 6.8 .

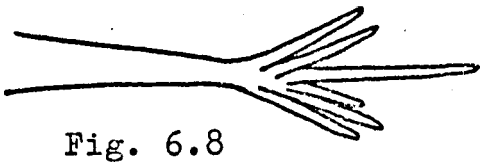

Fig. 6.8

If this were not the case then it would not be possible for each new craze-fan to be formed at the tip of a single tapered craze, and be caused by the arrival of a stress-pulse generated during the rupture of a previously formed craze or set of crazes.

The self-regeneration mechanism may also provide an explanation for the mode of expiry of the bands within a given banded region formed during double torsion fracture. If the formation of each new band relies on the arrival of a stress-pulse generated during the rupture of some previously formed craze or set of crazes, and if for some reason this pulse has less effect than normal, (e.g. it causes a relatively small deflection of the dominating crack-tip craze), then the band formed at that site may be less prominent than the earlier bands. Once a reduction in band prominence has occurred this could have a cumulative effect, in that the stress-pulses generated during the formation of this first low-dominance band could be even less effective, and so on, until eventually the stress-pulses generated at some later stage are unable to lead to the development of a new craze fan. Once this

stage has been reached, the banding process cannot be re-established until a suitable, perhaps chance, shock wave of large amplitude arrives at the crack-tip craze. The banding process could then re-commence by producing bands of the same prominence as those produced during the early stages of the previous banded region.

6.5 The Relationship between Banding and Fracture-Branching

The banded zone is not the pre-branching zone; there is a further zone before branching occurs, (zone D), and this has a similar structure to the immediate pre-branching zone of the second tensile sequence, in which, it will be remembered, no separate banded zone occurs.

In the pre-branching zones of both sequences there is apparently sufficient energy to maintain the banded fracture mode at different levels, although not yet continuously at two levels across the whole fracture area. The situation is therefore rather complex, since it involves cracking at different levels by a process which by itself produces multiple cracks. The mechanism leading to these major level differences might simply be one of secondary nucleation, although there is no direct evidence to support this at the present time. The existence of these major levels, (as compared with the level differences within the bands), indicates, however, that there is a further difference between banding in polystyrene and in pmma. In pmma the banded zone is the pre-branching zone, and the width of the bands gradually increases until eventually one band continues

to form a branch. This suggests that in this material the mechanism of branching is the banding mechanism. In polystyrene, on the other hand, it appears that the banding process, although of considerable interest, may not be directly related to the mechanism of fracture branching: the band-width remains substantially constant and the branch is formed by the continued propagation of two major fractures, both of which involve the banding process in their development.

The fact that both polystyrene zone sequences showed the same structure immediately before branching occurred, suggests that material contamination affects the early stages of fracture only, when the fracture progresses relatively slowly. By the time branching occurs contaminated and uncontaminated material behave in the same way, and there is no significant difference between the mean values of $\sigma c_b^{\frac{1}{2}}$ in the two cases. For the Borst polystyrene, (uncontaminated), the mean value of $\sigma c_b^{\frac{1}{2}}$ at branching was $1.83 MNm^{-3/2}$ and for B.P. material it was $1.65 MNm^{-3/2}$. A Student-t test showed there was no significant difference between these two values.

6.6 Discussion of Previous Results

During the course of this work a series of papers were published on some of the points arising from our own, independent, investigations, (e.g. Hull, 1970, Murray and Hull, 1970). These workers studied *inter alia* the

Mackerel pattern, (Murray and Hull's own phrase), and the banded structure. They argued that the Mackerel pattern was formed by ruptures at the craze polymer interface, and noted the progressive decrease in craze thickness as the banded zone was approached. On these two accounts their ideas are in agreement with our own. They argued that the banded structure was similar in form and was produced by the same mechanism as the banded structure on pmma. In these respects our ideas differ.

In this section we shall examine Murray and Hull's interpretations of the Mackerel pattern and the banded structure.

(i) The Mackerel Pattern

Murray and Hull argue quite explicitly that the Mackerel lines demarcate successive positions of the same crack front as it progresses through the specimen, and the wavy form of the Mackerel lines are due to local variations in crack speed along the crack front. The crack is envisaged as propagating down one craze-polymer interface, thereby increasing the local stress within the craze and causing decohesion at the other interface. The main crack then jumps from its original interface to the decohesion at the other and drawing is caused by adiabatic heating. The process then repeats, the local decohesion now occurring at the original interface.

There are clearly many unsubstantiated assumptions in this model, and it is difficult to see how it could be developed to account for the island structures of zone B,

which is effectively a variant of the Mackerel pattern. Moreover it is not legitimate to draw the conclusion that the Mackerel lines demarcate loci of the same crack front at different times, using only fracture surface observations. Indeed, our own observations have shown that the Mackerel lines were often oriented in completely different directions on adjacent sections of fracture surface, Plate 6.33, which indicates that they could not, at least on these occasions, all have been produced by successive positions of the same crack front.

Murray and Hull make no attempt to explain the tapered shape of the craze within which the Mackerel pattern is formed. The notion of crack propagation down a craze towards its tip is regarded as a natural consequence of the static crack-tip craze geometry; crack propagation is frequently discussed in isolation from the craze, the latter being treated as if it were a static region within which the crack advanced.

In a later paper Hull (1970), argues that the Mackerel lines and the boundary of the banded zone are loci of the same crack front at different times as it progresses through the material; i.e. he assumes that the tapered craze ruptures completely before the boundary to the banded zone has been established. We have previously argued that the chronology of the fracture in this region is far from clear, although the sharpness of the banded-zone boundary suggested that it had in fact been fixed before the tapered craze completely ruptured. Hull makes no reference to the sharpness of this boundary.

Our own observations have indicated that it is very unlikely that the Mackerel lines and the banded-zone boundary demarcate successive positions of the same crack front. Plate 6.34 shows an example where the radius of curvature of the Mackerel pattern is completely different from that of the banded zone boundary; it is unlikely that both could have been produced by a single advancing crack. Plate 6.35 illustrates a case where the Mackerel lines were perpendicular to the banded-zone boundary, which more obviously implies that they could not both have been produced by the same crack front.

It is the author's view that Hull and co-workers too readily interpret tacitly the more basic fracture features and thereby propose models which are based on many unsubstantiated premises about the progress of the crack. We acknowledge that this may have been done in our own discussion, although hopefully with rather more caution.

(ii) The banded structure

To account for the banded structure in polystyrene, (and evidently in pmma), Hull argues that the crack moves in jumps. The smooth strips between bands are thought to be formed by a rapidly moving crack propagating towards the tip of a (stationary) tapered craze. This rapid propagation, it is argued, leads to stress-relaxation, and consequently the crack slows, and thereby allows sufficient time for a field of crazes to developoff the axis of the crack. The establishment of this field of crazes enables

the stress level to build up once more. Some of these new crazes then rupture by cracks 'jumping' down them rapidly, and the process repeats.

This is clearly a tacit interpretation of the fracture surface observations, and contains several assumptions for which no supporting experimental evidence is given. For example, it is not legitimate to conclude from fracture surface observations alone that the crack moves in jumps. Furthermore it is not clear why a crack should slow down under conditions of increasing G. No attempt is made to account for the sharpness of the transition to the banded zone, or to explain why crazes retain their tapered shape, and it is difficult to account for the behaviour of polystyrene under double torsion conditions with this general model.

It is acknowledged that our own discussion of the process of banding is far from complete. However, we feel that it reflects more realistically the complexities of the fracture process in the banded zone. Hull's tacit interpretation, it seems to the author, underestimates at least to some degree the complexities of this fracture process. Furthermore, by relating the prima facie similarities between the banded zones on polystyrene and pmma fracture surfaces the important differences between the two structures is not acknowledged. These differences clearly imply that the mechanism of banding is different in the two materials.

A very simple, and direct demonstration of the difference between the development of the banded structures in the two cases can be obtained by breaking a sample of each material in simple bending and comparing the fracture surfaces so produced. Polystyrene gives rise to the structure shown in Plate 6.36 and pmma to that of Plate 6.37. It will be noted that the shape of the respective zone-boundaries to the two banded zones is quite different: in polystyrene the zone-boundary is roughly concentric about the fracture origin, whereas in pmma the banded morphology is restricted to two lateral "wings".

Johnson and Holloway (1966), have shown on theoretical grounds that if the onset of a particular zone can be characterised by a critical value of $\sigma c^{\frac{1}{2}}$, then for specimens broken in simple bending, the shape of the boundary to this zone may be the same as that found here for the banded zone in pmma. Conversely, it would be impossible for the transition to the banded zone on polystyrene to have the shape shown in Plate 6.36 if it were determined by a critical value of $\sigma c^{\frac{1}{2}}$.

6.7 Summary and Conclusions

This chapter has been concerned mainly with the fracture surface morphology and the related fracture processes in polystyrene, although where it was considered to be appropriate comparisons were made with pmma.

Two sequences of fracture surface zones were identified and their production was shown to depend on the presence of certain chemicals: viz intrinsic mineral oil, sebum and machine oil. Most of the discussion centred on the zones of the first sequence.

Two modes of craze failure were identified. The first mode occurs during slow crack propagation and consists of rupture of a craze roughly mid-way between the craze-polymer interfaces. During this mode of craze failure, the craze, which has a tapered shape, moves forward with the crack, so that to a first approximation the distance between the tip of the crack and the tip of the craze is substantially constant. Conic features are formed during slow crack growth when this first mode of craze rupture occurs. The second mode of craze failure consists of interfacial ruptures, and local drawing of craze material, in a craze which has retained its tapered shape; this occurs immediately before the onset of the banded zone and within the banded zone. By contrast, pmma crazes always fail by rupture between the interfaces, and never at the interface.

From an examination of the morphology of Conic features we were led to propose that the dominant craze thickening process in polystyrene is internal expansion of the craze structure formed within the initial tapered interfaces. Here too there appeared to be an important difference between polystyrene and pmma, for crazes in the latter would appear to thicken predominantly by the accretion of new craze matter.

It was tentatively suggested that the controlling factor in the establishment of the banded structure was the arrival of a stress pulse at the craze-tip, which led to the development of a fan-shaped craze field. It was suggested that the banding process might be self-regenerative. Several important differences were identified between the banded zone in polystyrene and zone D, (the analogue of the banded zone), in pmma. Notably, the sharpness of the zone-boundary in polystyrene compared with pmma; the observation that the banded structure in polystyrene could occur at a wide range of values of G, whereas in pmma it occurred only at a critical value of G; and the constancy of the band width in polystyrene as compared with the gradual increase in band width in pmma as G increased. It was also suggested that whereas the mechanism of banding in pmma was likely to be the mechanism of branching, this may not be the case in polystyrene.

At the time of writing there are many problems which remain unresolved; it is not entirely clear how or why interfacial craze rupture occurs, or why the craze retains its tapered shape when it fails in this manner. The response of a crack and its tip-craze to a stress wave which causes the formation of bands on conchoidal fracture surfaces, and possibly on tensile surfaces, is not yet resolved, although craze deflection was suggested as one possible response. In this respect it might be useful to attempt to induce ripples on the fracture surface using similar techniques to those employed by Kerkhof on glass, (1969).

Finally, it might be useful to extend the comparisons made here between polystyrene and pmma to other polymers. This has been achieved to a certain extent in the next chapter where we discuss the fracture process in an epoxy resin; and some preliminary experiments with the fracture of polycarbonate have shown that defined bands occur on the fracture surfaces, and their production might be influenced by stress pulses. Plate 6.38 shows, for example, some interesting polycarbonate band patterns which resemble Wallner lines.

CHAPTER 7

THE FRACTURE SURFACES OF AN EPOXY RESIN

7.1 Introduction

When specimens of Araldite CT200 resin are broken in simple tension, in common with the previous two materials they develop a characteristic morphology of the fracture face, Plate 7.1. Three distinct zones are produced, the general sequence of which resembles that found on the fracture surfaces of other materials, (e.g. glass and pitch). Andrews, (1959), introduced the terminology mirror, mist and hackle to describe this three-zone structure. Here, the mist zone corresponds to the area of striated and stippled surface contiguous to the smoother mirror zone, and the hackle to the fracture surface which follows branching at the mist-hackle boundary. In this chapter we discuss the results of a detailed examination of the microstructure of the mist zone.

7.2 Classification of the features which occur in the mist zone.

The mist zone of any single fracture surface of this resin consists of a collection of localised features superimposed on a general corrugated background, Plate 7.2. Most of these features are approximately parabolic or elliptical in outline, but they have different peripheral and internal markings.

In this section we shall briefly describe and illustrate these features enabling seven different types

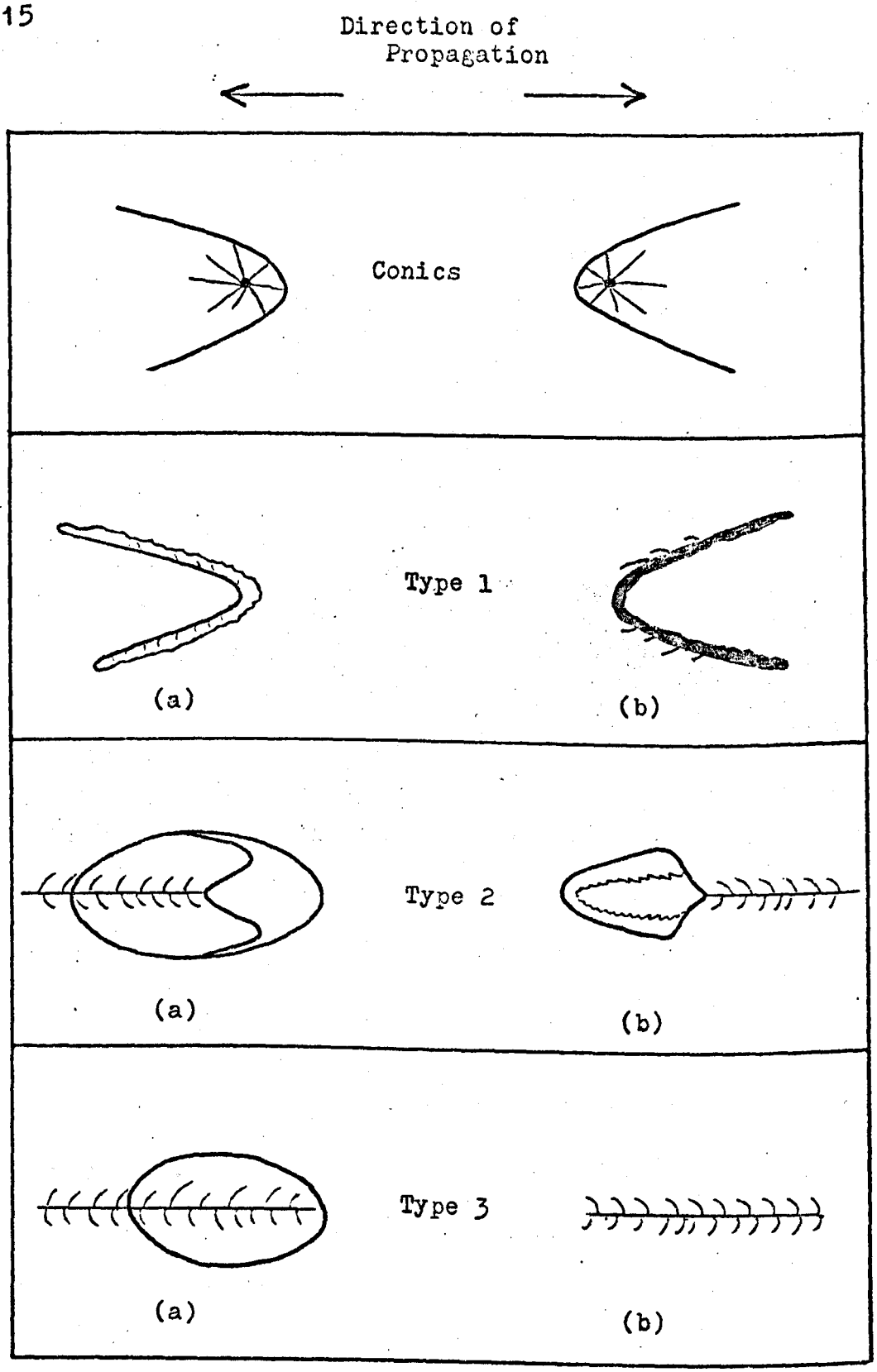

Essential Characteristics of main Fracture Surface Features.

Fig. 7.1

to be identified. Later, it will emerge that six of the features so categorised can be sub-grouped into three complementary pairs, the members of each pair being different manifestations of the same local fracture process as displayed on matching fracture surfaces. Fig. 7.1 illustrates the essential characteristics of each of the seven different features.

The first pair of diagrams in Fig. 7.1 illustrate a Conic feature, so-called because of its resemblance to the Conic features observed on the fracture surfaces of pmma and ps. These are parabolic lines with the closed end facing the origin of fracture. Each parabola has small streaks radiating from a point near to its 'focus'. (The use of the term 'parabola' in this context carries the same limitations as in Chapter 5).

Type 1a features are parabolic stripes, (rather than lines), the closed end again facing the origin of fracture. The stripe itself may vary in width, and usually shows interference contrast or fringes along part of its length when viewed in reflected illumination, and the inside edge of the stripe is more sharply defined than the outside.

Type 1b features also appear as a parabolic stripe, but are distinguished from Type 1a features by the absence of any interference effects along the stripe. Also, in this case, the outside edge of the stripe is the sharper, and small curved striations are present around the outside of the stripe.

Type 2a features are elliptical in outline, although a striation normally extends beyond the end of the feature which is furthest from the mirror zone, and smaller striations curve to meet it on either side, as shown in the diagram. The fracture surface within the elliptical boundary of the feature consists of two well-defined regions separated by a "W-shaped" boundary.

Type 2b features bear a superficial resemblance to a fish which has had the flesh of the body and tail removed, but not that of the head. The analogy breaks down with the "ribs" however, which are curved in the wrong direction. The "fish-head" lies at the end nearest the origin of fracture; it has a central featureless band running from front to back, and a more structured peripheral boundary which thickens at the rear of the head. When viewed in reflected illumination, interference contrast effects can be observed along this outer boundary.

The final two feature types have been designated Type 3a and Type 3b respectively. Type 3a features have a sharply defined elliptical boundary upon which is superimposed a "fish-bone" structure without the "head". The "back-bone" of this structure lies along the major axis of the ellipse, and normally extends with its associated "vertebrae" beyond the end of the elliptical boundary furthest from the origin of fracture. In reflected illumination quasi-elliptical interference fringes can be observed within the elliptical boundary of the feature.

Type 3b features, consist of a "fish-bone" structure without the head.

Comparison of equivalent regions on matching fracture surfaces revealed that the Type 1a, 1b, the Type 2a, 2b, and the Type 3a, 3b, were, respectively, matching pairs, and this is reflected in the choice of nomenclature employed in their categorisation. Of the features, Type 1 and Type 2 were more common than Type 3, and Conics were the most common of all. Apart from Conics, Type 1 features were predominant near the mirror boundary, while Type 2 features gradually increased in number with distance from the mirror zone until they became predominant near the hackle boundary.

A study of the topography of the fracture surface around each feature was undertaken using the optical microscope and attachments previously described in Chapter 4, and in the next section the results of these observations are summarised.

7.3 The Fracture Surface Topography around the Features

(i) Conics

Unlike the Conics observed on the fracture surfaces of the two thermoplastics, the Conics observed here had no interference fringe patterns associated with them. Indeed, there was no evidence of any thin film interference effects similar to those described in the previous two chapters.

Conic features were present over the whole of the mist zone, although the number per unit area of fracture surface increased with increasing distance from the fracture origin. Sometimes one of the parabolic arms of a Conic

feature was terminated by a second Conic formed in its path. Also, small Conic features were often observed within the boundary of a larger one, and these frequently terminated one of the radial streaks which emanated from the focus of the parent Conic. Furthermore, the closed ends of these small Conics invariably pointed towards the focus of the parent Conic.

The parabolic boundary of any given Conic resulted from a sharp step on the fracture surface, of height typically $\sim 0.3\mu$: i.e. the fracture surface immediately inside the Conic boundary was either higher or lower than that immediately outside by this amount. The fracture surface between the 'focus' and boundary of a Conic was invariably curved, and Fig. 7.2 shows the general form of this curvature for a typical feature. The fracture surface on the matching feature, would, of course, be curved in the opposite sense.

The small streaks referred to earlier, which radiated from the focus of a Conic were found to be small steps of height $\sim 0.1\mu$ or less.

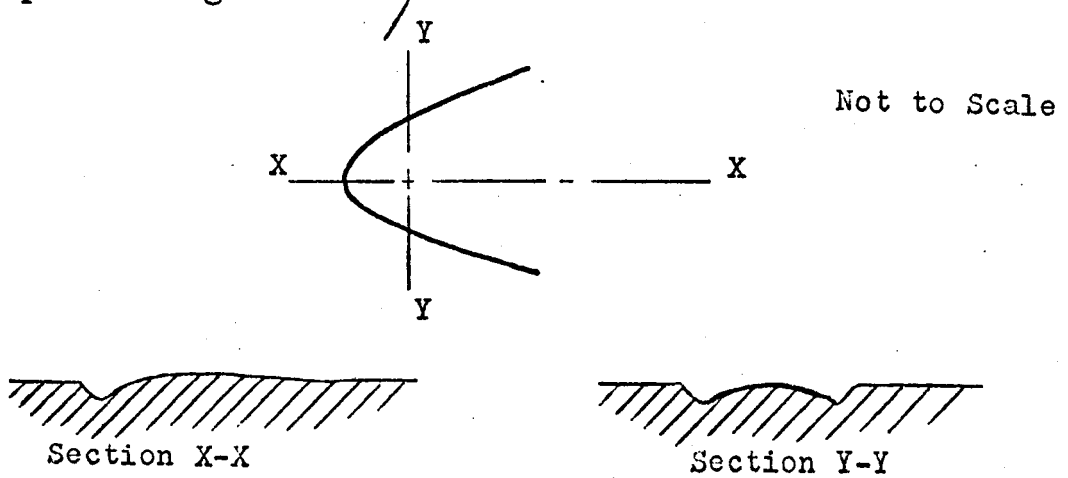

Fig. 7.2

(ii) Type 1 Features

The fracture surface inside the stripe of the Type 1a features was always lower than that immediately outside; the characteristic stripe itself was often at a higher level than the two fracture surfaces which it separated, and sloped sharply to meet these levels on either side. In some cases, the stripe was completely separated from the fracture surface, when it appeared as a strip or sliver which pointed upwards from the fracture plane.

On the larger features of this type the fracture surfaces on either side of the stripe showed a level difference of up to $\sim 80\mu$, and the smallest examples had a level difference typically of a few microns on either side of the stripe. Plate 7.3 shows an example of a large Type 1a feature, and Plate 7.4 shows a smaller feature of this type.

The fracture surfaces in and around Type 1b features were shown to be complementary to those of Type 1a: i.e. the fracture surface inside the stripe of the Type 1b features was always found to be higher than that immediately outside. The magnitude of the level difference on either side of the stripe of a Type 1b feature was the same as the matching Type 1a feature. Plate 7.5 shows a typical Type 1b feature.

Distortions from the relatively straightforward instances of Type 1a and 1b features were occasionally observed. Very infrequently for example, the outer boundary of a feature was completely closed to form an approximate

ellipse, Plate 7.6; and sometimes when the feature which mated with a Type 1a feature was examined, it too appeared to be a Type 1a feature, in that a section of its paraholic boundary displayed interference fringes; one essential characteristic of Type 1a features. This latter variant was subsequently found to be due to a section of the stripe of the Type 1a feature becoming completely separated and adhering to the Type 1b feature on the matching fracture surface. Once experience of this effect had been obtained, subsequent cases were categorised as Type 1b when the area of surface inside the parabolic boundary was higher than that immediately outside. A further ambiguity arose with the smaller Type 1 features, which so closely resembled Conics that it was sometimes difficult to place them into either category. The very nature of this ambiguity suggested however, that Type 1 features and Conics might arise as a result of a similar fracture process, and/or that a Conic was a limiting case of a Type 1 feature.

(iii) Type 2 Features

Plate 7.7 is a micrograph of a typical Type 2a feature, and Fig. 7.3 illustrates this feature schematically. Region A, (Fig. 7.3), was always closest to the fracture origin, usually contained a series of striations which curved towards the elliptical boundary, and was always lower than the surrounding fracture surface. Region B was higher than the surrounding fracture plane.

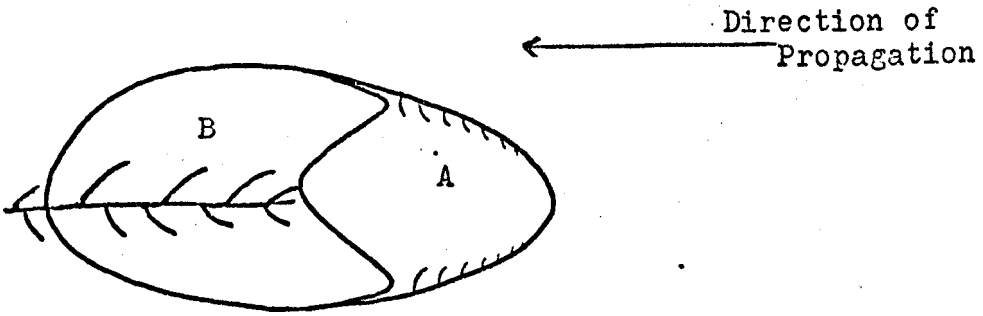

Type 2a Feature: Regions A and B

Fig. 7.3

When observed in reflected illumination, approximately elliptical interference fringes were normally present within region B, Fig. 7.3, but after slowly etching away the top layer of the fracture surface with N/6 chromic acid until the boundary between regions A and B just disappeared, these interference fringes were no longer present. This suggested that the crack which produced region A also extended beneath the exposed fracture surface of region B.

Plate 7.8 shows a typical example of a Type 2b feature. The fracture surface in and around this type of feature was found to be complementary to that of the Type 2a features. The "fish-head" of the type 2b features effectively slotted into region A of Type 2a features, and the "vertebrae" mated with the striation pattern observed on region B.

(iv) Type 3 Features

The elliptical boundary of each Type 3a features was shown to demarcate the periphery of a totally sub-

surface crack; by etching away the exposed fracture surface with N/6 chromic acid this crack was revealed directly, and it was found to be of the same size as the elliptical boundary of the former Type 3a feature. This sub-surface crack often sloped away from the fracture plane at the end furthest from origin of fracture.

The fish-bone structure which was superimposed upon this elliptical boundary, an example of which is shown in Plate 7.9, always matched in detail with the "fish-bone" structure of the Type 3b feature found on the complementary fracture surface. Plate 7.10 shows the Type 3b feature which matched the Type 3a feature shown in Plate 7.9. For obvious reasons, no matching counterpart to the elliptical boundary of Type 3a features was observed on the Type 3b. The "backbone" of the 'vertebrae' structure of Type 3a features was invariably slightly higher than the surrounding fracture surface level, and it was slightly lower in the case of Type 3b features.

7.4 Other Fracture Surface Markings

The features just described were the more prominent fracture surface markings found in the mist zone. Other fracture surface markings were observed both in the mist and the mirror zones, and two of these are described and discussed below.

(i) The origin of fracture when fracture initiated internally.

Although not a feature in the sense of a regularly repeated structure on the fracture surface, the morphology

of the surface around the origin of internally initiated fractures was of some interest. Whenever fracture initiated internally, a complex region was produced at the origin of fracture, similar to that shown in Plate 7.1. A close examination of this region revealed that miniature mirror and mist zones were present within it. Within the miniature mirror zone an inclusion was usually present. Plate 7.11 shows an example.

The surface morphology within this miniature mist zone was quite different from the macroscopic mist zone described above. The individual features of this first small mist zone closely resembled those found on fracture surfaces of partially-cured resin, (containing only about one sixth the normal amount of hardener), and this similarity suggested that there could be local regions within the nominally fully cured samples which had a cross-link density much below the average for the completely cured material.

Griffiths, (1969), has shown that the fracture energy of this resin, when cured with only one-sixth the recommended amount of hardener, was much lower than that of the fully cured material, ($\sim$3.5 Jm^{-2} as compared with $\sim$100 Jm^{-2}). Therefore a localised region at which the cross link density was lower than normal could easily act as a site at which a crack, once formed, could propagate to a catastrophic size.

If this is the case then the existence of these localised, low toughness sites might impose a limitation on

the useful strength of this material, especially if, as was the case here, an inclusion was always present to act as a stress raising agent in the vicinity of such a site. The presence of such inclusions might of course be more than a coincidence, but this possibility was not examined in any detail.

(ii) Craze-like Features

Small dark lines were visible on the fracture surfaces of all specimens examined. These lines lay in a direction roughly perpendicular to the general direction of fracture propagation, and many Conics and small Type 1 features were observed with one such line at their focus, Plate 7.12.

It was impossible to focus the microscope on these lines so as to produce a sharp image, although by focussing slightly below or above the fracture surface an effect similar to Becke Line interference was observed. This suggested that there might be small strips with a different refractive index from the bulk resin lying roughly normal to the general direction of fracture propagation, and that the lines were simply sections through such regions.

Simple experiments established, however, that it was most unlikely that the lines on the surface were simply sections through imperfections or irregularities within the cured resin. They appeared to be related to the fracture process. On tensile fracture surfaces, for example, the number of lines formed per unit area of

surface increased with distance from the fracture origin, and the orientation of the lines depended only on the direction that the fracture took through the material. On fracture surfaces formed by breaking double-cantilever-beam specimens the lines were straighter and more nearly parallel to one another than those observed on tensile fracture surfaces. Furthermore, when a specimen was broken under these conditions, (except for the case when the crack was allowed to propagate under dead-loading), the crack extended by a series of discrete jumps, and the number of lines formed on the resulting fracture surfaces was greater around each crack arrest position.

These observations suggest that the lines are related to the fracture process itself. They might of course develop from some microstructural feature within the material when this is acted upon by the stresses associated with the moving crack. Possible microstructural features might be inclusions similar to those found at the origin of internal fractures, or local regions with significantly lower cross-link density than normal, similar to those discussed in the previous section.

Although the origin of these fine lines is still unknown, their resemblance to the fine dark lines found on the fracture surfaces of pmma is quite striking. Like these lines, those found on the resin fracture surfaces matched in location although not always in length, and they had no pronounced effect on the fracture surfaces around them. It was argued in Chapter 5 that small oblique

crazes could account for the presence of the lines on the fracture surfaces of pmma. It is possible that a similar explanation might account for their formation in the resin, especially in the light of recent work undertaken in these laboratories in which craze-like markings were observed around the tip of a loaded crack in this, and in other, epoxy resins, (Lilley and Holloway, 1973). Plate 7.13 shows a field of these "crazes" formed around the tip of a crack which had been loaded by driving a wedge into its open end.

The observation that a high proportion of the Conic features had one such line present at their foci has not yet been accounted for, but this behaviour might be consistent with the hypothesis that the lines are produced by an intersection of a craze with the fracture surface. Conics are produced by the interaction of the main crack with a smaller secondary crack formed by advanced nucleation (see Chapter 5 and the next section), and it is possible that the stress magnification around the site at which the secondary crack was formed might, in some cases, be sufficiently great to cause crazing. If so, a craze would be present near to the foci, (i.e. the origin of the secondary crack), of many Conic features.

7.5 Discussion of the Formation of the Mist Zone Features

Earlier in this chapter we classified the mist-zone features using evidence obtained directly from the fracture surfaces. In this section we shall argue that the formation of each feature can be accounted for in terms of an

interaction between the main crack and a secondary crack formed in the unbroken material ahead of the main crack.

It has already been mentioned in Chapter 5 that Conic features are now commonly regarded as one hallmark of secondary nucleation, but there is other evidence which suggests that this is the dominant, if not the only, mechanism giving rise to secondary cracks in this material. Beneath some parts of the exposed fracture surfaces, sub-surface cracks could be observed as a consequence of the interference fringes to which they gave rise. These cracks were evidently formed so far from the plane of the main crack that they caused no significant perturbation of the fracture surface above them. Their very presence is strong evidence for secondary nucleation in this material however. Type 3a features could also be related to the presence of totally sub-surface cracks, and in some cases inclusions could be found within the boundaries of Type 1 and 2 features. It is likely that such inclusions acted as local stress raising agents at which secondary cracks could form. Plate 7.14 shows a micrograph of a Type 1a feature within whose boundary an inclusion is clearly visible.

It is possible to account for the structure of each feature in terms of an interaction between the main crack and a smaller secondary crack formed by advanced nucleation in the unbroken material ahead of the main crack. The form which this interaction takes will clearly depend in part on the normal separation between the plane of the

main crack and the plane of the secondary crack when the two cracks approach. If this separation is less than the average value of the two crack-tip radii then the two cracks will effectively "collide" as discussed in Chapter 5. If this separation is greater than the average crack-tip radius, however, the two cracks can overlap to some extent prior to joining. These two possibilities are shown diagramatically in Fig. 7.4(a) and Fig. 7.4(b) respectively, which are views from a plane which is parallel to the propagation direction and normal to the leading edges of the cracks.

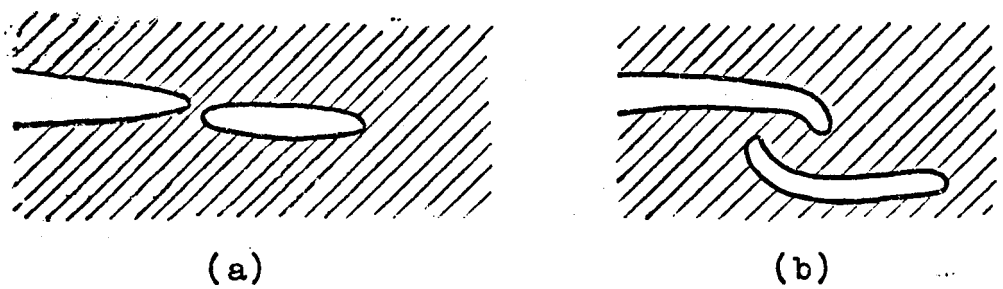

Fig. 7.4

A third mode of interaction is <u>a priori</u> possible; viz: the two cracks may overlap and then repel one another. This case might arise, for example, if the secondary crack had propagated in a plane which was oblique to the plane of propagation of the main crack as shown in Fig. 7.5, (p. 230).

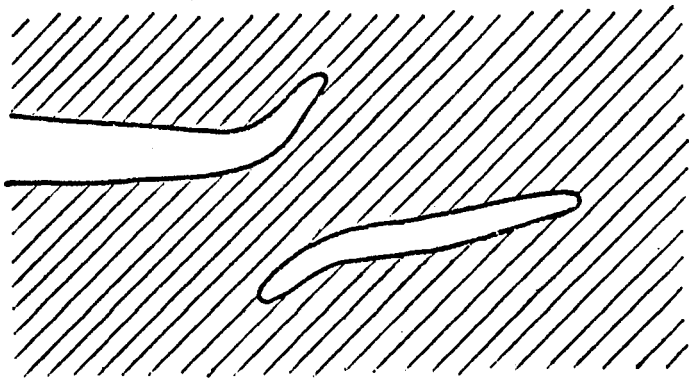

Illustrating a third possible mode of interaction.

Fig. 7.5

From the observations made on the features it is clear that if this mode of interaction does occur, it arises only very infrequently.

(i) The formation of Conic Features

The formation of Conics has already been discussed in Chapter 5. There it was argued that when the lateral distance separating the main crack and the secondary crack was less than the average value of the two crack-tip radii, a Conic feature would be formed. Such a condition would result from the collision mode of interaction just described.

The Conic features formed on the fracture surfaces of this resin have a structure consistent with this model, since it can be shown that the step height across the parabolic boundary of each Conic is less than the average tip radius of the two interacting cracks.

Plate 7.15 shows the tip of a crack formed in this material by loading the open end of a crack with a small wedge. The radius of this crack tip is $\sim 1.0\mu$. This, being the tip of a static crack, may not be a true representation of the radius of the tip of a moving crack

however, which is thought to be somewhat smaller, (Lilley, 1973). Nonetheless, the measured step height across a typical Conic boundary: i.e.~0.3μ, is substantially less than this estimate of the crack tip radius, and this supports the contention that Conic boundaries are formed by crack-crack collision.

(ii) Type 1 Features

The fracture process which leads to the formation of Type 1 features is thought to be similar to that which leads to a Conic, except that the planes of the interacting cracks are now separated by a distance which is greater than the average crack tip radius. Every feature which was unambiguously Type 1 showed a level difference across the boundary of at least a few microns, and if this is compared with Lilley's estimate of the maximum crack tip radius of $\sim 1.0\mu$, then the planes of the two cracks which led to any Type 1 feature must have been separated by a normal distance greater than the average crack tip radius. Fig. 7.6 illustrates the sort of interaction which is thought to occur when a Type 1 feature is produced. (Both views are from a plane normal to the crack fronts and parallel to the direction of propagation.)

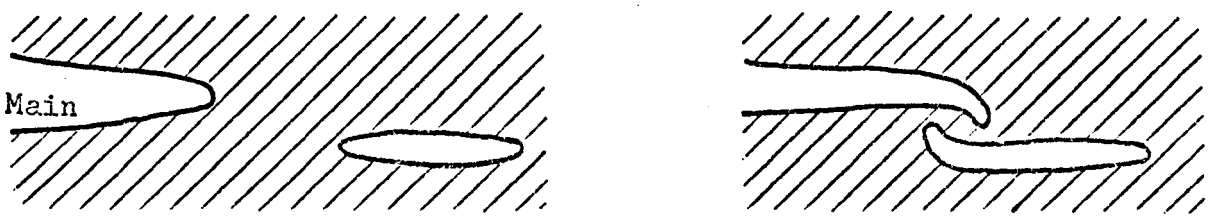

(a) Main and Secondary Cracks Approach

(b) Cracks overlap and then join

Fig. 7.6

The two fracture surfaces which are formed by this interaction are shown in section on Fig. 7.7. (For clarity a plan view of each structure is included.)

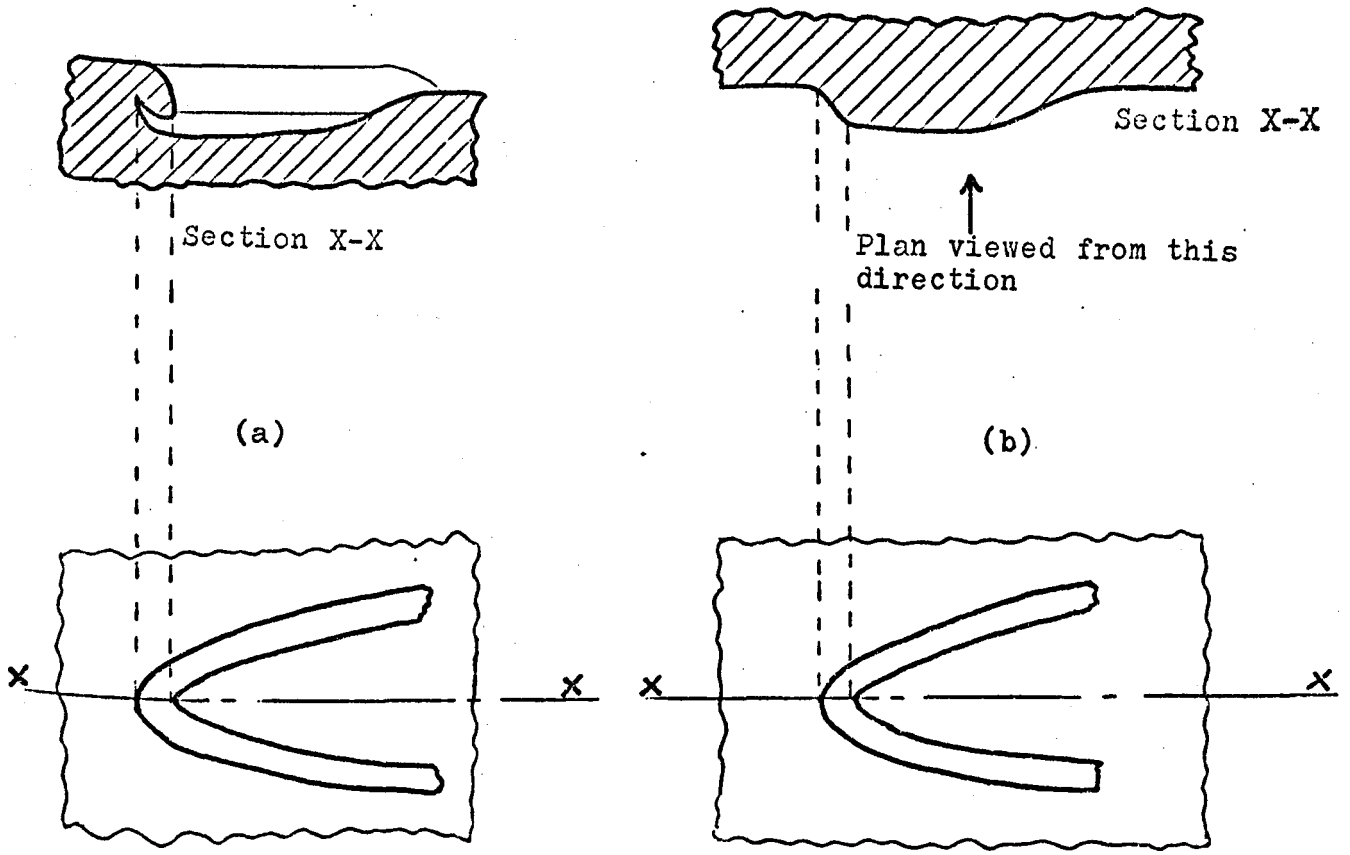

Fig. 7.7

When viewed in reflected illumination the boundary of the structure shown in Fig. 7.7(a) could show interference contrast in the region where the two cracks overlapped. It would also be feasible for this boundary region to become completely separated during final parting of the fracture surfaces, since in some cases it might only be fastened to the fracture surface below it by a thin strip of material. This would account for the slivers sometimes observed on the edges of Type 1a features.

The structure illustrated in Fig. 7.7(b), when viewed normally in reflected illumination, would show a dark boundary where the main and secondary crack joined, the width of which would depend on the sharpness of the step between the two levels. The plan view of this interaction would be similar to that drawn by Berry, (1964), to represent the formation of Conic features. On one fracture surface a parabolic stripe displaying interference contrast would be formed, and a dark parabolic stripe would be formed on the other. This model is therefore consistent with the general structure of the boundaries of Type 1a and 1b features. It also accounts for the observation that the surface within the boundary of any Type 1a feature was lower than the surrounding fracture surface, whereas the boundary of any Type 1b feature was higher.

(iii) The formation of Type 2 features

The structure of the surface in and around Type 2 features can also be accounted for in terms of a crack interaction in which the perpendicular distance between the planes of the two cracks is greater than the average crack-tip radius. In this case, a section of the main crack front is thought to be terminated very abruptly after overlapping the secondary crack. The secondary crack continues to expand in the general direction of fracture propagation, but at a slower rate than the sections of main crack front adjacent to the local section whose growth has been terminated. The secondary crack

is overtaken by these two sections of main crack front, and consequently its growth is eventually arrested. The two sections of main crack front sweep across the secondary crack and subsequently join. Fig. 7.8 illustrates this general process, in views looking down on to the fracture plane. At some stage the end of the secondary crack closest to the origin of fracture sweeps up towards and joins the main crack.

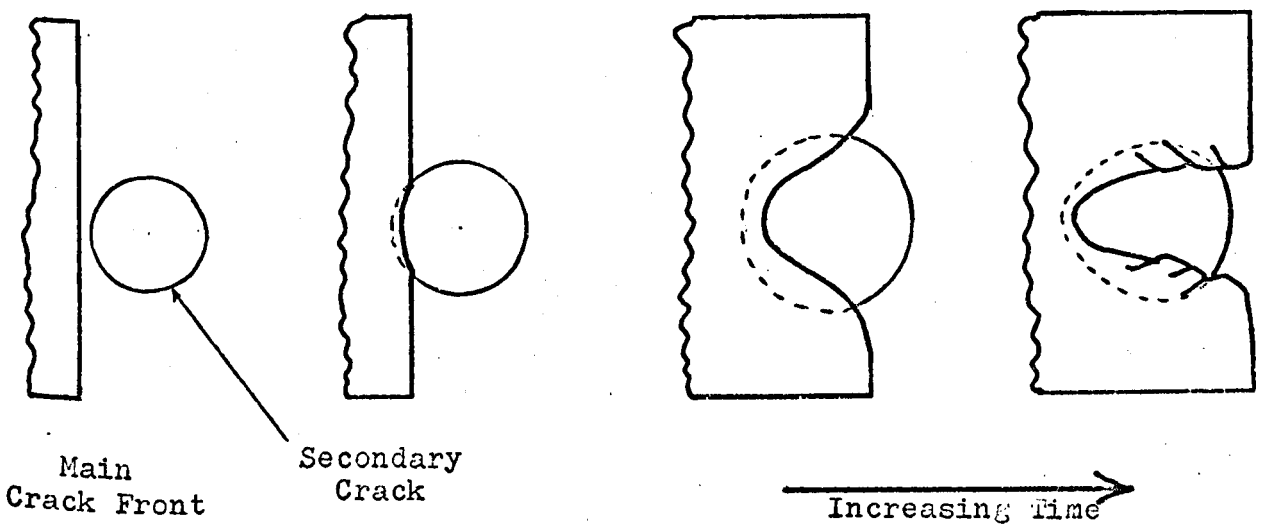

Fig. 7.8

Fig. 7.9 shows sections through the final crack arrays. (p. 235).

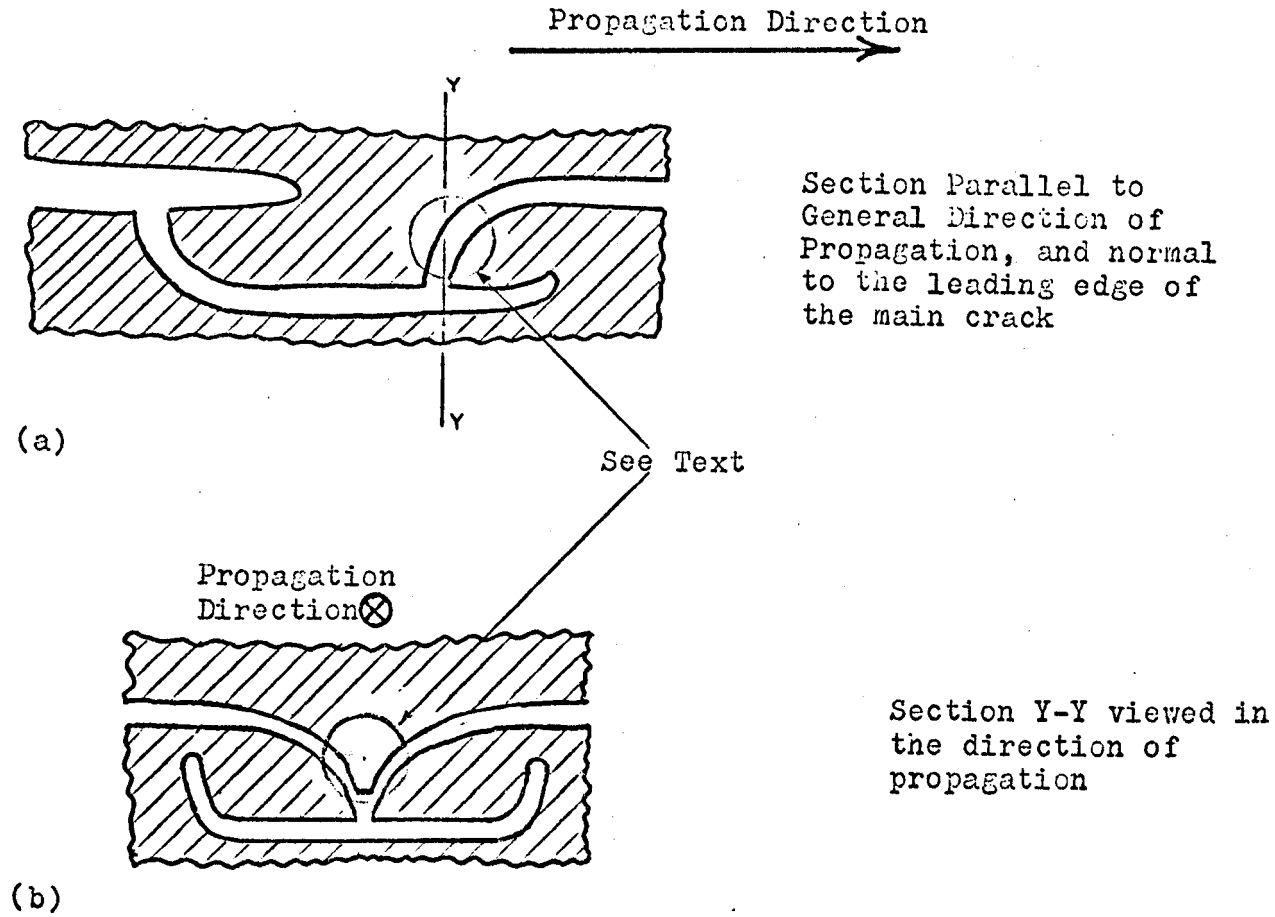

Fig. 7.9

A brief consideration of the crack arrays depicted in the preceding figure will indicate that the surfaces will tend to stick together at the encircled region. Complete severance of this local region will occur by tertiary cracking between the sidesweeping sections of main crack front and the secondary crack.

Fig. 7.10 illustrates the resulting structures formed on the fracture surfaces as a consequence of this crack interaction, (p. 236).

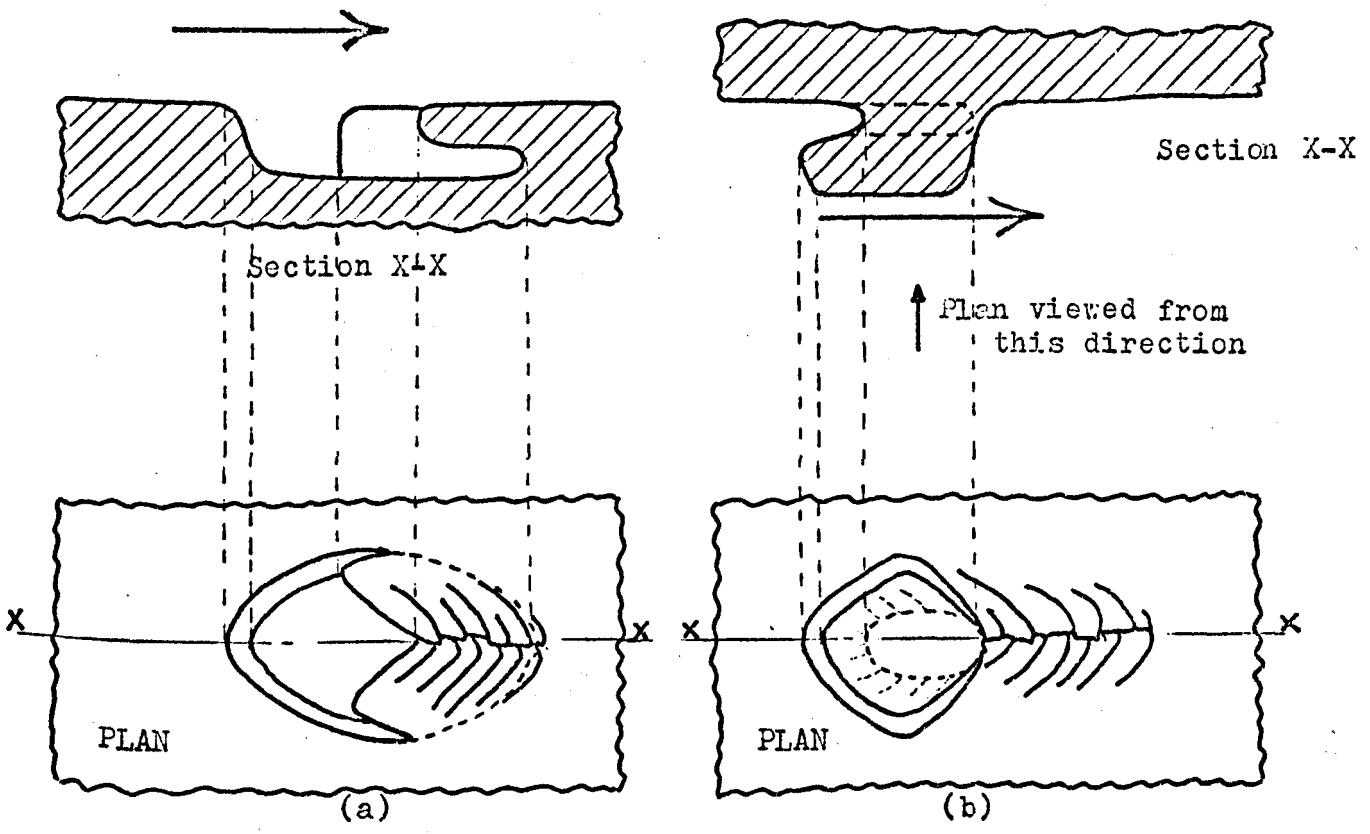

Fig. 7.10

(The arrows indicate the direction of propagation)

These structures are consistent with the observations made on Type 2 features. Fig. 7.10(a) shows a subsurface crack beneath the end of the feature furthest from the origin of fracture, and a subsurface crack was observed in this region on all Type 2a features examined. Fig. 7.10(b) indicates that the main crack undercuts the secondary one, which is again consistent with observations; the boundary running along the sides of the 'fish-head' of Type 2b features was found to be due to the presence of a crack beneath the exposed fracture surface. This model also explains why the 'fish-head' was always higher than the surrounding fracture plane.

The process just described to account for the formation of Type 2 features would consume more energy than the process which is thought to lead to Type 1 features, since a greater total surface area is produced. One might therefore expect that Type 2 features would be more frequently produced in the later stages of the mist zone, where the available energy is greater. As reported earlier, observation shows that this is the case.

(iv) Type 3 Features

The formation of Type 1 and Type 2 features both involve the main and secondary cracks joining. Observation shows that the secondary crack which leads to the formation of a Type 3 feature does not itself form part of the final fracture surface, which means that in this case the main and secondary crack do not join.

Type 3 features are thought to arise from a similar process to that which leads to Type 2 features, except that the sidesweeping pincer action of the sections of main crack front adjacent to the local section which overlaps the secondary crack severs the local area of the specimen completely before the main and secondary crack have had time to join. This process is shown in Fig. 7.11, (p.238).

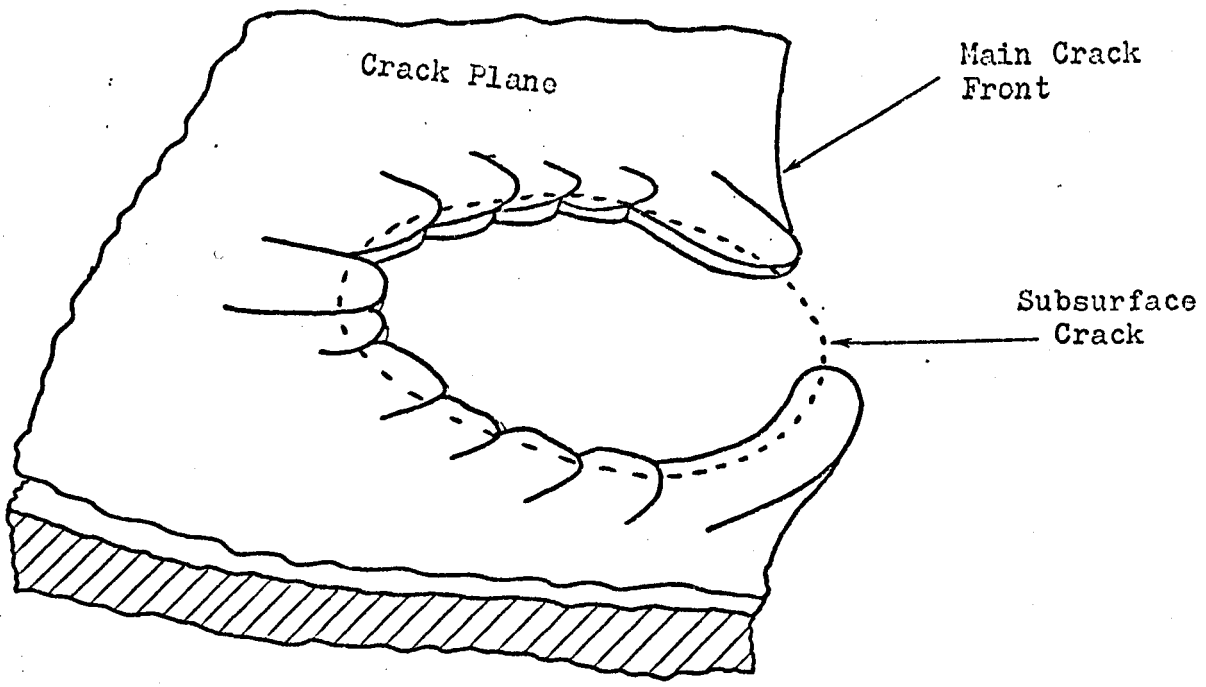

Fig. 7.11

Fig. 7.12 shows sectional views of the resulting crack arrays formed by this process.

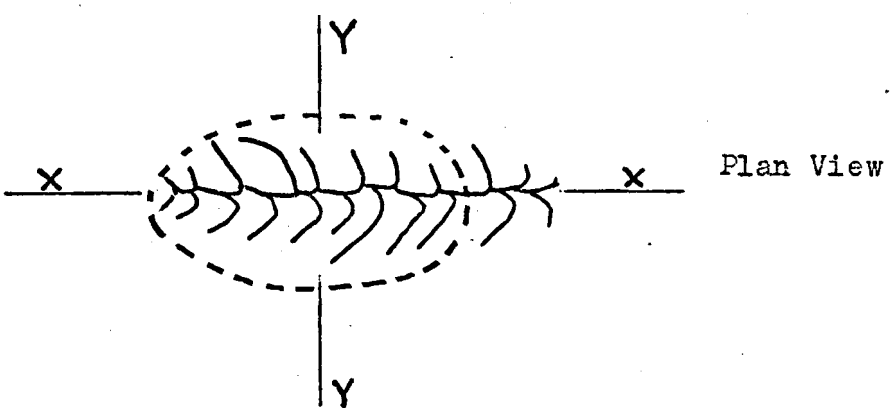

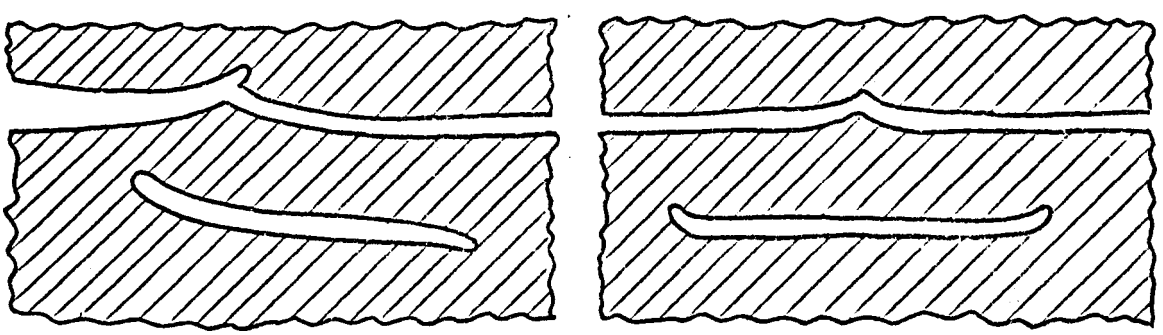

Section X-X

Section Y-Y

Fig. 7.12

If we are correct in thinking that the essential difference between the process leading to the formation of a Type 3 and a Type 2 feature is that in the former case there is insufficient time for the secondary crack to join the main one before a complete surface of separation exists above the secondary crack, then one possible reason for this is that the level difference between the main and secondary crack planes is generally larger when a Type 3 feature is produced.

Measurements on typical features indicate that there is a definite trend in this direction. For example, a typical level difference between the fracture plane and the subsurface crack beneath small Type 3a features was $\sim 12\mu$. For comparable Type 2 features the level difference across the boundary tended to be somewhat less than this, ($\sim 8\mu$).

7.6

Further Discussion

The models proposed for the formation of each of the dominant fracture surface features are material-independent, apart from the implicit assumption that there was no preferred plane of propagation which influenced the direction taken by either the main or the secondary crack. For this reason, if the account of the formation of each feature is correct in this material, then the features observed on the fracture surfaces of this resin should be similar in form, although perhaps different in scale, to fracture surface features formed by secondary nucleation in any isotropic solid.

One group of isotropic materials for which it has been commonly assumed without supporting experimental evidence that a secondary nucleation mechanism operates, are the inorganic oxide glasses, (see, e.g. Clark and Irwin, (1966), Congleton and Petch, (1967). It is of interest to compare the fracture surface features formed here with those formed on the mist zone of glass fracture surfaces.

Johnson and Holloway, (1968), have described the results of a detailed examination of the microstructure of the mist zone on the fracture surfaces of glass specimens broken in simple tension and bending. They found that the mist zone consisted of a collection of separate features which could be divided into two basic types. In normal incident illumination the first type had a central bright optically smooth area bounded on each side by a dark, slightly curved band. Plate 7.16 illustrates a prominent example. The second type had a dark narrow central band which broadened at the end nearer the origin of fracture, and was flanked with bright, often striated, but otherwise optically smooth areas on either side. Plate 7.17 shows an example of this type of feature.

The surface topography of both types of feature was examined with a Linnik interferometer, and it was found that the first had a long narrow strip of fracture surface which arched quite abruptly from the original plane of propagation, and then subsequently joined the original

level more slowly. The second type was essentially two optically smooth areas separated by a sharply rising step which had a complex depression or elevation at the end nearer the fracture origin.

By lightly etching the surface with dilute HF the structure of many of the features on the exposed un-etched surface could be related to subsurface microcracks. If these subsurface cracks were formed by secondary nucleation then we might expect there to be a basic similarity between the features to which they gave rise and those formed on the fracture surfaces of the Araldite resin. The subsurface cracks formed in glass are generally much smaller than those in the resin, and this difference has been borne in mind in the following discussion.

There are obvious similarities between the broad structures of Type 1 and 2 glass features, and Type 1 and 2 resin features respectively. One main difference, however, at least between the larger, well resolved glass features and the resin features concerns the ends of the features closest to the fracture origin. In the resin, the Type 1 and 2 features have a well defined, fairly sharp boundary, which results from the main and secondary cracks joining; in the glass features there is no clear indication of the existence of such a well defined boundary.

One possible explanation of this structural difference between the glass and resin features could be that the mechanism leading to the formation of the features in

glass is not one of advanced secondary nucleation. It is possible to account for the structures of the glass features in terms of a mechanism involving local bifurcations of small sections of the main crack front. This is not possible for the resin features. In a local bifurcation mechanism the first type of glass feature would be formed when one of the local bifurcations failed to propagate and fracture continued by growth of the second. The second type would be formed if both local bifurcations failed to propagate, and the fracture continued by expansion of the segments of main crack front adjacent to the locally bifurcated section.

The apparent absence of a well defined step at the head of the glass features might, on the other hand, simply be a consequence of the size of the step.

Types 1 to 3 resin surface features were explained in terms of crack interactions in which the perpendicular distance between the planes of the main and secondary cracks was greater than the average crack-tip radius. In glass, the radius of a crack tip is thought to be $\sim$ 0.8nm (see, e.g. Weidmann, 1973), and in principle secondary nucleation would lead to features like Types 1, 2 and 3 resin features, provided the secondary crack were nucleated at a distance exceeding 0.8nm from the main crack plane. But in order to see a step at the head of each feature, the secondary crack would need to form at a distance corresponding to many crack-tip radii above or below the

plane of the main crack, and it is unlikely that the stresses would be large enough to nucleate secondary cracks so far off the axis of the main crack, unless, of course, much larger stress raising agents than are normally present were available. (Johnson (1963) has shown that features with a clearly resolvable step at their heads could be produced in glass if silica particles were present to act as stress raising agents. Such features were very similar to the resin Type 1 features.)

A simple comparison between the structures of the resin and glass features does not provide sufficient evidence to make a decision either way on the mechanism in glass. Other circumstantial evidence does seem to suggest that a local bifurcation mechanism is the more likely, but we shall not enter into discussion of this here.

7.7 Summary and Conclusions

This chapter describes and discusses the information obtained from a largely qualitative inspection of the mist zone of Araldite CT200 resin. The most significant result is that the fracture surface features were found to be capable of a division into a few basic types, and all of these could be explained in terms of an interaction of the main crack with a smaller, secondary crack formed by advanced nucleation.

The multiplicity of these secondary cracks draws attention to the energetics of the fracture process, as

well as providing the basis for an explanation of the morphological appearance of the mist features. In terms of the energy argument for branching discussed in Chapter 3, we would expect crack branching to occur when both the main and secondary crack receive sufficient energy from the store of strain energy in the specimen to propagate together. Throughout the mist region this condition is not fulfilled. In the case of the Type 2 and 3 mist features, for example, the secondary crack is arrested, and the fracture advances by extension of the main crack only.

Finally, the presence of the secondary cracks in the mist zone should, as indicated in Chapter 2, have a marked effect on the terminal fracture speed in this material. The terminal speed in epoxy resins tends to be a low fraction of the longitudinal wave speed. This could be related to the relatively early stage, (in terms of the corresponding value of G), at which these secondary cracks form, as witnessed by the location of surface features to which they give rise. If secondary cracks form at a relatively low value of G, then this might set an early, and correspondingly low limit on the ultimatekinetic energy acquired by the main crack.

In conclusion, a general point which has arisen from the experienced gained from the fractography studies of this, and to a large extent the other materials, is that although it is relatively easy after the event to account for what has happened, it is much more difficult to explain

why. For example, why on a given occasion, a secondary crack and main crack join to form a Type 2 feature, and on another occasion a Type 3 feature. This distinction between what has happened and why it happened, and the relative paucity of information regarding the latter not only points to our present incomplete stage of understanding, but encourages further work to be undertaken on the question of why certain events have occurred at specific stages during fracture. We feel confident that in the case of the resin a satisfactory answer to the "what" question has been given, although for the two thermoplastics a complete answer to even this, the simpler of the two questions, is still awaited.

REFERENCES

Andrews, E.H. (1959), J. App Phys. 30, 740

Andrews, E.H. (1967), Fracture in Polymers, (Oliver and Boyd, London)

Anthony and Congleton, (1968), Metals Sci. J. 2, 158

Anthony S.R., Chubb J.P., and Congleton, J., (1970), Phil Mag July 1972

Bateson, S. (1960) Phys. Chem. Glasses 1 139

Beardmore, P. (1968) Phil.Mag. 19, 389

Berry, J.P. (1959) Fracture ed. Averbach B.L. et al (Wiley, New York)

Berry, J.P. (1960) J.Mech. Phys. Solids 8, 194

Berry, J.P. (1961) J. Poly. Sc. 50, 107

Berry, J.P. (1962) J. App. Phys. 5, 1741

Berry, J.P. (1964) Fracture Processes in Polymeric Solids, ed. Rosen, B. (Wiley, New York)

Bessonov, M.I. and Kuvshinskii, E.V. (1959) Fiz. Tverd. Tela 1, 1441

Bowden, P.B. (1970) Phil Mag. 22, 455

Busse, W.F., Orowan, E., and Neimark, J.E. (1956) Symposium on Ultimate Strength of Polymers. Polytechnic Inst. of Brooklyn.

Charles, R.J., (1961) Progress in Ceramic Science, Vol.1, J.E.Burke ed., Pergamon, (New York), p.1.

Clark, A.B.J. and Irwin, G.R. (1966), Expl. Mech. 23, 321

Condon, E.U. (1954), Am. J. Phys. 22 224

Congleton, J., Petch, N.J., and Shiels, S.A. (1968) Phil. Mag. Nov. 1968

Congleton, J., and Petch, N.J. (1967), Phil.Mag. 16, 749.

Cottrell, A.H. (1963), The Mechanical Properties of Matter, (Wiley, New York)

Craggs, J.W., (1963), J. Mech. Phys. Solids, 8, 66

Erdogan, B. (1967), Fracture Vol. 2 ed. Leibowitz, (Academic Press, New York)

Eshelby, J.D., (1969) J. Mech. Phys. Solids 17, 177

Field, J. (1971) Contemporary Physics Jan. 1971

Glennie, E.B. (1971) J. Mech Phys. Solids 19, 255

Griffith, A.A. (1920), Phil. Trans. R. Soc. A 221 163

Griffiths, R. (1969), MSc Thesis, University of Keele

Haward,R.N. (1973) in Amorphous material, ed Douglas. R.W and Ellis,B (Wiley Interscience)

Haward, R.N., Murphy B.M., and White, E.F.T. (1971) J. Poly. Sc. 9, 801

Higuchi, M. (1958) Repts. Research Inst. Appl. Mechs., Kyushu University, 6, 173

Hiorns, F.J. and Venables, J. (1961), Brit. Coal Utilisation R.A. Bulletin, 25,369

Holloway, D.G. (1973), The Physical Properties of Glass, (Wykeham Publications, London)

Hsiao, C.C. and Sauer, J.A. (1950), J.App. Phys. 21, 1071

Hsiao, C.C. and Sauer, J.A. (1953), Trans. ASME 75,895

Hull, D. (1970), J. Mat. Science. 5, 357

Inglis, C.E. (1913), Trans. Inst. Naval Arch. 55, 219

Irwin, G.R. (1948), American Society of Metals Symposium on Fracturing of Metals, Cleveland, Ohio

Irwin, G.R. (1956), Proceedings, Ninth International Congress of Applied Mechanics, Brussels, paper 11-101

Irwin G.R. (1960), Proceedings, Seventh Sagamore Ordnance Materials Conference, Syracuse University, p. IV-63

Irwin, G.R. and Kies J.A. (1952) Weld. J. Lond., Res. Suppl. 17,95a

Johnson J.W. (1963) PhD thesis, University of Keele

Johnson, J.W. and Holloway, D.G. (1966) Phil.Mag. 14, 731

Johnson, J.W. and Holloway, D.G. (1968) Phil. Mag. 17, 899

Kambour, R.P, (1964), J.Poly.Sc. A. 2 4165

(1965), J. Poly. Sc. A. 3 1713

(1966), J. Poly. Sc. A2.4, 349

(1968), Applied Polymer Symposia 7, 215

(1969), J. Poly. Sc. A-2 7, 1393

Kirchoff, F. (1969), International Conference on Fracture, University of Sussex, Brighton, 1969. Conference Proceedings

Kostrov, B. (1964), J. App. Math. Mech. 28, 793

Lilley, J. (1973), PhD thesis, University of Keele

Lilley, J. and Holloway, D.G. (1973) Phil. Mag. 28, 215

Linger, K. (1967) PhD thesis, University of Keele

Love, A.E.H. (1944). The mathematical theory of Elasticity. (Cambridge)

MacMillan, N.H. (1972), J. Mat. Sc. 7, 239

Maxwell, B. and Rahm, (1949), Ind. Eng. Chem., 41, 1988

(1950), SPE, 6, 7

Mott, N.F. (1948), Proc. Conf. Brittle Fracture in Mild Steel Plates, B.I.S.R.A., p. 82(1945); Engineering, 165, 16.

Murgatroyd, J.B. (1942), J. Soc. Glass Tech. 26, 156

Murray, J. and Hull, (1969), Polymer, (London), 10, 451

(1970), J. Polymer Sc. A2 8 1970

Newman, S.B. and Wollock, I. (1957), J. Res. Natl Bur. Stan. 58, 339

(1962) Adhesion and Cohesion, ed. P. Weiss, Elsevier, New York.

Orowan, E. (1934), Z Krist. A 89 327

(1945), Trans. Inst. Eng. Shipbuilders, Scotland 89 165

(1946), as above

(1948), Rep. Prog. Phys. 12 185

(1955), Weld. J. Lond. Res. Supp. 34 157s

Outwater, J.O. and Gerry, D,J. (1966), Report on Contract NONR 3219, (01) (X), Office of Naval Research, Washington, D.C.

Paris, P.C. and Sih, G.C. (1964), Symposium on Fracture Toughness Testing and its Applications, Chicargo 1964.

Polanyi, M. (1921), Z. Phys. 7 323

Roberts, D.K and Wells, A.A. (1954), Eng. London, 178, 820

Russel, E.W. (1950), Nature, 165, 91

Saibel, E. (1948), Fracturing of Metals. A.S.M. Cleveland.

Schardin, H. (1959), Fracture, ed. Averbach et al (Chapman and Hall)

Shand, E.B. (1954), J. Am. Ceramic Soc. 37 559

Spurr, O.K. and Niegisch, W.D. J. App. Poly. Sc. 3,168

Sternstein, S.S., Ongchin, L., and Silverman, (1968), Applied Polymer Symposia, 7, 175

Tolansky,S. (1954), An Introduction to Interferometry. (Longmans) (1963), Encyclopaedia Britannica.

Wallner,H. (1939), Z. Phys. 114, 368

Weidmann, G.W. (1973), PhD thesis, University of Keele

Wells, A.A. (1963) BWRA Res. Report M13/63

Westergaard, H.M. (1939), J. App. Mech. 6, 49

Wiederhorn, S.M. and Townsend, P.R. (1970), J. Am. Ceramic Soc. 53, 486

Williams, J.G., Radon, J. and Turner, (1968) Pol. Eng. and Sci., April, 1968

Wolock, I., Kies, J.A., and Newman, S.B. (1959) Fracture, ed. by Averbach et al(Chapman and all)

Wolock, I., Newman, S.B., and Weissberg, S.G. (1960) Paper presented to Meeting of Division of High Polymer Physics, American Physica Society, Detroit, Mich., March 1960.

Wolock, I. Kies, J.A. (1964) in Fracture of Polymeric Solids, ed Rosen (Wiley, New-York)

Yoffé, E. (1951) Phil. Mag., 42 739

Zandman, F. (1954), Etude de la Deformation et de la Rupture des Matieres Plastiques, Publications Scientifique et Technique du Ministere de l'Air, No. 291, Paris.

PHOTOGRAPHS FOR CHAPTER 5

THE NUMBER IN EACH MARGIN INDICATES, IN MICRONS, THE ACTUAL LENGTH REPRESENTED BY THE VERTICAL EDGE OF EACH PRINT.

UNLESS OTHERWISE STATED THE DIRECTION OF FRACTURE PROPAGATION IS FROM RIGHT TO LEFT.

List of Plates for Chapter 5.

Plate 5.1 .... Surface crazes on pmma

Plate 5.2 .... Crazes around a crack-tip

Plate 5.3 .... Fracture surface of pmma

Plate 5.4 .... Conic-shaped features

Plate 5.5 .... Conics and background structure

Plate 5.6 .... Structure of zone D

Plate 5.7 .... Localised roughening in Conic zone

Plate 5.8 .... Detail of zone A

Plate 5.9 .... Detail of cleaved surface

Plate 5.10 ... Interference fringes associated with linear features

Plate 5.11 ... Interference contrast along Conic boundaries

Plate 5.12 ... Local heating of craze film

Plate 5.13 ... "Polygonal Conics"

Plate 5.14 ... Matching D-zones

Plate 5.15 ... Detail of a rough strip

Plate 5.16 ... Matching rough strip to that shown in Plate 5.15

Plate 5.17 ... Fan of crazes

Plate 5.18 ... Result of heating a craze-fan

Plate 5.19 ... Fracture surface of oriented pmma loaded parallel to the orientation

Plate 5.20 ... Fracture surface of oriented pmma loaded normal to the orientation

1500

Pl. 5.1 Surface crazes on pmma

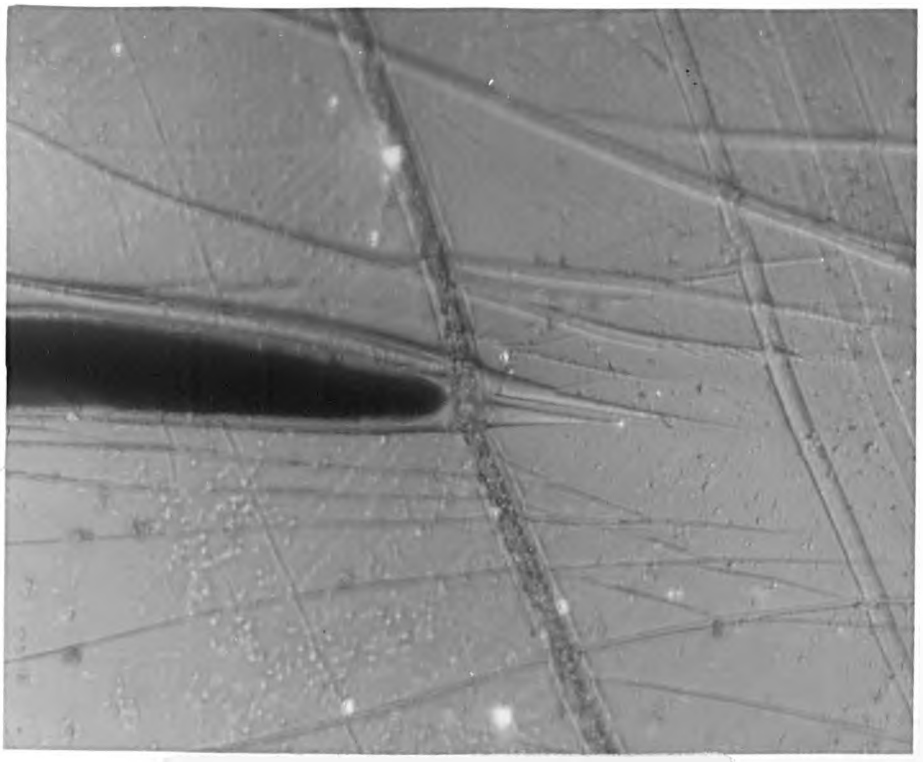

15

Pl. 5.2 Crazes around a crack-tip. Note displacement of surface scratch.

6000

Pl. 5.3 Fracture surface of pmma

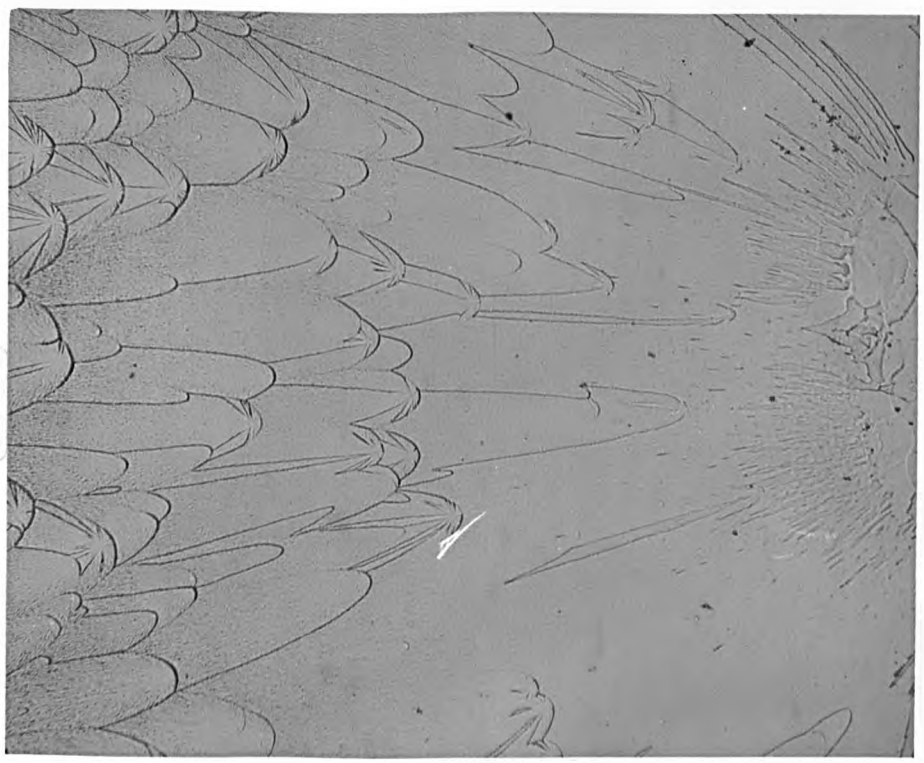

1500

Pl. 5.4 Conic-shaped features

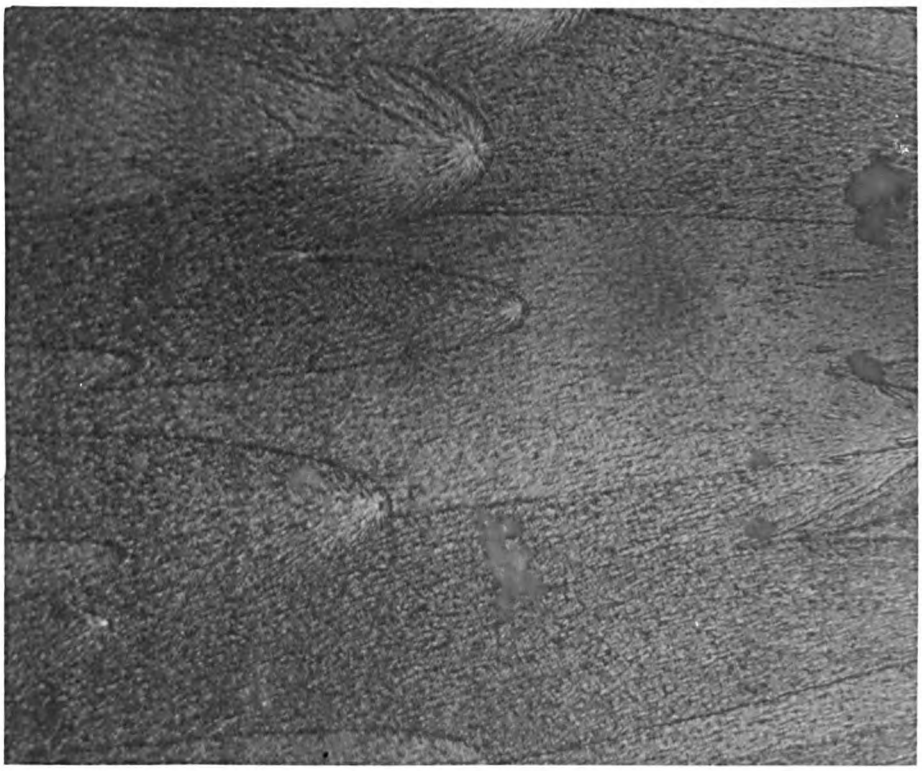

530

Pl. 5.5 Conics and background structure

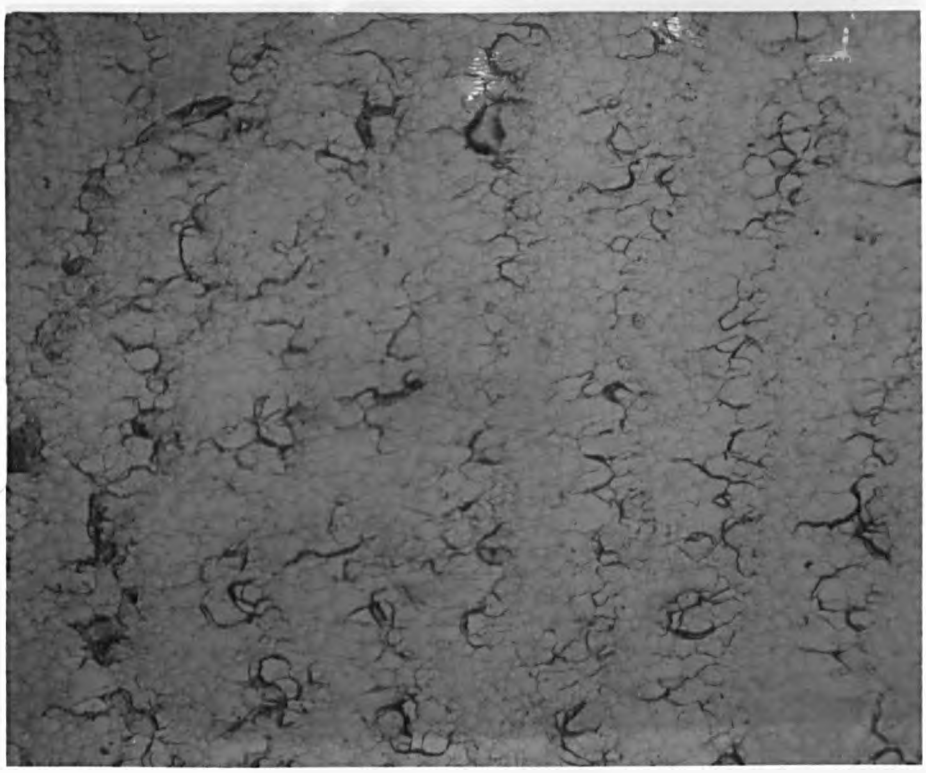

4300

Pl. 5.6 Structure of zone D

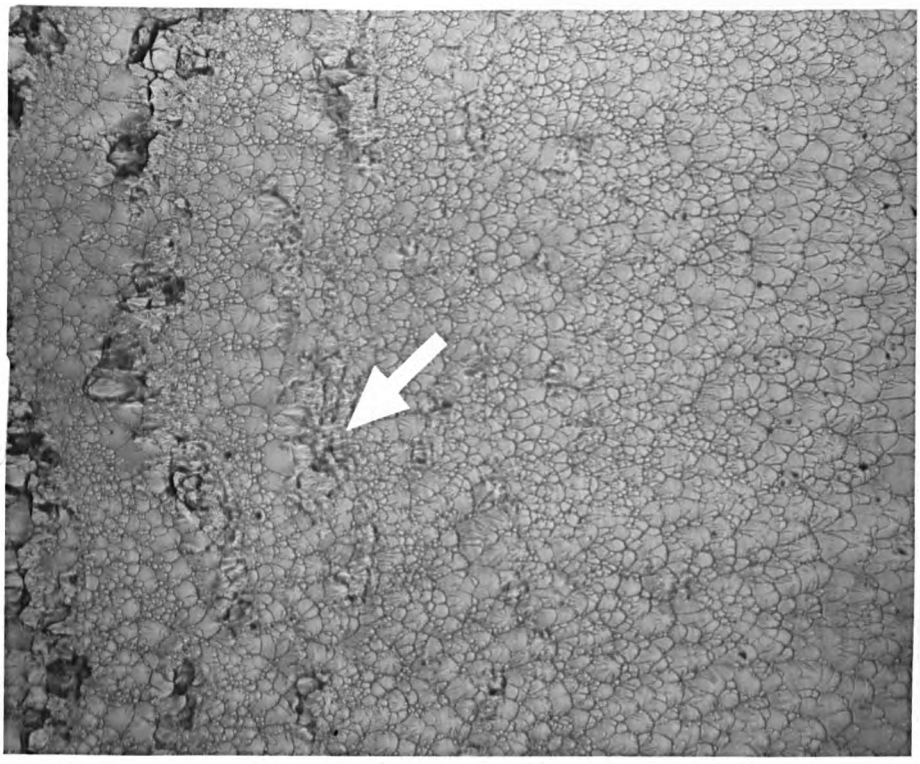

4000

Pl. 5.7 Localised roughening in conic zone. (An example is arrowed)

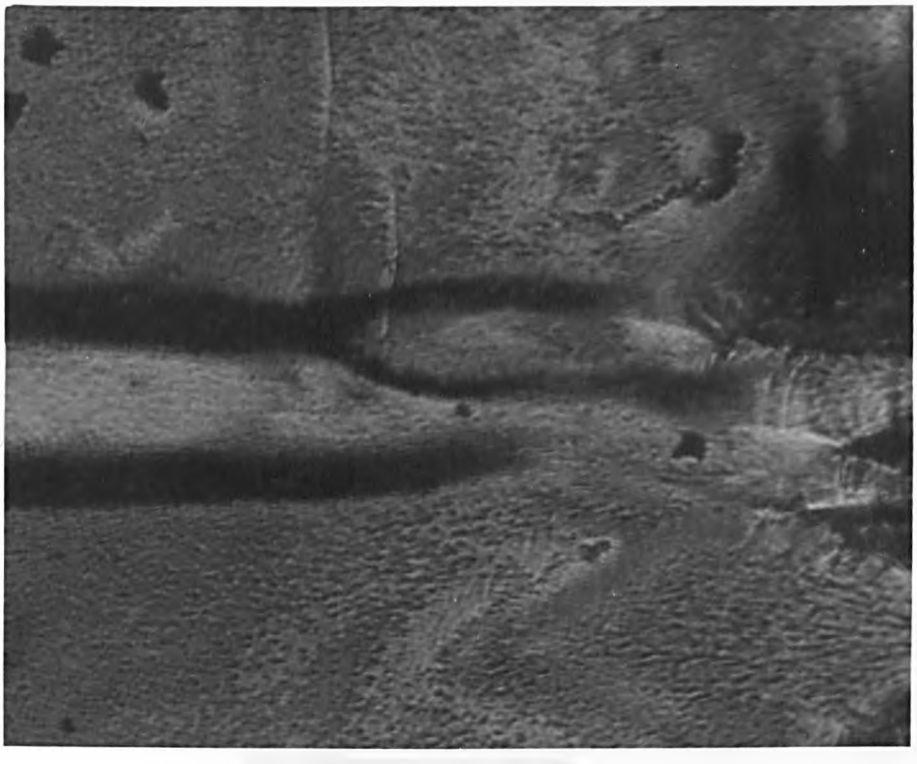

700

Pl. 5.8 Detail of zone A

710

Pl. 5.9 Detail of cleaved surface

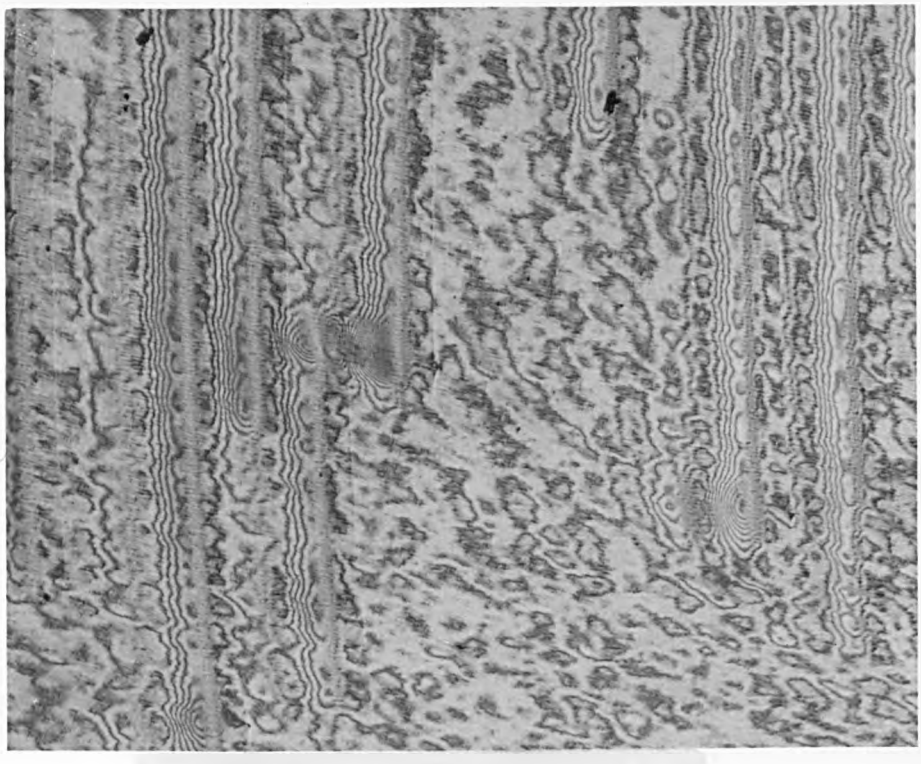

1000

Pl. 5.10 Interference fringes associated with linear features

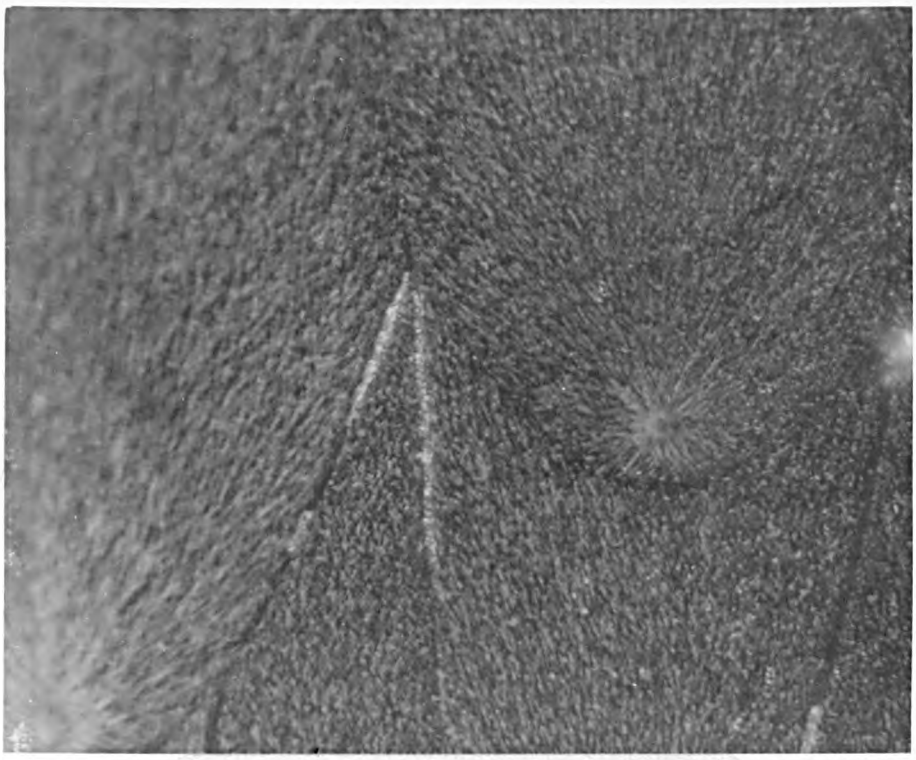

100

Pl. 5.11 Interference contrast along Conic boundaries.

460

Pl. 5.12 Local heating of craze film

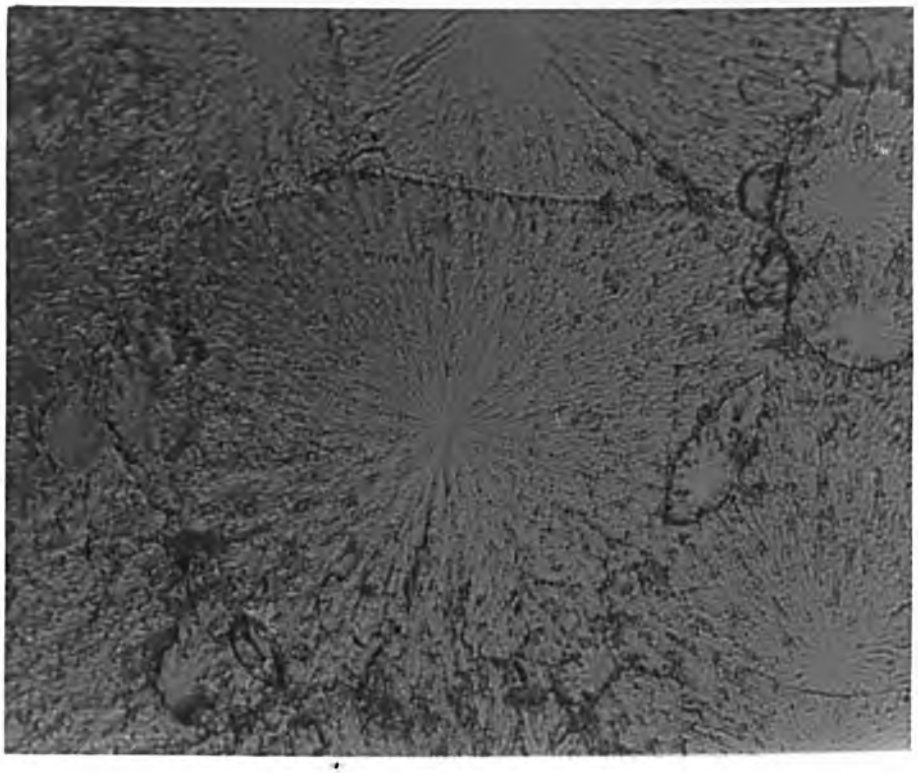

130

Pl. 5.13
"Polygonal Conics"

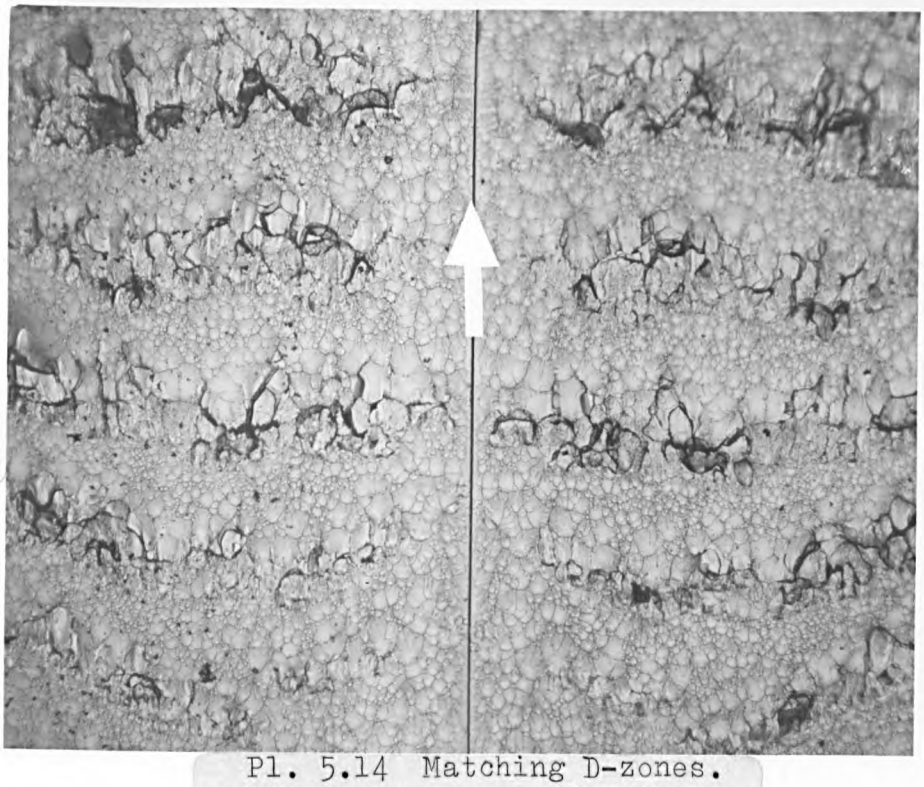

4800

Pl. 5.14 Matching D-zones.
(The arrow shows direction
of propagation).

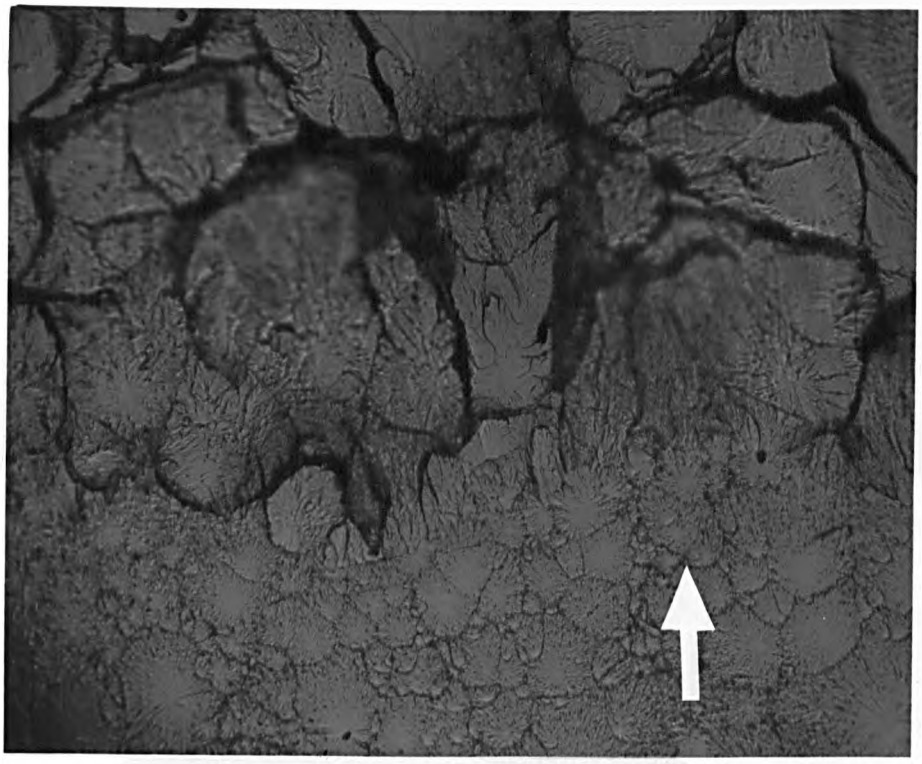

500

Pl. 5.15 Detail of a rough strip. The arrow indicates the propagation direction.

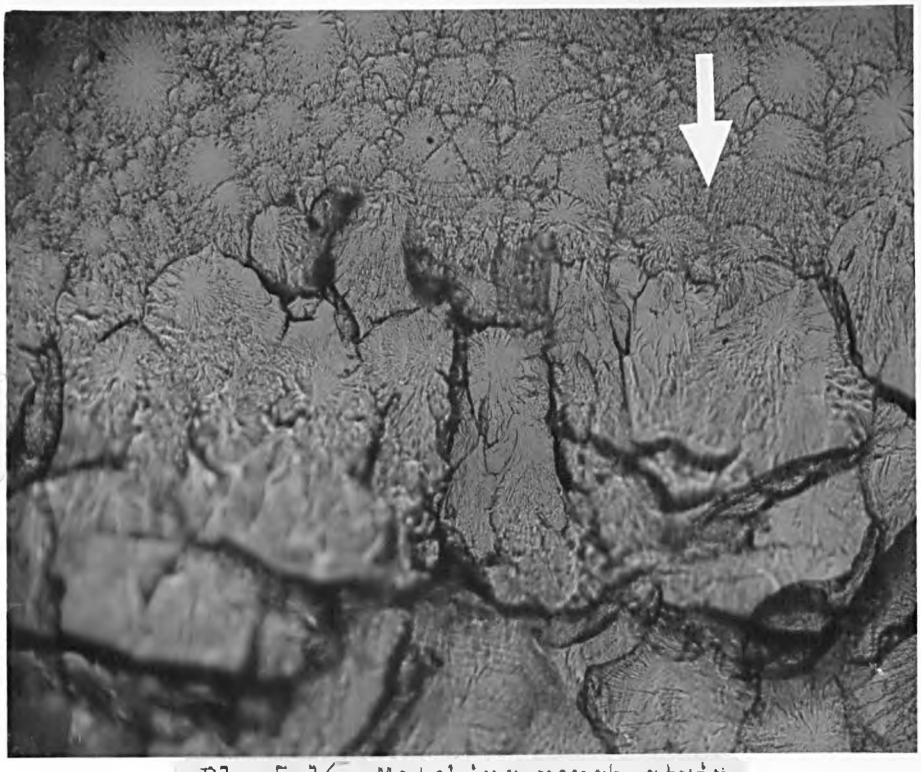

500

Pl. 5.16 Matching rough strip to that shown in Pl. 5.15. (Arrow shows propagation path)

1700

Pl. 5.17 Fan of crazes.
The propagation direction is
from left to right.

1700

Pl. 5.18 Result of heating
a craze-fan.

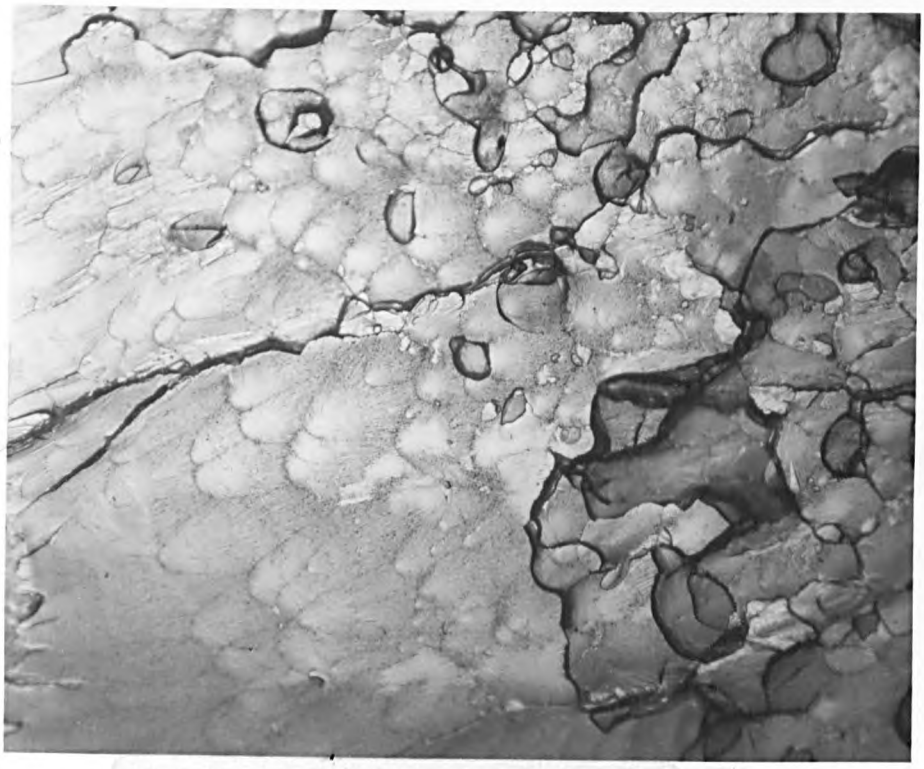

4500

Pl. 5.19 Fracture surface of oriented pmma loaded parallel to orientation.

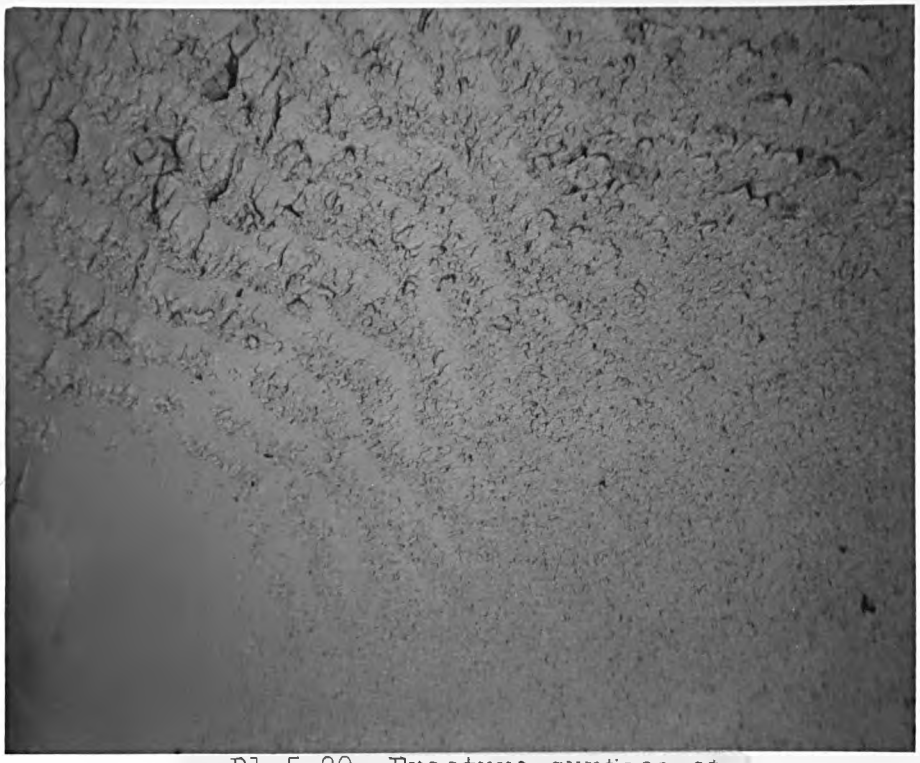

4000

Pl 5.20 Fracture surface of oriented pmma loaded normal to orientation.

PHOTOGRAPHS FOR CHAPTER 6

THE NUMBER IN EACH MARGIN INDICATES, IN MICRONS, THE ACTUAL LENGTH REPRESENTED BY THE VERTICAL EDGE OF THE PRINT.

UNLESS OTHERWISE STATED THE FRACTURE DIRECTION IS FROM RIGHT TO LEFT

PLATES FOR CHAPTER 6

Plate 6.1 .... Zone Sequence 1

Plate 6.2 .... Zone Sequence 2

Plate 6.3 .... The 'Island' Structure

Plate 6.4 .... The 'thin-wedge' Structure

Plate 6.5 .... Showing Thickness of Wedge

Plate 6.6 .... The Mackerel-pattern

Plate 6.7 .... Wedge Structure

Plate 6.8 .... Wedge Structure

Plate 6.9 .... Drawn Fibrils on Island Structure

Plate 6.10 ... B-C Zone Transition

Plate 6.11 ... Banded Structure

Plate 6.12 ... Craze-fans

Plate 6.13 ... Craze-fan

Plate 6.14 ... Beginning of Band Corresponding to Craze-fan of Plate 6.13

Plate 6.15 ... Island Structure-Change of Scale

Plate 6.16 ... Islands Formed as Rib-marks

Plate 6.17 ... Tensile Zone D

Plate 6.18 ... Crazes Beneath Zone A

Plate 6.19 ... Structure of Zone A

Plate 6.20 ... Zone B of Sequence 2

Plate 6.21 ... Detail of Plate 6.20

Plate 6.22 ... Zone C of Sequence 2

Plate 6.23 ... Decrease in the scale of the Island Structure in Zone C of Sequence 2

Plate 6.24 ... Level differences in Zone C

Plate 6.25 ... Level Change at the C-D Zone boundary

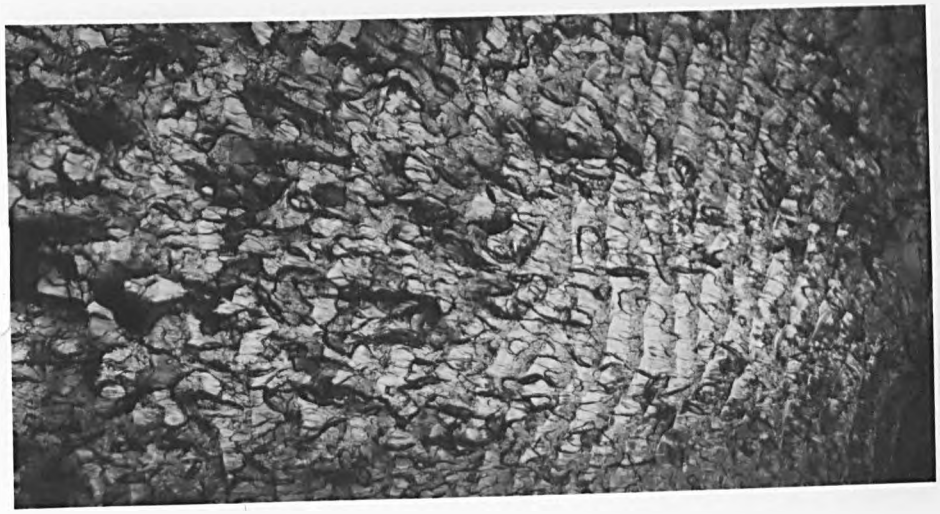

Pl. 6.1
Zone Sequence 1

Pl. 6.2
Zone Sequence 2

420

Pl. 6.3
The 'island' structure

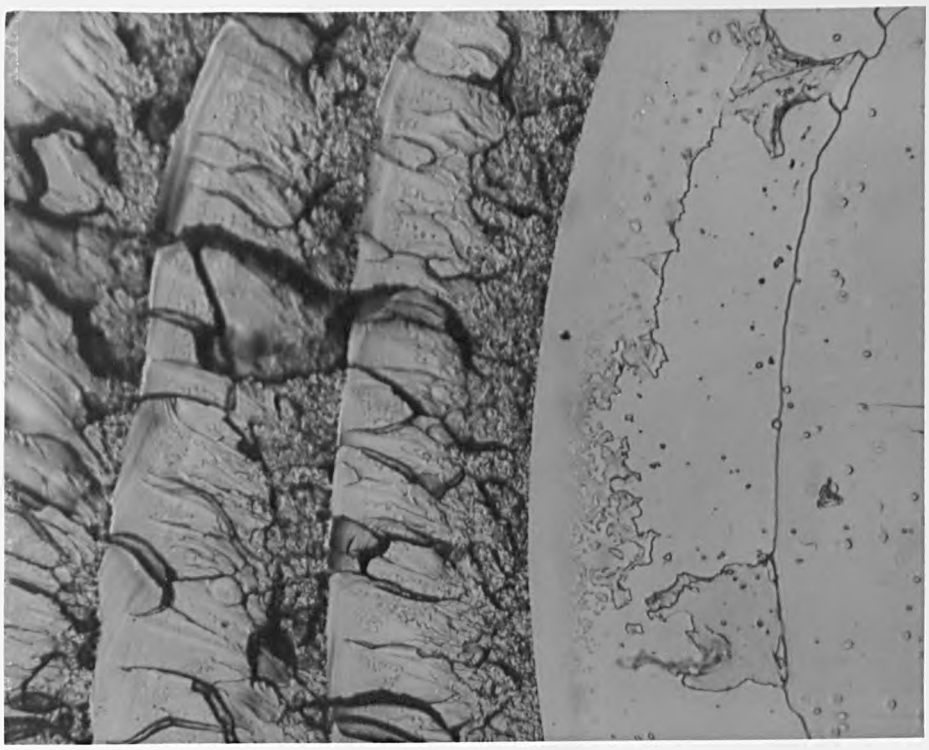

1075

Pl. 6.4
The 'thin-wedge' structure

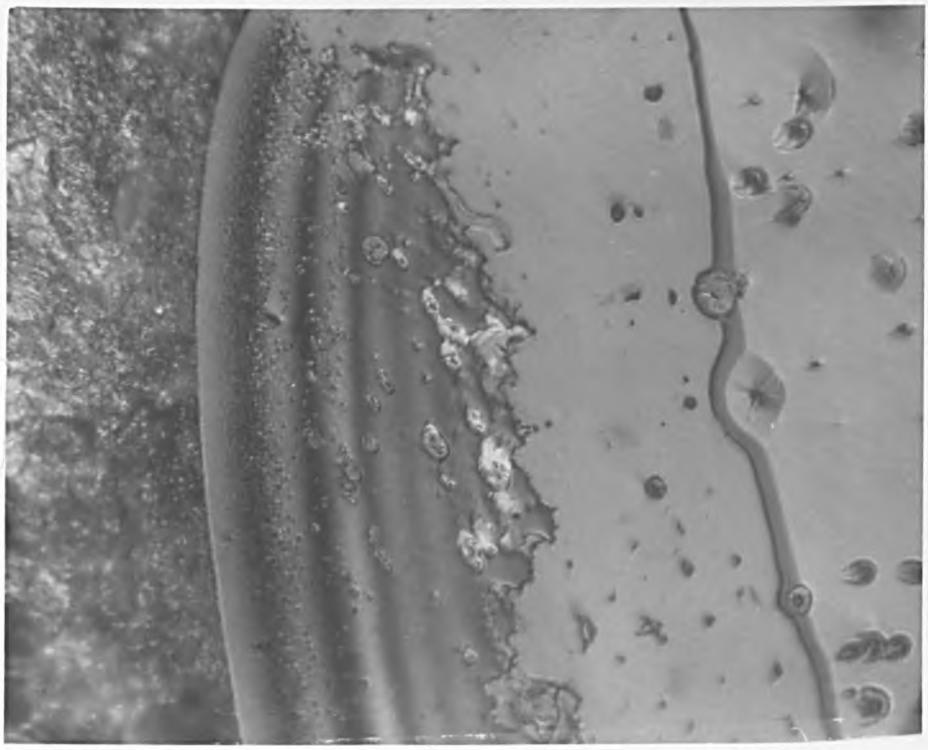

Pl. 6.5 Showing thickness of wedge

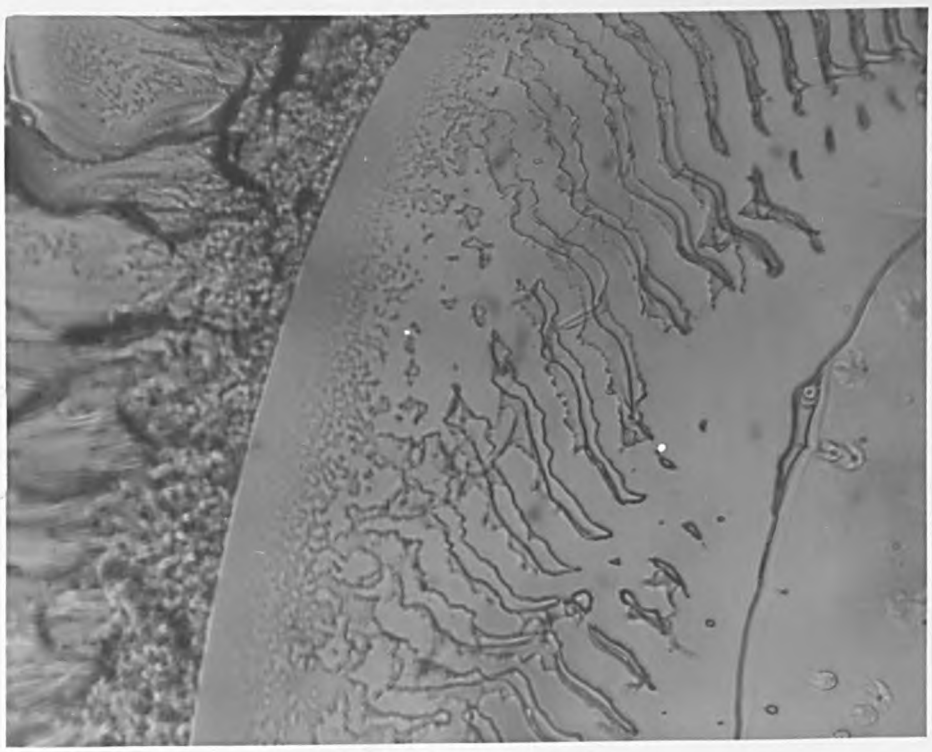

Pl. 6.6 The Mackerel pattern

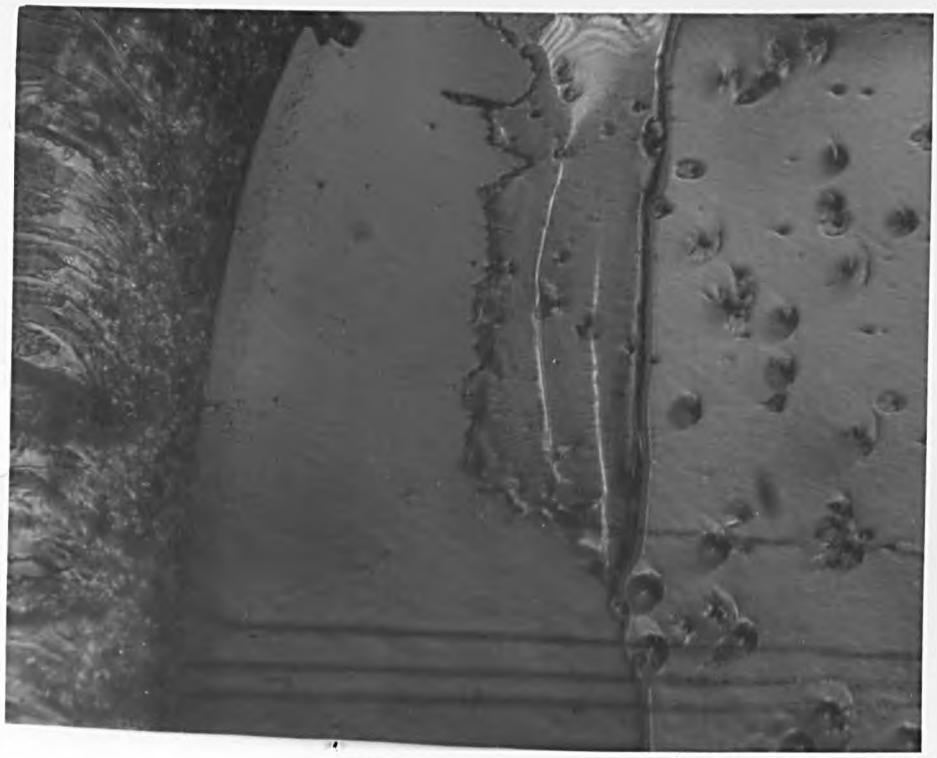

580

Pl. 6.7 Wedge structure (A)

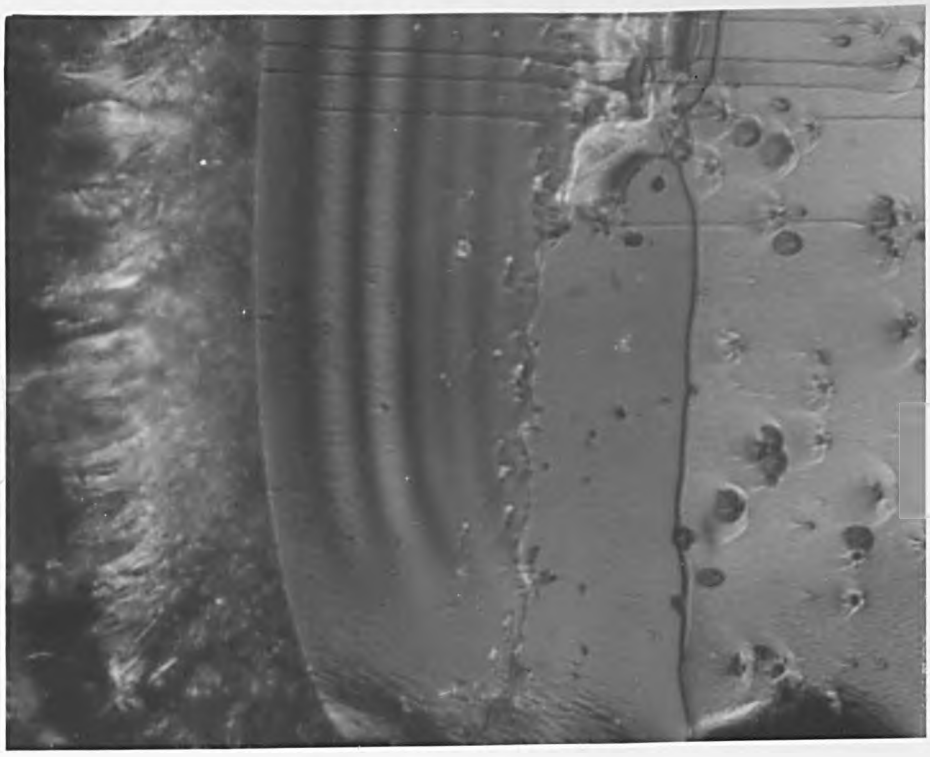

580

Pl. 6.8 Wedge structure (B)

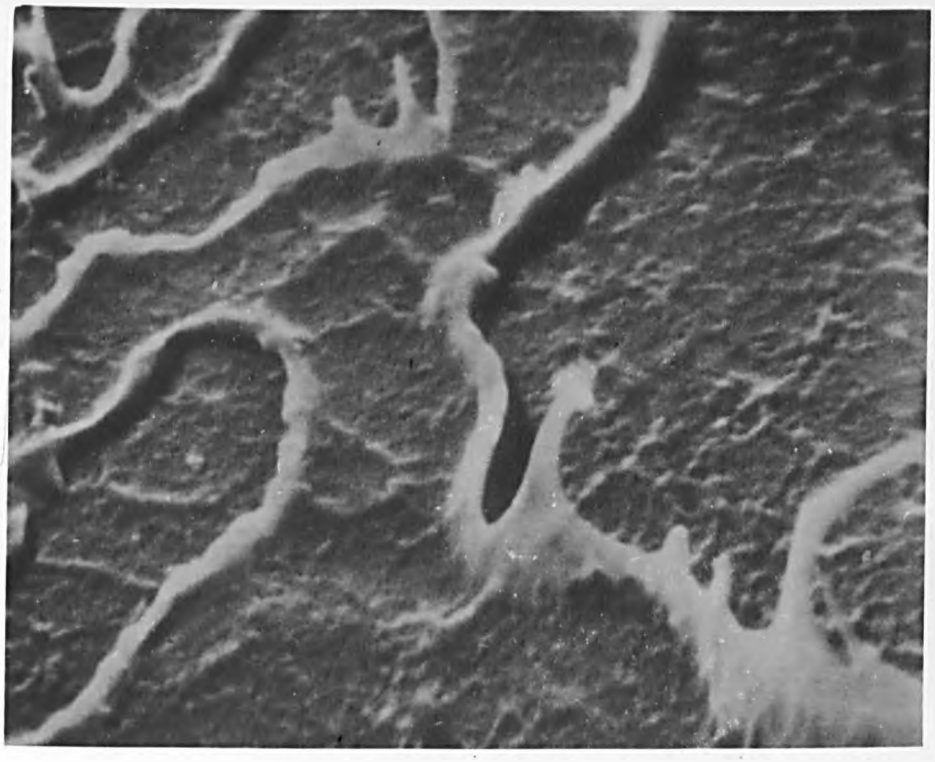

20

Pl. 6.9 Fibrils
on edge of island

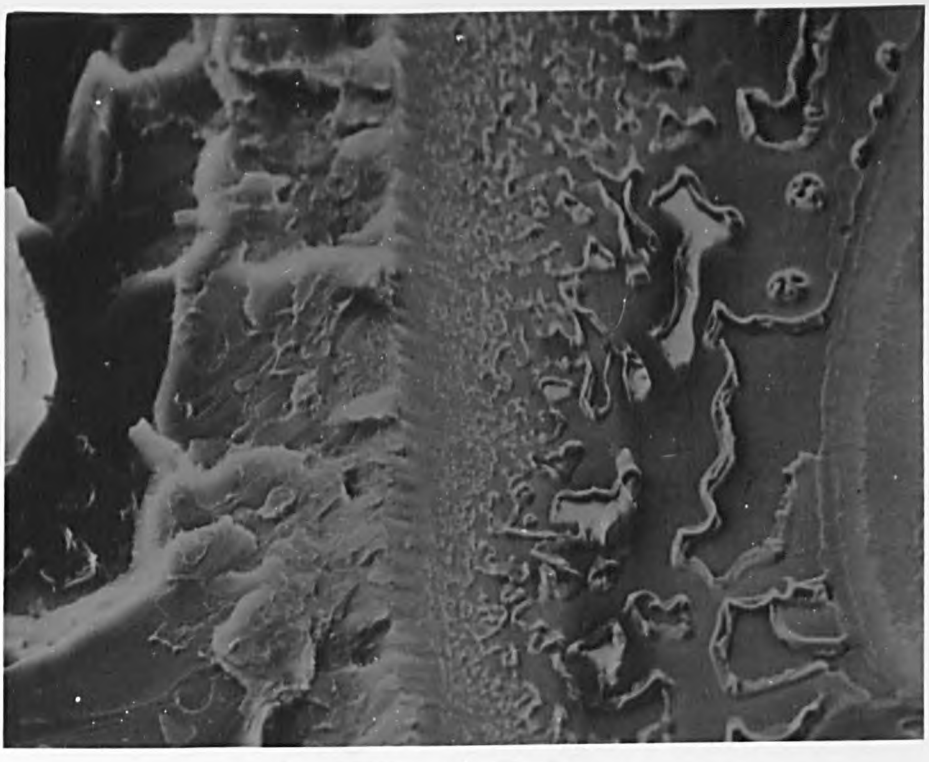

50

Pl. 6.10 B-C
zone transition

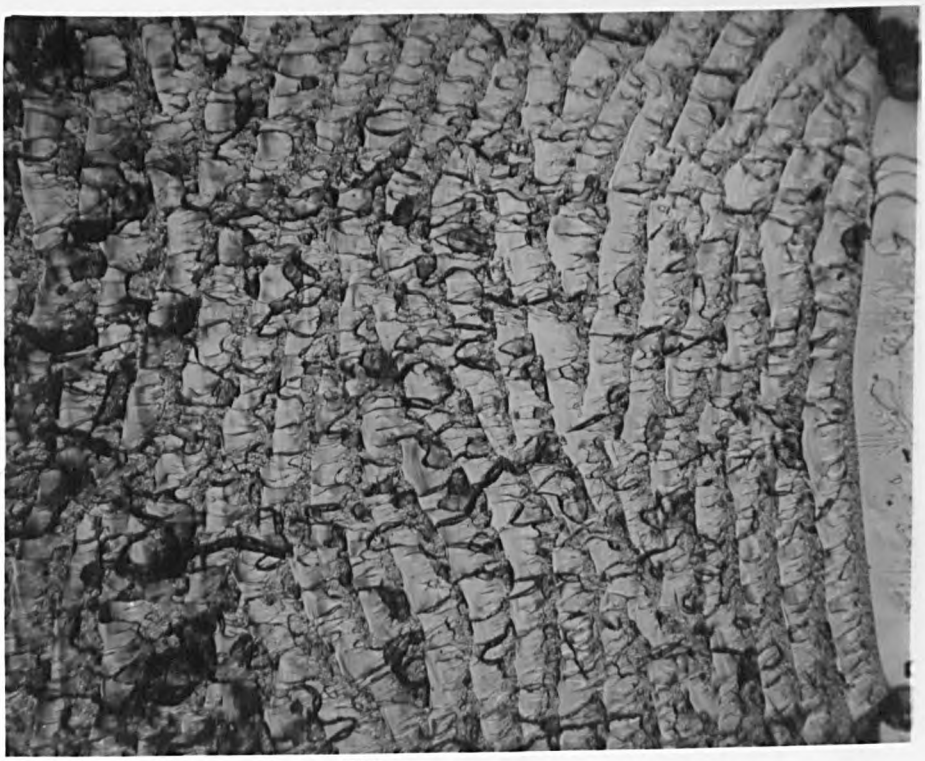

4550

Pl. 6.11
Banded structure

520

Pl. 6.12
Craze-fans

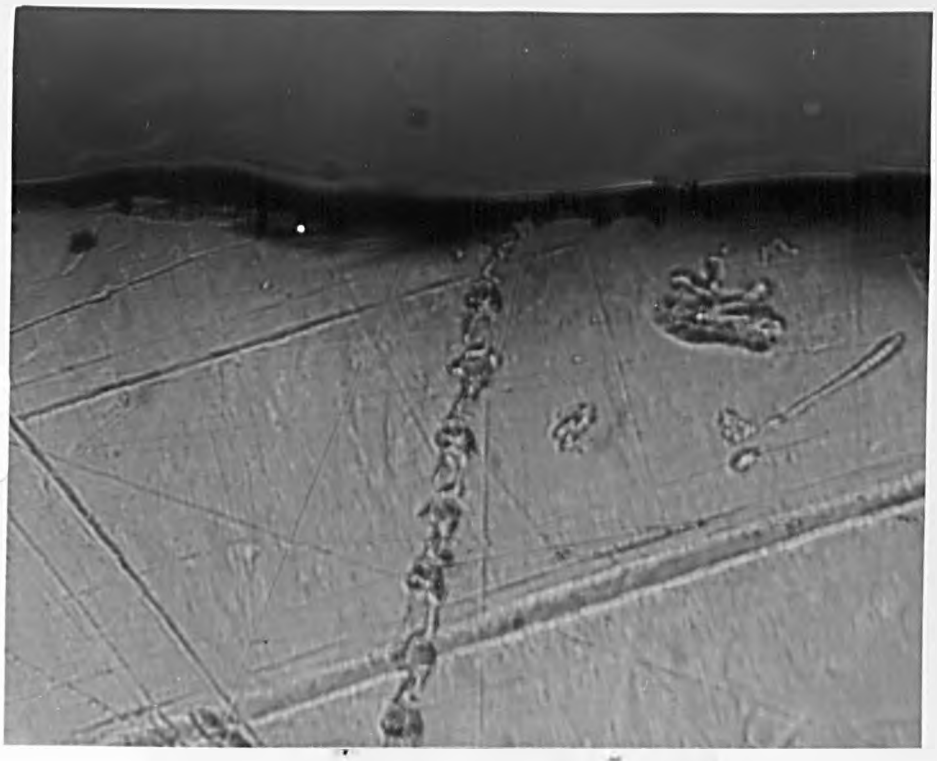

Pl. 6.13 Fan of crazes. (Note the coincidence with the fortuitous surface scratch

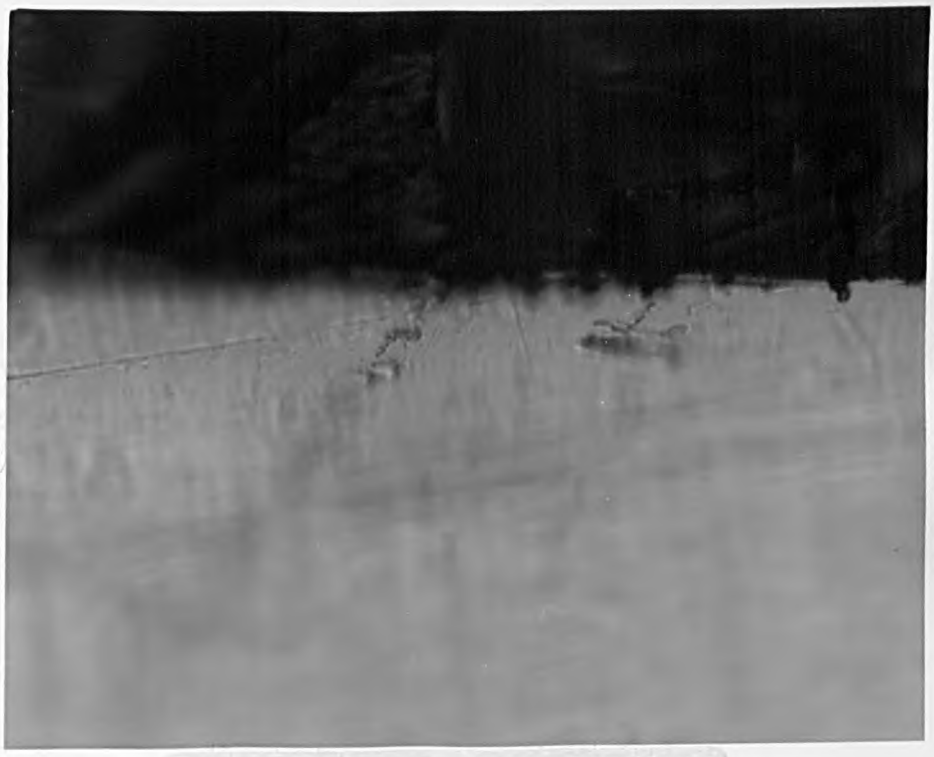

Pl. 6.14 Beginning of band corresponding to craze-fan of Plate 6.13

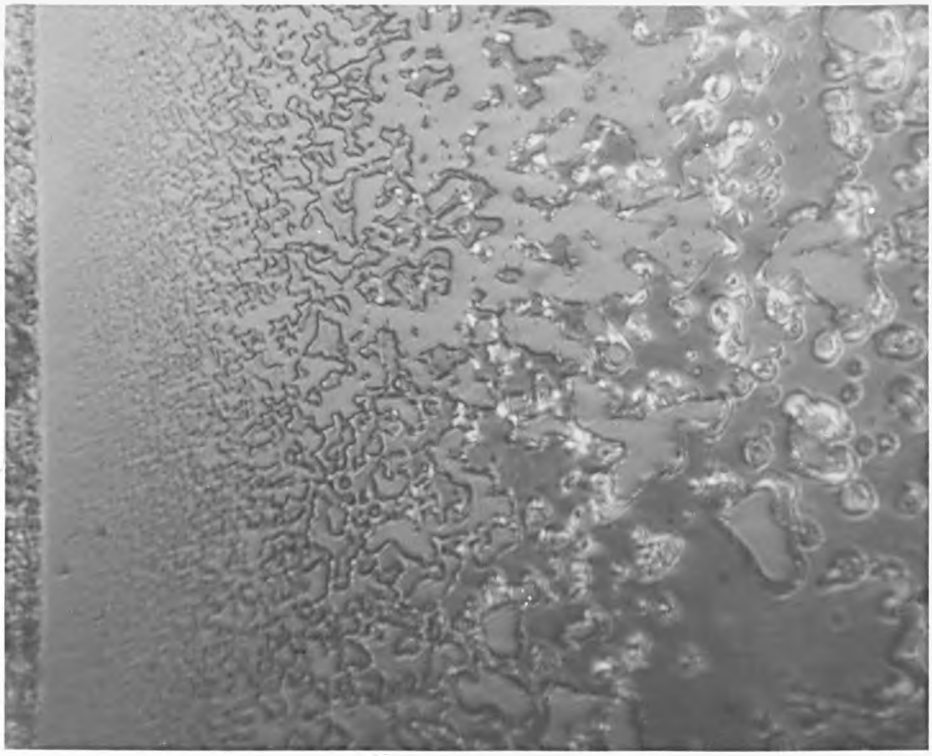

Pl. 6.15 Island structure-change of scale

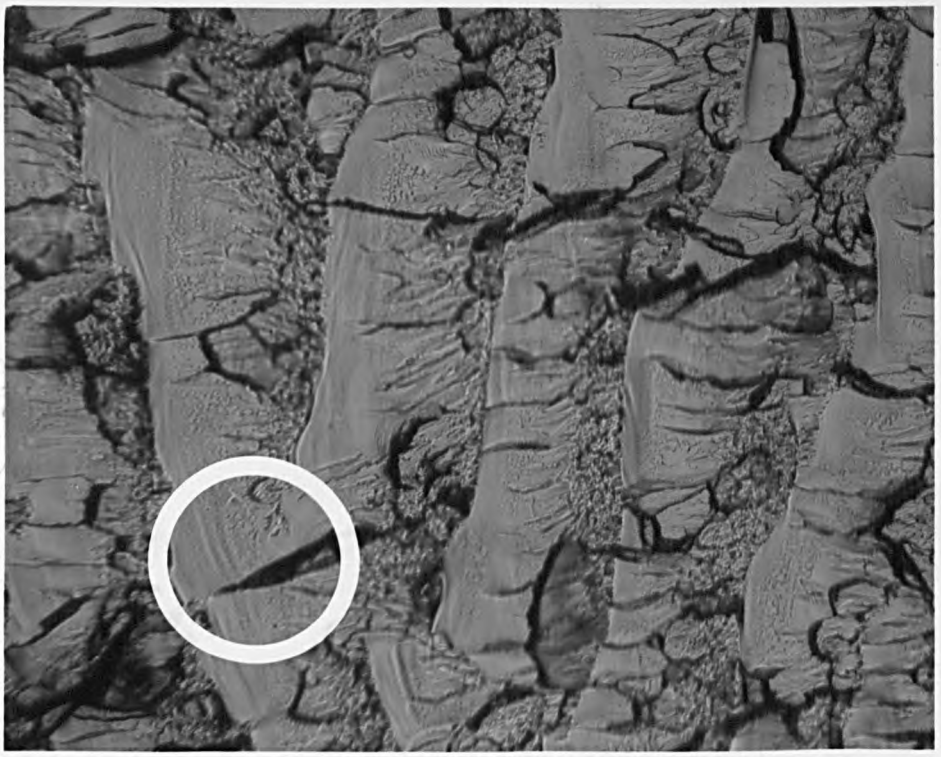

Pl. 6.16 Islands formed as rib-marks

1300

Pl. 6.17
Tensile zone D

570

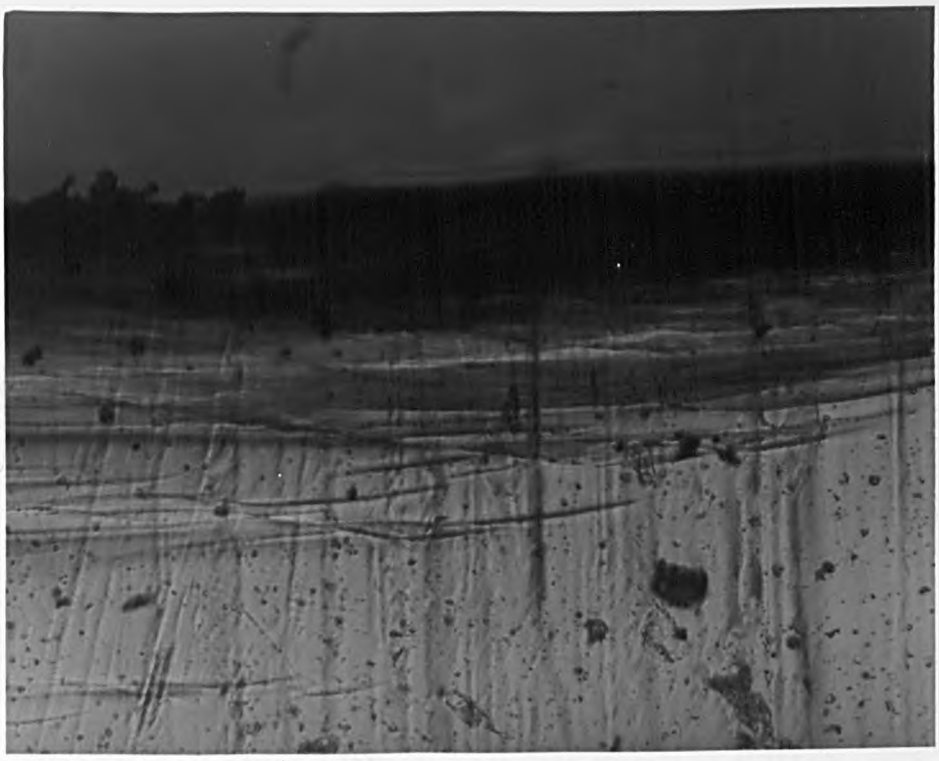

Pl. 6.18 Crazes
beneath zone A

120

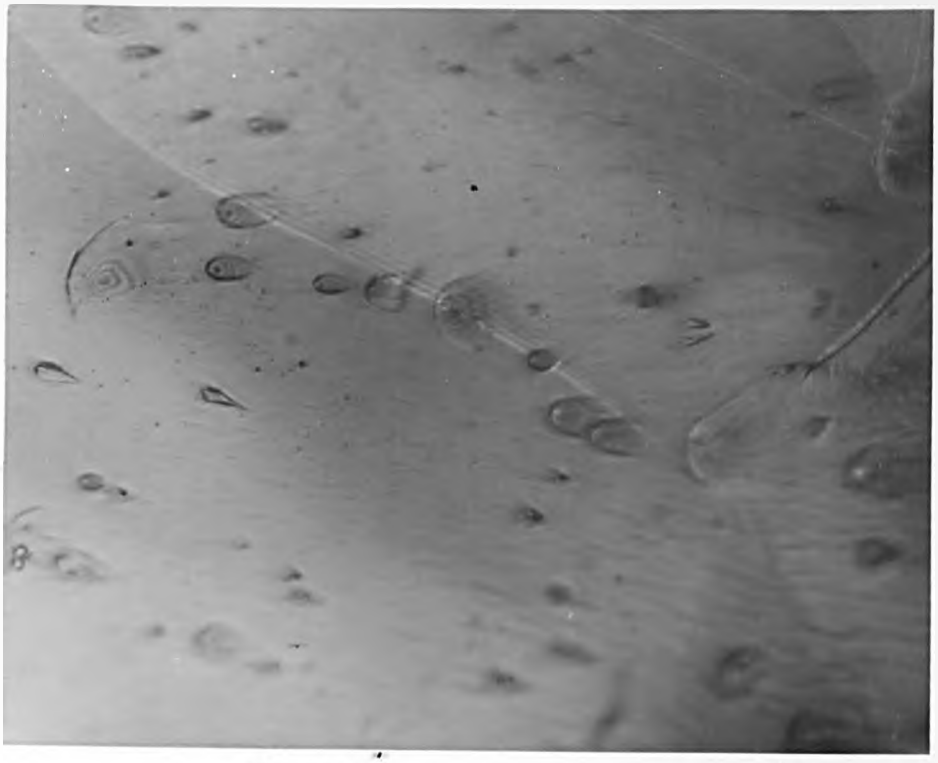

Pl. 6.19
Structure of
zone A

4500

Pl. 6.20 Zone B
of Seqance 2

Pl. 6.21 Detail
of Plate 6.20

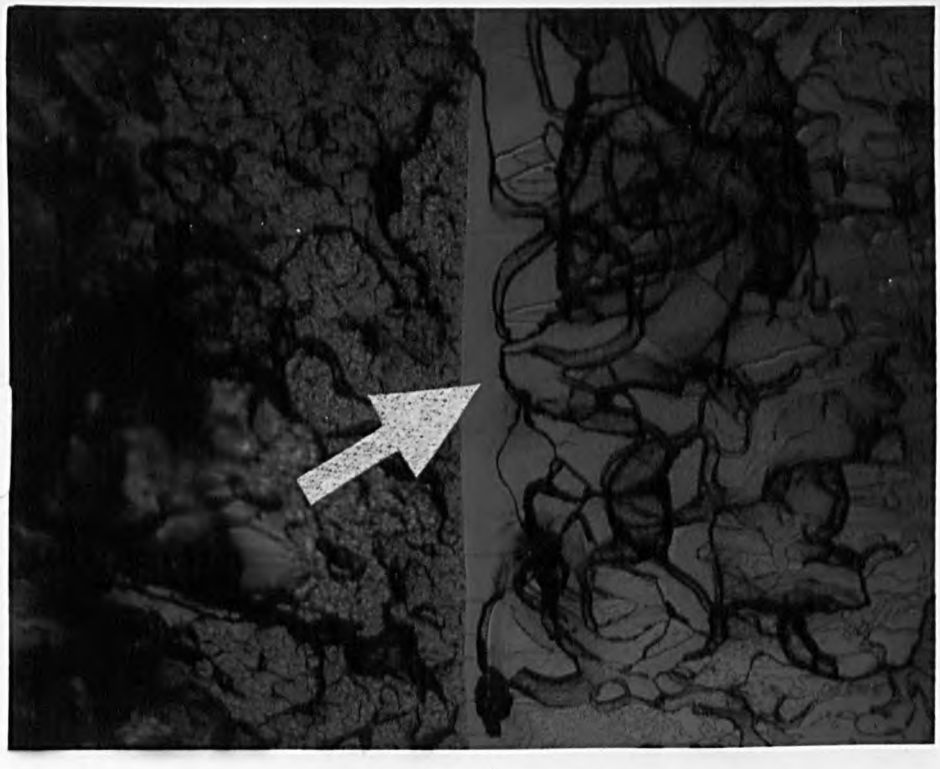

Pl. 6.22 Zone C
of Sequence 2
(Arrowed)

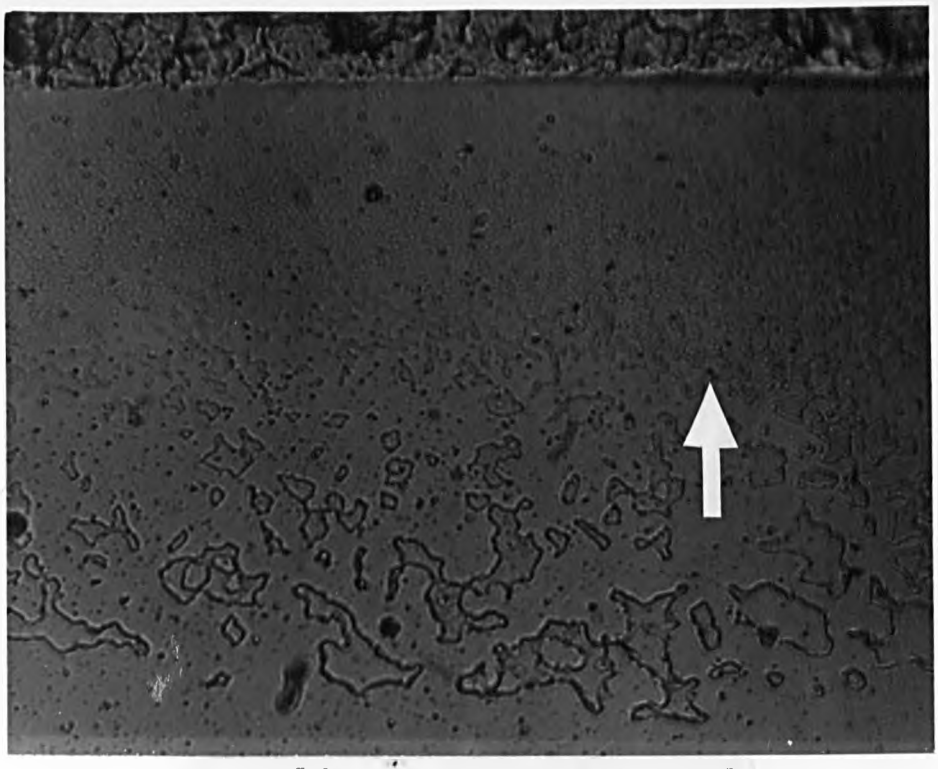

120

Pl. 6.23 Decrease in the scale of the island structure in zone C of Sequence 2.

240

Pl. 6.24 Level differences in zone C

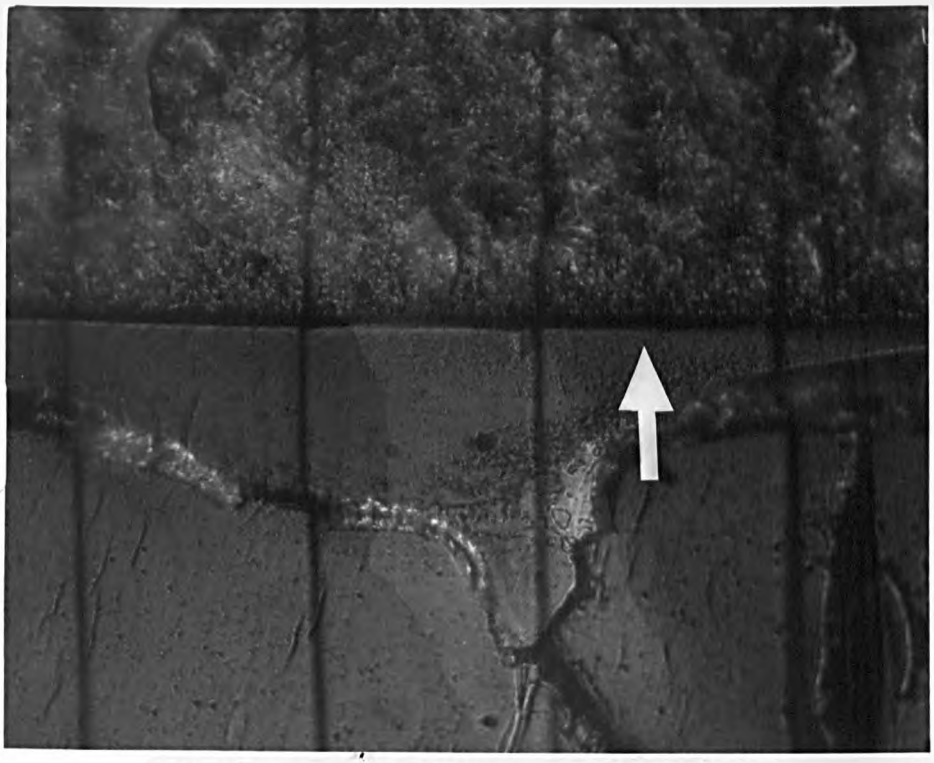

Pl. 6.25 Level change at C-D zone boundary. The lines are from the light-cut graticule.

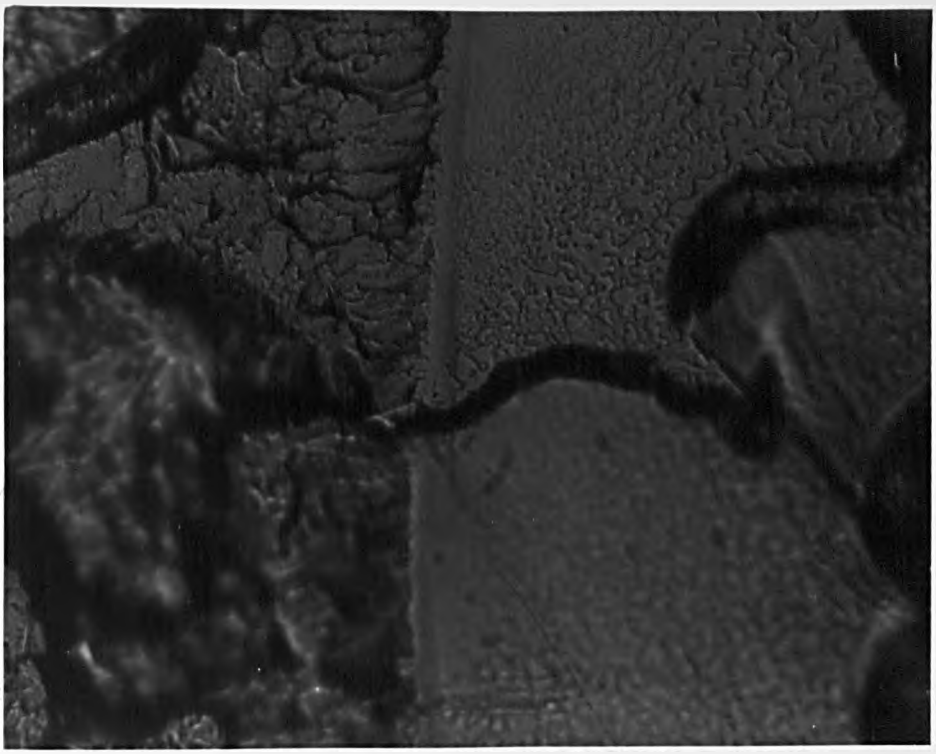

Pl. 6.26 C-D zone transition at different levels

Pl. 6.27 Conic features-surface A

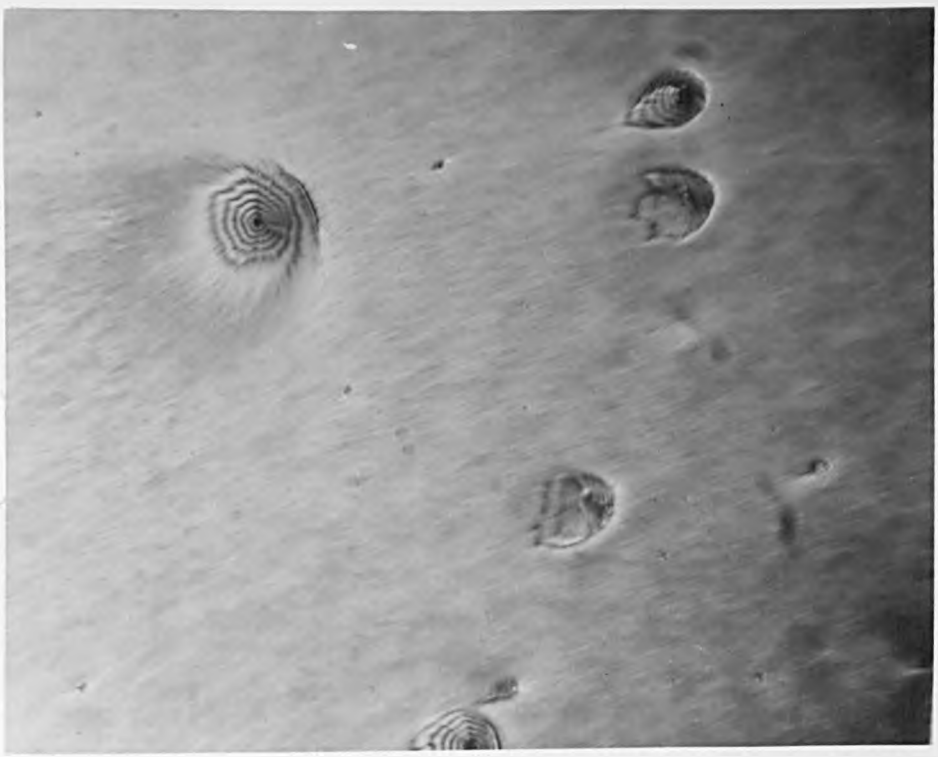

Pl. 6.28 Conic features-surface B

Pl.6.29 Effect of striations on the fine structure in the banded zone.

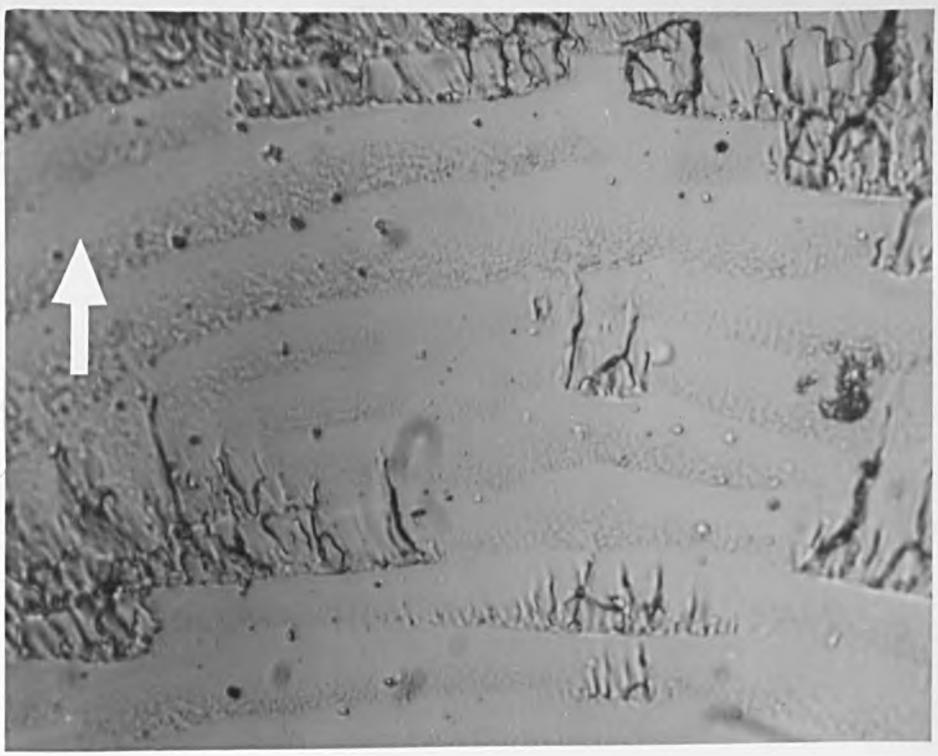

Pl. 6.30
Conchoidal surface

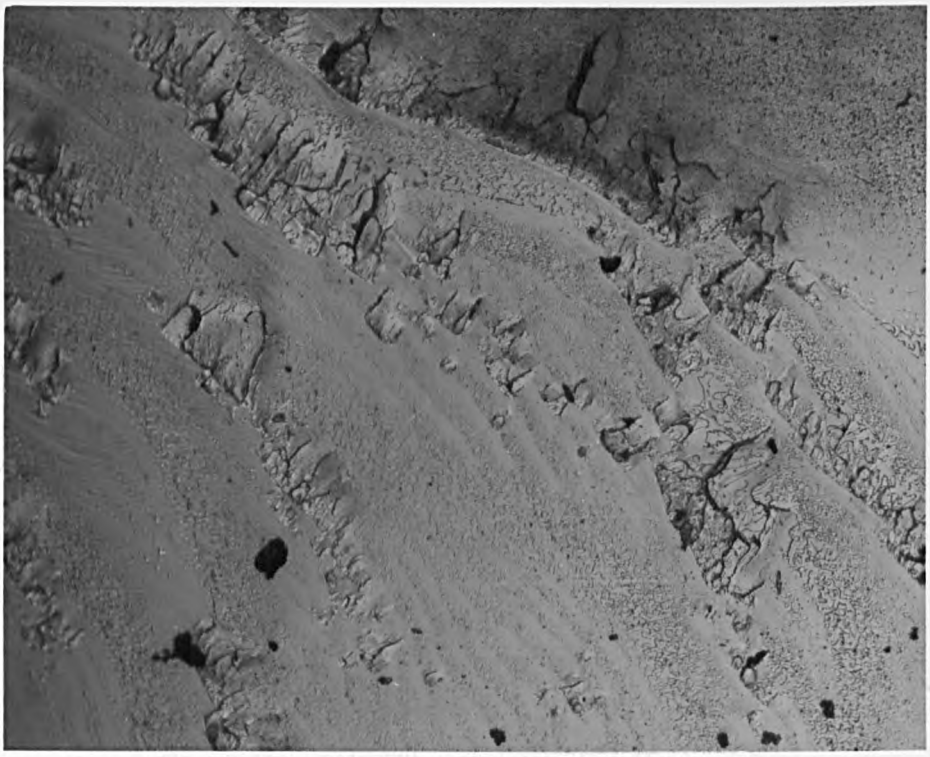

1370

Pl. 6.31 End of double-torsion banded region

1370

Pl. 6.32 Beginning of (next) double-torsion banded region

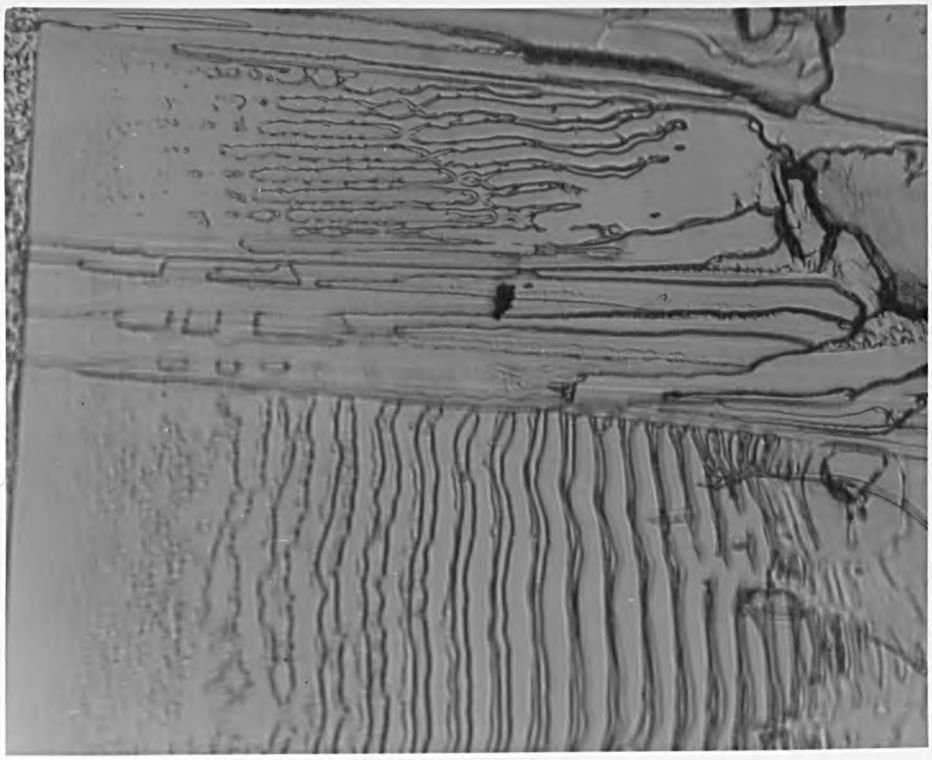

500

Pl. 6.33
Mackerel line
orientation

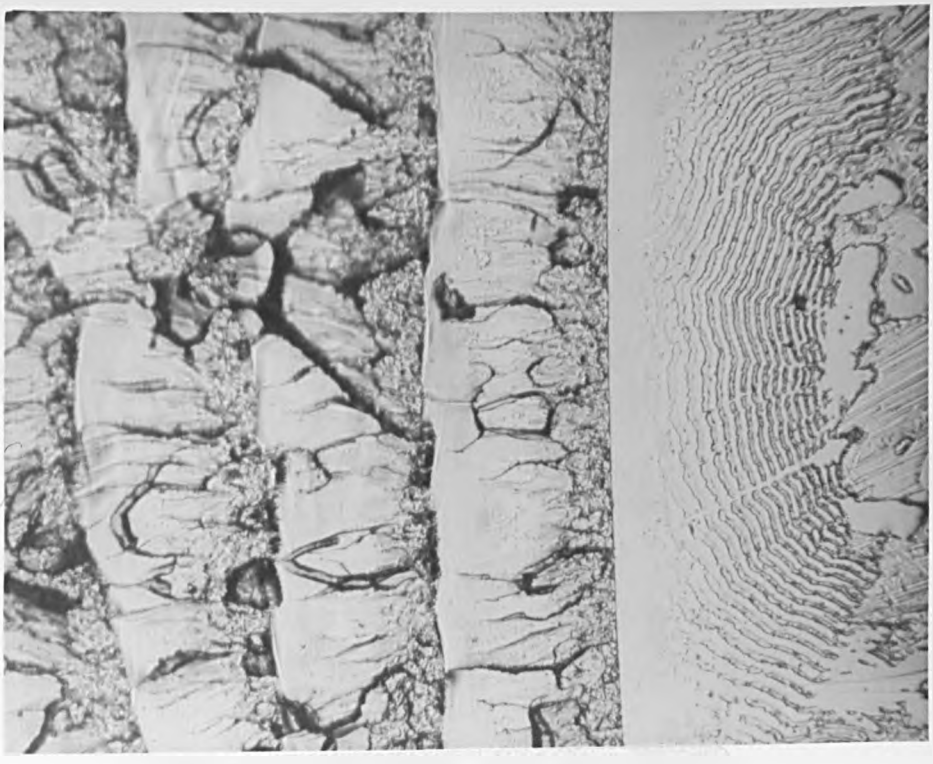

1250

Pl. 6.34 Showing radii of
Mackerel lines and banded zone
boundary.

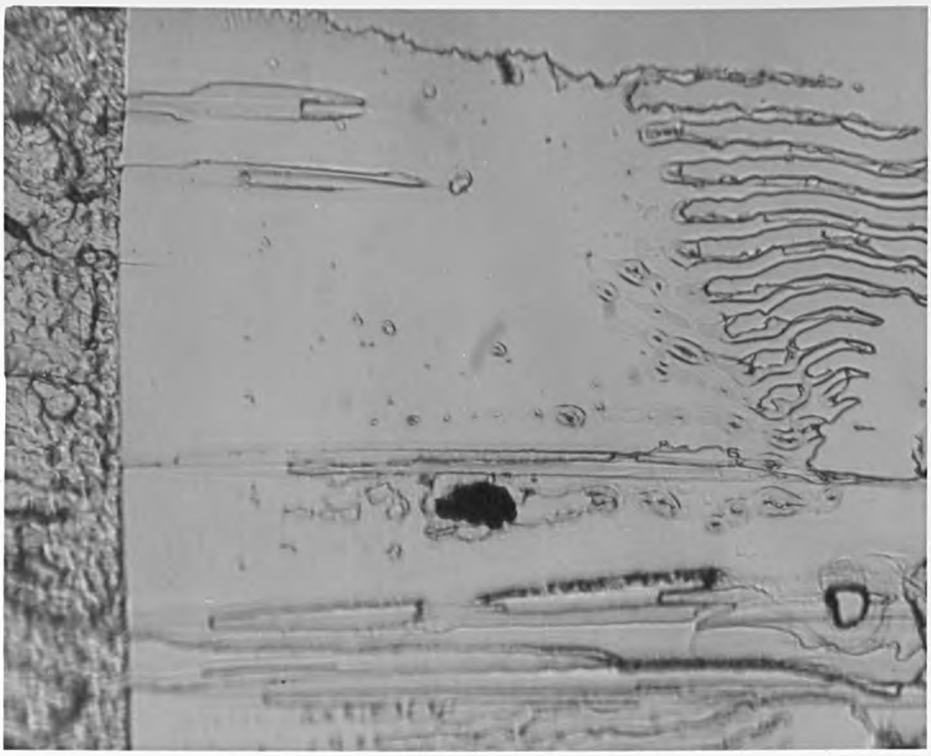

Pl. 6.35 Mackerel lines normal to zone C boundary

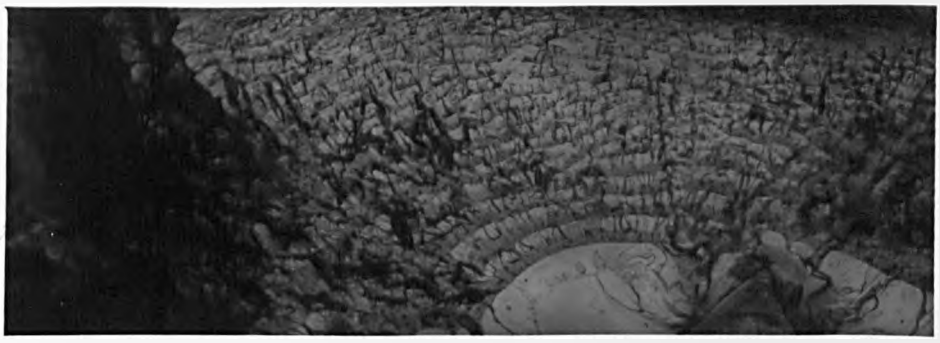

Pl. 6.36 Fracture surface of polystyrene broken in bending

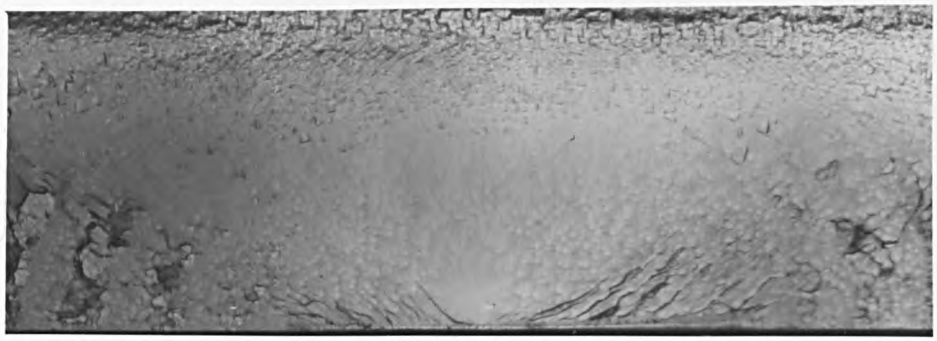

Pl. 6.37 Fracture surface of pmma broken in bending.

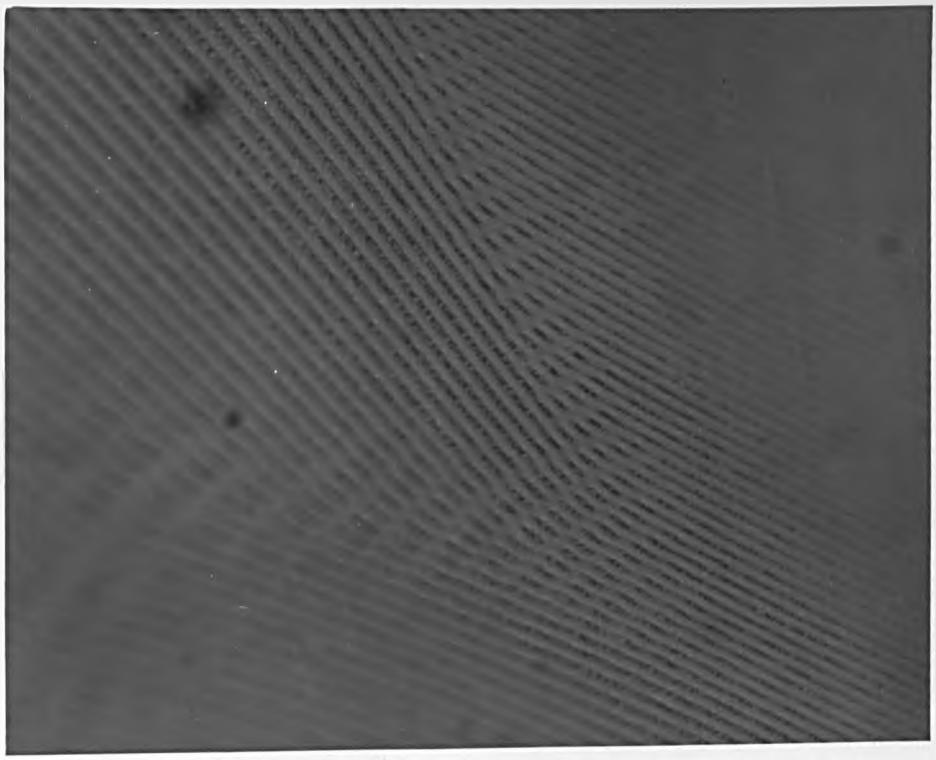

Pl. 6.38 "Bands" on polycarbonate fracture surface

PHOTOGRAPHS FOR CHAPTER 7

THE NUMBER IN EACH MARGIN INDICATES, IN MICRONS, THE ACTUAL LENGTH REPRESENTED BY THE VERTICAL EDGE OF THE PRINT.

UNLESS OTHERWISE STATED THE DIRECTION OF FRACTURE PROPAGATION IS FROM RIGHT TO LEFT

List of Plates for Chapter 7.

Plate 7.1 .... Fracture surface of CT200

Plate 7.2 .... The Mist Zone

Plate 7.3 .... Large Type 1a feature

Plate 7.4 .... Small Type 1a feature

Plate 7.5 .... Type 1b feature

Plate 7.6 .... Variants of Type 1 features

Plate 7.7 .... Type 2a feature

Plate 7.8 .... Type 2b feature

Plate 7.9 .... Type 3a feature

Plate 7.10 ... Type 3b feature

Plate 7.11 ... Miniature mirror and mist zones close to the fracture origin

Plate 7.12 ... Craze-like markings

Plate 7.13 ..."Crazes"around a crack-tip in CT200

Plate 7.14 ... Inclusion in a Type 1a feature

Plate 7.15 ... Crack-tip in CT200

Plate 7.16 ... Type 1 Glass feature

Plate 7.17 ... Type 2 Glass feature

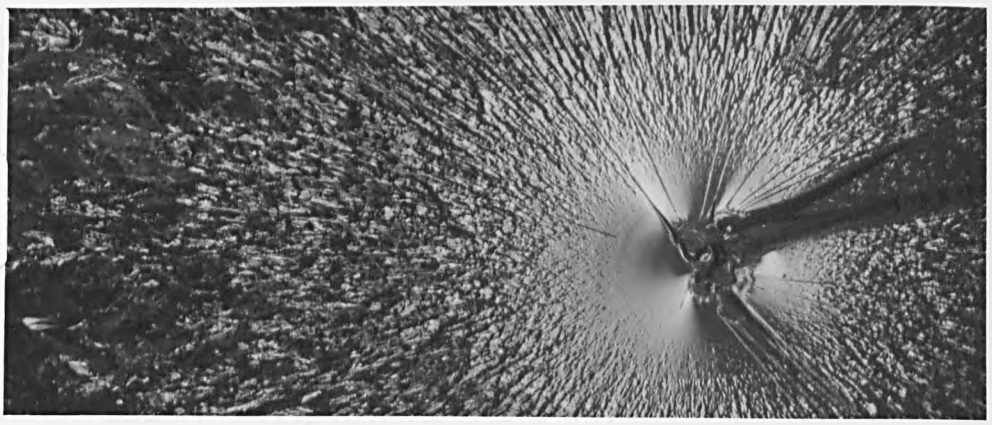

Pl.7.1 Fracture surface of CT200

Pl. 7.2
The mist zone

210

Pl. 7.3 Large
Type la feature

75

Pl. 7.4 Small
Type la feature

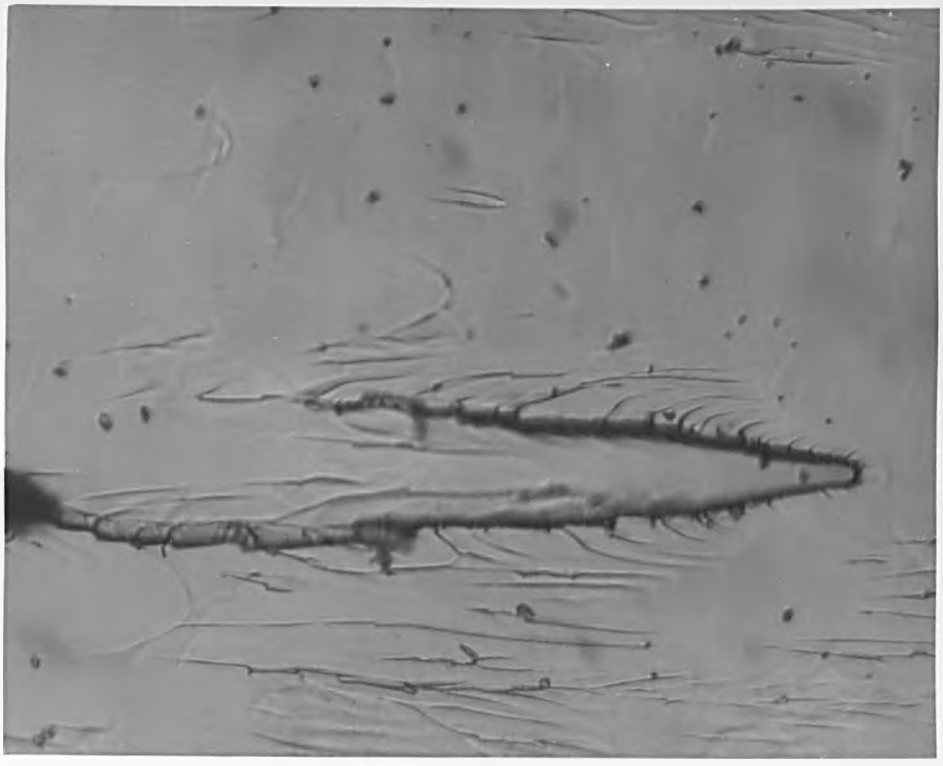

Pl. 7.5
Type 1b feature

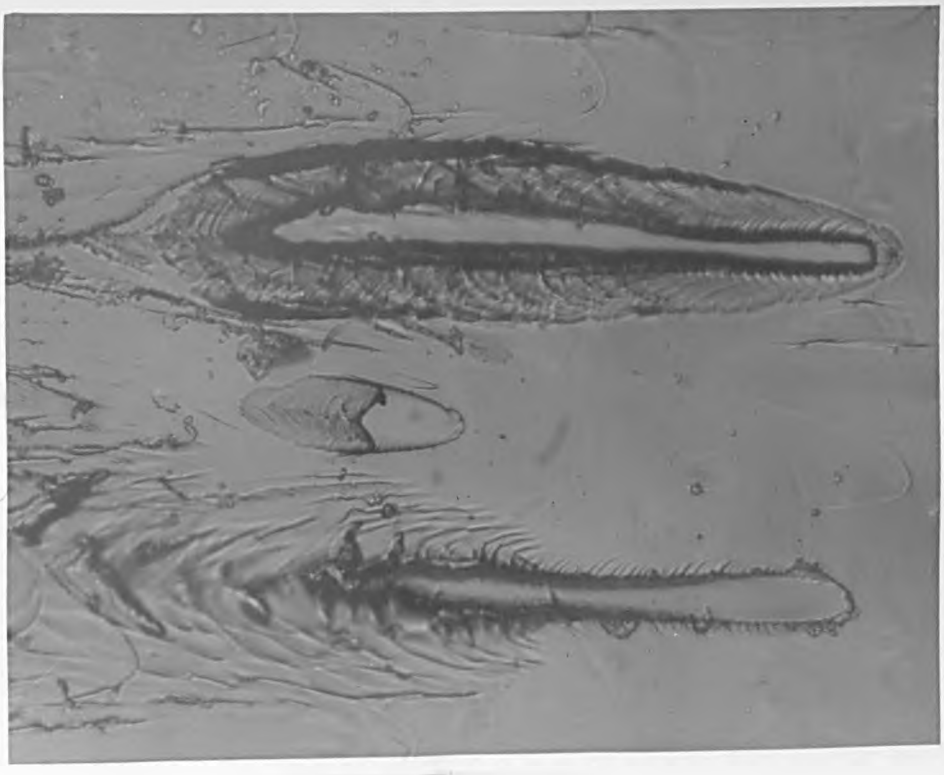

Pl. 7.6 Variants
of Type 1 features

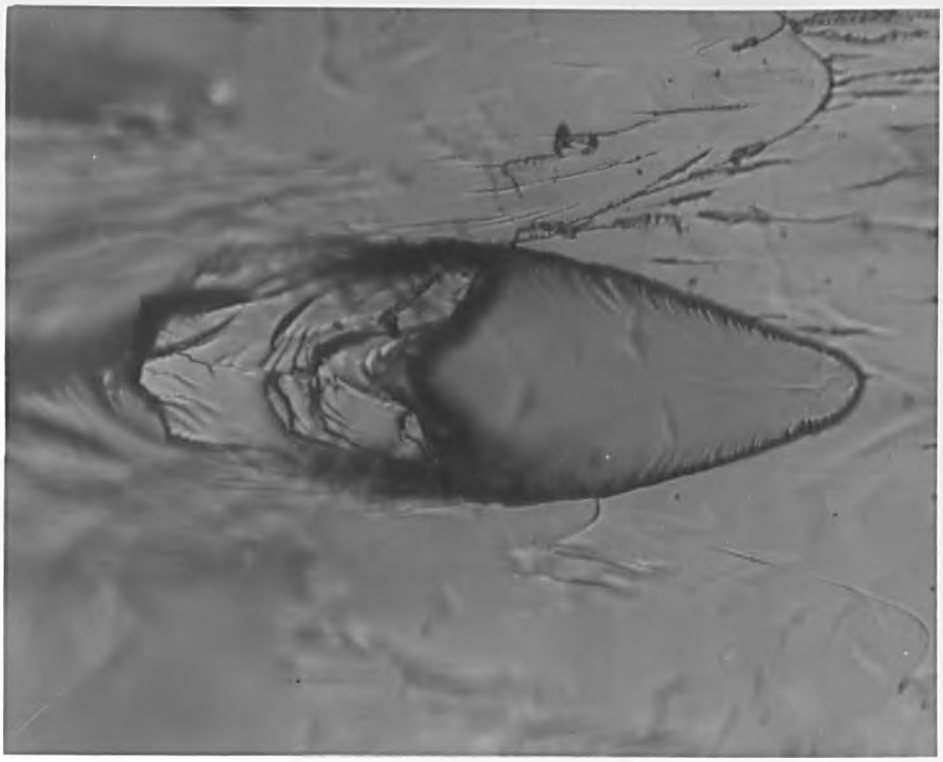

250

Pl.. 7.7
Type 2a feature

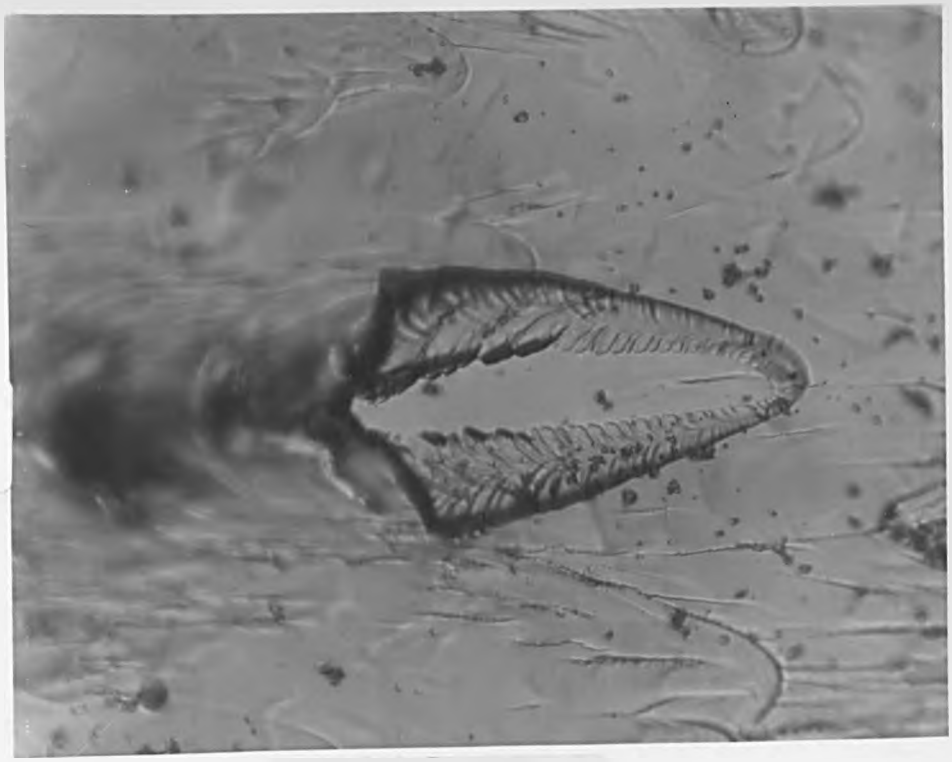

250

Pl.7.8
Type 2b feature

Pl. 7.9.
Type 3a feature

Pl. 7.10
Type 3b feature

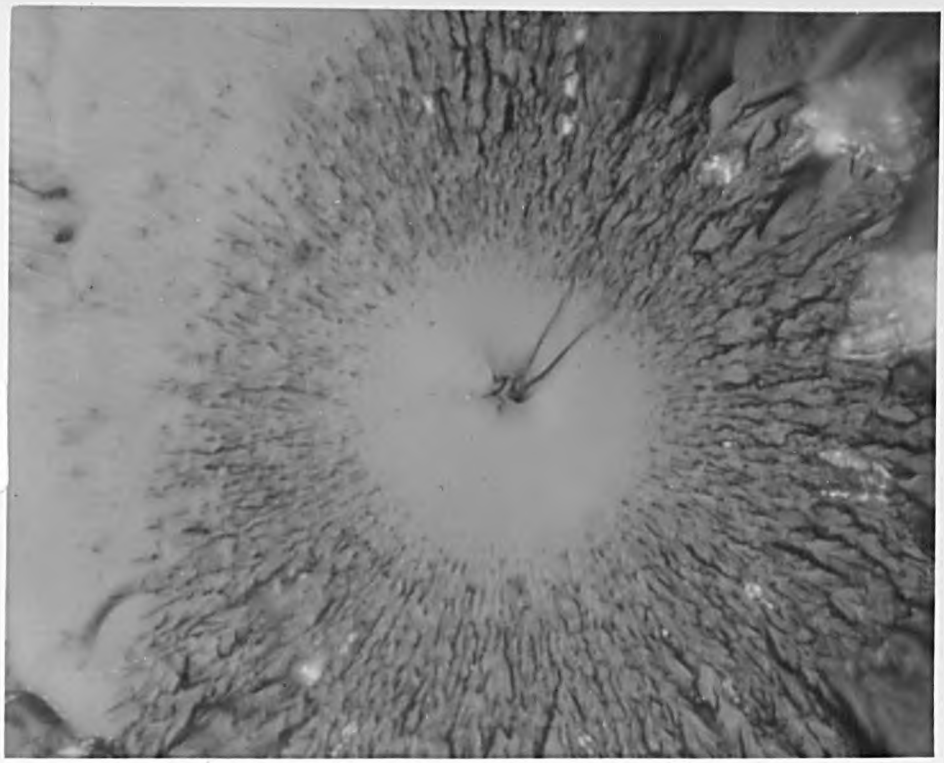

125

Pl. 7.11 Miniature mirror and mist zones close to the fracture origin.

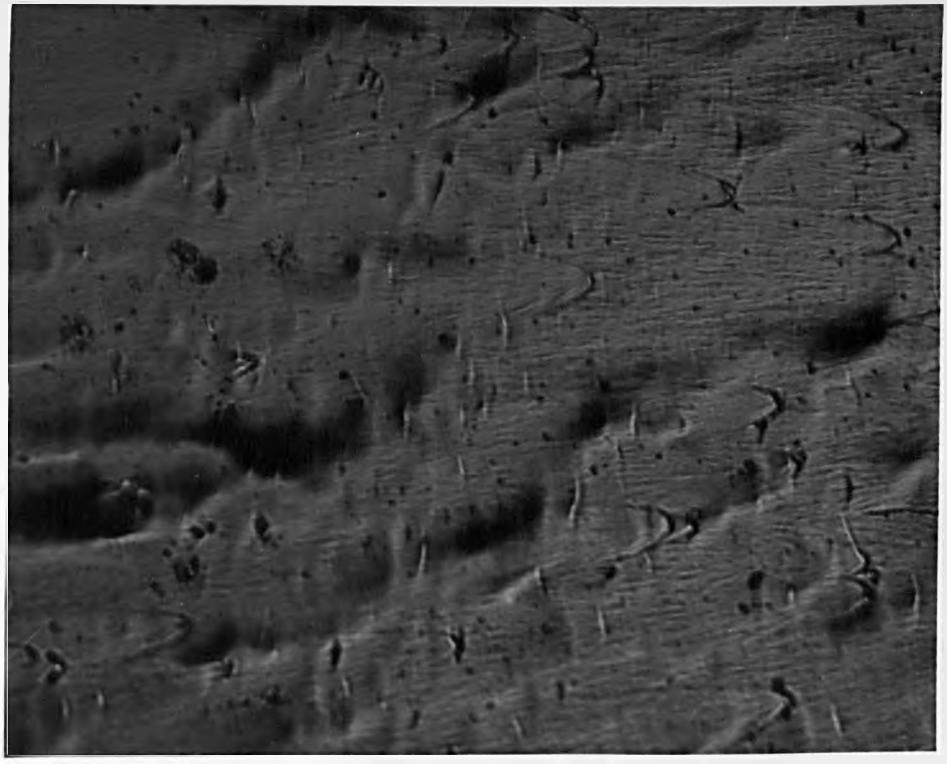

500

Pl. 7.12
Craze-like markings

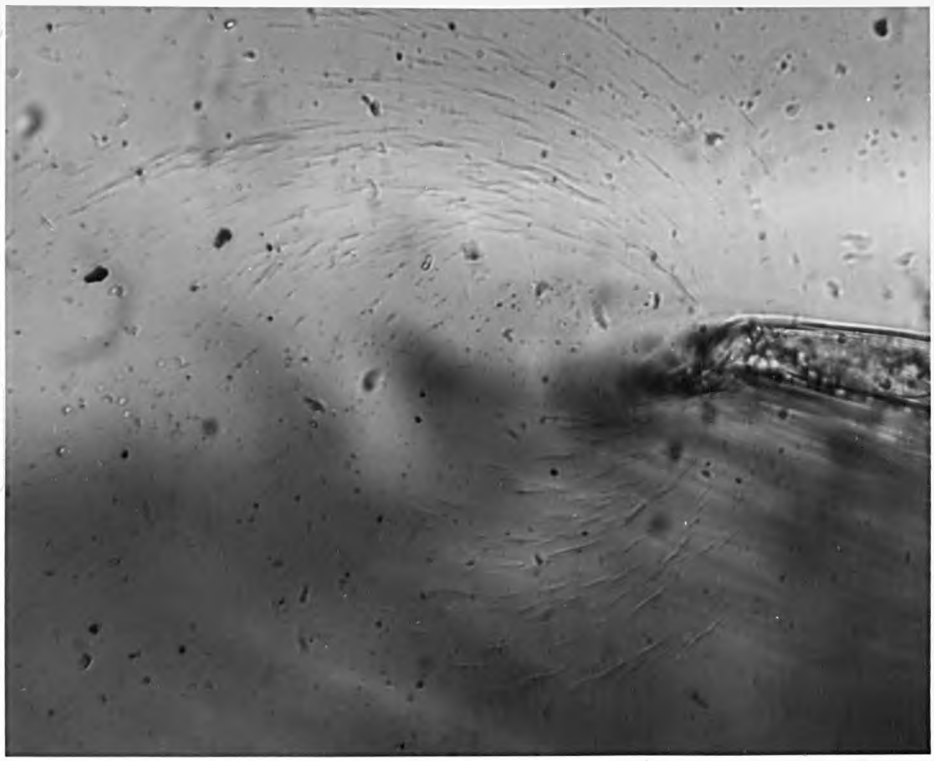

250

P. 7.13 "Crazes" around a loaded crack

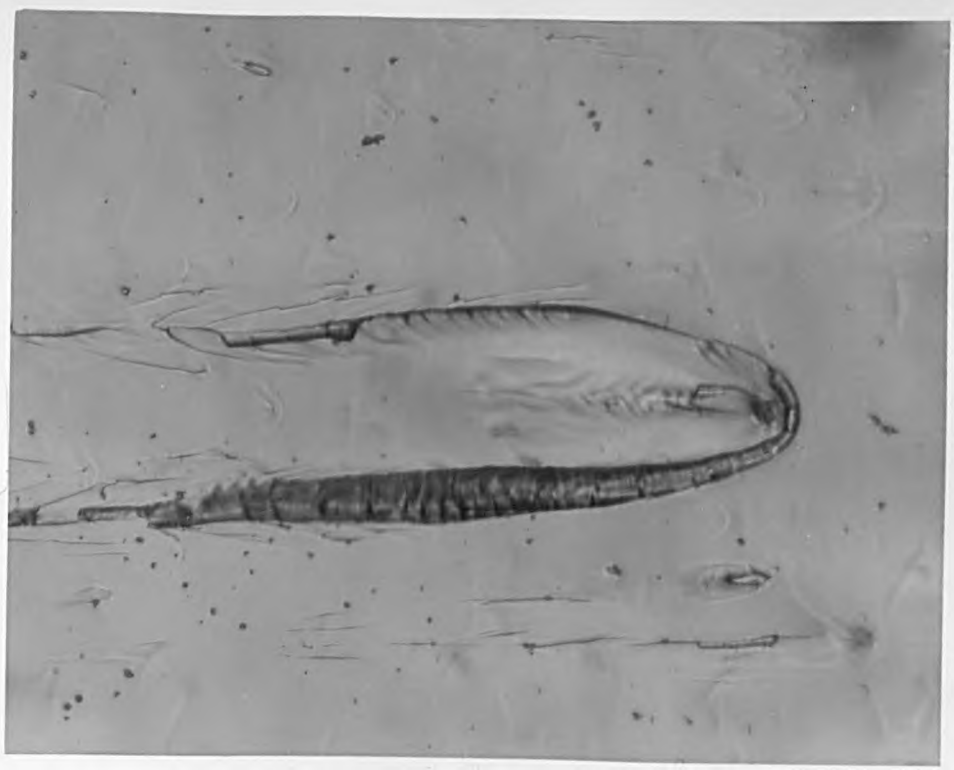

230

Pl. 7.14 Inclusion in a Type Ia feature

Pl. 7.15
Crack-tip in CT200

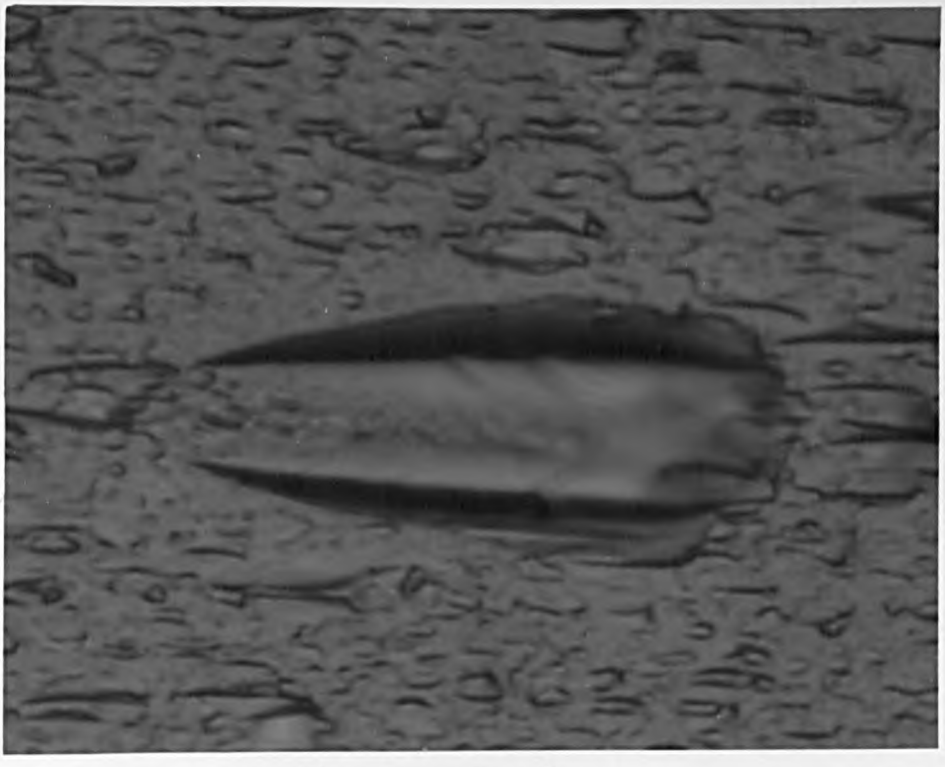

Pl. 7.16 Type 1
Glass feature

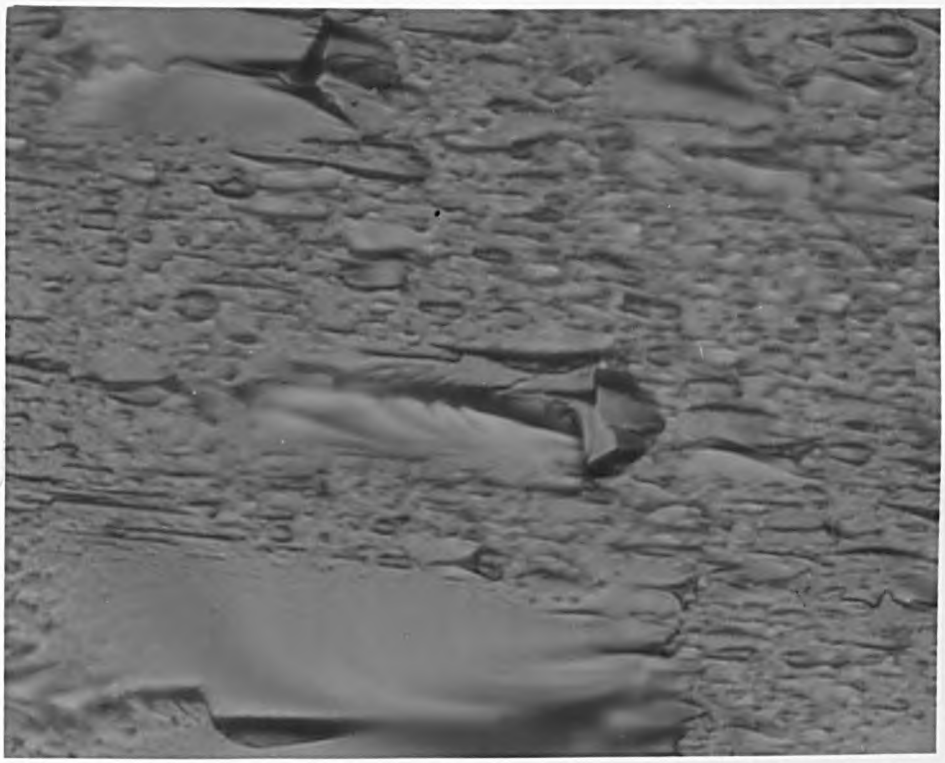

Pl.7.17 Type 2
Glass feature.